10. SITE 654: UPPER SARDINIAN MARGIN[1]

Shipboard Scientific Party[2]

HOLE 654A

Date occupied: 3 February 1986

Date departed: 8 February 1986

Time on hole: 5 days, 4 hr

Position: 40°34.76′N; 10°41.80′E

Water depth (sea level, corrected m, echo-sounding): 2208

Water depth (rig floor, corrected m, echo-sounding): 2217

Bottom felt (m, drill pipe length from rig floor): 2218.4

Total depth (m): 2701.8

Penetration (m): 483.4

Number of cores: 53

Total length of cored section (m): 483.4

Total core recovered (m): 239.5

Core recovery (%): 49.5

Deepest sedimentary unit cored:
Depth sub-bottom (m): 415.6
Nature: continental series
Age: unknown
Measured vertical sound velocity (km/s): 1.96 to 6.25

Igneous or metamorphic basement: none

Principal results: Site 654 is located on a fault-bounded, tilted block on the upper margin of Sardinia (Fig. 1). Seismic lines across Site 654 exhibit a geometry suggestive of pre-, syn-, and post-rift sequences. Hole 654A penetrated the wedging seismic unit which is interpreted as the syn-rift sequence, but was terminated in coarse conglomerate before reaching the subparallel dipping reflectors interpreted as the pre-rift sequence (Fig. 2).

Hole 654A was not logged because the bit failed to release. A series of four heat-flow measurements gave an average thermal gradient of 4.2 °C/100 m or a heat flow of approximately 50 mW/m^2.

Six major sedimentary units have been identified of Pleistocene to Tortonian (and possibly older) age (Fig. 3).

Unit I: Cores 107-654A-1R to 654A-27R-1, 3 cm; 0–242.7 mbsf; age: Pleistocene and Pliocene.

Unit I is dominated by nannofossil oozes with subordinate calcareous muds, with minor terrigenous clastics, volcanic ashes, and probable sapropels. An interval of nonvesicular, aphanitic, olivine-phyric basalt was encountered between 71 and 73 mbsf, within a few meters of the Pliocene/Pleistocene boundary.

Unit II: Cores 107-654A-27R-1, 3 cm, to 654A-36R-1, 110 cm; 242.7–312.6 mbsf; age: Messinian.

Unit II comprises gypsum interbedded with calcareous clay, mudstone, minor sandstone, breccia, dolostone, anhydrite, and very rare nannofossil chalk. Numerous discrete intercalations of laminated, balatino-type gypsum were penetrated, ranging in thickness from 0.15 to 7 m, and cumulatively accounting for approximately one-third of the total sediment thickness. Structures indicative of current activity (ripples, microcross-laminations, and small scours) are common in the intra-gypsum clastic layers. Evidence of sedimentary instability is sparse.

Unit III: Cores 107-654A-36R-1, 110 cm to 654A-40R-1, 7.5 cm; 312.6–348.9 mbsf; age: inferred early to middle Messinian. Unit III is dominated by dark colored, finely laminated, organic-carbon-rich claystone and dolomitic/calcareous siltstone, with minor volcanic ash. A sparse biota comprises radiolarians, diatoms, sponge spicules, and fish teeth. Synsedimentary debris flows, convolute laminations, and microfaults are common.

Unit IV: Cores 107-654A-40R-1, 7.5 cm to 654A-45R-5, 145 cm, 348.9–403.9 mbsf; age: late Tortonian to earliest Messinian.

Unit IV comprises homogeneous, highly burrowed nannofossil oozes. The benthic foraminifer assemblages can be interpreted as suggesting shoaling of the water depth downsection; while the nannofossil assemblages suggest a downsection trend from open marine to more restricted marine. Trace quantities of asphaltic hydrocarbons were found in the upper part of this unit.

Unit V: Core 107-654A-45R-5, 145 cm, to 654A-46R-CC; 403.9–415.7 mbsf; age: not determined.

This unit comprises polymict glauconitic sandstone and marly calcareous chalk with large foraminifers and fragments of mollusks and echinoderms. The base of the unit is marked by large, thick-walled oyster shells.

Unit VI: Cores 107-654A-47R through 654A-52R; 415.7–473.8 mbsf; age: indeterminate.

Unit VI comprises reddish-colored gravel-bearing calcareous mudstones, underlain by matrix-supported conglomerate, gravel, and gravelly mudstone. The pebbles consist mostly of limestone, marble, dolostone, and quartzitic rocks, and are subrounded. (Core 107-654A-53R, 473.8–483.4 mbsf, was empty.)

---

[1] Kastens, K. A., Mascle, J, Auroux, C., et al., 1987. *Proc., Init. Repts. (Pt. A), ODP*, 107.

[2] Kim A. Kastens (Co-Chief Scientist), Lamont-Doherty Geological Observatory, Palisades, NY 10964; Jean Mascle (Co-Chief Scientist), Laboratoire de Géodynamique Sous-Marine, Université Pierre et Marie Curie, BP 48, 06230 Villefranche-sur-Mer, France; Christian Auroux, Staff Scientist, Ocean Drilling Program, Texas A&M University, College Station, TX 77843; Enrico Bonatti, Lamont-Doherty Geological Observatory, Palisades, NY 10964; Cristina Broglia, Lamont-Doherty Geological Observatory, Palisades, NY 10964; James Channell, Department of Geology, 1112 Turlington Hall, University of Florida, Gainesville, FL 32611; Pietro Curzi, Istituto di Geologia Marina, Via Zamboni, 65, 40127 Bologna, Italy; Kay-Christian Emeis, Ocean Drilling Program, Texas A&M University, College Station, TX 77843; Georgette Glaçon, Laboratoire de Stratigraphie et de Paleoécologie, Centre Saint-Charles, Université de Provence, 3, Place Victor Hugo, 13331 Marseille Cedex, France; Shiro Hasegawa, Institute of Geology, Faculty of Science, Tohoku University, Aobayama, Sendai, 980, Japan; Werner Hieke, Lehrstuhl für Allgemeine, Angewandte und Ingenieur-Geologie, Abt. Sedimentforschung und Meeresgeologie, Technische Universität München, Lichtenbergstrasse 4, D-8046 Garching, Federal Republic of Germany; Floyd McCoy, Lamont-Doherty Geological Observatory, Palisades, NY 10964; Judith McKenzie, Department of Geology, University of Florida, 1112 Turlington Hall, Gainesville, FL 32611; Georges Mascle, Institut Dolomieu, Université Scientifique et Médicale de Grenoble, 15 Rue Maurice Gignoux, 38031 Grenoble Cedex, France; James Mendelson, Earth Resources Laboratory E34-366, Department of Earth, Atmospheric and Planetary Sciences, Massachusetts Institute of Technology, 42 Carleton Street, Cambridge, MA 02142; Carla Müller, Geol. Paläont. Institut, Universität Frankfurt/Main, 32–34 Senckenberg-Anlage, D-6000 Frankfurt/Main 1, Federal Republic of Germany (current address: 1 Rue Martignon, 92500 Rueil-Malmaison, France); Jean-Pierre Réhault, Laboratoire de Géodynamique Sous-Marine, Université Pierre et Marie Curie, BP 48, 06230 Villefranche-sur-Mer, France; Alastair Robertson, U.S. Geological Survey, 345 Middlefield Road, Menlo Park, CA 94025 (current address: Department of Geology, Grant Institute, University of Edinburgh, Edinburgh, EH9 3JW, United Kingdom); Renzo Sartori, Istituto di Geologia Marina, Via Zamboni, 65, 40127 Bologna, Italy; Rodolfo Sprovieri, Istituto di Geologia, Corso Tukory, 131, Palermo, Italy; Masayuki Torii, Department of Geology and Mineralogy, Faculty of Science, Kyoto University, Kyoto, 606, Japan.

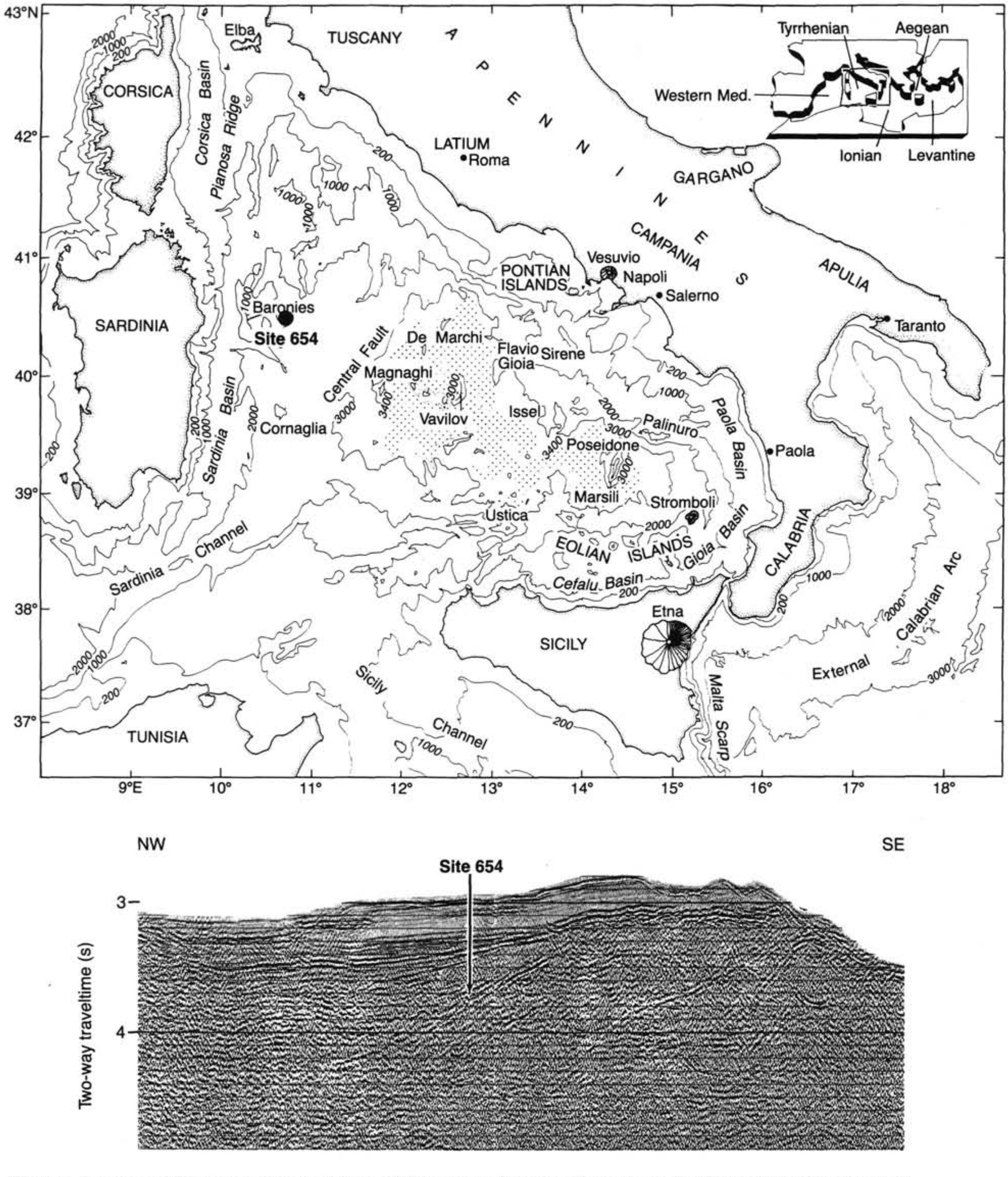

Figure 1. Location of Site 654 on bathymetric map of the Tyrrhenian Sea and on seismic line ST06. Bathymetry in meters.

BACKGROUND AND OBJECTIVES

Regional Setting and Previous Work

Site 654 is a companion study to Site 652, with similar tectonic setting and objectives. Like Site 652, Site 654 is located on the continental margin of Sardinia (Figs. 4–6), on a tilted block which is apparently bounded by seaward-dipping listric normal faults. As at Site 652, seismic reflection profiles across Site 654 exhibit a geometry appropriate for pre-, syn-, and post-rifting sequences (Fig. 7). But whereas Site 652 was close to the transition between inferred oceanic and continental crust in 3375 m water depth, almost 200 km from the coast of Sardinia, Site 654 is located high on the continental margin in only 2175 m water depth, less than 75 km from the shoreline. At Site 652, the thickness of the crust as inferred from seismic refraction experiments (Recq et al., 1984; Steinmetz et al., 1983) is 7–8 km, whereas at Site 654 the crust is 20 km thick (Fig. 8).

The motivation for drilling on two different tilted blocks on the thinned continental crust was to test the hypothesis that extension did not occur uniformly in space and/or time. The difference in crustal thickness between Sites 652 and 654 implies that the two areas have not been stretched equally (in the terminology of McKenzie, 1978, the two areas have locally different Beta values). Exactly how this difference in Beta value is accommodated across the transition zone from extremely-thinned to slightly-thinned continental crust is not clear either from theory or from observation at other passive margins. In the idealized case, one could imagine that either the region of extremely-thinned continental crust accommodated greater horizontal extension per unit time than the region of slightly-thinned crust, or that the region of extremely-thinned crust experienced horizontal extension over a longer interval of time than the region of slightly-thinned crust. In the first case, timing of extension at Site 652 and 654 should be the same, but the rate of extension would differ; whereas in the second case the rate of extension should be the same at both sites, but extension at Site 652 should have begun earlier than at Site 654. Extension cannot be directly measured; the tie between observation and theory requires an assumption that the timing and rate of extension are related to the timing and rate of subsidence, and the timing and rate of rotation of fault-bounded, tilted blocks.

In the Tyrrhenian, an additional complication is introduced by the possibility that there has been more than one phase of stretching. Based on seismic stratigraphy, Moussat (1983) and Rehault et al. (1984) have suggested the following possibilities:

1. The whole margin (including both Sites 652 and 654) was affected by an early (18–10 Ma) rifting phase, and then a second phase of rifting (10–6 Ma) was concentrated in the central basin (including Site 652 but not Site 654);
2. An early, abortive phase of extension occurred on the Sardinian margin (including Site 654), and later extension was confined to the central basin (including Site 652); and
3. The entire basin was affected by two distinct, sequential stretching phases.

Site 654 is located on the westernmost tilted block which has an obvious pre-, syn-, and post-rift geometry on the seismic reflection profiles. To the west of Site 654 lies a north-trending ridge with approximately 1000 m of relief, called Baronie Ridge or Monte delle Baronie (Figs. 4 and 5). Dredge hauls and cores from this ridge have yielded a diverse assemblage of primarily continental rocks, which may be similar to the pre-rift assemblage to be expected at Site 654. Paleozoic to Triassic quartzite and conglomerate accompany lower and middle Pliocene shallow water carbonates. Other rock types which have been recovered but not dated include serpentinite, alkali-olivine basalt, mica schist, carboniferous [sic] phyllite, sandstone, and granite or granodiorite (Colantoni et al., 1981).

To the east of Site 654 lies a north-trending terrace or region of flat seafloor, about 2800 m deep, called the Cornaglia Terrace or Cornaglia Basin (Figs. 4 and 5). The flat seafloor of the terrace is underlain by a north-trending structural trough. As has been pointed out in discussion of the earlier sites, the interpretation of Messinian facies in most of the Tyrrhenian Sea is controversial; the one point of consensus concerns the Cornaglia Basin. There, the distinctive strong subparallel reflectors typical of the upper evaporites, overlying the more transparent unit deformed by sporadic diapirs typical of the lower evaporites, have persuaded all investigators (Fabbri and Curzi, 1979; Malinverno et al., 1981; Moussat, 1983) that thick salt-bearing evaporites are present. The inference that within the Tyrrhenian thick evaporites only occur toward the western margin has been presented as evidence that the Cornaglia Basin was the deepest part of the Tyrrhenian Sea during the Messinian desiccation (Hutchison et al., 1985; Duschenes et al., 1986). If this scenario is correct, then Site 654 would lie on the margin of this pre-Messinian older basin; whereas Site 652 would lie on the margin of a younger basin that subsided or "foundered" during or after the Messinian.

Objectives

Passive Continental Margin Evolution

The primary objective at Site 654 was to document the timing of extension and subsidence of a young passive margin by dating the pre-/syn-rift contact and the syn-rift/post-rift contact, plus intermediate reflectors within the syn-rift. The timing of extension and subsidence on the upper Sardinian margin, as determined at Site 654, will be compared to the timing and rate of subsidence on the lower Sardinian margin (Site 652) and at other passive margins not bounding marginal basins.

Messinian Paleoenvironment

As at each previous site, the Messinian facies in the vicinity of Site 654 had been variously interpreted. Fabbri and Curzi (1979) mapped this region as "evaporites of the marginal zone" (i.e., evaporites lacking the lower halite-bearing evaporites); this assessment is shared by Moussat (1983). On the other hand, on the Messinian facies map of Malinverno et al. (1981), Site 654 falls on a boundary between a pocket of salt-bearing evaporites (to the east) and a subaerial erosional facies (to the west).

Pre-Messinian Paleoenvironment

The pre-rift sequence at Site 654 is expected to be Tortonian or older in age. Of particular interest would be to determine whether the sediments deposited prior to the present phase of rifting were already in a marine environment; such an observation might support the hypothesis that the Tyrrhenian opened in two or more separate rifting phases.

Site Selection

Site 654 is located on the farthest westward tilted block which exhibits a clearcut geometry of pre-, syn-, and post-rift sediments on seismic reflection profiles (Fig. 7). The challenge in choosing the exact site was to avoid potential structural hydrocarbon traps, avoid evaporites capable of forming a cap rock for a hydrocarbon reservoir, and yet find a site where the pre-rift sediments might be accessible with a single-bit hole. A suitable site was selected on site survey line ST06 (shotpoint 1531) near its intersection with line ST07.

OPERATIONS

Strategy

Site 654 was expected to reach 600 mbsf and to end in a unit with a seismic velocity of 4.4 km/s. Because of the relatively deep penetration and potentially very hard unit at depth, the site was scheduled for rotary drilling. Heat flow runs with the Uyeda probe were planned every fourth core to a maximum of four good or five total measurements. The planned logging program comprised standard Schlumberger logs, plus selective use of the borehole televiewer.

The Safety Panel had placed several restrictions on drilling at Site 654. Drilling was to be terminated if "evaporites capable of serving as a [hydrocarbon] seal" were encountered, or if hydrocarbons monitored by gas chromatography in the Pliocene-Quaternary cores exceeded 200 times background where "background is defined as 10^{-8} to 10^{-4} standard volumes of C_1-C_6 hydrocarbons per volume of sediment, or the levels observed in cores at Site TYR-2 [653]." The Safety Panel had specified a very precise location at shotpoint 1531 on seismic line ST06, constrained in both the updip and downdip direction by structures they considered dangerous.

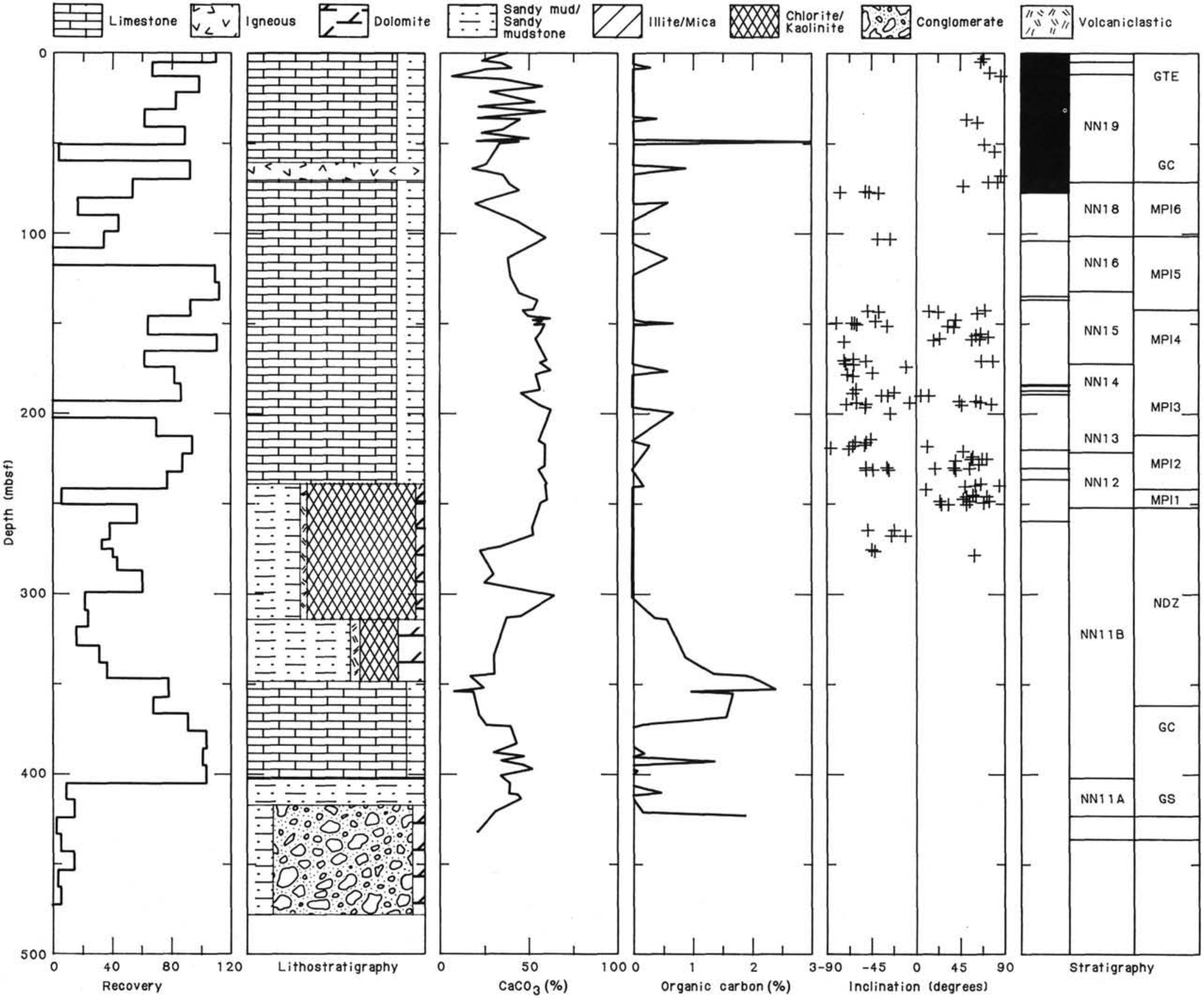
Limestone
Igneous
Dolomite
Sandy mud/ Sandy mudstone
Illite/Mica
Chlorite/ Kaolinite
Conglomerate
Volcaniclastic
Depth (mbsf)
0
100
200
300
400
500
Recovery
0
40
80
120
Lithostratigraphy
CaCO$_3$ (%)
0
50
100
Organic carbon (%)
0
1
2
3
Inclination (degrees)
-90
-45
0
45
90
Stratigraphy
GTE
NN19
GC
NN18
MPl6
NN16
MPl5
NN15
MPl4
NN14
MPl3
NN13
MPl2
NN12
MPl1
NN11B
NDZ
GC
NN11A
GS

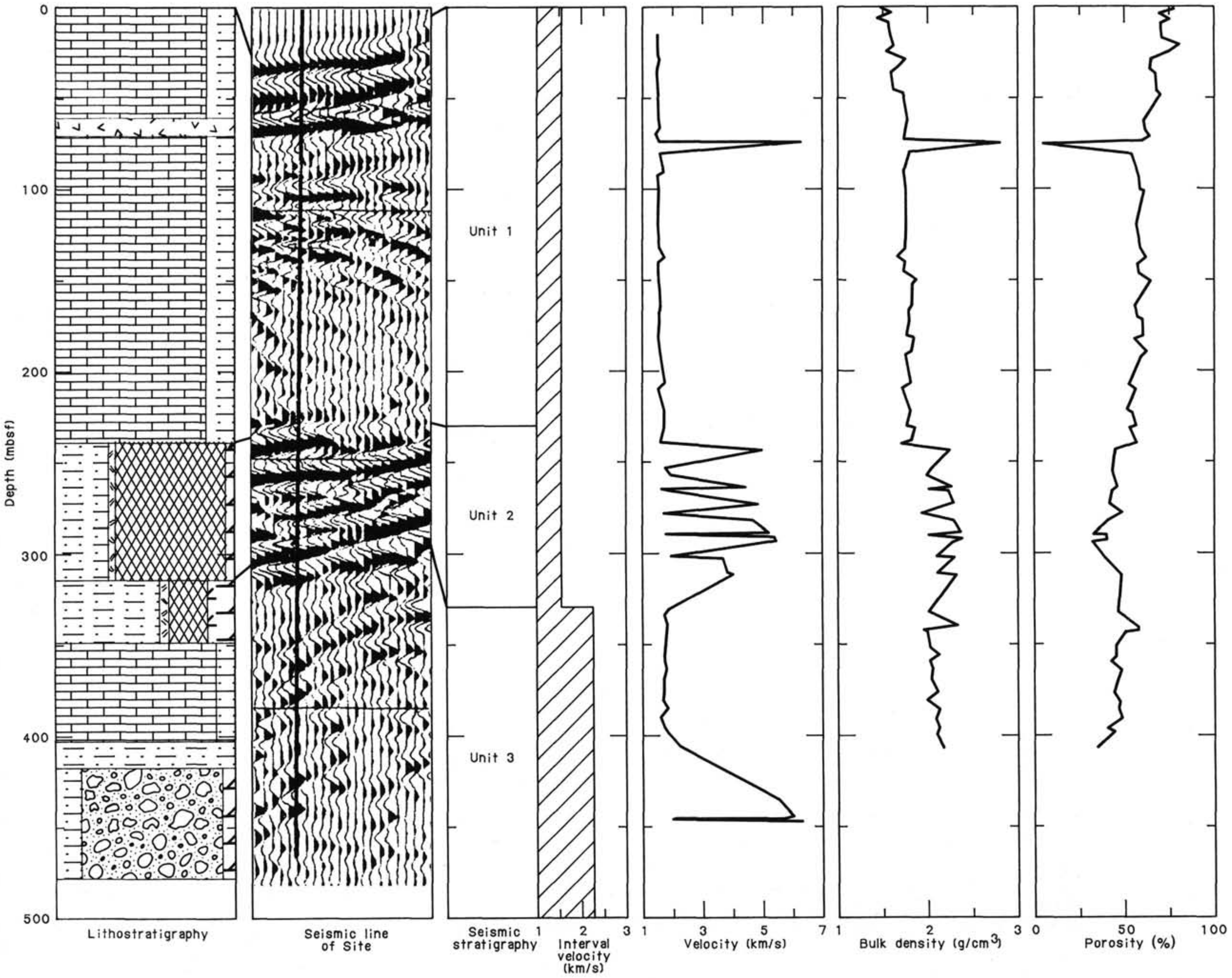

Figure 2. Summary of measurements made at Site 654.

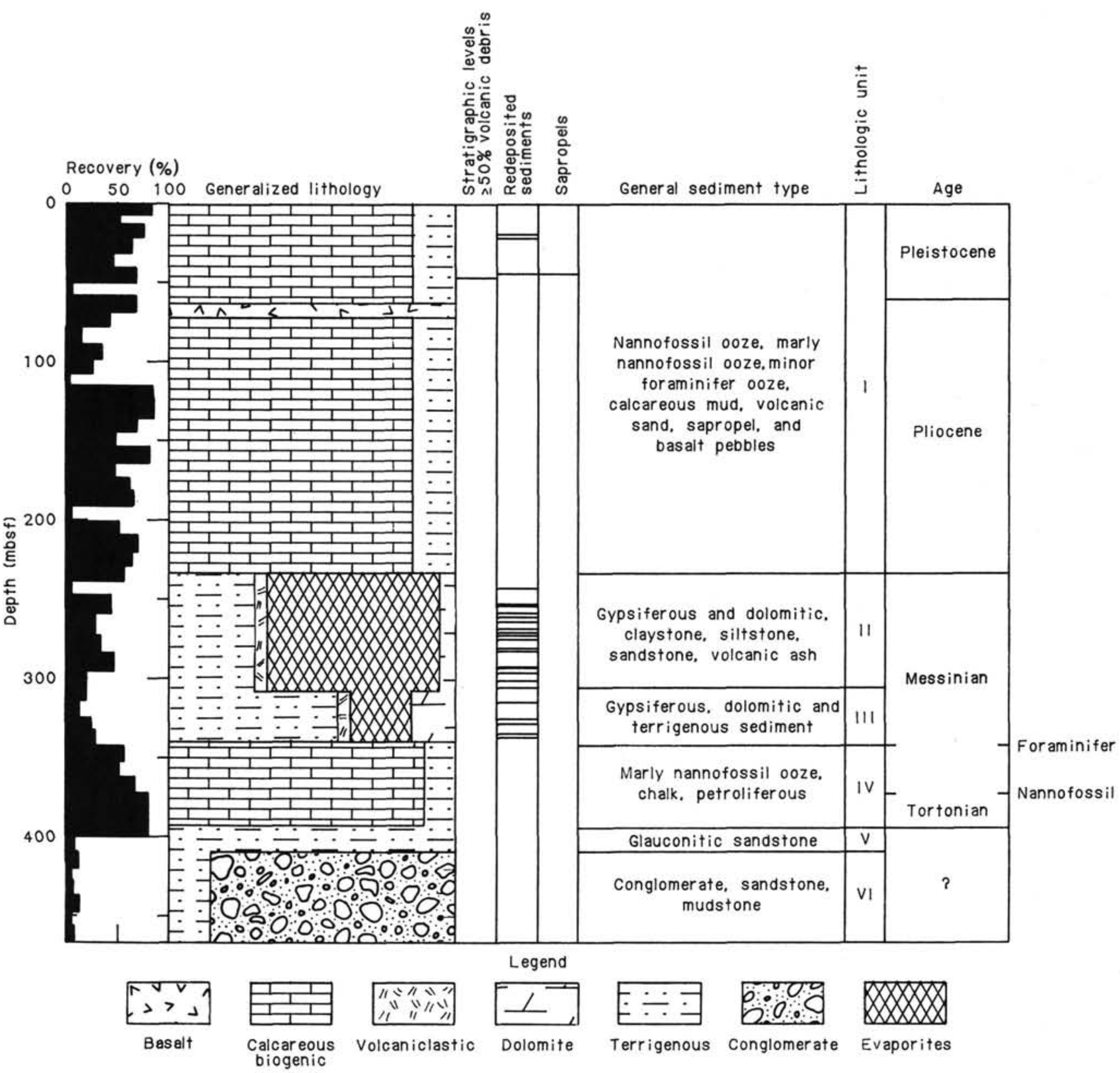

Figure 3. Lithostratigraphic summary for Site 654.

The approach to the site was planned to duplicate site survey line ST06 from southeast to northwest. Because the acceptable drilling position was tightly constrained, the beacon drop was planned for the second pass over the site.

Approach to Site

Unlike the previous four site approaches, the approach to Site 654 was blessed by good navigation data from both the Loran C and Global Positioning System (GPS). Good weather, without atmospheric disturbance, as well as the timing of the site approach during daytime rather than at dawn, dusk, or night, probably contributed to the stability and accuracy of the Loran positions.

On the transit from Site 653, the ship was navigated by Loran C, using X and Z slaves. The 3.5-kHz profiles collected in transit at 12 kt are unusually good, probably because of flat, calm seas. At 0650 on 3 February, the ship slowed to 5 kt and changed course to 311° to follow the track of site survey profile ST06. Seismic gear were streamed at 0700, and a few minutes later the experimental towed 3.5-kHz transducer array was lowered off the port crane. At 0726, the 3.5-kHz system was switched from the hull-mounted transducer to the towed transducer array; record quality immediately deteriorated.

As the ship followed the track of line ST06, navigating by Loran C, good agreement was noted between our seismic and bathymetric profiles and the site survey profiles. The streamer passed over the target at 0838. At 0924 the ship began a Williamson turn to a reciprocal course. During the turn the 3.5-kHz system was switched back to the hull-mounted transducer, and the towed fish was brought back aboard. The turn was completed and the ship was steadied on course 130° by 0941. The daytime GPS window was predicted to begin at 1000, and

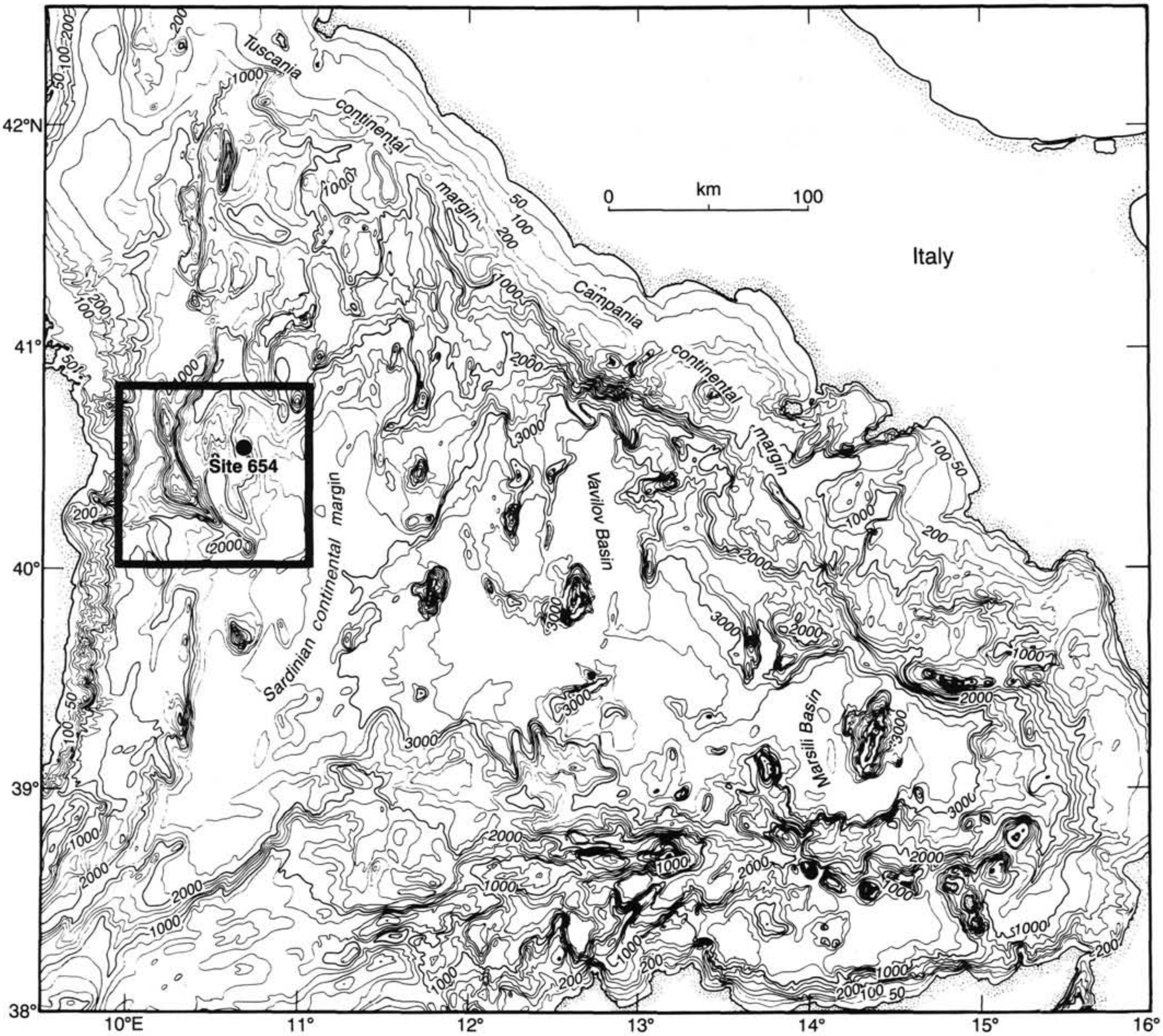

Figure 4. Bathymetric map of the Tyrrhenian Sea, showing location of Site 654 on the upper Sardinian continental margin.

the first GPS fix arrived on schedule. The first GPS fix gave a position 0.7 nmi northeast of the Loran position. Over the next 15 min the GPS position converged on the Loran position, as the elevation of GPS satellite 11 rose from 3° to 11°; by 1015, the GPS positions were tracking consistently 0.1 nmi northeast of the the Loran positions. At 1040, the ship reached (simultaneously) the target Loran position and the target water depth as recorded on the northeastbound track, and the beacon was dropped. The Loran C drop position was 40°34.60′N, 10°41.65′E, and the GPS drop position was 40°34.73′N, 10°41.86′E.

The seismic survey was terminated at 1045 and seismic gear pulled aboard. At 1056 the ship reversed course to return to the beacon to begin dynamic positioning. The drill site was located 17 m west of the beacon. An average of GPS and transit satellite fixes received while on station gave a final site position of 40°34.76′N, 10°41.80′E.

Hole 654A

The standard RCB bottom-hole assembly was used, with a newly developed hydraulic bit release and RBI, C-3 bit. A mudline punch core was taken at 1611, 3 February, establishing the water depth at 2218.4 m by drill pipe measure. Routine coring continued in hemipelagic ooze using virtually no circulation to avoid washing away the soft material. In Core 107-654A-9R, still well within the hemipelagic sequence, a totally unexpected layer of basalt was cored; although only 0.24 m were recovered, the marked drop in rate of penetration suggested that the basalt layer extended from 71 to 73 mbsf. Below the basalt, the marly ooze continued growing gradually stiffer but presented no penetration problems.

At 249.5 mbsf the first of the anticipated Messinian evaporites was contacted and readily identified by a drastic reduction in rate of penetration coupled with moderate vibration and jump-

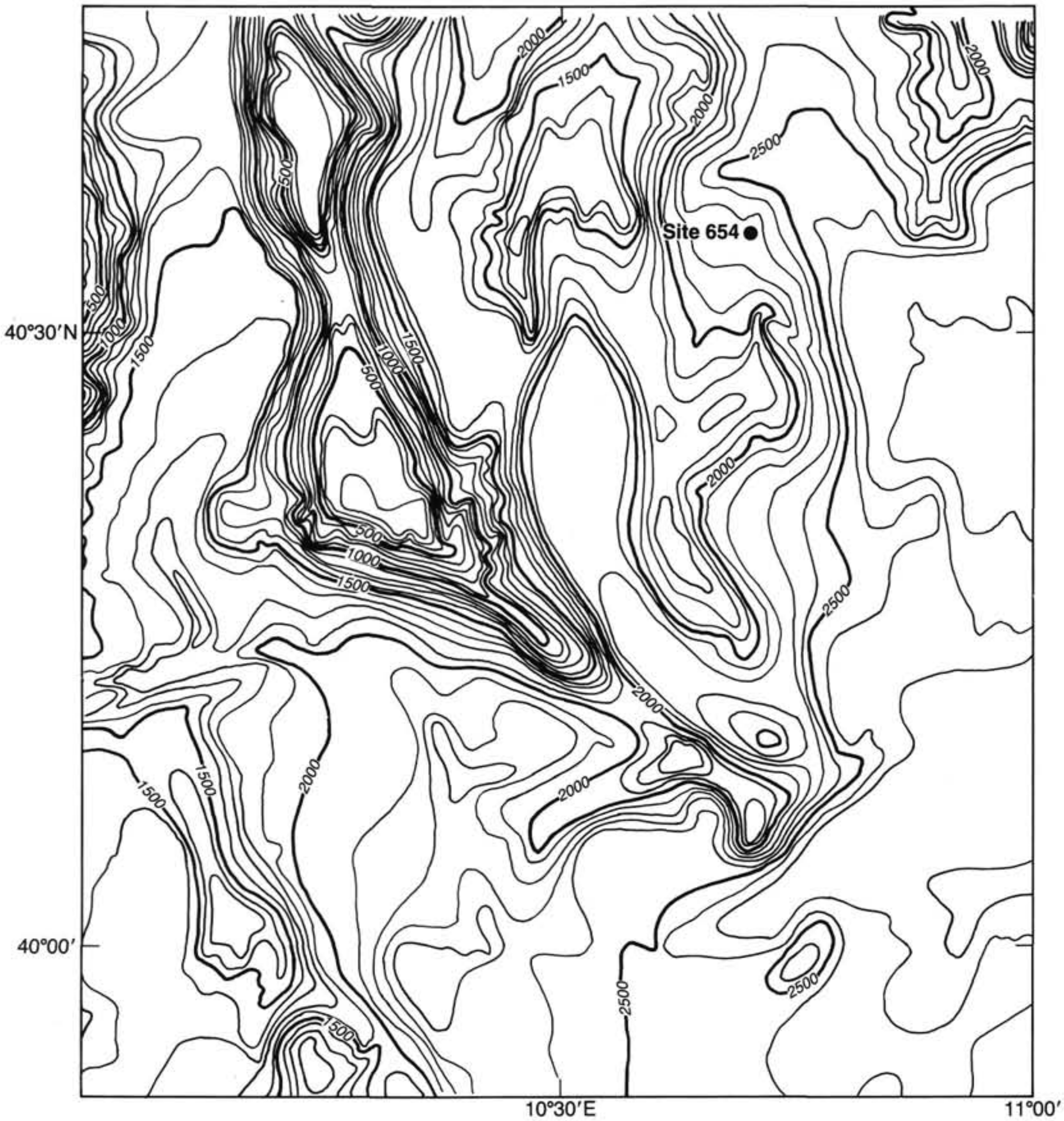

Figure 5. Detailed bathymetric map of the Site 654 area. The Baronie Mountains are just west of the site location.

ing of the entire drill string. This behavior continued for the final 2 m of Core 107-654A-27R. When recovered the core was found to contain about 1/2 m of hard, laminated, balatino-type gypsum. This lithology was considered to be exactly what the JOIDES Safety Panel had in mind when they placed a restriction on penetrating through "evaporites capable of forming a [hydrocarbon] seal." Thus drilling would have to terminate if a layer of such gypsum more than 3 or 4 m thick were encountered.

The top 1 1/2 m of the next core also drilled very slowly, with the drill string jumping and shaking, indicating more of the same gypsum. At 1 1/2 m into Core 107-654A-28R, the rate of penetration suddenly increased, indicating that the first gypsum layer had been only 3-1/2 m thick. The mud recovered from below the gypsum layer was tested for hydrocarbons by both vacutainer and head space analysis. Less than 5 ppm methane was measured with no heavier hydrocarbons in evidence. In consultation with ODP headquarters, it was decided that in view of the very low measured hydrocarbon values, we could continue to drill through laminated gypsum layers, provided that each core contained intra-gypsum mud layers suitable for hydrocarbon analysis, and provided gas content stayed very low.

The sequence of events outlined for Cores 107-654A-27R and 654A-28R repeated themselves with minor variations for the next 62.5 m of penetration. At least five discrete layers of gypsum a meter or more in thickness, interbedded with mud, were penetrated. No methane readings in excess of 6 ppm were recorded in the mud layers.

The base of the evaporites was reached at 312 mbsf; rate of penetration increased as firm, finely-laminated mudstones were penetrated (lithostratigraphic Unit III). At about 350 mbsf, in the uppermost core of the open marine oozes (lithostratigraphic Unit IV), a small hydrocarbon show was discovered. The hydrocarbons appeared as two 1-mm-thick laminae visible under black light in the split core. These were determined by extract analysis to be asphaltines. C_1, C_2, and C_3 volumes measured by headspace analysis were 12, 1, and 2 ppm, respectively. In the next two cores, only pinhead-sized specks of hydrocarbons were visible under black light, and hydrocarbons measured by headspace analysis quickly decreased to the normal background level of 3 ppm methane with nothing heavier.

Coring continued into a conglomerate of probable continental origin containing pebbles of all sizes. Recovery in the conglomerate sequence dropped to generally less than 1 m per core.

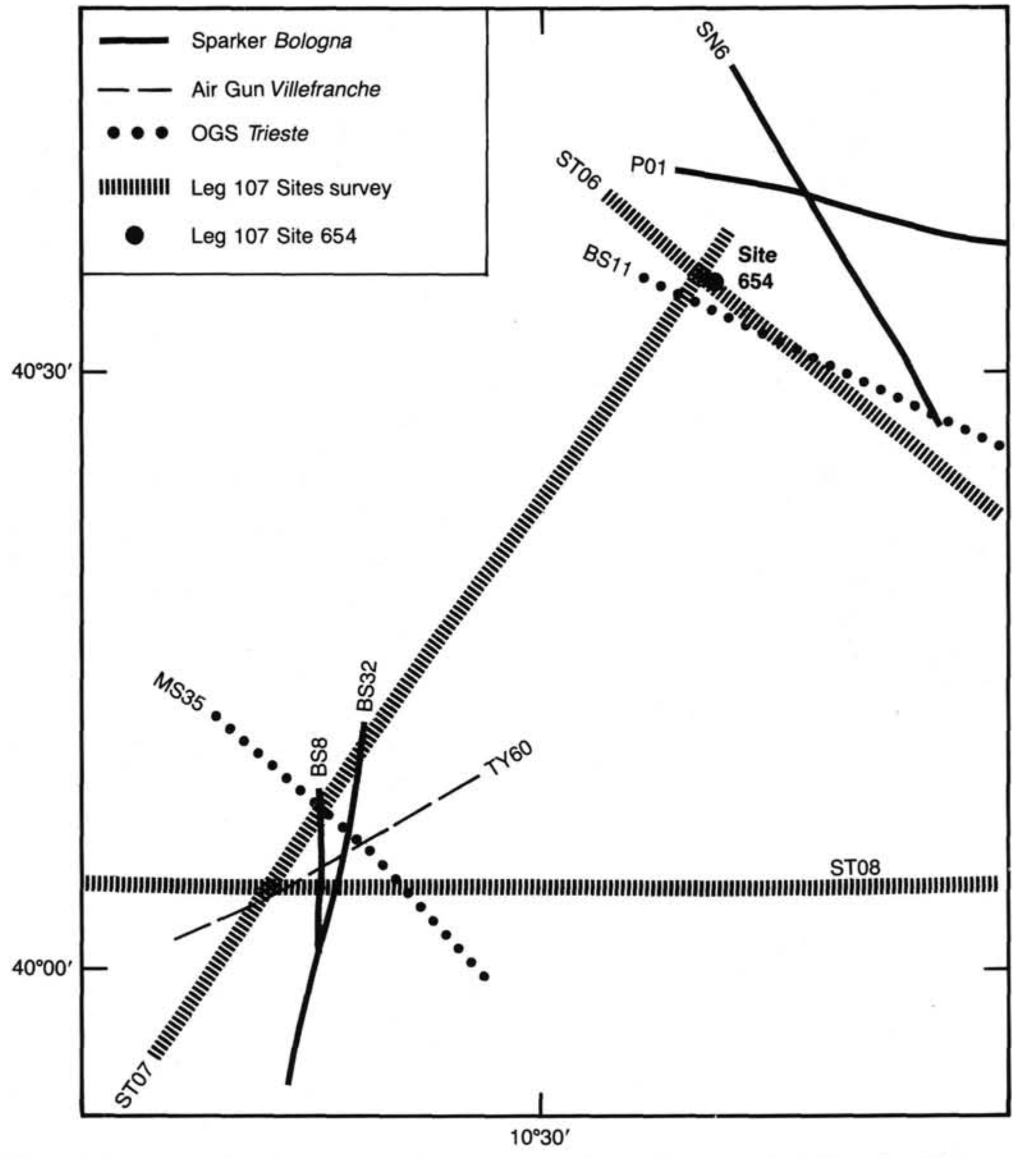

Figure 6. Seismic track lines in the vicinity of Site 654, which is located at shotpoint 1531 on line ST06.

After six cores in the unstable mixture, not-too-surprising hole problems developed. Torquing and a momentarily plugged bit were experienced in Core 107-654A-51R. Core 107-654A-52R had fill in the bottom of the hole and Core 107-654A-53R came up completely empty. The empty liner suggested that a piece of rock might be stuck in the throat of the bit preventing the core barrel from latching into place. A core barrel with a bit deplugger was dropped to dislodge such a rock. While recovering the bit deplugger barrel, the pipe became very stuck and required 3 1/2 hr of strenuous working of the pipe with up to 265,000 lb overpull to free. While the pipe was stuck, it became evident that continuation of the hole would not be advisable even if the pipe could be worked free. An attempt was then made to activate the hydraulic bit release in hopes that releasing the bit would enable the pipe to be torqued or pulled loose, leaving the hole accessible for logging. The go-devil seated and pressured up properly, but the release mechanism would not activate. The pipe was then worked for a few more minutes and suddenly came free. The bit was then pulled two stands uphole where hole conditions were assumed to be stable. A final unsuccessful attempt was made to release the bit, and the go-devil was retrieved.

The pipe was pulled to a depth of 2539 m and a 50 bbl cement plug was set across the evaporite sequence (approximately 100 m). The pipe was then pulled to the ship and the hole was abandoned. The bit arrived on deck at 1515, 8 February, and the ship was underway at full speed for Site 655 by 1530.

LITHOSTRATIGRAPHY

Introduction

At Site 654 six major sedimentary units are recognized ranging from Pleistocene to Tortonian and possibly older in age (Fig. 9). The location of the site is on a fault-bounded tilted block of inferred continental crust on the upper continental margin of Sardinia. The lithostratigraphic units are first outlined, then discussed in more detail (coring summary in Table 1).

Unit I: Cores 107-654A-1R-1 to 654A-27R-1, 3 cm; 0–242.7 mbsf; age: Pleistocene and Pliocene. The unit is dominated by nannofossil oozes with subordinate calcareous muds, with minor terrigenous clastics, volcanic ashes, and sapropels. A layer of nonvesicular aphanatic olivine-phyric basalt was encountered between 71 and 73 mbsf.

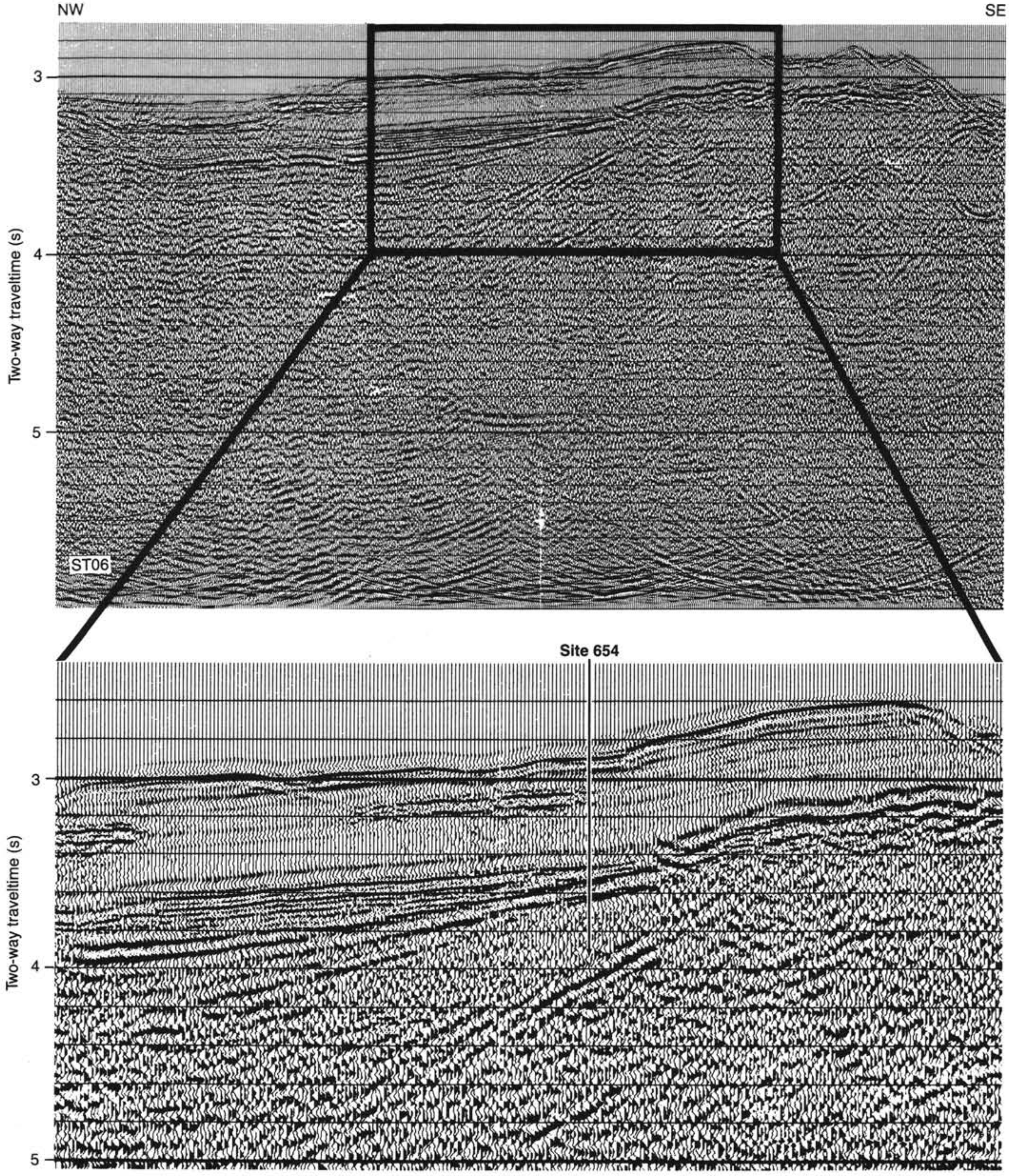

Figure 7. Section of MCS Line ST06 showing location of Site 654. The geometry of the seismic units is interpreted in terms of post-rift, syn-rift, and pre-rift sediments.

Unit II: Cores 107-654A-27R-1, 3 cm, to 654A-36R-1, 110 cm; 242.7–312.6 mbsf; age: Messinian. Unit II comprises gypsum interbedded with calcareous clay, mudstone, minor sandstone, breccia, dolostone, anhydrite, and very rare nannofossil ooze.

Unit III: Cores 107-654A-36R-1, 110 cm, to 654A-40R-1, 7.5 cm; 312.6–348.9 mbsf; age: inferred to be early to middle Messinian. The unit is dominated by very dark colored, finely laminated, organic-carbon-rich claystone and siltstone, with minor volcanic ash. There is a sparse biota composed of radiolarians,

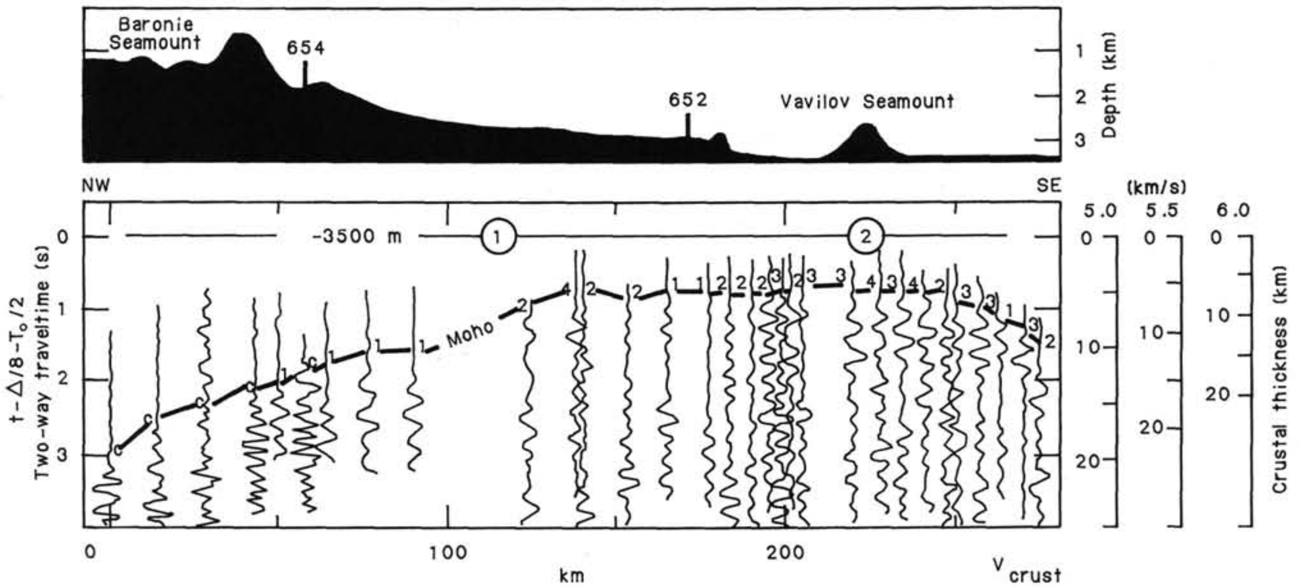

Figure 8. Crustal section across the Sardinian margin (after Steinmetz et al., 1983), showing the progressive thinning of the margin toward the Vavilov Basin. Projected locations of Sites 652 and 654 are indicated.

diatoms, sponge spicules, and fish teeth. Synsedimentary debris-flows, convolute lamination, and microfaults are common.

Unit IV: Cores 107-654A-40R-1, 7.5 cm to 654A-45R-1, 145 cm, 348.9-403.9 mbsf; age: late Tortonian and earliest Messinian. This unit comprises highly burrowed nannofossil oozes which contain a microfauna suggestive of shoaling downward into a more restricted marine setting.

Unit V: Cores 107-654A-45R-5, 145 cm, to 654A-46R-CC; 403.9-415.7 mbsf; age: not determined. The unit comprises polymictic glauconitic sandstone and marly calcareous chalk with large foraminifers and fragments of mollusks and echinoderms. The base of the unit contains large thick-walled oyster shells.

Unit VI: Cores 107-654A-47R through 654A-52R; 415.7-473.8 mbsf; age: indeterminate. Unit 6 comprises reddish gravel-bearing calcareous mudstones, underlain by matrix-supported conglomerate, gravel, and gravelly mudstone. The pebbles consist mostly of limestone, marble, dolostone, and quartzitic rocks, inferred to have been derived from a deformed and metamorphosed carbonate unit and its continental basement.

Unit I

Cores 107-654A-1R to 654A-27R-1, 3 cm (inclusive); Depth: 0-242.7 mbsf; thickness: 242.7 m; age: Pleistocene and Pliocene.

Unit I (0-242.7 mbsf) is composed mostly of bioturbated nannofossil oozes, often rich in planktonic foraminifers, with minor carbonate mud, organic-rich layers, true sapropels, and volcanic ash. The minor lithologies mostly occur in the upper 90 m of the succession, within the Pleistocene and the upper part of the Pliocene succession. The Pleistocene/Pliocene boundary is defined at about 80 mbsf (see "Biostratigraphy" section, this chapter). The whole unit has been extensively disturbed by drilling, in some cases to the extent of complete homogeneity. The average carbonate content increases markedly below 90 mbsf (107-654A-11R; see "Geochemistry" section, this chapter). Details of the succession from the top downward are as follows:

From the seafloor down to 12.0 mbsf (107-654A-2R) the recovery consisted only of soupy nannofossil ooze with scattered pteropod shell fragments. Several coarse-grained terrigenous and volcaniclastic layers are present from 0 to 4.6 mbsf (107-654A-2R). At 12.3 mbsf (107-654A-3R-3, 20-33 cm) volcanic ash is present, and appears again as a minor lithology from 21.4 to 30.8 mbsf (107-654A-4R). In smear slides the volcanic ash consists mostly of volcanic glass particles that are extensively replaced and overgrown by zeolites. The nannofossil ooze is extensively burrowed, as recorded by generally gray mottling attributable to the presence of iron monosulfide (hydrotroilite). Some intervals, as thick as several tens of centimeters, exhibit a diffuse orange stain that probably indicates the presence of limonite (37 mbsf; Section 107-654A-5R-5).

Beginning at 30.8 mbsf (107-654A-5R), there is the appearance of several dark colored, apparently organic-rich, layers. Of these only 3 of 17 analyses exhibit values of organic carbon >1%, and of these only one contains >2% organic carbon and is thus a true sapropel. Each of the organic-rich sediments with >1% organic carbon occurs between 44.93 and 46.45 mbsf (107-654A-4R, 133-135 cm, 1.88%; same section, 142-144 cm, 3.68%; same core Section 5, 15-17 cm, 1.35%. Most of the dark colored, apparently organic-rich, layers in Unit I are enriched in pyrite, either finely disseminated or as pyritized worm burrows (e.g., Section 107-654A-4R-4, 60 cm; 26.5 mbsf). Volcanic ashes were recognized again slightly lower in the succession (Section 107-654A-6R-5, 100-110 cm; 45.8 mbsf).

In the interval from 69.3 to 79.0 mbsf (107-654A-9R) four pieces of dark gray olivine-phyric basalt were recovered. While drilling this core, a marked decrease in the rate of penetration was noted between 71 and 73 mbsf, suggesting that the recovered few tens of centimeters of basalt came from a unit as thick as 2 m. The contact with the sediment was, however, not retrieved and there is no evidence of any alteration (e.g., baking, chemical changes) of the sediment recovered. Details of the basalt are given following the lithostratigraphic description.

Below the basalt, the very homogeneous nannofossil ooze continues with scattered planktonic foraminifers, and abundant pyrite. Pyrite is again abundant, especially so in Section 107-654A-11R-3, 67-72 cm, and in the same core section at 103-104.5 cm (99.5-100 mbsf). Individual foraminifer shells are commonly filled with pyrite. Discrete volcanic ash layers were not noted, but volcanic ash was occasionally seen in smear slides (e.g., 107-654A-14R-6 and -7; 123.5-125.5 mbsf). Downwards the alternations of more and less foraminifer-rich nannofossil ooze become more conspicuous, imparting a weak color banding (e.g., 107-654A-16R-4, 100-101 cm; 143.9 mbsf). Such foraminifer-rich zones are particularly well developed in 107-654A-

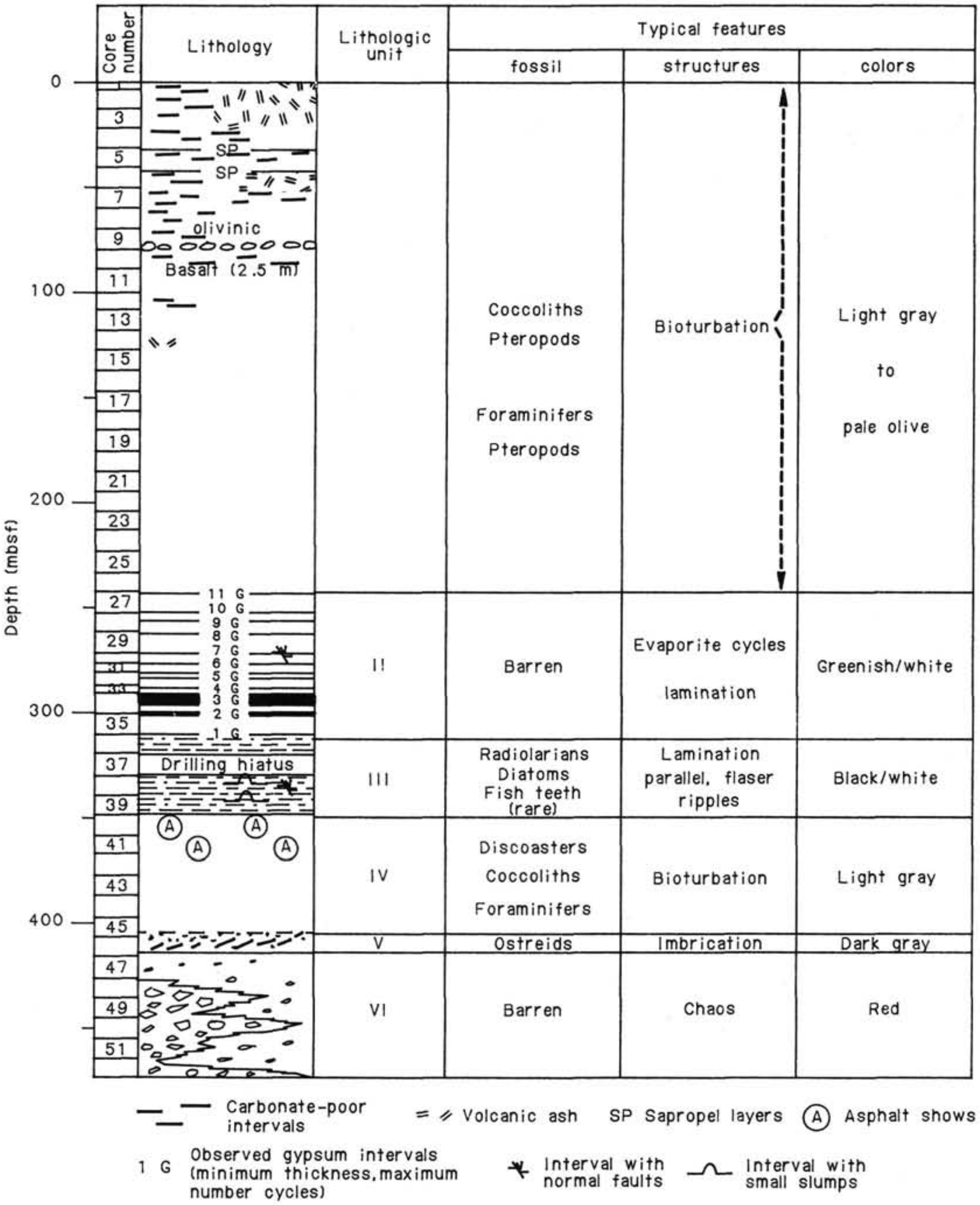

Figure 9. Summary of the lithostratigraphic succession at Site 654.

27R (242–252 mbsf) at five intervals. Burrowing becomes more intense and many burrows are pyritized (e.g., 107-654A-24R, CC, 10 cm; 222.8 mbsf).

The unit ends abruptly in 107-654A-27R-1 at 3 cm. Below this there is the first appearance of gypsum which is taken as the top of Unit II. Immediately above the base of Unit I, there is a short transitional interval (107-654-26R-4, -5, and CC; 237.2–242.0 mbsf), in which the nannofossil ooze becomes more argillaceous and exhibits a range of yellow, brown, and red colors.

Depositional Environment

Unit I of Pleistocene and Pliocene age records open marine pelagic deposition of foraminifer-bearing nannofossil ooze, which was more calcareous in the Pliocene than during the Pleistocene. During the Pleistocene, occasional layers of air-fall volcanic ash accumulated, followed by reworking and later extensive conversion to zeolites. Occasional sapropelic layers are attributable to short-lived episodes of bottom-water stagnation and/or enhanced organic-matter input during the Pleistocene. The abundance of presumed iron monosulfide and of pyritization attests to generally reducing early diagenetic conditions in the Unit I succession as a whole. Relatively constant pelagic depositional conditions persisted throughout the Pliocene. The short basal interval of brightly colored nannofossil mud immediately above the gypsum (top of Unit II, see below) possibly reflects the presence of iron-rich clays and other oxidized particles derived from the earlier Messinian landmass.

Table 1. Coring summary table for Site 654.

Core no.	Date (Feb. 1986)	Time	Sub-bottom depths (m)	Cored (m)	Recovered (m)	Recovery (%)
1R	3	1700	0.0–4.6	4.6	4.6	100.4
2R	3	1800	4.6–12.0	7.4	4.5	61.1
3R	3	1930	12.0–21.4	9.4	8.5	90.4
4R	3	2030	21.4–30.8	9.4	7.1	75.7
5R	3	2145	30.8–40.3	9.5	5.3	55.7
6R	4	0030	40.3–49.7	9.4	7.7	82.0
7R	4	0145	49.7–59.1	9.4	0.2	2.6
8R	4	0315	59.1–69.3	10.2	8.7	85.4
9R	4	0545	69.3–79.0	9.7	4.8	49.4
10R	4	0715	79.0–88.7	9.7	1.4	14.9
11R	4	0930	88.7–98.4	9.7	4.0	40.9
12R	4	1030	98.4–108.0	9.6	3.0	31.6
13R	4	1145	108.0–117.7	9.7	0.0	0.4
14R	4	1315	117.7–127.4	9.7	9.8	101.0
15R	4	1615	127.4–136.9	9.5	9.8	103.4
16R	4	1800	136.9–146.4	9.5	8.1	85.5
17R	4	1945	146.4–156.1	9.7	5.8	60.0
18R	4	2145	156.1–165.8	9.7	9.9	101.6
19R	5	0000	165.8–175.0	9.2	5.3	57.1
20R	5	0130	175.0–184.6	9.6	7.3	75.9
21R	5	0245	184.6–194.2	9.6	7.6	79.6
22R	5	0400	194.2–203.8	9.6	0.0	0.1
23R	5	0700	203.8–213.4	9.6	6.2	65.0
24R	5	0830	213.4–223.1	9.7	8.4	86.8
25R	5	1000	223.1–232.7	9.6	7.7	80.6
26R	5	1130	232.7–242.4	9.7	6.9	71.6
27R	5	1345	242.4–252.0	9.6	0.6	6.0
28R	5	1600	252.0–261.7	9.7	5.1	53.0
29R	5	1830	261.7–271.3	9.6	3.4	35.3
30R	5	2045	271.3–276.3	5.0	1.5	30.4
31R	5	2230	276.3–280.9	4.6	1.7	37.8
32R	6	0145	280.9–287.6	6.7	2.7	40.3
33R	6	0315	287.6–290.6	3.0	1.7	55.3
34R	6	0830	290.6–300.3	9.7	5.5	56.4
35R	6	1115	300.3–310.0	9.7	1.9	20.0
36R	6	1330	310.0–319.6	9.6	2.1	21.5
37R	6	1600	319.6–329.3	9.7	1.5	15.3
38R	6	1730	329.3–338.6	9.3	2.7	29.0
39R	6	1915	338.6–348.2	9.6	3.2	33.8
40R	6	2145	348.2–357.8	9.6	6.9	72.3
41R	6	2345	357.8–367.4	9.6	6.1	63.1
42R	7	0115	367.4–377.1	9.7	8.2	84.3
43R	7	0245	377.1–386.8	9.7	9.2	95.2
44R	7	0500	386.8–396.4	9.6	8.9	93.1
45R	7	0645	396.4–406.1	9.7	9.3	95.5
46R	7	0900	406.1–415.7	9.6	0.8	8.0
47R	7	1045	415.7–425.4	9.7	1.2	12.8
48R	7	1245	425.4–435.1	9.7	0.2	2.2
49R	7	1500	435.1–444.7	9.6	0.5	5.0
50R	7	1645	444.7–454.4	9.7	1.2	12.6
51R	7	1845	454.4–464.1	9.7	0.3	2.8
52R	7	2200	464.1–473.8	9.7	0.5	5.2
53R	8	0015	473.8–483.4	9.6	0.0	0.0

Unit II

Cores 107-654A-27-1, 3 cm (242.7 mbsf) to 107-654A-36R-1, 110 cm (312.6 mbsf); thickness: 69.9 m; age: Messinian.

Unit II comprises gypsiferous sediments interbedded with a heterogeneous lithological assemblage comprising clays, mudstones, sandstones, breccias, dolostone, anhydrite, and very minor nannofossil ooze.

The recovery was very variable, often poor. Soft facies were difficult to recover by rotary drilling. Soft lithologies are penetrated much faster than harder ones and thus the record of drill rate vs. time (Fig. 10) is a useful means of identifying the relative thicknesses of hard vs. softer layers, in this case the presence or absence of gypsum. The drilling rate data suggest that the hard layers identified as gypsum occur throughout Unit II, but are thickest in the middle to lower part (Cores 107-654A-32R to 654A-35R inclusive); overall, the drilling-rate data suggest that five main gypsum-rich intervals are present, separated by six other intervals composed of softer sediment.

In terms of the recovered material, a total of 11 horizons of pure balatino-type gypsum are present. These are located within the five main gypsum-rich intervals identified by the drill-rate data, separated by four intervals in which little gypsum is present (gypsum-poor intervals).

Gypsum-rich interval 1: The first occurrence of gypsum forms the top of Unit II and extends down to 107-654A-28R-1, 50 cm (253.5 mbsf). The gypsum is of fine-grained alabastrine (balatino) type, exhibiting a variety of forms of lamination. Gypsum in this interval shows the following microcycles of millimetric scale (Fig. 11): (1) laminae that typically occur between partings of greenish gray clay-rich sediment; (2) laminae separated by a greenish lamination (that may represent a surface of dissolution); and (3) laminae that coarsen upward giving rise to reverse-graded microunits, that are overlain by greenish gray clay-rich sediment. The laminae between the gypsum are often very calcareous (e.g., carbonate 52.70%; 107-654A-28R-1, 103–107 cm; 262.3 mbsf). Zeolites are locally common. Nannofossils were identified with the scanning electron microscope within a minor interval of the calcareous sediment (Fig. 12A, -B).

Gypsum-poor interval 1: This interval from 107-654A-28R-2, 0 cm, down to 107-654A-29R-2, 122 cm, is dominated by weakly consolidated gypsiferous and dolomitic mud and graded gypsiferous silts and muds. Typically, the graded muds and silts exhibit sharp, sometimes scoured bases, overlain by greenish gray calcareous siltstones and silty clays, that fine upward into weakly calcareous nearly homogeneous clays (e.g., over 80 such depositional units occur in 107-654A-28R-2, 70–120 cm; 254.2 mbsf; see Fig. 13). Other sedimentary structures in this interval include microcross-lamination, centimetric-scale asymmetrical ripples, and microflaser structures. Some individual gypsiferous laminae also comprise numerous tiny (<0.5 mm diameter), rounded detrital gypsum grains and more angular clay intraclasts.

Physical diagenesis is recorded by the presence of subvertical fractures filled with gypsiferous sand and silty sand (e.g., 107-654A-29R-1; 261.8 mbsf). The most notable chemical diagenetic feature is the presence of large (4.5 mm diameter) concretions of selenitic gypsum (107-654A-29R-2, 16 cm; see Fig. 14).

Gypsum-rich interval 2: Pure balatino-type finely laminated gypsum reappears from 107-654A-30R-1, 70 cm, and near the base of the same core at 276.1 mbsf. The sedimentary features are essentially as already described. However, in the core catcher of 107-654A-30R (276 mbsf) there is a prominent reverse-graded unit, composed of greenish gypsiferous silt, passing up through medium- and coarse-grained sandstone with numerous rip-up clasts composed of gypsum. A very well preserved normal fault was cored intact in the interval from 107-654A-30R-1, 100–122 cm (272 mbsf; see Fig.15). At this level the apparent dip of primary lamination is 34°; the dip of the fault plane is 85° and the vertical throw is 1.5 cm. A small wrench as well as normal fault motion is implied. The fault plane is irregular and cavities within it have been filled and cemented by sparry gypsum. Further analysis is given at the end of this section.

Gypsum-poor interval 2: There is a return to more heterogeneous sedimentation for a short interval of 107-654A-31R-1 down to 105 cm (276.3–277.3 mbsf). Characteristic of this interval is the occurrence of repeated normal-graded units each <5 cm thick. The graded units are composed of sand and silt that passes up into poorly calcareous silty mud, enriched in limonite. One other notable feature of this interval is the occurrence of a 10-cm-thick microbreccia containing well-rounded sand grains of possibly eolian origin (107-654A-31R-1, 95–105 cm; 277.4 mbsf).

Gypsum-rich interval 3: Downhole, the next gypsum-rich interval to be encountered was considerably thicker, beginning at

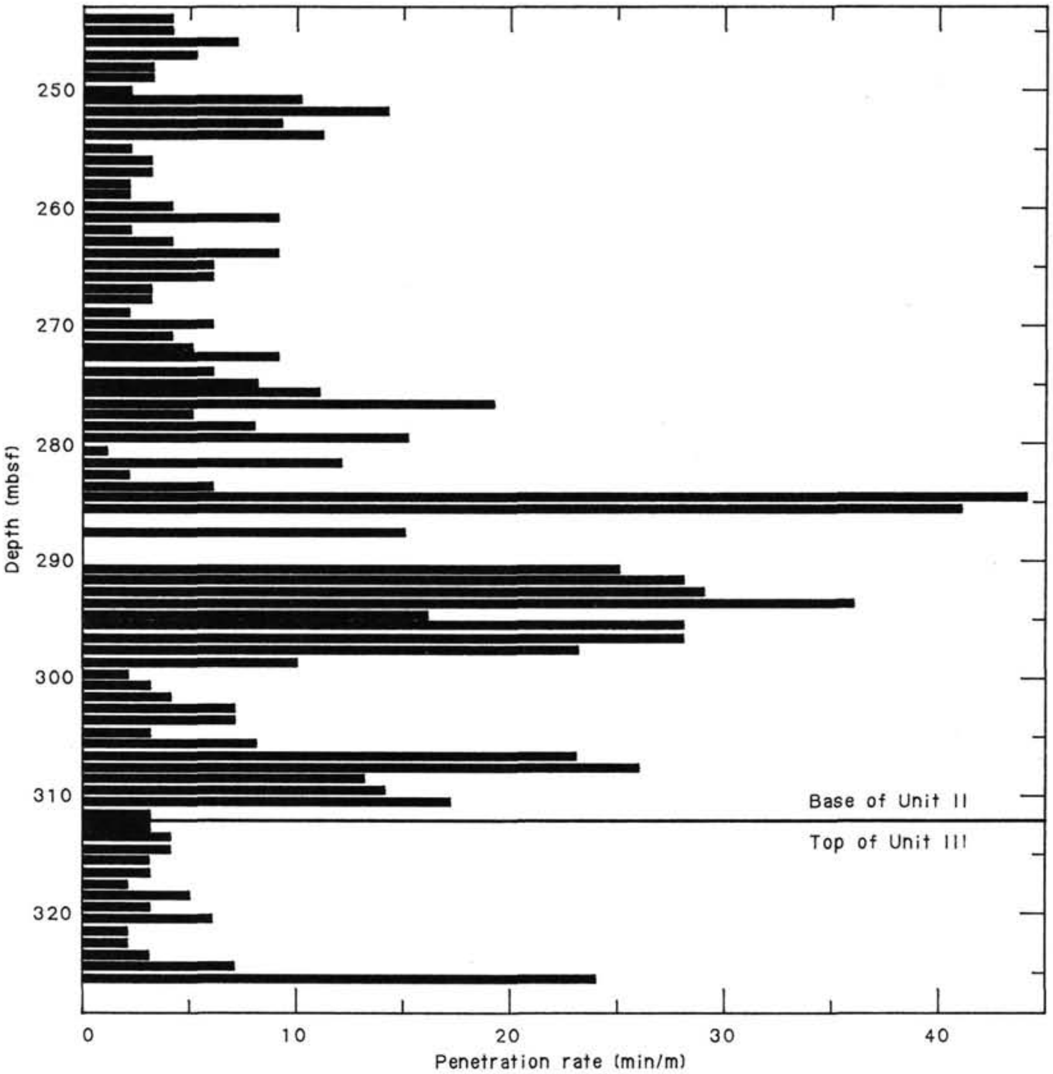

Figure 10. Graph of drilling rate vs. time. The bar chart shows the downhole progress of the drill string vs. the time needed to drill that meter of hole. The penetration rate is measured on the "Geolograph," which monitors the motion of a pulley between the travelling block and a stationary anchor. Drilling time is predominantly related to lithology, but may also be influenced by changes in rock texture, weight on the bit, or even the weather conditions. The possible error is ± 1 m per core. On this graph the longer bars are correlated with occurrences of gypsum that were more resistant to drilling.

107-654A-31R-1, 106 cm (277.3 mbsf) and extending down to the base of the recovery in the same core (107-654A-31R, CC). Additional gypsum was recovered in Sections 1 and 2 and in the core catcher of the next core (107-654A-32R). The drill rate vs. time data (Fig. 10) suggest that intercalations of softer sediment are present that were not cored. The sedimentary features of this interval are essentially as already described above.

Gypsum-poor interval 3: A further short interval of the more heterogeneous sediments occurs in 107-654A-33R-1 and in the core catcher (287.6–290.6 mbsf). Most of this interval comprises alternations of centimeter-thick well-layered dark gray calcareous muds with very fine (millimeter-scale) gypsiferous laminae. In 107-654A-33R-1, 60–75 cm, the mud units are as thick as 2–3 cm. In the same core in Section 1 from 112 to 130 cm, white marls were found to contain abundant nannofossils.

Gypsum-rich interval 4: The thickest of the recovered gypsum layers was then encountered from 107-654A-34R-1, 14 cm (290.74 mbsf) to Section 3, 85 cm in the same core (295.8 mbsf). The gypsum mostly occurs as laminae, each 0.5 to 1.0 cm thick, that are either parallel or wavy. In this horizon the laminae appear to be organized in microcycles, as in the gypsum-rich intervals described above.

Gypsum-poor interval 4: This occurs from 107-654A-34R, CC (300.1 mbsf) down to 107-654A-35R, CC (309.95 mbsf). One feature of note in this interval is the presence of poorly sorted gypsiferous/calcareous breccia with clasts that include laminated gypsum and sediment rich in zeolite, set in a fine-grained calcareous matrix. In the core catcher of 107-654A-35R (309.90 mbsf) finely laminated gypsum exhibits tiny (millimeter-scale) cracks, that could be syneresis cracks, dissolution cracks, or possibly sun-cracks, although the possibility that they were formed by drilling can not be totally ruled out.

Gypsum-rich interval 5: The last of the gypsum horizons, marking the base of Unit II, occurs in 107-654A-36R-1, 110 cm (311.1 mbsf). Although again characterized by very finely laminated balatino-type gypsum (<0.5-mm-thick laminae), this horizon is notably darker, medium to dark gray, in contrast to the pale grays and white colors of the previous gypsum intervals.

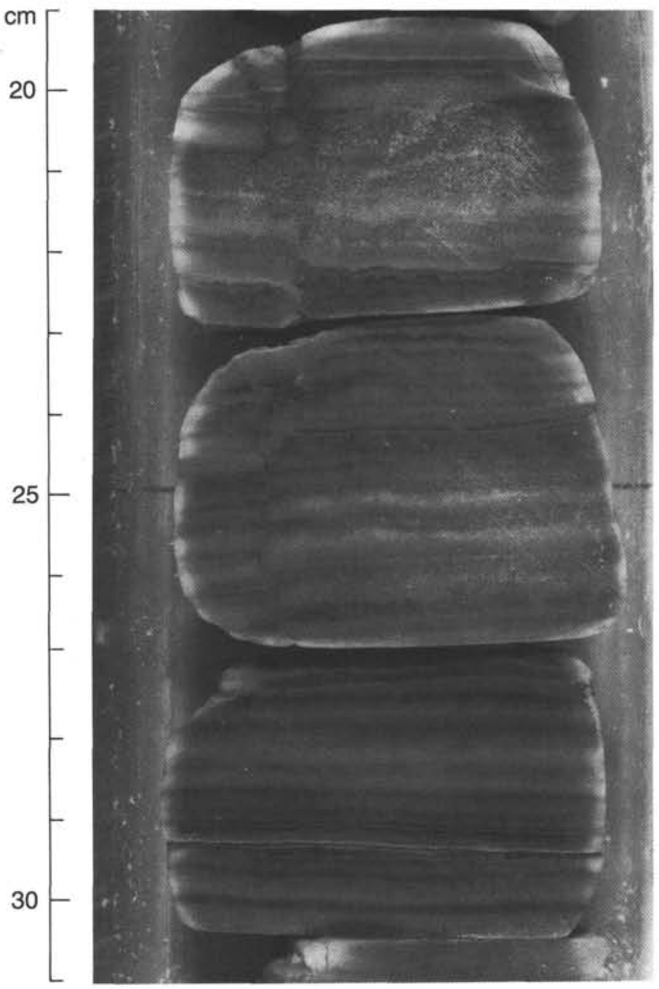

Figure 11. Finely laminated balatino-type gypsum; note the sand-filled cracks in the upper part of the photograph; see text for explanation. Close-up photograph from Core 107-654A-28R-1, 20–30 cm. From 19 to 27 cm microfaults are present in the gypsum.

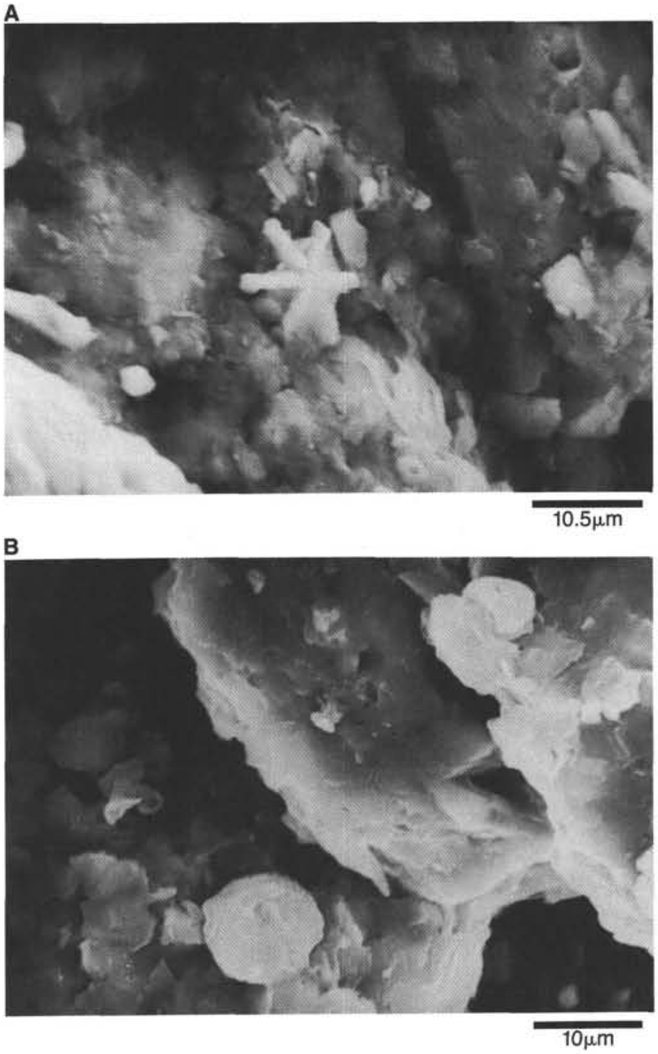

Figure 12. Scanning electron micrographs of nannofossils in greenish gray mud, from 1-mm-thick laminae located between two gypsum layers of balatino-type gypsum (Core 107-654A-27R-1, 18 cm). A. Calcareous discoaster. B. *Cyclococcolithus leptoporus* algal filaments associated with the laminated gypsum.

Depositional Environment

For convenience of description, Unit II was divided into five main intervals dominated by finely laminated balatino-type gypsum, interstratified with four other intervals that are lithologically more diverse, including gypsiferous and calcareous muds, silts, sands, and minor breccias, as well as minor dolomitic sediments and nannofossil marls. Throughout the unit, generally, there is considerable evidence of bottom-current activity, manifested in the occurrence of intraformational rip-up clasts, ripples, microcross-lamination, and small scours. The millimeter- to centimeter-scale grading, best developed in the gypsiferous and calcareous beds, is attributed to turbiditic deposition and/or resuspension effects. There is a general absence of convolute lamination, or slumps, in contrast to lower in the succession (see below) and this suggests that the seafloor was relatively tectonically stable during the deposition of Unit II.

The clastic intervals are mostly normal graded. However, the balatino-gypsum typically exhibits tiny (< a few millimeters) cycles that are reverse graded, interspersed with greenish calcareous and clay-rich seams which are in some cases anastomose. The microcycles can be tentatively interpreted in terms of episodic seafloor salinity variations: when the waters were more saline the gypsum precipitated; when the waters were less saline, partial dissolution of the gypsum gave rise to the clay-rich laminae. Planktonic foraminifers and nannofossils occur mainly in the calcareous gypsum-poor sediments. Three possibilities to explain this are: (1) the presence of balatino-type gypsum indicates desiccation, while the fossiliferous gypsum-poor sediments record marine events; (2) the Messinian sea persisted but was well stratified and the balatino gypsum precipitated from deep saline waters, while normal marine plankton continued to live in the surface waters; and (3) the marine microfauna were washed into the basin from outside. The observation that microfossils do occasionally also occur within the balatino-type gypsum suggests that (2) may be plausible.

Diagenetic changes began immediately after deposition. The alabastrine gypsum shows a tendency to undergo aggrading neomorphism. Coarse selenitic gypsum was precipitated in muds. How much of the sulfate is now gypsum, as opposed to anhydrite, must await shore-based X-ray diffraction determination. The sulfate-rich layers appear to have been lithified early in diagenesis, while the more argillaceous intervals remained softer and have undergone greater compaction. The few well-developed steep normal faults that were observed are taken to indicate post-depositional tectonic instability (see the following discussion).

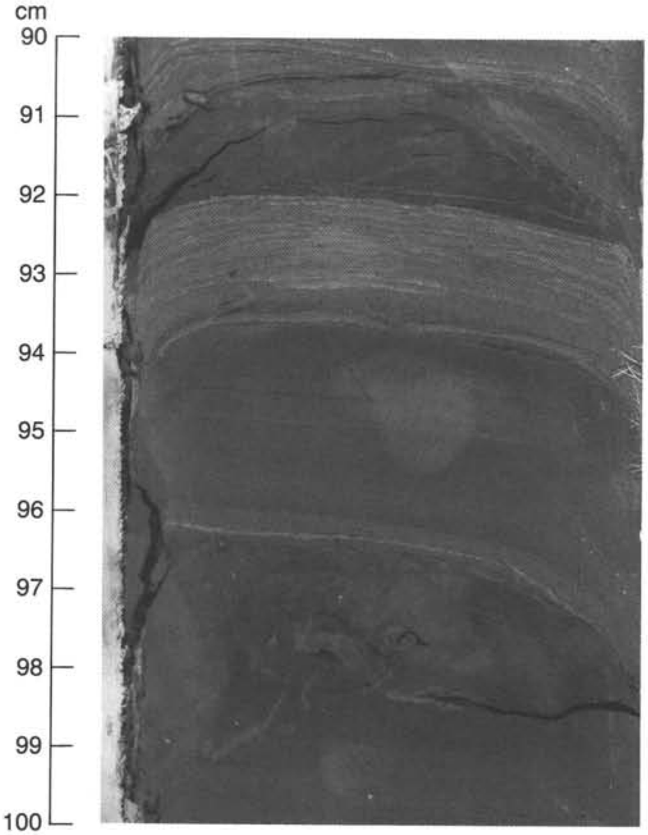

Figure 13. Normally graded calcareous silts and muds in a Messinian intra-gypsum horizon; see text for explanation. Close-up photograph from Core 107-654A-28R-3, 90–100 cm.

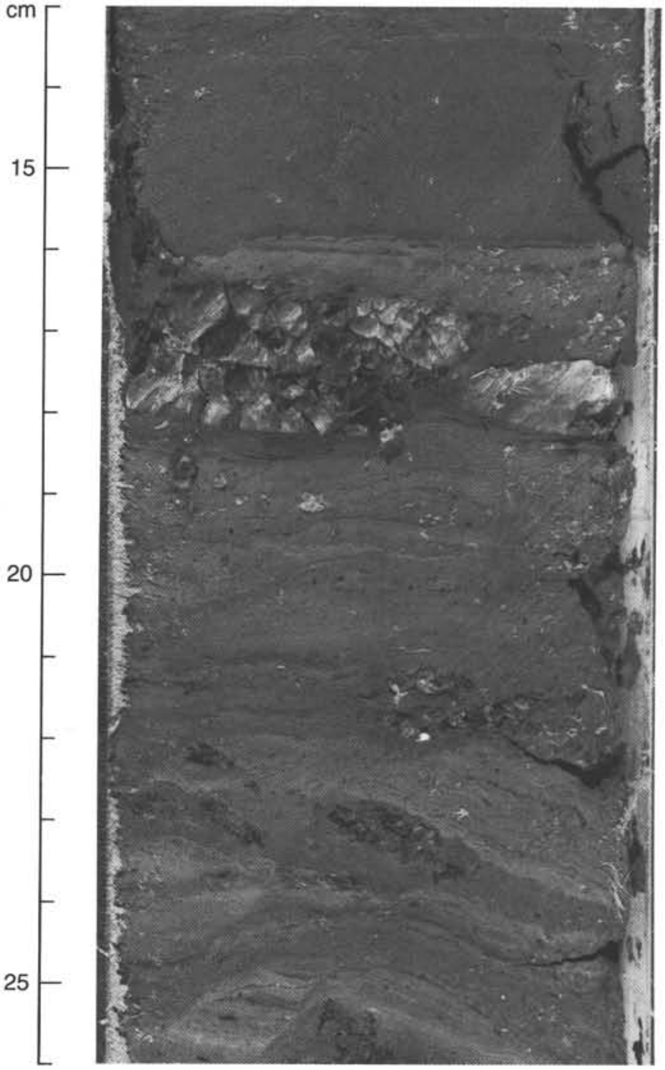

Figure 14. Large diagenetically-formed selenitic gypsum concretions within gypsiferous and calcareous mudstone. Close-up photograph from Core 107-654A-29R-2, 13–26 cm.

Unit III

Cores 107-645-36R-1, 110 cm (312.6 mbsf) to 107-654A-40R-1, 7.5 cm (348.9 mbsf); thickness: 36.3 m; age: early to middle Messinian.

Unit III begins abruptly with the first appearance of dark colored, finely laminated, fine-grained sediments which contrast sharply with the much paler gypsiferous sediments at the base of Unit II (see above). Overall, Unit III is relatively homogeneous, composed of thinly bedded and finely laminated claystone and siltstone that is alternately dolomitic and calcareous with local volcanic ash. In contrast to Unit II, which is mostly barren, Unit III contains rare radiolarians, sponge spicules, diatoms, and occasional fish teeth and fish scales. The age is presumed to be lower Messinian, based on the occurrence of this unit between Unit II that is Messinian and Unit IV that is Tortonian to early Messinian. Unit III was recovered in three cores (107-654A-36R, 654A-38R, and 654A-39R); Core 107-654A-37R comprises only drilling breccia composed of various lithologies washed down from above. Carbonate analyses performed on Unit III sediments range from 8.69% to 32.25%; values of organic carbon vary from 0.96% to 2.40% (see "Geochemistry" section, this chapter). The dominant sedimentary structures in Unit III are, first, very fine, millimetric lamination that resembles varves (Fig. 16) and, secondly, numerous thin, centimetric, graded siltstones and claystones. Other sedimentary structures include normal-grading, parallel-lamination, flaser-lamination, microcross-lamination, and small scour structures. These features are not notably different from the base of Unit II (see above), but there are, in addition, numerous millimetric-sized particles that are rounded and indicate reworking by currents (fecal pellets?). There is a distinct color banding picked out by varying hues of gray; the lighter gray lithologies are more calcareous than the darker ones (e.g., darker 107-654A-38R-1, 40 cm; 329.7 mbsf); lighter ones in the same core at 110 cm (330.4 mbsf). In a few cases dolomicrite rich in altered volcanic ash was noted together with black well-lithified concretions (107-654A-38R-1, 79–94 cm), compact layers (same core section at 60 cm) and coarse-grained intervals (same section, 70 cm, and 104–108 cm). In the next section down, thin white laminae are rich in tuff, with zeolites.

There are a number of high-angle normal faults, accompanied by low-angle normal faults (Fig. 16). Many, but probably not all, of these faults can be attributed to drilling disturbance (see further discussion at the end of this section).

Unit III culminates in an interval of dark colored laminated sediments with organic carbon values as high as 2.40% (107-654A-39R; 338.6–341.7 mbsf). A marked feature of this interval is its fine lamination and numerous intraformational rip-up clasts and thin (<20 cm) debris-flows (Fig. 17). For example, in 107-654A-39R, the interval 15–36 cm comprises rounded and stretched clasts floating in an argillaceous matrix. The fine lamination is disturbed by slump-folding and/or convolute lamina-

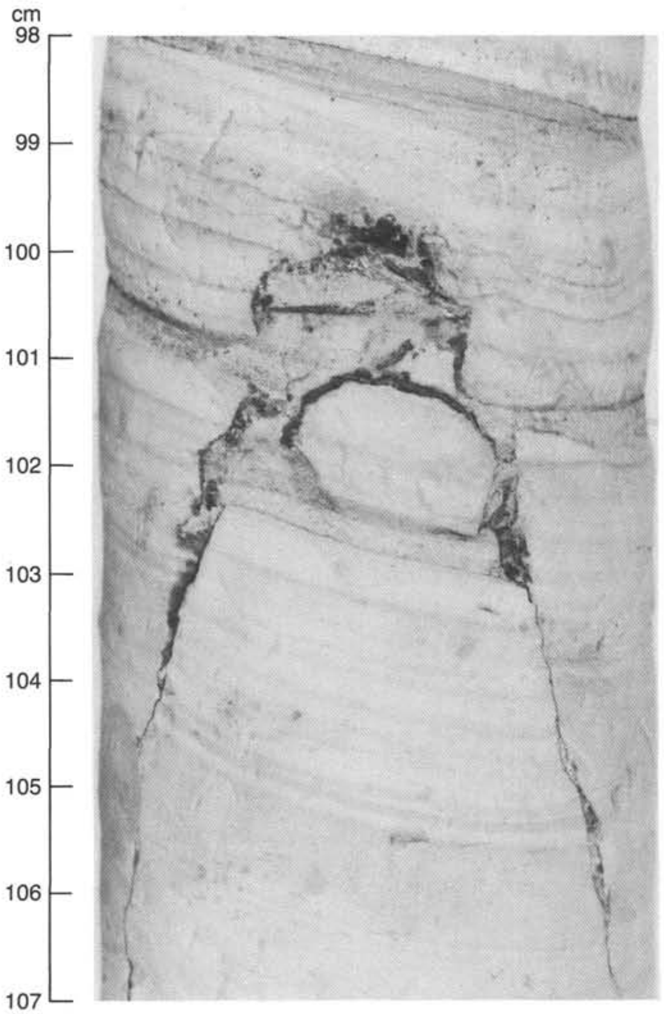

Figure 15. Normal fault with a small wrench component that was cored intact within the balatino-type gypsum; see text for explanation. Close-up photograph from Core 107-654A-30R-1, 98–107 cm.

tion. In addition, some siltstone partings in this interval are offset by moderately dipping (26°) fractures with a component of reversed motion.

Depositional Environment

In contrast to Unit II, the siliceous biogenic components and the fish remains of Unit III, although rare, indicate accumulation in open marine waters in which productivity was possibly high. A marked feature of the unit is its organic-carbon-rich nature, combined with fine lamination, abundant pyrite, and the general absence of burrowing. Together, these features indicate that the sediments were anoxic. Two alternatives are: (1) the basin was silled and the deep waters were anoxic like the modern Black Sea, or (2) the bottom waters were essentially oxic, but the input of reactive organic matter was sufficiently rapid for abundant organic matter to be buried, thus making the sediment anaerobic below the sediment-water interface (similar to the modern Gulf of California). Unit III can be considered equivalent to the Tripoli Formation, exposed in Sicily, where similar finely laminated claystones exist (Catalano et al., 1978). The Tripoli Formation, however, is rich in diatoms which are rare in Unit II.

As in Unit II, there was a continued input of muds that were probably deposited by dilute turbidity currents. By contrast, however, Unit III exhibits considerably more evidence of local sediment instability, which apparently persisted during and after deposition. The synsedimentary and structural features are consistent with tilting and faulting related to rifting during the accumulation of Unit III in lower to middle Messinian time.

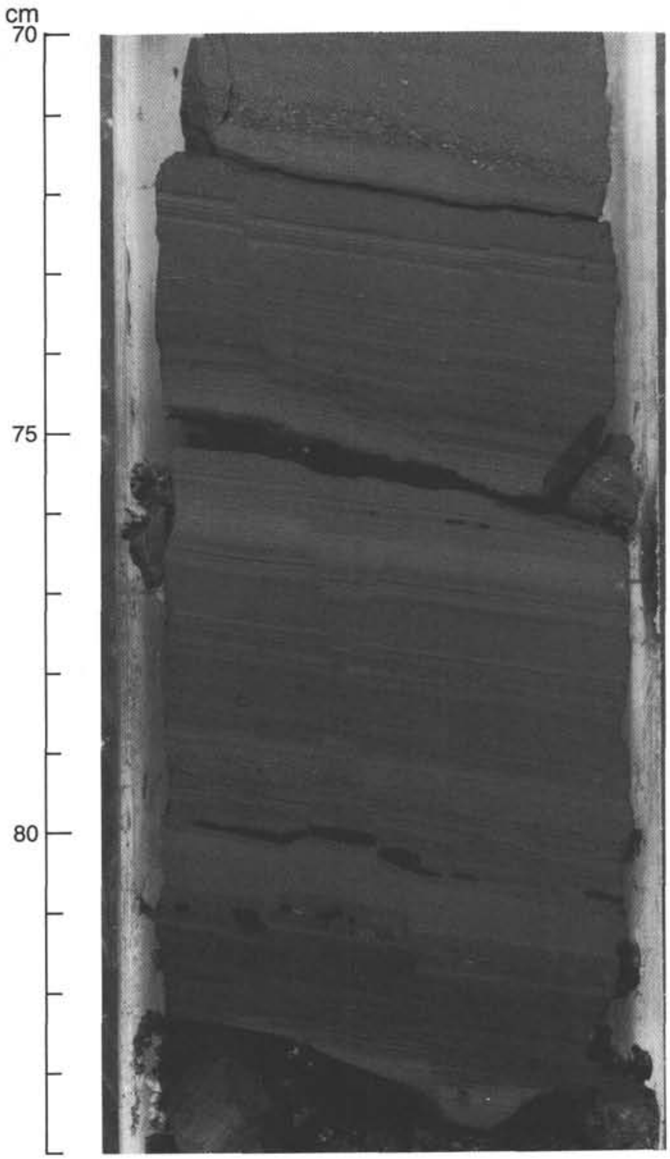

Figure 16. Varve-type laminated organic-rich mudstone typical of the inferred Messinian interval represented by lithostratigraphic Unit III. Note also the normal-graded siltstone in the upper part of the photograph. The small faults, with sigma 1 parallel to the drill string (lower part of photograph), are considered to have been formed by the drilling. Close-up photograph from Core 107-654A-38R-1, 70–84 cm.

Unit IV

Cores 107-654A-40R-1, 7.5 cm (348.9 mbsf) to 107-654A-45R-5, 145 cm (403.9 mbsf); thickness: 55.0 m; age: late Tortonian and early Messinian. Planktonic foraminifer occurrences place the Messinian-Tortonian boundary in 107-654A-42R-2, 70 cm, while, on the basis of nannofossils, this boundary is assigned to 107-654A-43R, CC.

Unit IV is homogeneous and composed almost entirely of strongly burrowed nannofossil oozes with little surviving primary depositional texture. Carbonate content ranges from 30.41% to 48.32%. The sediments recovered in the upper part

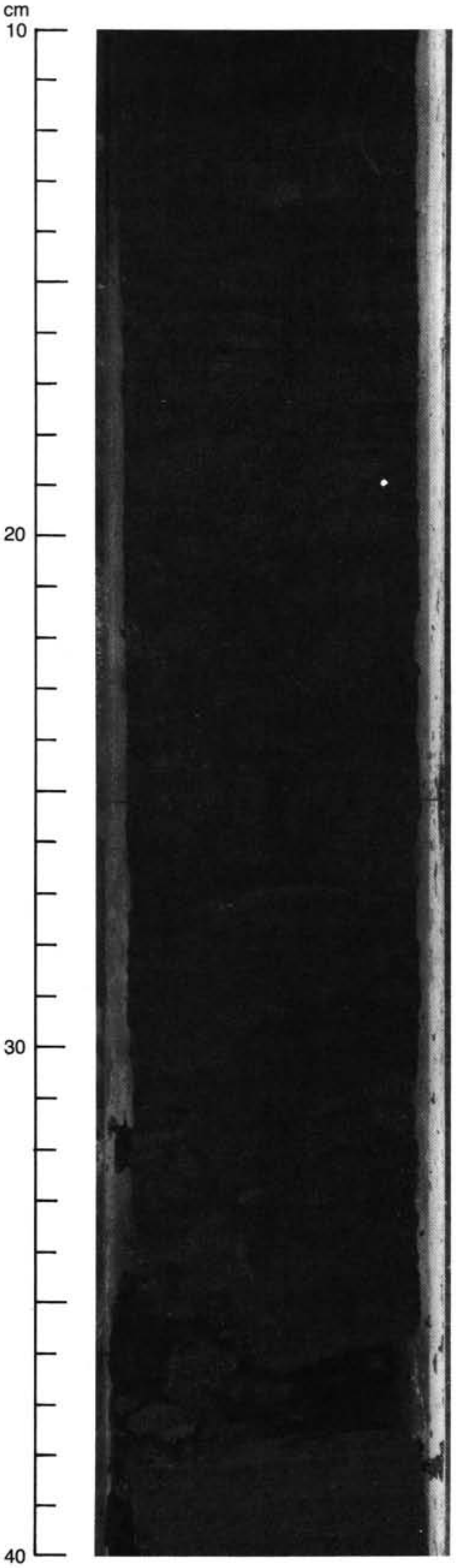

Figure 17. Debris flows typical of the inferred Messinian interval of Unit III. Marked tectonic instability apparently related to rifting took place at this time. Close-up photograph from Core 107-654A-39R-1, 10–40 cm.

of the unit (107-654A-40R and 654A-41R; 348.2–367.4 mbsf) gave off a distinct petroliferous odor when the cores were cut. Examination of the split cores under ultraviolet light indicates the presence of small quantities of asphaltine hydrocarbons, mostly concentrated in worm burrows. The asphaltines are black in normal light. The burrows in this unit include *Chondrites* type. Many of the individual worm burrows are pyritized, usually as dense masses of small (millimetric) pyrite framboids; more complete replacement by massive pyrite also occurs (e.g., 107-654A-41R-3, at 55–60, 103, and 112 cm). Planktonic foraminifers are commonly concentrated in centimetric layers (e.g., orbulinids in 107-654A-43R-4; 380.1–381.1). In many cases individual foraminifer shells are filled with pyrite.

Toward the base of Unit IV, there is an increase in silt (e.g., 107-654A-44R-2, 120 and 140 cm), marking a transition to the sediments of Unit V. The base of Unit IV comprises 5.2 m of nannofossil-rich calcareous chalk with abundant foraminifers and a few large mollusk fragments (e.g., 107-654A-45R-2, 131–138 cm). In general, these bioclasts increase in number and size downward toward the contact with Unit V. Within 105-654-45R, the abundance of the sand fraction increases markedly in Section 1 at 125 cm, and persists down to the base of the unit at Section 6, 10 cm, in the same core. The contact with the underlying unit is gradational.

Depositional Environment

Unit IV records an open marine environment during upper Tortonian and earliest Messinian time. The background sedimentation was nannofossil ooze that is similar to upper Tortonian and early Messinian lithofacies, for example, in Sicily. The intense burrowing indicates an abundance of nutrient materials in the surface sediment. Occurrences of fish teeth also tend to indicate that the seas were quite fertile. Minor oil was generated essentially *in situ*, and this also suggests fertile seas during deposition of the nannofossil oozes. Sufficient reactive organic matter found its way into the sediment to generate subsurface anoxia. This, in turn, favored the widespread, probably early diagenetic, development of pyrite framboids, particularly within foraminifer shells. The intense burrowing and the downward increase in silt and sand are quite consistent with accumulation in relatively shallow seas (i.e., several hundred meters), as also suggested by the size and diversity of the microfauna (see "Biostratigraphy" section, this chapter).

In marked contrast with Unit III, there is little evidence of sediment instability, possibly because such structures were totally destroyed by bioturbation.

In summary, Unit IV accumulated during the late Tortonian and earliest Messinian in relatively shallow, well ventilated, fertile, open marine seas that deepened through time.

Unit V

Cores 107-654A-45R-5, 145 cm, and 654A-46R, CC; 403.9–415.7 mbsf; thickness: 11.8 m; age not determined.

Unit V comprises polymictic glauconitic sandstone and marly calcareous chalk. Carbonate values of 46.0%, 31.0%, and 18.0% were recorded. Biogenic fragments are common.

Unit V commences with a 25-cm-thick interval of sandy calcareous mudstone with numerous matrix-supported gravel to small pebble-sized fragments that are mostly angular to subangular. The clasts exhibit no obvious preferred orientation. There are numerous bioclasts, mostly large foraminifers, mollusks and probable echinoderm plates that become more numerous toward the top of this interval (107-654A-45R-5, 130–150 cm). The matrix-to-large-clast ratio increases upward. Below this (Core 107-654A-46R-1) occurs sandstone which is matrix rich, poorly sorted, and contains quartz, mica, gypsum, glauconite, pyrite, and carbonates (based on limited smear slide data). Where bioclasts are numerous and large, they display a weak imbrication. The largest Ostreid shells occur in 107-654A-46R-1 at 9–12 cm. Some of the oyster shells (Fig. 18) are bored by Cliona-type sponges. Large benthic foraminifers are abundant.

Depositional Environment

Unit V comprises clastic and calcareous sediments that were laid down in a marginal, near coastal, setting. The fauna is neritic, with scarce pelagic microfossils (see "Biostratigraphy" section, this chapter). In the modern oceans glauconite forms during early diagenesis close to the sediment surface, in areas undergoing low rates of sediment accumulation, often in a local reducing environment within an oxidizing one overall. The presence of pyrite also indicates the development of at least local diagenetic anoxia.

The matrix-supported nature of the sand and gravel suggests that the sediment accumulated on a relatively quiet seafloor that either was protected (e.g., a bay), or was located below the wave base. However, the basal few centimeters of the unit do show imbrication of the shell fragments, pointing to the existence of active currents, as would be anticipated near a coastline. A plausible setting may be the subaqueous part of a coastal fan delta, as to be found today, for example, around the margins of the Red Sea.

Unit VI

Core 107-654A-47R through 107-654A-52R; 415.7–473.8 mbsf; thickness: 58.1 m; age: not determined.

Unit VI comprises gravel-bearing calcareous sandy mudstone at the top, underlain by pebbles, cobbles, gravelly mudstone, and muddy gravel. Much of this conglomerate unit is matrix-supported. The matrix sediment is reddish in contrast to the clasts, which are mostly of subdued grayish and buff color.

In the upper part of Unit VI (107-654A-47R-1), the small recovery mostly comprised reddish gravel-bearing sandy calcareous mudstone. The gravel and pebble clasts are as large as 10 mm in diameter; there is also one 3-cm-diameter dolomitic pebble at the base of the recovered Section in 107-654A-47R-1. Most of the clasts are angular to subrounded, but there are a few quartz grains that are well rounded.

Similar lithologies were again recovered in 107-654A-50R, 40–50 cm, and from 90 to 143 cm in the same core, as well as in 107-654A-52R-1, 15–50 cm. Between the three intervals (listed above) of clastic sediment, four horizons were recovered consisting only of pebbles and cobbles. Any matrix, if originally present, was washed out during drilling.

The individual pebbles and cobbles (Fig. 19) are as large as 9 cm. The larger ones tend to be subrounded, while the smaller ones are mostly subangular. Based on a binocular microscope examination of all the pebbles and examination of thin sections of six pebbles, the following lithologies were identified in decreasing abundance: recrystallized limestone, marble, quartzitic rock, and dolostone. Several of the more metamorphosed rocks contain small greenschist inclusions. Apparently primary sedimentary structures, including plane- and microcross-lamination, are visible in several of the dolostone pebbles. In addition, examination of the internal fabrics revealed the following structures: pressure solution cleavage, tension gashes, sparry calcite-filled veins, and small-scale brittle shear structures.

Depositional Environment

The red color, taken with the absence of fossils, points to a continental depositional setting for Unit VI. A probable environment is a braided alluvial fan. Few of the clasts are well rounded, suggesting only limited alluvial transport. The strongly oxidized nature of the exteriors of the individual pebbles suggests they may have been exposed to prolonged reworking after erosion, as in many modern fluvial systems. The relatively immature nature of the pebbles is most consistent with local (i.e., kilometer to several tens of kilometers) derivation, quite possibly from a nearby tilted rift-block. Such derivation is supported by the presence of an erosional unconformity that is visible on the seismic records updip on the same tilted block. The strong reddening of many of the clasts is consistent with a hot, arid to semiarid climate during the time of erosion.

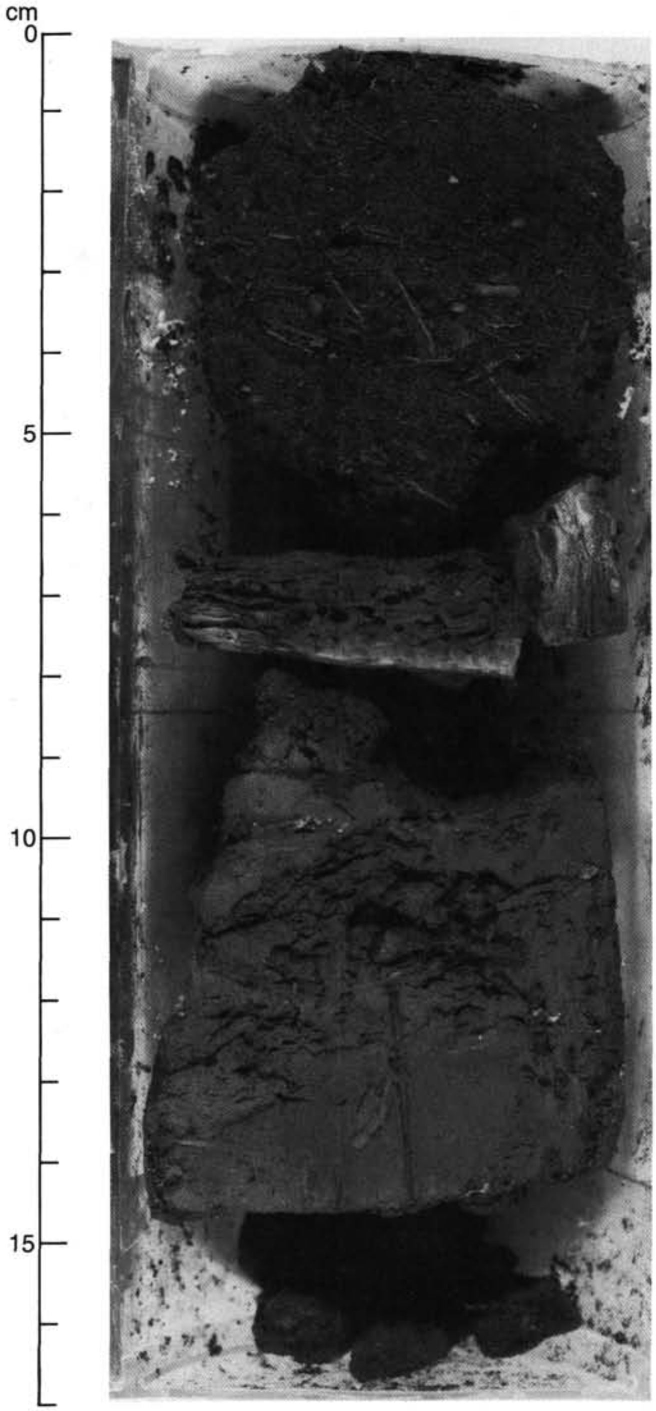

Figure 18. Broken thick-walled oyster shell (center of photograph) together with numerous small benthic foraminifer shells (upper) that are broken and imbricated by currents; near the base of Unit V. Close-up photograph from Core 107-654A-46R, CC.

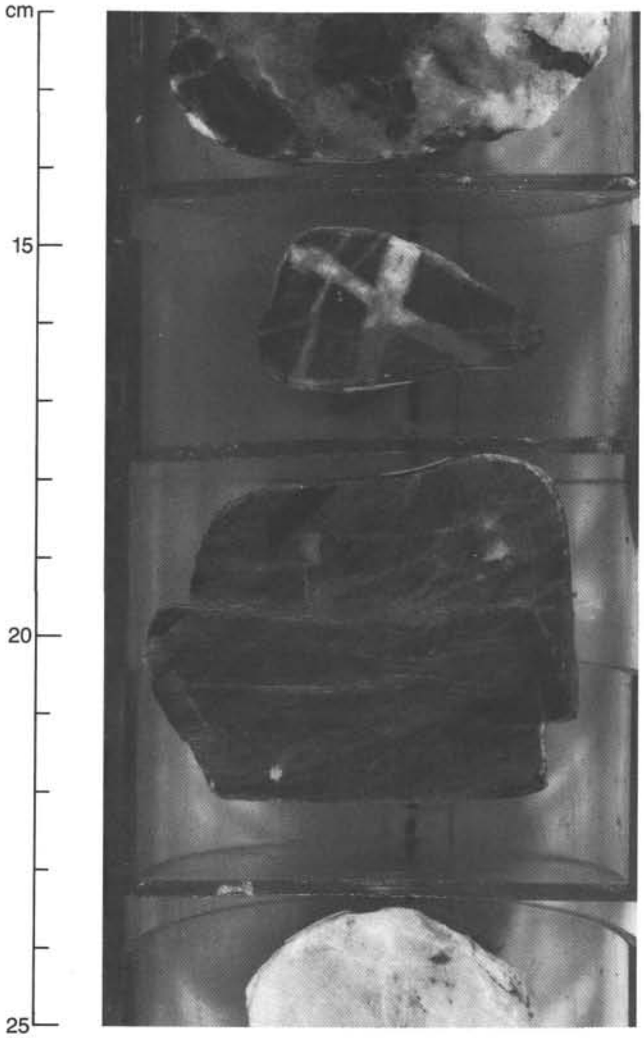

Figure 19. Pebbles from the matrix-supported conglomerate. Examples of pebbles in Unit VI. Note the subrounded and subangular shape and the presence of calcite veining within the second pebble from the top of the photograph. The pebbles comprise marble, recrystallized limestone, and quartzitic metamorphic rocks. Close-up photograph from Core 107-654A-49R-1, 12-25 cm.

The pebbles were mainly derived from carbonate and quartzose rocks. The provenance is probably a carbonate unit and its immediate basement rocks. These units underwent regional metamorphism, apparently in the greenschist facies. A few limestone samples are less metamorphosed and indicate a carbonate platform of possibly Paleozoic age (crinoidal biosparite with calcispheres and agglutinating foraminifers). Others, more recrystallized and affected by stylolite formation, are impure basinal carbonates comparable with, for example, the middle Paleozoic (Devonian) rocks of Sardinia.

Sedimentary Instability

Microfractures of tectonic origin are encountered in laminated gypsum intervals in Core 107-654A-28R-1, 17-26 cm (252.0-261.7 mbsf) and 107-654A-30R-1, 99-118 cm (271.3-276.3 mbsf).

The first example mentioned above shows several minor fracture surfaces (Fig. 11), which exhibit a Riedel pattern in lateral view and a conjugate pattern in zenithal view, but then merge into a single fracture downsection. The angle between the major fracture and the stratification is 75°, and throw is 6 mm. The Riedel pattern is inferred to be syntectonic because it forms a small grabenlike feature which is filled by sandy gypsum of the overlying layer.

The second fracture (Fig. 15) shows the angle between stratification and fracture plane to be 85°, antithetic to the dip which is 15°. The angle between the strike of the fault and the strike of the layers is 130° (Fig. 15). The vertical component of throw is 15 mm and the left-lateral component is 8 mm; this gives a pitch close to 62° for the slickensides. Small pull-apart features, which reflect irregularities on the faulted surface, are filled by sparry gypsum. If we assume that the general dip is toward west or west-northwest, as shown by the seismic profiles in the area of Site 654, the fault would be oriented between N40° and N85°, with a southeastward, or southward, downthrow and a small left-lateral component. This is consistent with a general N120° extensional pattern proposed for the Tyrrhenian area (Moussat, 1983; Moussat et al., 1985).

In addition, several minor fault planes have been observed in Cores 107-654A-38R and 654A-39R. They show a well-expressed conjugate pattern and, with the exception of those seen in Section 107-654A-39R-3, they may well have been created by the drilling. This interval is also rich in microbrecciated and slumped zones of uncertain origin.

IGNEOUS PETROLOGY

A basaltic unit was cored between 69.3 and 79.0 mbsf (Core 107-654A-9R). Though a section only about 30 cm long was recovered, drilling rate data suggest that the basalt layer is about 2 m thick. Basalt/sediment upper and lower contacts were not recovered.

The basalt is nonvesicular and aphanitic. A relatively high compressional-wave velocity was measured in a sample of the rock, i.e., 6.38 km/s. The rock is mildly altered; it has intersertal texture, with microphenocrysts of euhedral olivine and Ca-plagioclase in a groundmass with scattered skeletal plagioclase microliths and alteration products. Glass was probably present originally.

The basalt appears to have cooled rapidly; therefore, it probably represents a lava flow erupted on the seafloor rather than a sill. Given the thickness of the drilled basalt, it probably represents an *in-situ* flow from a close-by center of activity rather than an allocthonous block. If Site 654 basalt indeed represents an *in-situ* flow, its stratigraphic position within sediments of uppermost Pliocene (MPl6 foraminifer biozone; NN18 nannofossil biozone; see "Biostratigraphy" section, this chapter) places its age at about 1.7 m.y. ago. Absolute age determinations will have to confirm this evaluation.

No serious statement can be made on the petrochemical affinity of Site 654 basalt before more analytical work is carried out on the samples. Site 654 is clearly on continental crust, though probably thinned and stretched. The basalt might indicate basaltic melt injections into thinned continental crusts, as is commonly observed in rifted margins. We note that Pliocene/Pleistocene basalts with alkaline affinity are known from the Sardinian margin of the Tyrrhenian not far from the location of Site 654 (Keller, 1981), and from the Orosei region of eastern Sardinia (Marinelli, 1975).

BIOSTRATIGRAPHY

Summary

A sequence of 242.0 m of Pliocene-Pleistocene age was recovered at Site 654 overlying a series of evaporitic to open marine sediments deposited during late Tortonian-Messinian time (Core 107-654A-27R to Core 107-654A-45R-6, 243.0-406.0 mbsf). They are underlain by a few meters of glauconitic sands of unknown age. These sands are transgressive upon continental deposits made of red clay and conglomerates (Fig. 20).

A thin layer of basalt (about 2 m) was recovered intercalated in Core 107-654A-9R sediments dated as early Pleistocene.

Changes of fauna and flora assemblages throughout the Pliocene are mainly controlled by climatic events; they seem to be more distinct at Site 654 than at the previous sites.

An unconformity might exist at the Miocene/Pliocene boundary either due to nonrecovery or to a real stratigraphic gap.

The Pliocene is underlain by Messinian evaporitic to open marine sediments from 242.0 to 356.0 mbsf. The upper part of the sequence (242.0–348.0 mbsf) consists of greenish and gray clay and balatino-type gypsum. The clay of Cores 107-654A-27R to 107-654A-29R are rich in nannoplankton indicating normal marine surface water. Planktonic foraminiferal assemblages of these sediments are characterized by small *Globigerinita quinqueloba* and *Globigerinita glutinata* indicating a marine environment which is also confirmed by benthic foraminiferal assemblages. In the lower part of the sequence (Core 107-654A-30R to Core 107-654A-39R), micro- and nannofossil abundance decreases and the assemblages are of lower diversity. However, diagenesis is very strong within this interval which might have destroyed a great part of the fossils. These observations could show that marine conditions continued to exist throughout the Messinian.

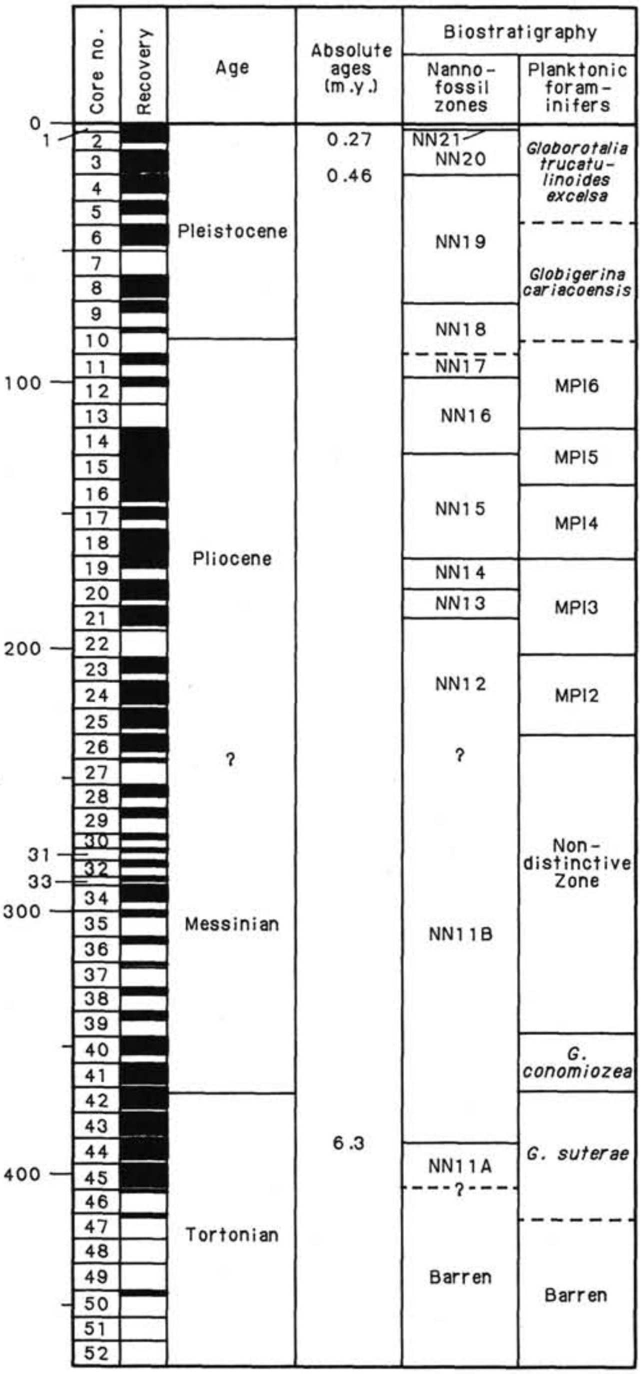

Figure 20. Summary of biostratigraphic determinations made at Site 654.

In Cores 654A-28R and 654A-29R an assemblage very rich in *Ammonia beccarii tepida* and *Cypridus* sp. was found. This represents the first sure recovery of Caspish "brackish" shallow water fossils in the Tyrrhenian deep-sea record.

The lowermost part of the Messinian and the upper Tortonian (Cores 107-654A-40R to 654A-45R) are rich in micro- and nannofossils with well-diversified assemblages. The glauconitic sands contain only few fossils which do not allow an age determination. They are transgressive upon continental deposits. The Tortonian/Messinian boundary was recognized at two slightly different levels by the two groups of fossils.

Planktonic Foraminifera

Holocene

Holocene was observed at the top of Core 107-654A-1R with the characteristic planktonic assemblage described by Cifelli (1975) from plankton tows and by Parker (1955), Todd (1958), and Thunell (1978) from surface sediments. *Globorotalia truncatulinoides excelsa* is left coiled. Pteropods are frequent. The presence of *Styliola subula* and *Hyalocylix striata* characterizes the sediments younger than 4000 years old.

Pleistocene

The Pleistocene interval was recovered from Core 107-654A-1R to about 80 mbsf. On the base of the few samples studied (only from core catchers), the base of the Pleistocene is not very clear and shore-based studies will probably revise the boundary. Two planktonic foraminiferal biozones (Ruggieri and Sprovieri, 1983; Ruggieri et al., 1984) were recognized. The *Globorotalia truncatulinoides excelsa* biozone is present from the top to about 40.3 mbsf (Sample 107-654A-5R, CC). The base of this biozone is only indicative, and further studies on all the samples are needed for a better refined recognition. The *Globigerina cariacoensis* biozone appears at 66 mbsf (107-654A-8R, 92 cm). The Pliocene/Pleistocene boundary on the base of the first peak of sinistral *Neogloboquadrina pachyderma* is between the top of 107-654A-10R-1 and the top of 107-654A-11R-1 (about 80 mbsf). Due to the poor recovery the Pliocene/Pleistocene boundary itself is recognized only in an approximate way.

If it is present, Termination I (Broecker and Van Donk, 1970) should be in Core 107-654A-1R because 107-654A-1R, CC shows a cold assemblage dominated by *Globigerina bulloides* and *Limacina retroversa* older than 18,000 years.

Pliocene

The Pliocene interval is present between about 80 mbsf and about 242 mbsf (107-654A-26R, CC), where the MPl1 biozone is present. The six foraminiferal biozones (Cita, 1975; Rio et al, 1984a) were recognized. MPl6 (*Globorotalia inflata*) biozone is present between about 80 and 119.5 mbsf (Sample 107-654A-14R-2, 32–36 cm). *Globorotalia truncatulinoides, Globorotalia tosaensis*, and *Sphaeroidinella dehiscens* are present from 92 to 98.5 mbsf (Samples 107-654A-11R-3, 32 cm, to 654A-11R, CC).

MPl5 (*Globigerinoides elongatus*) biozone is present between about 119.5 and 143.0 mbsf (Sample 107-654A-16R-3, 70-72 cm) where the last occurrence of *Sphaeroidinellopsis* spp. was detected. MPl4 was recognized between 143.0 mbsf and 166.5 mbsf (Sample 107-654A-19R-1, 70-72 cm). The MPl3 (*Globorotalia margaritae-Globorotalia puncticulata*) biozone is recognized between 166.5 mbsf and 203.8 mbsf (Sample 107-654A-22R, CC). MPl2 (*Globorotalia margaritae*) biozone is present between 203.8 and 239.4 mbsf (Sample 107-654A-26R-3, 70-72 cm) where the first *Globorotalia margaritae* was found. The MPl1 biozone (probably the top) was recognized between this level and Sample 107-654A-26R, CC. Sediment belonging to the MPl1 (*Sphaeroidinellopsis* acme) biozone should be present within Core 107-654A-27R. At the base of Core 107-654A-27R (252 mbsf), Messinian sediments (gray marls and gypsum) are present.

Messinian

Messinian sediments have been recognized between 242.4 and 369.6 mbsf (Sample 107-654A-42R-2, 70-72 cm). In the upper interval (between 252 and 338.6 mbsf; Cores 107-654A-27R through 654A-38R), a sequence with marls, clays, sands, pyrite, gypsum, and thin limestone levels has been recognized. Dwarfed planktonic foraminifers are present in core catchers of Cores 107-654A-27R to 654A-33R (352-291 mbsf) indicating "normal" marine environment (see "Benthic Foraminifers" below).

In Sample 107-654A-39R, CC (348 mbsf) pyrite is extremely abundant. In the very poor faunistic assemblage, sponge spicules, rare small gastropods, fish teeth, and rare radiolarians are present. These sediments are tentatively correlated with the Tripoli formation. From 348.2 mbsf (Sample 107-654A-40R-1) downhole, a fully marine assemblage, with abundant planktonic and benthic foraminifers is present. *Globorotalia conomiozea* is present between 107-654A-40R-3, 70-72 cm, and 654A-42R-2, 70-72 cm (351.9-369 mbsf) and therefore the *Globorotalia conomiozea* biozone (D'Onofrio et al., 1975) is recognized. By correlation with the Falconara Tortonian-Messinian boundary stratotype (D'Onofrio et al., 1975), the base of the Messinian stage is recognized at 369.6 mbsf (Sample 107-654A-42R-2, 70-72 cm).

Tortonian

The middle-upper Tortonian is recognized between 369.6 and 415.7 mbsf (Samples 107-654A-42R-2, 70-72 cm, and 654A-46R, CC). *Globorotalia miozea conoidea, Neogloboquadrina humerosa, Globorotalia merotumida, Globorotalia limbata*, and *Globorotalia suterae* are present, indicative of the *Globorotalia suterae* biozone (D'Onofrio et al., 1975) at the top of the Tortonian stage. The middle-upper Tortonian marine sequence is followed downhole by a continental sequence of unknown age.

Benthic Foraminifers

The benthic foraminiferal assemblage recovered in the Pliocene-Pleistocene interval of Site 654 is the most abundant and diversified of all the sites of Leg 107.

Benthic foraminifers occur from the top, down to 415.7 mbsf of Hole 654A. In all the samples between the top of the hole and 242.4 mbsf (Core 107-654A-26R, CC), abundant well-preserved specimens are present. The top sample of Core 107-654A-1R includes several specimens of *Articulina tubulosa, Gyroidina neosoldanii, Melonis pompilioides, Ammolagena clavata*, and *Glomospira charoides*. In the upper Pleistocene (6-40 mbsf; Cores 107-654A-1R, CC to 107-654A-5R, CC), the species number per sample is relatively low. *A. tubulosa, Cassidulina carinata, Cibicidoides kullenbergi, Parafissurina* spp., *Gyroidina neosoldanii*, and *Pyrgo depressa* are consistently found in this interval. This assemblage resembles that of the upper to middle Pleistocene sequence between 17 and 58 mbsf of Hole 652A, but differs slightly from the latter in including more various species. Displaced specimens are found in a few horizons.

In the Pliocene and lower Pleistocene (Core 107-654A-6R, CC to Core 107-654A-26R, CC), many species were found. The displaced specimens are very rare. The species diversity through the interval shows a single cycle with an increasing abundance upward in the Pliocene of Sites 652 and 653. Indeed at the very base of the Pliocene are a fairly large number of species. A maximum abundance can be found in the interval between Cores 107-654A-16R and 654A-15R (146-128 mbsf). This interval corresponds to the upper part of MPl4 Zone through the lower part of MPl5 Zone of planktonic foraminifers. The bottom level of *A. tubulosa* is found at 79 mbsf (Core 107-654A-9R, CC) in the basal part of the *Globigerina cariacoensis* Zone. In the Pliocene sequence *Cibicidoides italicus* is not present above 135.6 mbsf (Core 107-654A-15R-6, 70-72 cm) in the lower part of MPl5 Zone.

In the samples from the gypsiferous Messinian (lithostratigraphic Unit II) between 261.7 mbsf (Core 107-654A-27R, CC) and 290 mbsf (Core 107-654A-33R, CC), some specimens can be found in a few sandy layers. Many different species are recognized, but all of the specimens are broken or recrystalized, and seem to be displaced and/or reworked.

In the interval between Samples 654A-28R-4, 33-35 cm, and 654A-29R-3, 4-6 cm, quite rich assemblages with *Ammonia beccarii tepida* and *Cyprideis* sp. (with instals) are present, indicating shallow, brackish environment. In the top two sections of Core 654A-29R, few pyritized Lamellibranchia are present.

Between 357.8 mbsf (Core 107-654A-40R, CC) and 406 mbsf (Core 107-654A-45R-6; lithostratigraphic Unit IV and upper part of Unit V), many moderately- to ill-preserved specimens occurred. Species closely related to those of the Pliocene, some of which seem to be the same species, can be found in some genera such as *Cibicidoides, Gyroidina, Pullenia, Sigmoilopsis*, and *Oridorsalis*. Through the interval, *Bolivinoides miocenicus, Burseolina calabra, Cassidulina laevigata, Gyroidina altiformis, Lenticulina directa, L. spinulosa, Spiroplectammina carinata*, and *Uvigerina barbatula* (these last two species are present only in the lower part of the Tortonian sequence) are present with many other benthic foraminiferal species. In Core 107-654A-45R, CC with glauconite (406 mbsf), the specimens are very ill preserved, but their faunal association is essentially similar to the others in this interval.

In the sample at 416 mbsf (Core 107-654A-46R, CC) below the glauconitic layers, several shallow-water species are present. This fauna is characterized by low species diversity and low equitability. *Ammonia beccarii* is very abundant and is associated with lesser *Cibicides* sp., *Elphidium* sp., and *Hanzawaia* sp. Based on the compiled data of Murray (1973), such faunal association suggests an abnormal marine condition like a hyposaline lagoon. The general benthic assemblage indicates a transition from a very shallow environment just above the continental sequence and below the glauconitic interval to an epibathyal environment several hundreds of meters in depth in the uppermost part of the Tortonian sequence.

Nannoplankton

At Hole 654A, a sequence of 242.0 m of Pliocene-Pleistocene sediments was recovered overlying a series of evaporitic to open marine sediments deposited during late Tortonian-Messinian time. These overlie glauconitic sands and conglomerates of unknown age.

The Pleistocene comprises a series of 73.8 m thickness. Nannoplankton Zone NN21 (*Emiliania huxleyi* Zone) was determined from Core 107-654A-1R to Sample 107-654A-2R-3, 110 cm (0-8.70 mbsf) underlain by the *Gephyrocapsa oceanica* Zone (NN20) recognized from Sample 107-654A-2R, CC to Sample

107-654A-4R-1, 150 cm (12.0–23.0 mbsf). Nannofossils are generally abundant and well preserved. Reworked older species are few in several layers together with detrital carbonates. The small *Gephyrocapsa* sp. becomes very abundant at two horizons within Zone NN20 (Samples 107-654A-3R-1, 40 cm, and 107-654A-3R-2, 100 cm) as also observed at Site 651. *Helicosphaera* sp. (two large pores) occurs again within the lower part of the *Gephyrocapsa* Zone (Samples 107-654A-3R-4, 20 cm, to 107-654A-3R-5, 120 cm). This species has been observed also at the other sites and seems to be a good marker for the lower part of Zone NN20 at least in the Tyrrhenian Sea.

Nannoplankton Zone NN19 (*Pseudoemiliania lacunosa* Zone) is present from Sample 107-654A-4R-2, 50 cm, to 107-654A-9R-3, 30 cm (23.4–72.6 mbsf).

The acme zone of the small *Gephyrocapsa* sp. occurs from Core 107-654A-4R-4 to Core 107-654A-6R-3. Sapropel layers are present from Core 107-654A-5R-3 to Core 107-654A-6R-5, i.e., within the interval of the Jaramillo magnetic event. Further sapropel layers are concentrated around the Pliocene/Pleistocene boundary (Samples 107-654A-8R-4, 42 cm, and 107-654A-9R, CC). The last occurrence of *Helicosphaera sellii* was observed in 107-654A-8R-1, 50 cm, below the small *Gephyrocapsa* Zone. Common large specimens of *Braarudosphaera bigelowi* were found in Samples 107-654A-8R-4, 20 cm, and 107-654A-9R-2, 30 cm, just above the Pliocene/Pleistocene boundary.

The Pliocene/Pleistocene boundary was determined between Samples 107-654A-9R-3, 30 cm, and 107-654A-9R-3, 100 cm, by the extinction of *Cyclococcolithus macintyrei*. Discoasters are absent or extremely rare in Cores 107-654A-9R and 107-654A-10R. They become slightly more common from Core 107-654A-11R and abundant from Section 107-654A-14R-3.

Nannoplankton Zone NN18 (*Discoaster brouweri* Zone) of the upper Pliocene combined with Zone NN17 was encountered from Samples 107-654A-9R-3, 100 cm, to 107-654A-12R-1, 110 cm (73.3–99.5 cm). This zone is characterized by certain horizons less rich in nannoplankton but with abundant small carbonate fragments. Discoasters are absent within these layers. Marly nannofossil oozes rich in nannoplankton with rare-to-few discoasters are intercalated. These alternations are probably due to climatic fluctuations which are more pronounced within the uppermost Pliocene.

The interval from Samples 107-654A-12R-2, 30 cm, to 107-654A-14R, CC belongs to Zone NN16 (100.4–127.4 mbsf). The extinction level of *Discoaster tamalis* was observed in Sample 107-654A-14R-2, 50 cm. Discoasters are rare within the upper part of the this zone; they become common from Sample 107-654A-14R-3, 100 cm, downsection with the dominance of *Discoaster surculus* and *Discoaster brouweri*.

Zone NN15 (*Reticulofenestra pseudoumbilica* Zone) was determined from Samples 107-654A-15R-1, 50 cm, to 107-654A-19R-3, 120 cm (128.0–149.4 mbsf). The top of this zone was recognized by the last occurrence of a smaller *Reticulofenestra pseudoumbilica*. Large specimens of this species are present only from Sample 107-654A-16R-1, 50 cm. In Core 107-654A-15R-3 discoasters are common; they are of large size (*Discoaster tamalis, Discoaster surculus*). The same phenomenon was observed within the same stratigraphic interval at Hole 652A (uppermost part of NN15).

The *Discoaster asymmetricus* Zone (NN14) is present from Samples 107-654A-19R-3, 130 cm, to 107-654A-20R-3, 30 cm, (170.1–178.3 mbsf), underlain by the *Ceratolithus rugosus* Zone (NN13) from Samples 107-654A-20R-3, 120 cm, to 107-654A-21R-5, 120 cm (180.0–192.0 mbsf). This interval is characterized by the presence of *Discoaster variabilis* within the lowermost Zone NN14 and at least the upper part of Zone NN13 (Samples 107-654A-20R-3, 120 cm, to 107-654A-21R, CC) indicating a climatic deterioration. At the same time a decrease of discoasters within Core 107-654A-20R can be observed.

The interval from Samples 107-654A-21R, CC to 107-654A-26R, CC (194.2–242.4 mbsf) belongs to Zone NN12 (*Amaurolithus tricorniculatus* Zone) of the lower Pliocene. Nannofossils are common to abundant throughout the sequence. There are slight fluctuations in the abundance of discoasters. *Discoaster surculus* and *Discoaster pentaradiatus* predominate.

The Pliocene is underlain in Core 107-654A-27R by balatino-like gypsum with intercalations of greenish clay. An unconformity might exist between the Pliocene and the evaporitic sequence of the Messinian, either due to a stratigraphic gap or poor recovery. From Cores 107-654A-26R to 107-654A-36R nannofossils are present. Generally they are common, decreasing within intervals of stronger diagenesis downhole (formation of dolomite and gypsum). They are of smaller size than normal. The assemblages consist mainly of *Coccolithus pelagicus, Reticulofenestra pseudoumbilica, Helicosphaera carteri, Cyclococcolithus leptoporus, Sphenolithus abies, Cyclococcolithus rotula, Cyclococcolithus macintyrei*, and *Discolithina multipora*. *Amaurolithus delicatus* and discoasters are rare to few throughout this sequence. Discoasters are of different size and preservation indicating that a part of them is reworked from older sediments of the Miocene. At the same time there are always few reworked species from the Cretaceous and Paleogene, but they never become abundant. These observations show that at this time somewhat restricted conditions existed.

The underlying dark gray mudstones with fine laminations recovered from Cores 107-654A-37R to 107-654A-39R are barren of nannofossils. Pyrite, gypsum, and dolomite are abundant; few plant fragments were observed. There is a very distinct change between Sections 1 and 2 of Core 107-654A-40R. Downhole from 107-654A-40R-2, nannofossils become abundant, indicating an open marine environment for the lower Messinian (Zone NN11b).

The boundary between Zones NN11a and NN11b (Tortonian-Messinian) lies between Samples 107-654A-43R-5, 92 cm, and 107-654A-43R, CC (386.0 mbsf) defined by the first occurrence of *Amaurolithus primus* and *Amaurolithus delicatus* at about 6.3 m.y. The Tortonian/Messinian boundary as determined by nannoplankton lies slightly deeper than that based on planktonic foraminifers.

The upper Tortonian (Zone NN11a) was determined from Samples 107-654A-43R, CC to 107-654A-45R, CC (386.0–406.0 mbsf). The glauconitic sands are very poor in nannoplankton. Discoasters are absent due to very shallow-water conditions. Core 107-654A-46R is barren of nannoplankton. The shallow-water sediments of unknown age are transgressive upon continental deposits of red clays and conglomerates.

PALEOMAGNETISM

Two hundred two discrete 7-cm^3 samples were collected at this site. Most of the Pliocene/Pleistocene samples were analyzed on board. The Miocene samples are generally very weakly magnetized and are being studied using more sensitive magnetometers on shore. The remanent magnetization of the Pliocene/Pleistocene sediments was easily cleaned using alternating field (AF) demagnetization, the secondary overprints at this locality having low coercivity. Thermal demagnetization on shore has further improved the data quality. The primary magnetite magnetization is often isolated after demagnetization in peak fields as low as 100 Oe. From the base of Core 107-654A-15R (136.9 mbsf) downward, the undisturbed recovery is sufficiently good to allow us to interpret this magnetic stratigraphy (Table 2). Above this level, undisturbed recovery is very meager.

As at Site 652, the Miocene/Pliocene boundary is clearly within the oldest reversed interval of the Gilbert chron. This site should prove very valuable for stratigraphic correlation in the lower Pliocene.

Table 2. Preliminary determination of magnetozone boundaries for Site 654. The samples which bracket the magnetozone boundaries are given.

Magnetozone boundary	Core	Section	Interval	Depth (mbsf)
Top of Kaena	between 15R	7	46–48	136.87
	and 15R	7	55–57	136.96
Base of Kaena	between 15R	7	55–57	136.96
	and 16R	3	128–130	141.19
Top of Mammoth	between 16R	4	41–43	141.82
	and 16R	4	64–66	142.23
Base of Mammoth	between 16R	5	142–144	144.33
	and 16R	6	3–5	144.44
Top of Gilbert	between 17R	4	68–70	151.59
	and 18R	5	20–22	162.31
Top of Cochiti	between 19R	4	63–65	170.94
	and 20R	3	99–101	179.00
Base of Cochiti	between 20R	5	96–98	181.97
	and 20R	5	102–104	182.03
Top of Nunivak	between 21R	1	24–26	184.85
	and 21R	1	47–49	185.08
Base of Nunivak	between 21R	2	45–47	186.56
	and 21R	2	75–77	186.86
Top of Sidufjall (C_1)	between 23R	5	5–7	209.86
	and 23R	CC	11–13	211.42
Base of Sidufjall (C_1)	between 24R	5	112–114	220.53
	and 24R	5	137–139	220.78
Top of Thvera (C_2)	between 24R	6	48–50	221.39
	and 25R	4	123–125	228.84
Base of Thvera	between 26R	4	132–134	238.53
	and 26R	5	6–8	238.77
Below 654A-26R-5, 6–8 cm	No data			

PHYSICAL PROPERTIES

Introduction

Coring Site 654 on the northern Sardinian margin sampled a 473.6-m sedimentary sequence, ranging from Recent to at least upper Tortonian. Routine physical properties measured on the sediments included porosity, bulk density, shear strength, thermal conductivity, and compressional-wave velocity.

The methods of analysis are described in the "Explanatory Notes" chapter, this volume.

Results

Index Properties and Compressional Velocity

Grain density, porosity, bulk density, and compressional velocity are plotted relative to sub-bottom depth in Figures 21 and 22 and are listed in Tables 3 and 4.

The grain density appears heterogeneous and a careful study of such data has to be conducted later.

The bulk density values are in good agreement with the porosity values and reflect the same trend changes along the cores. In a first approach, four main physical property units can be distinguished in Hole 654:

1. Unit 1: From the seafloor to about 78 mbsf porosity values decrease from 76% to 59%, and bulk density values increase from 1.53 g/cm^3 at the mud line to about 1.85 g/cm^3. This unit ends with basalt which has a high bulk density (3.00 g/cm^3) and a low porosity (5%).
2. Unit 2: From 79 to about 240 mbsf with a constant porosity and bulk density: 55%–60% and 1.80–1.90 g/cm^3, respectively.
3. Unit 3: From 240 to 339 mbsf, this unit is characterized by variability of bulk density and porosity. In this interval, the porosity curve shows two trends: between 240–292 mbsf porosity decreases from 45% to 33% but between 292–339 mbsf, porosity increases from 33% to 57%. In the same interval (240–339 mbsf), the bulk density curve presents an alternation of high (2.45–2.50 g/cm^3) and low (2.05–2.10 g/cm^3) values corresponding to the alternation of gypsum and marly layers, respectively.
4. Unit 4: From about 339 to 405 mbsf this unit is characterized by well-marked porosity and bulk density trends. The porosity values range from about 50% at 341 mbsf to 35% at 405 mbsf. The bulk density increases from 2.05 to 2.29 g/cm^3.

The compressional-wave velocity plot (Fig. 21) shows also four main trends:

1. Unit 1: From the seafloor to about 240 mbsf the velocities measured on samples are very homogeneous and range from 1.54 km/s at the mud line to 1.679 km/s at 240 mbsf. The monotony of this unit is interrupted at 79 mbsf by a high-velocity measurement (6.38 km/s) related to the basalt interval.
2. Unit 2: This unit was sampled between 240 and 330 mbsf and is characterized by an alternation of high (3.80–5.44 km/s) and low (1.70–1.90 km/s) values, corresponding to the gypsum and marly layers respectively.
3. Unit 3: This unit (330–397 mbsf) contrasts with Unit 2 by its homogeneity. The velocity ranges between 1.69 and 1.88 km/s.
4. Unit 4. This unit is dominated by the pebbles lying between 397 mbsf and the bottom of the hole. The high-velocity measurements (5.51–6.25 km/s) were obtained in the pebbles (average of 5.878 km/s); the low values (average of 2.098 km/s) are linked to the red matrix of the pebbles.

Shear Strength Measurements

Measurements were made between the seafloor and 264.8 mbsf (Fig. 23 and Table 5). As a first approach, the following points can be established:

1. Shear strength increases from 5.69 kPa at 8 mbsf to 32.28 kPa at 73 mbsf.
2. From the basalt (at 74 mbsf) to 100 mbsf the shear strength remains low (13–15 kPa). Such data can be related either to a geological phenomenon or more probably drilling disturbances.
3. Below 100 mbsf, the shear strength increases to 130 kPa at 239 mbsf. This main trend interrupted by high and low values; the high values (175 kPa at 210–220 mbsf) are related to pyritic layers and the low values (38.5 kPa at 146 mbsf and 62.6 kPa at 189 mbsf) may be related to drilling disturbances.

Thermal Conductivity

Thermal conductivity test results are plotted on Figure 23 and listed in Table 6. Extensive discussion of these data appears in the "Downhole Measurements" section, this chapter.

Correlation with Lithology Results

The physical properties analysis at Site 654 correlates with the main lithologic units and their boundaries as follows:

1. Lithologic Unit 1, from 0 to 242.7 mbsf (see "Lithostratigraphy" section, this chapter), is characterized by well-defined velocity, bulk density, and porosity trends. The base of this unit also corresponds to the Miocene-Pliocene boundary, which is indicated by a change of porosity, density, and velocity. According to the physical property results, this lithologic unit can be divided into two subunits. From the seafloor to the basalt layer at 79 mbsf the interval is characterized by volcanic ash, sapro-

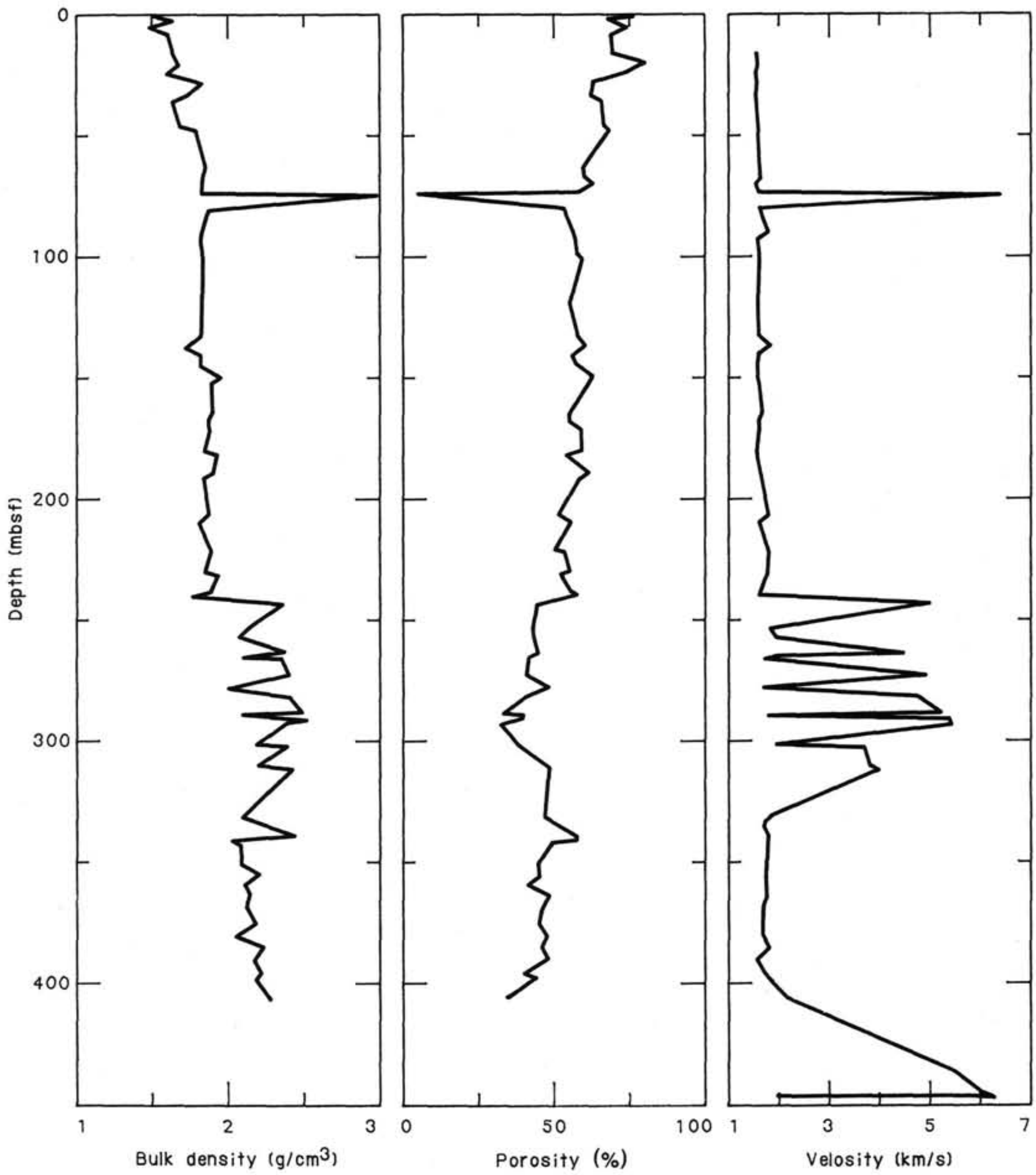

Figure 21. Bulk density, porosity, and velocity vs. depth at Site 654.

pels, and low carbonate content materials that give well-defined porosity and bulk density trends. Lower in the hole, the lithologic Unit I is homogeneous; the physical properties reflect this homogeneity.

2. Lithologic Unit II, between 242.7 and 312.6 mbsf, correlates with the physical-property measurements. The alteration of lithology (gypsum and marly deposits) appears on the bulk density, porosity, and velocity curves.

3. Lithologic Units III and IV, from 312.6 to 403.9 mbsf cannot be separated by the physical properties. The velocity is constant throughout the two units and the porosity and bulk density values are on the same trends.

4. Only one good measurement is available in lithologic Unit V (403.9–415.7 mbsf). Even so, a clear increase of velocity and bulk density (with a decrease of porosity) was noted.

5. Only velocity was measured on lithologic Unit VI. The data show high velocity related to the pebbles. The reddish matrix has an average velocity (2.098 km/s) which can be compared with that of the unconsolidated Tortonian sediments of lithologic Unit IV.

Correlation with the Seismic Reflection Data

It is interesting to compare the velocities computed from the site survey seismic data with the velocities measured on the cores:

1. The average measured compressional velocity between the mud line and 240 mbsf (deleting the measurement done on the basalt sample) is 1.625 km/s. This measurement is only 0.044 km/s higher than the 1.581 km/s velocity computed from the seismic line for Seismic Unit 1. The basalt was found at 79 mbsf; the average measured velocity above the basalt is 1.563 km/s; any reflector linked to this basalt should appear around 0.095 s below the sea floor.

2. The velocities measured between 240 and 330 mbsf have an average of 3.514 km/s. This average must be corrected: ten measurements were done on gypsum and seven come from marly samples. The recovery in this interval was poor and does not represent the real percentage of each lithologic facies comprising the unit.

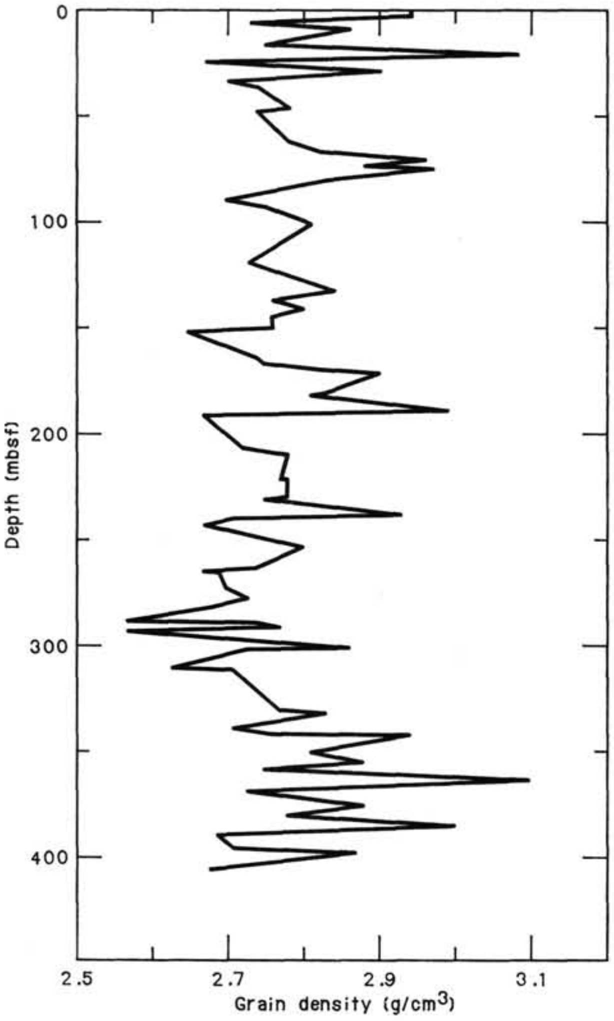

Figure 22. Grain density vs. depth at Site 654.

According to the rate of penetration during drilling (Fig. 10), this 90-m-thick layer is composed of 26 m of gypsum (29% of the unit) and 64 m of marly sediments (71% of the unit). The average velocity of the gypsum samples is 4.686 km/s, and the average velocity of the interbedded marly sediments is 1.840 km/s. From these data we compute an average velocity of 2.66 km/s for the interval 240–330 mbsf. As a consequence, this interval has a thickness of 0.067 s on the seismic line and corresponds probably to only the top of Seismic Unit 2. This thin seismic layer was not detected on the MCS velocity computation.

3. The sediments drilled between 330 and 404 mbsf have an average velocity of 1.769 km/s. The top of this interval (330 mbsf) does not correlate well with the boundary between the lithostratigraphic Units III and IV but was well documented by the physical properties. According to our computation, the thickness of this interval is 0.079 s. As a conclusion, the 0.053 s which constitutes the lower part of Seismic Unit 2 corresponds only to the drilled interval 330–377 mbsf. The lower part of the lithostratigraphic Unit IV (377–404 mbsf) constitutes the top of Seismic Unit 3.

4. The deeper lithologic unit (404–473.8 mbsf) was poorly recovered and is probably made of continental deposits. The pebbles recovered are not necessarily representative of the main lithology, and thus the velocities measured do not represent the *in-situ* velocity of these continental facies.

Table 3. Physical properties index.

Core section	Interval or piece no.	Depth sub-bottom (m)	Bulk density (g/cm^3)	Porosity (%)	Grain density (g/cm^3)
1R-1	67–70	0.68	1.53	76.S	2.94
1R-2	69–71	2.20	1.65	68.8	2.94
2R-1	73–76	5.35	1.49	74.4	2.73
2R-3	64–67	8.25	1.60	69.8	2.86
3R-3	60–63	15.62	1.65	70.5	2.75
3R-6	46–49	19.92	1.68	79.9	3.08
4R-2	78–81	23.70	1.60	74.5	2.67
4R-5	53–55	27.95	1.82	64.0	2.90
5R-2	54–57	32.85	1.74	63.4	2.70
5R-4	24–27	35.55	1.65	66.6	2.74
6R-4	79–82	45.60	1.69	67.6	2.78
6R-5	78–81	47.10	1.79	69.6	2.74
8R-2	100–103	61.62	1.85	60.3	2.78
8R-5	77–80	65.88	1.83	61.1	2.82
9R-1	60–63	69.91	1.83	63.4	2.96
9R-3	60–63	72.91	1.81	59.0	2.88
9R-CC	10–13	78.80	2.90	0.5	3.00
10R-1	78–80	79.79	1.88	54.0	2.83
11R-1	78–80	89.49	1.81	57.0	2.70
11R-3	76–80	92.48	1.81	57.7	2.75
12R-1	53–55	98.94	1.83	58.5	2.80
12R-2	53–55	100.44	1.83	60.0	2.81
14R-1	100–103	118.72	1.83	56.2	2.73
15R-4	17–20	131.99	1.82	59.0	2.84
15R-7	27–30	136.59	1.74	61.1	2.76
16R-3	39–42	140.20	1.82	56.8	2.80
16R-6	18–21	144.50	1.81	57.9	2.76
17R-2	117–120	149.50	1.96	63.7	2.76
17R-4	52–53	151.52	1.91	62.6	2.65
18R-5	146–149	163.60	1.90	55.9	2.74
18R-7	49–52	166.00	1.87	55.7	2.75
19R-3	22–23	169.04	1.87	56.5	2.82
19R-4	54–57	170.85	1.88	59.3	2.90
20R-4	47–50	179.98	1.85	60.0	2.83
20R-5	18–21	181.20	1.93	54.9	2.81
21R-3	80–82	188.41	1.91	62.0	2.99
21R-5	20–22	190.81	1.85	59.2	2.67
23R-2	73–76	206.05	1.89	52.1	2.72
23R-4	73–76	209.05	1.80	56.0	2.78
24R-5	132–135	220.74	1.91	51.4	2.77
24R-6	56–59	221.60	1.89	53.2	2.78
25R-5	42–45	229.54	1.85	56.2	2.78
25R-5	135–138	230.47	1.94	52.9	2.75
26R-4	60–64	237.82	1.90	56.1	2.93
26R-5	60–64	239.32	1.77	57.7	2.71
27R-1	44–46	242.84	2.37	44.6	2.67
28R-1	103–107	253.03	2.15	43.6	2.80
28R-3	145–149	256.45	2.09	44.2	2.78
29R-1	139–142	263.10	2.39	45.5	2.74
29R-2	114–117	264.35	2.12	44.4	2.67
29R-3	14–17	264.85			
30R-1	78–80	272.09	2.43	41.7	2.70
31R-1	90–93	277.22	2.01	48.7	2.73
32R-1	52–54	281.43	2.42	41.0	2.68
33R-1	61–64	288.23	2.52	33.6	2.57
33R-1	126–129	288.88	2.10	40.6	2.74
34R-1	44–46	291.05	2.52	40.6	2.77
34R-2	63–65	292.74	2.40	33.0	2.57
35R-1	88–92	301.20	2.20	39.2	2.86
35R-1	139–143	301.72	2.42	39.6	2.73
36R-1	30–32	310.31	2.21	49.1	2.63
36R-1	120–122	311.21	2.45	48.1	2.71
38R-1	113–115	330.43	2.11	46.3	2.77
38R-C	8–10	331.89	2.10	47.1	2.83
39R-1	39–42	338.99	2.47	57.7	2.71
39R-2	144–150	341.54	2.05	57.7	2.76
39R-C	3–5	341.63	2.09	50.0	2.94
40R-2	60–63	350.30	2.11	45.2	2.81
40R-5	65–67	354.85	2.22	45.4	2.88
41R-1	70–73	358.50	2.13	42.2	2.75
41R-4	69–72	362.99	2.16	48.2	3.10
42R-1	69–72	368.09	2.14	46.2	2.73
42R-6	21–24	375.11	2.21	44.9	2.88
43R-2	107–110	379.68	2.08	47.6	2.78
43R-5	130–133	384.42	2.24	46.7	3.00
44R-2	109–112	389.40	2.19	48.5	2.69
44R-6	98–100	395.29	2.23	40.4	2.71
45R-1	80–82	397.21	2.19	44.5	2.87
45R-7	6–8	405.46	2.29	35.4	2.68

Table 4. Compressional velocity.

Core section	Interval (cm)	Depth sub-bottom (m)	Compressional velocity (km/s)
3R-3	60–63	15.62	1.540
3R-6	46–49	19.92	1.554
4R-2	78–81	23.70	1.526
4R-5	53–55	27.95	1.584
5R-2	54–57	32.85	1.548
5R-4	24–27	35.55	1.534
6R-5	78–81	47.10	1.569
8R-2	100–103	61.62	1.592
8R-5	77–80	65.88	1.621
9R-1	60–63	69.91	1.538
9R-3	60–63	72.91	1.584
9R-C	17–19	74.00	6.378
10R-1	78–80	79.79	1.591
11R-1	78–80	89.49	1.756
11R-3	76–80	92.48	1.583
12R-1	53–55	98.94	1.611
12R-2	53–55	100.44	1.598
14R-1	100–103	118.72	1.595
15R-4	17–20	131.99	1.591
15R-7	27–30	136.59	1.769
16R-3	39–42	140.20	1.594
16R-6	18–21	144.50	1.573
17R-2	117–120	149.50	1.567
17R-4	53–56	151.55	1.607
18R-5	146–149	163.60	1.642
18R-7	49–52	166.00	1.627
19R-3	23–26	169.05	1.633
19R-4	54–57	170.85	1.615
20R-5	18–21	181.20	1.560
20R-4	47–50	179.98	1.604
21R-3	80–82	188.41	1.630
21R-5	20–22	190.81	1.633
23R-2	73–75	206.05	1.771
23R-4	73–76	209.05	1.622
24R-5	132–135	220.74	1.789
24R-6	56–59	221.60	1.758
25R-5	42–45	229.54	1.763
25R-5	135–138	230.47	1.758
26R-4	60–64	237.82	1.652
26R-5	60–64	239.32	1.679
27R-1	44–46	242.84	5.052
28R-1	103–107	253.03	1.827
28R-3	145–149	256.45	1.948
29R-1	139–142	263.10	4.420
29R-2	114–117	264.35	1.703
29R-3	14–17	264.85	1.948
30R-1	78–80	272.09	4.892
31R-1	90–93	277.22	1.718
32R-1	52–54	281.43	4.749
33R-1	61–64	288.23	5.280
33R-1	126–129	288.88	1.770
34R-1	44–46	291.05	5.440
34R-2	63–65	292.74	5.460
35R-1	88–92	301.20	1.966
35R-1	139–143	301.72	3.731
36R-1	30–32	310.31	3.842
36R-1	120–122	311.21	3.998
38R-1	113–115	330.43	1.884
38R-C	8–10	331.89	1.813
39R-1	39–42	338.99	1.824
39R-C	3–5	334.63	1.728
40R-2	60–63	350.30	1.796
40R-5	65–68	354.85	1.757
41R-1	70–73	358.50	1.762
41R-4	69–72	362.99	1.796
42R-1	69–72	368.09	1.719
42R-6	21–24	375.11	1.717
43R-2	107–110	379.68	1.698
43R-5	130–133	384.42	1.840
44R-2	109–112	389.40	1.615
44R-6	96–99	395.29	1.756
45R-1	80–82	397.21	1.827
45R-7	6–8	405.47	2.247
49R-C	no. 2	435.40	5.514
50R-1	no. 1	444.70	6.034
50R-1	no. 12	445.50	5.712
50R-1	93–96	445.65	2.080
50R-1	118–120	445.90	1.967
50R-1	no. 14	446.00	6.254

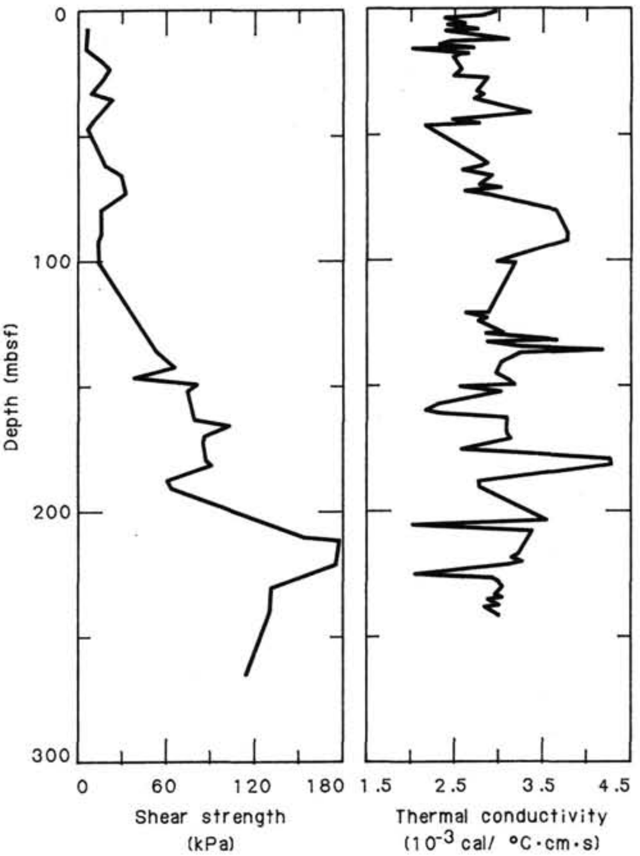

Figure 23. Thermal conductivity and shear strength vs. depth at Site 654.

Conclusion

The physical property measurements at Site 654 show a set of trends and units which are in good agreement with the lithology and which differ slightly from the acoustic stratigraphy.

INORGANIC GEOCHEMISTRY

Carbonate Analyses

Determinations of calcium carbonate content in numerous samples of Hole 654 yielded the following results.

The Pleistocene sequence drilled at this site displays significant fluctuations of $CaCO_3$ concentrations around a mean value of 33.5 weight % $CaCO_3$ with a standard deviation (1σ) of $\pm 11.7\%$. The shape of the depth plot of $CaCO_3$ (Fig. 24) reveals the sawtooth pattern typical for this interval. A gradual downhole increase in $CaCO_3$ from low Pleistocene values to high, fairly uniform middle Pliocene values probably reflects a phase of climatic deterioration in the upper Pliocene.

The middle Pliocene sediments of Hole 654 average 52.3% ($\pm 9.3\%$) $CaCO_3$, a value similar to those encountered in coeval sediments of Sites 650 to 653. The transition from Pliocene open marine to Messinian facies is less marked in terms of $CaCO_3$ abundance than in other sites, e.g., Site 652. Messinian sediments of Site 654 have a mean carbonate content of 32.9%, but vary widely, as expressed in a high standard deviation of $\pm$ 14.6%.

Marine sediments of Tortonian age cluster around a mean value of 38.7% $CaCO_3$ and display moderate variation ($1\sigma = \pm$ 9.3%). Results of $CaCO_3$ determinations are appended in Table 7.

Table 5. Shear strength measurements.

Core section	Interval (cm)	Depth sub-bottom (m)	Shear strength (kPa)
2R-3	66	8.26	5.6896
3R-3	61	15.61	4.4667
3R-6	45	19.45	14.4154
4R-2	76	23.66	20.5063
4R-5	56	27.96	16.8517
5R-2	53	32.83	9.3395
5R-4	28	35.58	22.9427
6R-4	83	45.63	7.5122
6R-5	82	47.12	5.0758
8R-2	105	61.65	18.6790
8R-5	81	65.91	29.2364
9R-3	84	73.14	32.2822
10R-1	82	79.82	15.2274
11R-1	74	89.44	15.0244
11R-3	73	92.43	13.1971
12R-2	83	100.73	14.2123
15R-7	24	136.45	53.8036
16R-4	82	142.12	65.5649
16R-C	10	146.30	38.5762
17R-2	119	149.10	79.4064
17R-4	47	151.47	73.5784
18R-5	158	163.68	77.9494
18R-7	47	165.57	103.4470
19R-3	123	170.03	85.2344
19R-4	52	171.53	83.7774
20R-4	59	179.50	86.6914
20R-5	51	181.51	90.3339
21R-3	45	188.05	60.3101
21R-5	25	190.85	62.5859
23R-5	5	209.85	153.6200
24R-5	122	211.02	176.3790
24R-6	37	221.27	174.1030
25R-C	7	230.67	130.8610
26R-C	10	239.58	130.8610
29R-2	10	264.80	113.7930

Table 6. Thermal conductivity.

Core section	Interval (cm)	Depth sub-bottom (m)	Thermal conductivity (10^{-3} cal/cm^2/s)	(W/H/C)
1R-1	75	0.75	2.959	1.239
1R-2	75	2.25	2.823	1.182
1R-3	75	3.00	2.365	0.990
2R-1	100	5.60	2.597	1.087
2R-2	50	6.60	2.409	1.009
2R-3	50	8.10	2.750	1.151
2R-3	100	8.60	2.371	0.993
3R-1	50	12.50	3.110	1.302
3R-1	100	13.00	2.415	1.011
3R-2	50	14.00	2.296	0.961
3R-2	100	14.50	2.544	1.065
3R-3	50	15.50	2.699	1.130
3R-3	100	16.00	1.998	0.836
3R-4	50	17.00	2.642	1.106
3R-4	100	17.50	2.629	1.101
3R-5	50	18.50	2.540	1.063
3R-5	100	19.00	2.476	1.037
4R-2	50	23.40	2.559	1.071
4R-3	50	24.90	2.515	1.053
4R-4	50	26.40	2.423	1.014
4R-5	50	27.90	2.870	1.201
5R-2	50	32.80	2.730	1.143
5R-3	50	34.30	2.807	1.175
5R-4	50	35.80	2.701	1.131
6R-1	50	40.80	3.346	1.400
6R-2	50	42.30	2.862	1.198
6R-3	50	43.80	2.439	1.021
6R-4	50	45.30	2.778	1.163
6R-5	50	46.80	2.152	0.901
8R-1	50	59.60	2.763	1.157

Table 6 (continued).

Core section	Interval (cm)	Depth sub-bottom (m)	Thermal conductivity (10^{-3} cal/cm^2/s)	(W/H/C)
8R-2	50	61.10	2.846	1.191
8R-3	50	62.60	2.811	1.177
8R-4	50	64.10	2.568	1.075
8R-5	50	65.60	2.887	1.209
9R-1	50	69.80	2.777	1.163
9R-2	50	71.30	2.797	1.171
9R-2	100	71.80	3.031	1.269
9R-3	50	72.80	2.620	1.097
9R-3	100	73.30	2.847	1.192
10R-1	100	80.00	3.627	1.518
11R-1	50	89.20	3.760	1.574
11R-2	50	90.70	3.750	1.570
11R-3	50	92.20	3.757	1.573
12R-1	50	98.90	3.169	1.326
12R-1	100	099.40	3.086	1.292
12R-2	50	100.40	2.935	1.229
12R-2	100	100.90	2.973	1.245
12R-2	132	101.22	3.192	1.336
14R-2	50	119.70	2.887	1.209
14R-2	100	120.30	2.629	1.100
14R-3	50	121.20	2.658	1.112
14R-3	100	121.70	2.825	1.182
14R-4	50	122.70	2.855	1.195
14R-4	100	123.20	2.743	1.148
14R-5	50	124.20	2.788	1.167
15R-1	100	128.40	3.058	1.280
15R-2	50	129.40	2.819	1.180
15R-3	50	130.90	3.655	1.530
15R-4	50	132.40	2.843	1.190
15R-5	100	134.40	3.223	1.349
15R-6	50	135.40	4.167	1.744
15R-6	100	135.90	3.268	1.368
15R-7	50	136.90	3.217	1.347
16R-3	50	140.40	3.006	1.258
16R-4	50	141.90	3.037	1.271
16R-5	50	143.40	2.935	1.229
16R-6	25	144.65	2.951	1.235
17R-2	100	149.40	3.172	1.328
17R-3	50	150.40	2.546	1.066
17R-4	50	151.90	3.044	1.274
18R-1	50	156.60	2.306	0.966
18R-3	50	159.60	2.160	0.904
18R-4	75	161.35	2.319	0.971
18R-5	50	162.60	3.090	1.294
19R-3	50	169.30	3.084	1.291
19R-4	50	170.80	3.151	1.319
20R-1	50	175.50	2.578	1.079
20R-2	50	177.00	3.068	1.284
20R-3	50	178.50	4.270	1.787
20R-5	50	181.50	4.290	1.796
21R-3	50	188.10	2.761	1.156
21R-4	50	189.60	2.817	1.179
21R-5	50	191.10	2.775	1.161
23R-1	50	204.30	3.562	1.481
23R-2	50	205.80	1.997	0.836
23R-3	50	207.30	3.376	1.413
23R-4	50	208.80	3.354	1.404
24R-3	50	216.90	3.231	1.353
24R-4	50	218.40	3.121	1.307
24R-5	50	219.90	3.193	1.337
24R-5	100	220.40	3.256	1.363
24R-6	50	221.40	3.142	1.315
25R-2	50	225.10	2.093	1.092
25R-3	50	226.60	2.575	1.078
25R-3	100	227.10	2.915	1.220
25R-4	50	228.10	2.981	1.248
25R-5	50	229.60	3.064	1.283
26R-1	50	233.20	2.982	1.248
26R-2	50	234.70	3.047	1.276
26R-3	50	236.20	2.892	1.211
26R-4	50	237.70	3.027	1.267
26R-4	100	238.20	2.846	1.191
26R-5	50	239.20	2.914	1.220
26R-C	10	242.30	2.998	1.255

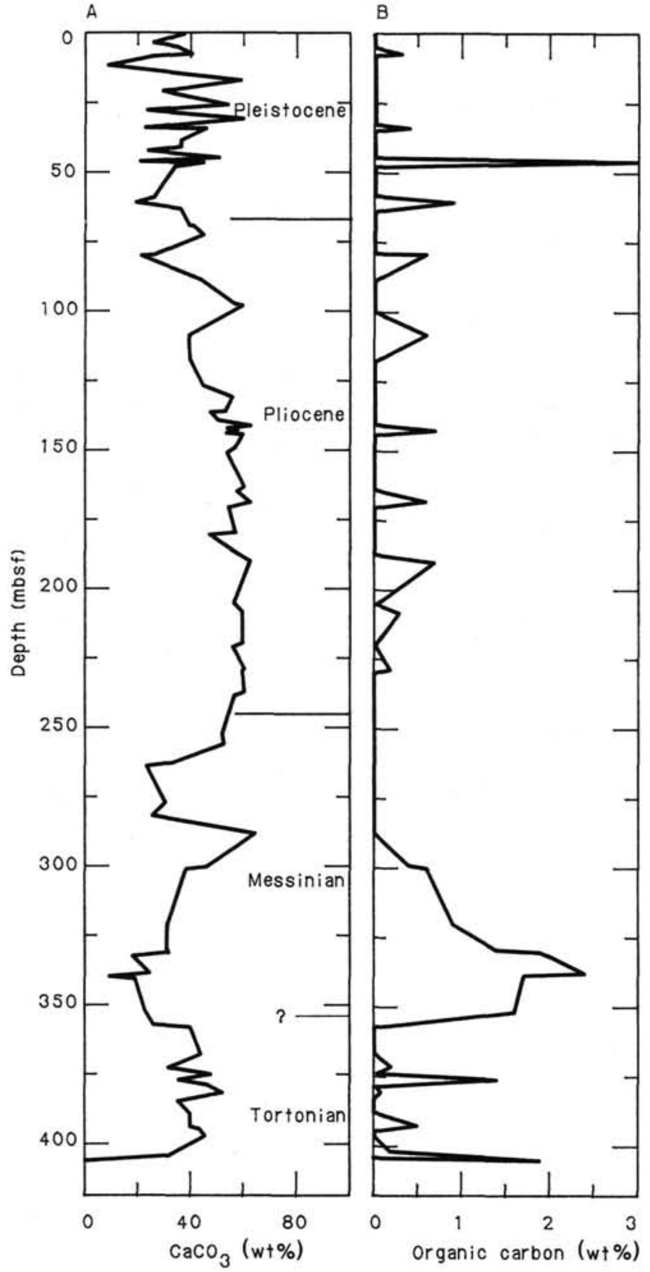

Figure 24. A. Plot of CaCO$_3$ weight % vs. depth, Hole 654A. B. Plot of C$_{org}$ weight % vs. depth, Hole 654A.

Interstitial Waters

Results of interstitial water analyses are given in Table 8 and Figure 25. Since all ions decrease gradually downsection within the first 200 mbsf, the presence of Messinian evaporites in this sequence—at a depth of 242 mbsf—could not be anticipated from interstitial water analysis. This is quite different from other sites in the Tyrrhenian, where prominent increases in chlorinity and dissolved calcium and the lack of magnesium depletion signaled dissolution of evaporites at depth and upward diffusion/migration of these dissolved solids.

In Site 654 sediments, the occurrence of high amounts of salts in samples including and underlying Sample 654A-26R-4, 140–150 cm, does obviously not lead to an upward migration of ions along the concentration gradient to younger samples. This is puzzling because no obvious lithological barrier restricts mi-

Table 7. Calcium carbonate and organic carbon.

Sample	Depth	CaCO$_3$ (%)	C$_{org}$ (%)
1R-1, 75–76	0.75	37.7	
1R-2, 75–76	2.25	32.1	
1R-3, 75–76	3.75	24.9	
2R-1, 73–76	5.33	31.0	
2R-1, 100–101	5.60	35.5	
2R-3, 30–31	7.90	40.7	0.34
2R-3, 64–67	8.24	40.2	
2R-3, 100–101	8.60	27.8	
2R-CC, 10–11	11.80	7.4	
3R-2, 49–51	13.99	36.4	
3R-5, 0–1	18.01	34.9	0.00
3R-5, 49–51	18.49	55.1	
3R-6, 49–51	19.99	29.2	
4R-1, 49–50	21.89	29.8	
4R-4, 74–75	26.64	54.2	
4R-5, 50–51	27.90	22.2	
5R-1, 50–51	31.30	60.5	
5R-2, 119–120	33.49	20.7	0.09
5R-3, 50–51	34.30	21.4	0.47
5R-3, 138–139	35.18	46.3	
5R-CC, 5–7	40.05	36.1	
6R-1, 50–51	40.80	36.4	
6R-2, 50–51	42.30	23.4	
6R-4, 50–51	45.30	51.7	
6R-4, 133–135	46.13	25.1	1.88
6R-4, 140–141	46.20	25.7	
6R-4, 142–144	46.22	20.1	3.68
6R-5, 15–17	46.45	39.2	1.35
6R-5, 50–51	46.80	45.9	
6R-6, 0–1	47.80	34.5	
7R-CC, 7–8	59.07	26.2	
8R-2, 49–50	61.09	18.5	0.97
8R-4, 42–43	64.02	36.1	
9R-1, 50–51	69.80	40.6	
9R-1, 60–63	69.90	41.4	
9R-3, 50–51	72.80	45.5	
9R-3, 60–63	72.90	45.1	
10R-1, 50–51	79.50	26.9	
10R-1, 78–80	79.78	20.5	0.66
11R-1, 50–51	89.20	44.4	
11R-1, 78–80	89.48	43.4	
11R-3, 50–51	92.20	47.4	
11R-3, 78–80	92.48	47.7	
12R-1, 50–51	98.90	57.4	
12R-1, 53–55	98.93	60.0	
12R-1, 74–76	99.24	59.0	
12R-2, 53–55	100.93	56.3	
13R-1, 100–103	109.00	39.2	0.61
14R-1, 89–90	118.59	40.4	
15R-1, 17–20	127.57	45.1	
15R-3, 100–103	131.40	56.2	
15R-7, 3–4	136.43	53.0	
15R-7, 27–30	136.67	52.7	
15R-7, 50–51	136.90	47.7	
16R-3, 39–42	140.29	51.9	
16R-4, 50–51	141.90	63.5	
16R-4, 139–140	142.79	53.3	0.20
16R-5, 50–51	143.40	58.4	0.79
16R-6, 10–21	144.50	53.7	
16R-6, 24–25	144.64	60.4	
17R-2, 117–120	149.07	57.4	
17R-4, 53–56	151.43	54.2	
18R-5, 146–149	163.56	61.3	
18R-7, 49–52	165.59	57.8	
19R-3, 23–26	169.03	63.5	0.68
19R-4, 54–57	170.84	54.3	
20R-4, 47–50	179.97	57.3	
20R-4, 119–120	180.69	46.3	
20R-5, 18–20	181.18	48.0	
21R-3, 80–82	188.40	58.7	
21R-5, 20–22	190.80	63.3	0.75
23R-2, 73–76	206.03	56.1	
23R-4, 73–76	209.03	60.0	0.31
24R-5, 132–135	220.72	60.0	
24R-6, 56–59	221.46	56.8	
25R-5, 42–44	229.52	61.5	0.20
25R-5, 135–138	230.45	60.0	0.02

Table 7 (Continued).

Sample	Depth	$CaCO_3$ (%)	C_{org} (%)
26R-4, 60–64	237.80	61.5	
26R-5, 60–64	239.30	57.9	
28R-1, 103–107	253.03	52.8	
28R-3, 145–149	256.45	53.4	
29R-1, 90–93	262.60	34.2	
29R-2, 114–117	264.34	23.7	
31R-1, 90–93	277.20	31.9	
32R-1, 110–111	282.00	25.6	0.00
33R-1, 129–130	288.89	65.5	
34R-CC, 9–10	300.29	46.1	0.45
35R-1, 75–76	301.05	38.4	0.60
37R-1, 149–150	321.09	31.3	0.96
38R-1, 126–132	330.56	31.0	1.45
38R-2, 33–39	331.13	32.3	1.99
38R-2, 148–149	332.28	17.3	2.01
39R-1, 7–10	338.67	25.7	2.40
39R-1, 102–104	339.62	8.7	1.01
39R-2, 6–9	340.16	19.1	1.70
40R-3, 139–140	352.59	23.0	1.61
41R-1, 0–1	357.81	27.2	0.20
41R-1, 70–73	358.50	40.1	
42R-1, 69–72	368.09	44.7	
42R-4, 61–64	372.51	30.6	0.22
42R-6, 21–24	375.11	48.3	
42R-CC, 9–10	377.09	34.6	1.48
43R-2, 107–110	379.67	47.4	
43R-4, 10–11	381.70	52.9	0.15
43R-5, 130–133	384.40	34.2	
44R-2, 109–112	389.39	40.0	
44R-5, 119–120	393.99	40.2	0.57
44R-6, 96–99	395.26	44.6	
45R-1, 80–82	397.20	46.0	
45R-6, 0–1	403.90	31.0	0.23
45R-7, 13–14	405.53	18.0	1.95

gration between Samples 654A-26R-4, 140–150 cm, at 238 mbsf and the next sample at 190.5 mbsf. In sediments of Messinian and Tortonian age, pore water concentrations of Ca^{2+}, Mg^{2+}, and SO_4^{2-} are higher than in younger strata. A slight decrease in sulfate in Sample 654A-40R-3, 140–150 cm, at 352 mbsf is associated with an increase in alkalinity. In this interval, traces of degraded oil were found. Possibly, bacterial sulfate reduction oxidized this oil to CO_2. Because this resulting alkalinity maximum coincides with a pronounced magnesium depletion, we may assume that magnesium carbonates formed in a reducing and low pH environment. All ions reach a maximum in the lowest sample at 404 mbsf.

Organic Geochemistry

Because of the geological and tectonic setting of Site 654 on the edge of a tilted block, safety considerations led to a stringent geochemical hydrocarbon monitoring program during drilling operations. Using downhole changes in volatile hydrocarbons (C_1 to C_{6+}) of Site 653 as a reference background, concentrations of these gases were monitored with vacutainer and headspace techniques. Although gas analysis yielded no significant concentrations of volatile hydrocarbons above background values (less than 15 ppm), concerns expressed by the Safety Panel proved to be justified. Although in minute amounts, hydrocarbons were indeed found trapped beneath the sealing upper Messinian evaporite sequence. When Cores 107-654A-40R to 107-654A-42R were opened, a heavy petroliferous odor emanated from the grey sediment of Tortonian age. Asphaltic material filled a crack in Core 654A-40R, Section 5. Excited by ultraviolet light, this material displayed a dull yellow to brown fluorescence typical of heavy crudes. Penetrating deeper into Tortonian marine nannofossil oozes, no further fluorescencing material was detected, and the petroliferous odor decreased and was absent in cores deeper than Core 107-654A-43R.

Gas analysis, as mentioned above, failed to show any significant increase in the amounts of volatile hydrocarbons upon approach to this "trap." This is not surprising, when we consider the dominance of high molecular weight hydrocarbons (dominated by compounds with carbon atom numbers higher than C_{36}) in this degraded oil. A gas chromatographic trace of the saturated fraction from Sample 107-654A-40R-5, 46–48 cm, is presented in Figure 26. A preliminary comparison of saturated hydrocarbons from underlying Tortonian and overlying Messinian organic-carbon-rich strata suggests that the oil originated from Tortonian source rocks (compare Fig. 26A with -B, -C, and -D).

Organic carbon concentrations of samples from all lithological units, including Pleistocene sapropels, are listed in Table 7 and plotted vs. depth in Figure 24B.

SEISMIC STRATIGRAPHY

Introduction

Site 654 is located on a tilted faulted block cutting across the upper Sardinian margin at the base of the slope of Monte Baronie, a ridge which parallels the upper slope. The site is located (see Fig. 7) on MCS line ST06 (shotpoint 1531 on the processed line just before the intersection with MCS line ST07). Four distinct seismic units are well expressed; no real acoustic basement is observed (Fig. 27).

Description of Units

Seismic Unit One

This unit extends from seafloor to the top of a high-amplitude reflector for a thickness of about 0.300 s. Using the inter-

Table 8. Composition of interstitial waters.

Sample no.	Depth	Sal.	Alk.	pH	Cl^-	SO_4^{2-}	Ca^{2+}	Mg^{2+}	Ca/Mg
1R-2, 140-150	2.9	38.0	3.01	7.49	601	29.2	10.3	55.1	0.19
6R-3, 140-150	44.7	38.0	3.56	7.40	588	28.4	10.3	53.7	0.19
11R-2, 140-150	91.6	38.0	2.98	7.54	582	22.9	9.2	46.8	0.20
16R-4, 140-150	142.8	36.5	2.49	7.45	576	20.7	9.5	44.2	0.22
21R-4, 140-150	190.5	38.0	2.03	7.15	528	15.1	7.3	26.5	0.27
26R-4, 140-150	238.6	39.0	2.00	7.33	595	39.7	27.1	54.7	0.49
40R-3, 140-150	352.6	39.0	2.94	7.15	587	24.8	27.0	34.4	0.78
45R-5, 140-150	403.8	39.5	1.74	7.61	598	38.2	35.16	76.41	0.46

Chemical analyses of interstitial water samples, Leg 107/Hole 654A. Sample no.: Hole 654A, Core-section, interval. Depth is given in meters below seafloor. Sal.: Salinity in parts per thousand; Alk.: Alkalinity in mmol/L; Cl^-, SO_4^{2-}, Ca^{2+}, Mg^{2+} are given in mmol/L. n.d. = not measured.

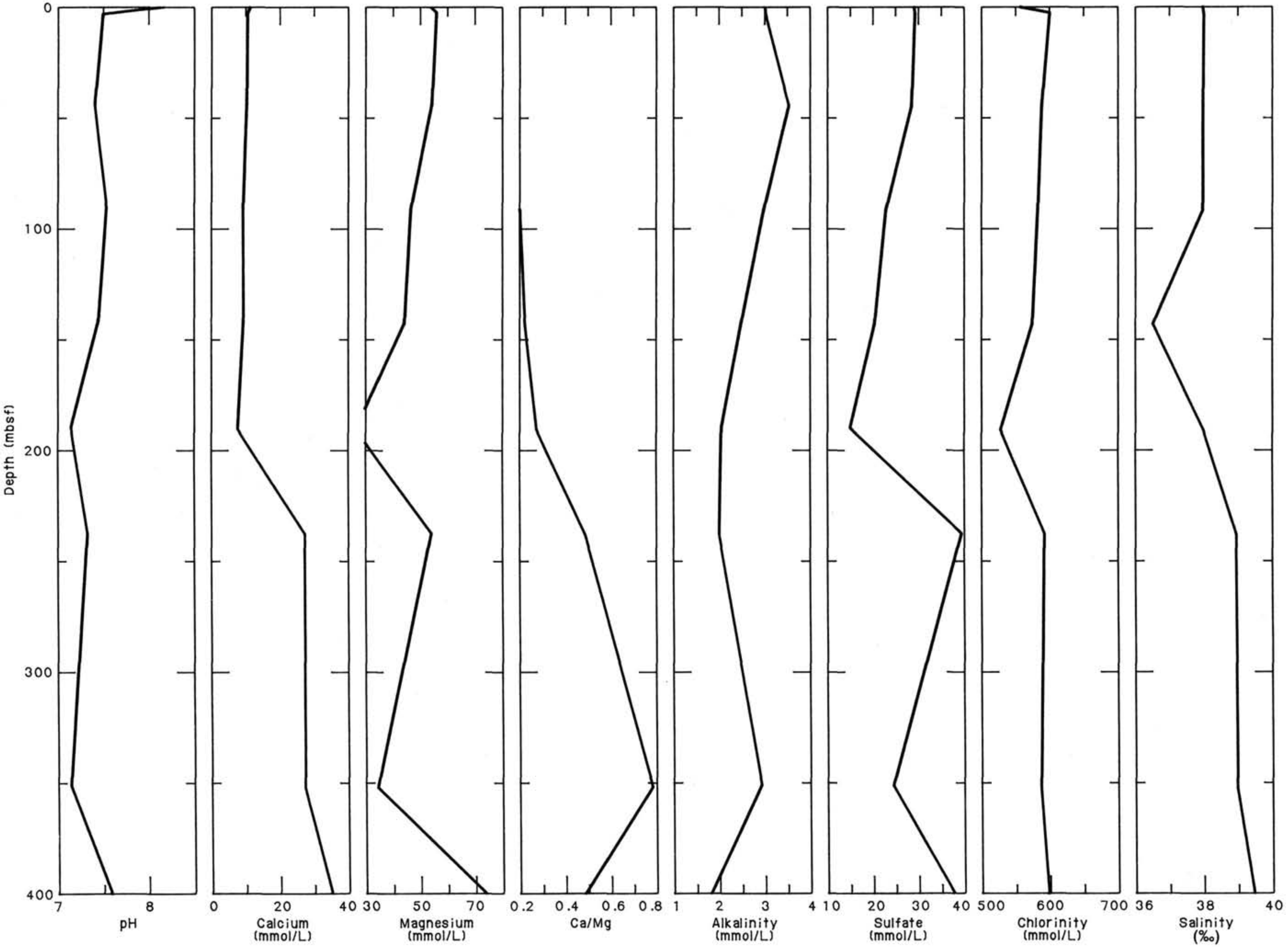

Figure 25. Downhole variations of pore water constituents, Hole 654A.

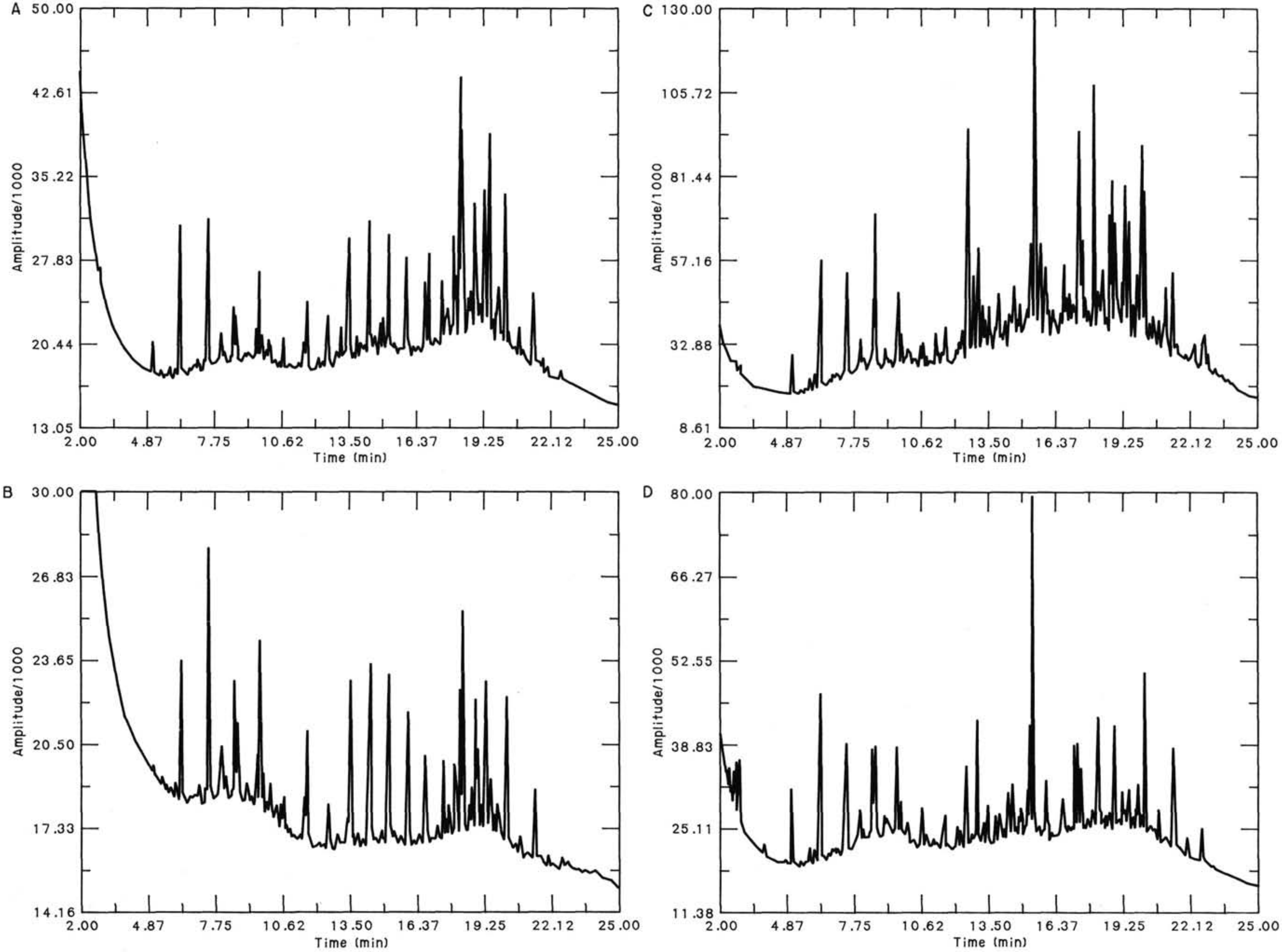

Figure 26. Gas chromatograms of saturated hydrocarbon fractions. A. Asphalt show, Sample 654A-40R-5, 46–48 cm. B. Tortonian mudstone, Sample 654A-42R-4, 61–64 cm; C_{org} = 0.22%. C. Messinian claystone, Sample 654A-38R-2, 33–39 cm; C_{org} = 1.99%. D. Messinian claystone, Sample 654A-39R-1, 7–10 cm; C_{org} = 2.40%.

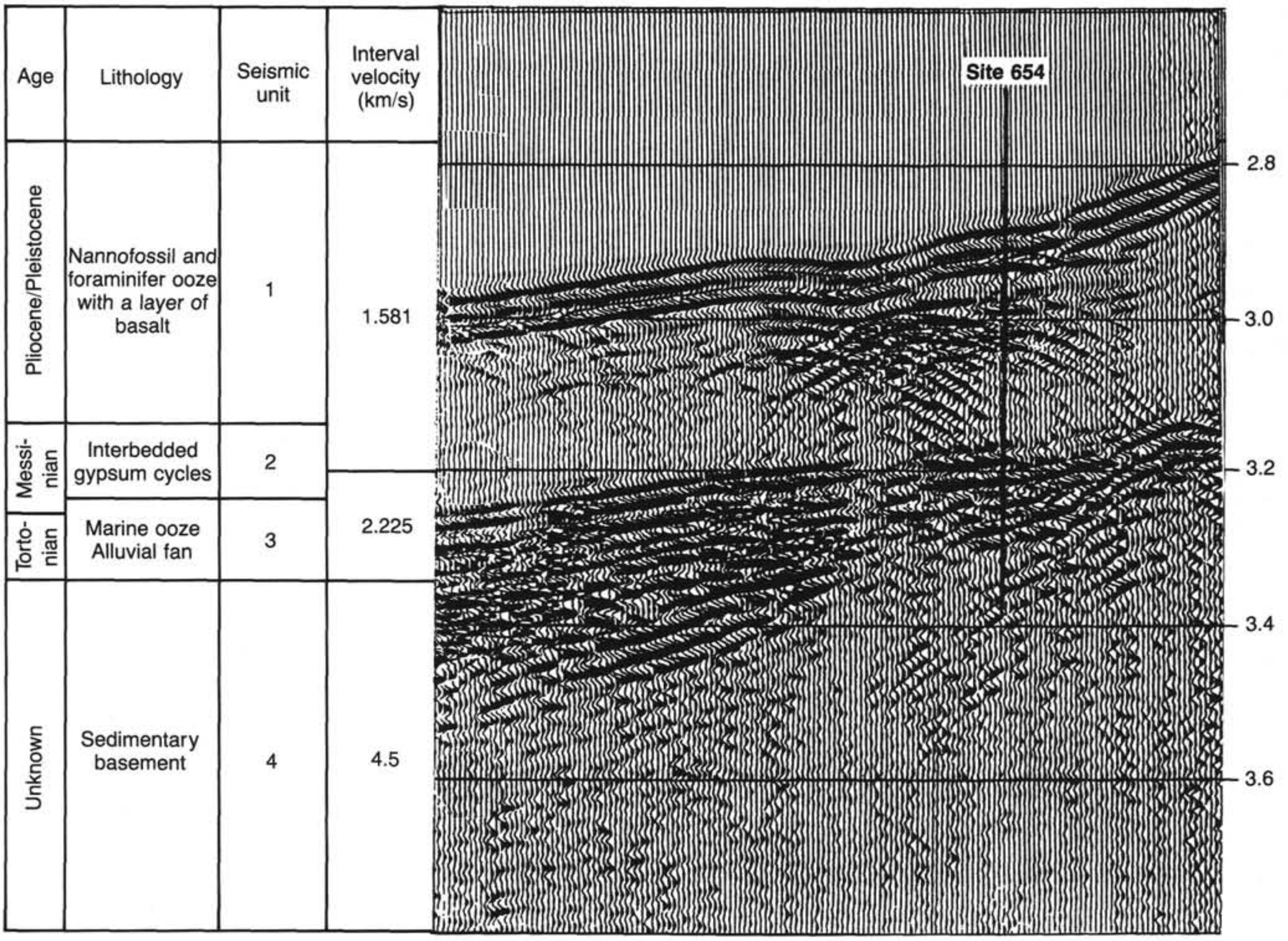

Figure 27. Section of the seismic line recorded during the approach to Site 654, showing the comparison between seismic units, lithology, and interval velocity at the site.

val velocity of 1.581 km/s, the base of the unit should be about 230–240 mbsf. The seismic character of Seismic Unit One is rather constant (only very few weak internal reflectors) with the exception of discontinuous strongly diffractive layers at about 90 mbsf. Such reflectors indicate a local and discontinuous change in lithology.

Seismic Unit Two

Unit Two consists of a series of well-layered, closely spaced, subhorizontal, high-amplitude reflectors (7–8 reflectors). The average thickness at the site location is 0.120 s. The computed interval velocity is surprisingly the same as that of the overlying sediments. If correct, the unit would be then about 100 m thick and its base would be situated at about 330 mbsf.

Seismic Unit Three

At Site 654, the thickness of this unit is on the order of 0.22 s. Using the interval velocity of 2.22 km/s, the thickness should be approximately 240 m and its base should lie at about 570–580 mbsf. Close examination permits the distinction of two subunits. Subunit 3A corresponds to a series of high-amplitude reflectors (about 90 m thick) while Subunit 3B is represented by an almost acoustically reflection-free sequence of about 0.14 s in thickness (150 m thick). This internal change in seismic character suggests a sharp change in lithology occurring at about 420 mbsf.

Seismic Unit Four

The top of this last unit is a very high-amplitude reflector dipping gently toward the north-northwest. The unit is characterized by a very high-interval velocity (4.5 km/s) and contains only a few discontinuous but well-marked reflectors showing the same general dip. It is impossible to observe a real acoustic basement. Unit Four progressively grades into a reflection-free sequence, thus indicating a thick and very lithified sedimentary section.

Discussion

The general geometric arrangement of the different seismic units described above and shown on MCS line ST06 (Fig. 7) can be considered as typical of, respectively, a post-rift (Unit One), syn-rift (Unit Three), and pre-rift (Unit Four) sequence deposited during the progressive creation and evolution of the Sardinian margin. Unit Two remains more difficult to interpret as it appears to onlap onto Unit Three, but shows a slight thickening toward the west-northwest.

Several authors have already proposed a stratigraphic interpretation of seismic lines across the Sardinian margin. Fabbri and Curzi (1979), Malinverno et al. (1981), as well as Moussat (1983), postulate that sedimentary layers of Miocene age exist below the Messinian evaporites. Furthermore, Fabbri et al. (1981), Moussat (1983), and Rehault et al. (1985) believe that an late Tortonian rifting phase created most of the asymmetric grabens cutting across the upper margin, while Malinverno et al. (1981) suggest a Serravalian/early Tortonian stage for the margin creation.

If the assumption of Moussat (1983) is correct, Seismic Unit Three, which lies directly over the pre-rift sediments, should be of late Tortonian age.

Synthetic Seismogram

As for previous sites, a synthetic *P*-wave seismogram has been generated using physical properties measurements of velocity and bulk density (Fig. 28). The synthetic seismogram shown here can easily be compared with both the seismic lines (Figs. 27 and 7) and simplified lithology (see "Lithostratigraphy" section, this chapter). The thin (about 2.5 m thick) layer (or boulder) of basalt recovered at about 74 mbsf is particularly well detected on the seismic line and on the seismogram, where it is expressed by a sharp contrast in amplitude. The Messinian gypsiferous complex is also well evidenced in the seismogram. It correlates on the synthetic with a series of high-amplitude reflectors between 230 and 320 mbsf, while their thickness as predicted from seismic lines should be 100 m (between about 230 and 330 mbsf). We note, however, a discrepancy between the base of Seismic Unit Two, as given in time and the base as deduced from the seismogram. This is due to an abnormally low velocity computed for Unit Two. In fact, if we consider that the massive gypsum layers represent one part of the gypsum sequences, one should adopt a mean velocity of about 2.7 km/s for the Messinian upper sequence. Unit Two, as deduced from the seismic profile, probably incorporates the finely laminated, almost barren 50 m of sediment just below the gypsum cycles.

The synthetic seismogram shows a high-amplitude acoustic character at about 410 mbsf. This marks the transition from marine sediments to continental-type deposits. Such a transition is barely detected on the seismic line. It may be correlated with a progressive transition from an almost transparent acoustic facies to a more layered, but discontinuous facies. The former represents the upper Tortonian marine sediments, the latter the appearance of interbedded conglomeratic layers.

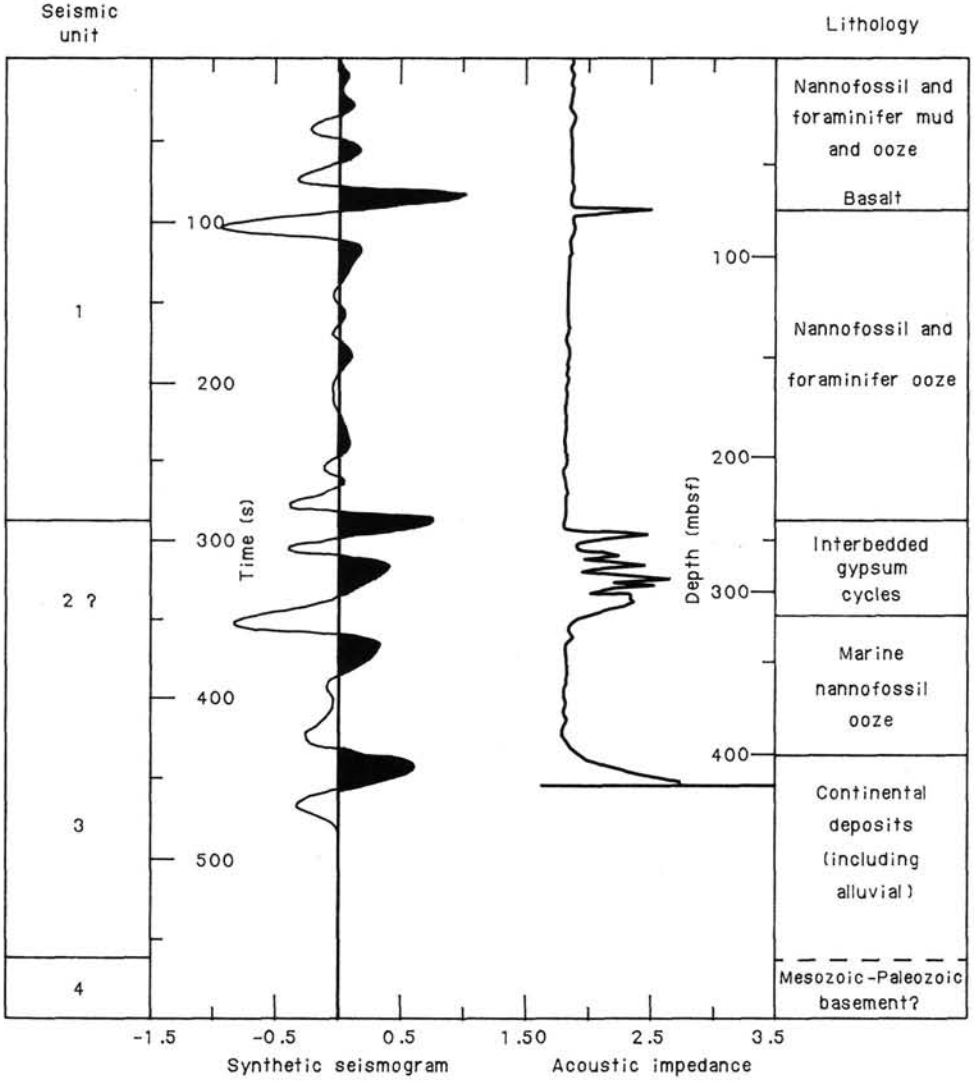

Figure 28. Acoustic impedance calculated from physical property data and synthetic seismogram generated from this data. Comparison between seismic unit and lithology is indicated.

Conclusion

Drilling at Site 654 established the following points:

1. A discontinuous but sharply reflective layer within the Pliocene-Quaternary sequence indicates the presence of basaltic rocks, either as boulders or as an *in-situ* flow.
2. The finely stratified sequences of seven to eight high-amplitude reflectors, interpreted as the upper evaporitic sequence, is made of distinct massive gypsum layers (as thick as 7 m), interbedded within marls which probably have been partially washed out.
3. The lower part of the syn-rift deposits corresponds to marine upper Tortonian sediments showing progressively shallower depth of deposition downhole.
4. The strong high-amplitude reflector (Fig. 7) interpreted as the top of the pre-rift sequence has not been documented. However, the recovery in Cores 107-654A-48R to 654A-51R (435–465 mbsf) of poorly sorted pebbles suggest that erosion of underlying strata (the pre-rift sequences) occurred during the tilting. The pebbles may represent most of the type rocks of the pre-rift sedimentary basement.

HEAT FLOW

Introduction

At Site 654 (Fig. 29), a constant 250-m thickness of onlapping Pliocene-Pleistocene series rests on upper Messinian evaporitic sequences and syn-rift deposits as well as an eroded "basement." This cover seals the whole geological structure and favors the occurrence of a conductive heat flow regime.

Five downhole temperature measurements were made at this site in order to investigate the detailed structure of the geothermal gradient within the deep Pliocene-Pleistocene section. These data also provide a reliable heat flow value against which shallow probe heat flow values obtained elsewhere in the Tyrrhenian Sea can be compared.

Temperature Measurements

Four of the five downhole measurements obtained are of excellent quality (Figs. 30 and 31 and Table 9) and are perfectly equilibrated. They were obtained with the same Uyeda probe downhole temperature recorder and the same thermistor, minimizing the possibility of calibration errors that may arise for the use of different measuring systems. Measurement 2 (located at

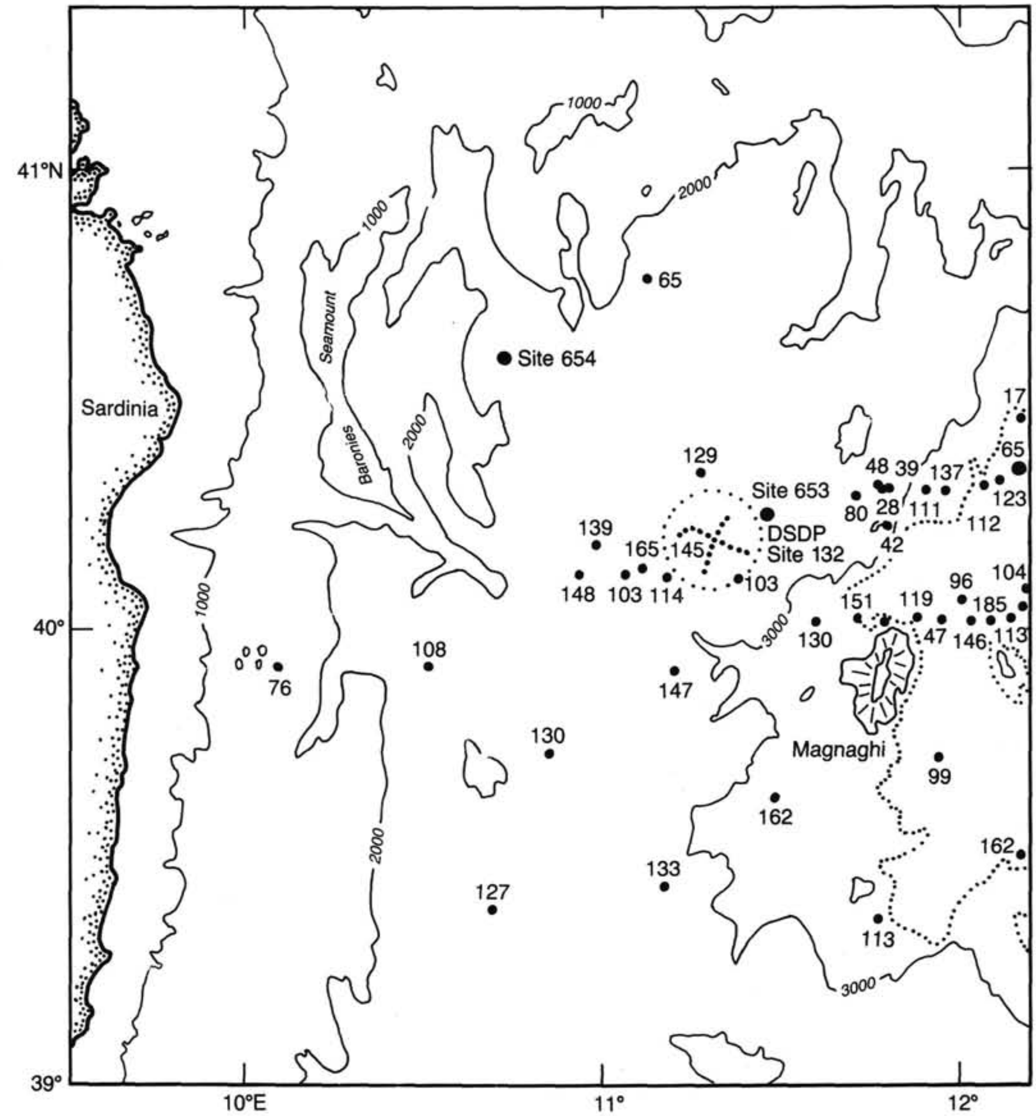

Figure 29. Location of Site 654 along with previously measured heat flow values. Previous measurements are after Della Vedova et al. (1984), in mW/m^2.

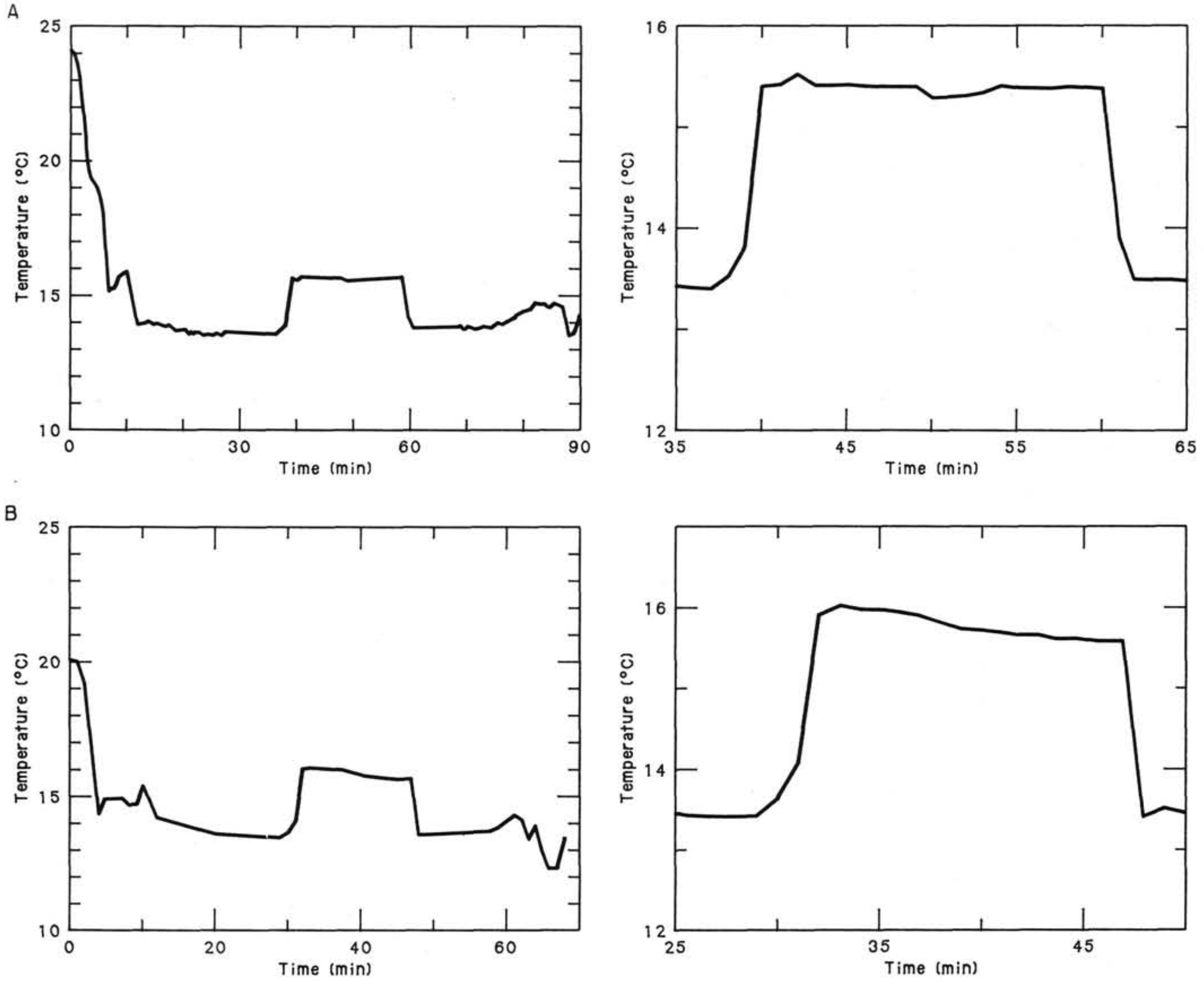

Figure 30. Temperature records. A. Station HF 1 (40.3 mbsf). B. Station HF 2 (88.7 mbsf).

88.7 mbsf) shows a slow decrease in temperature to an equilibrium temperature of 15.15°C from a 15.48°C initial temperature 2 min after penetration (Fig. 30B). We must point out that this measurement occurred after drilling encountered hard material (2-m-thick basalt) which led the drill crew to significantly increase pressure of the pumps. It is likely that the sediment below the basalt interval has been cooled by drilling fluids, (see "Lithostratigraphy" and "Physical Properties" sections, this chapter). This measurement is therefore considered inaccurate, and is not included in further heat flow determinations. The measurements are plotted vs. sub-bottom depth on Figure 32 to illustrate the structure of the geothermal gradient at Site 654.

A bottom water temperature of 13.30°C was measured during the stabilization times prior to the thermistor penetrations into the undrilled sediments.

Thermal conductivity has been measured on each section of cores which did not appear intensively disturbed by drilling. Values are reported vs. depth in Figure 23, and the mean thermal conductivity of each downhole temperature measurement interval is given in Table 9 with the number of thermal conductivity measurements.

Discussion

Heat flow at Site 654 decreases slightly with depth according to the plotted geothermal gradient on Figure 32, in spite of increasing thermal conductivities downward (Table 9).

In summary, one may consider two main intervals:

1. From seafloor to 127.4 mbsf where the heat flow is 56 mW/m^2 using geothermal gradients and the mean of thermal conductivity of this interval.
2. From 127.4 to 203.8 mbsf where the average heat flow is 45 mW/m^2 using geothermal gradient and the mean of thermal conductivity of this last interval.

The proximity of the upper Messinian evaporitic layers (having a conductivity two or three times greater than the sediments in which the temperatures were measured) may have caused local reduction of the regional heat flow, particularly near the pinch-out of the evaporites. Nevertheless, the average uncorrected heat flow value of 50 ± 5 mW/m^2 estimated for Site 654 is appropriate for a margin affected by a stretching factor of 1.4–1.5.

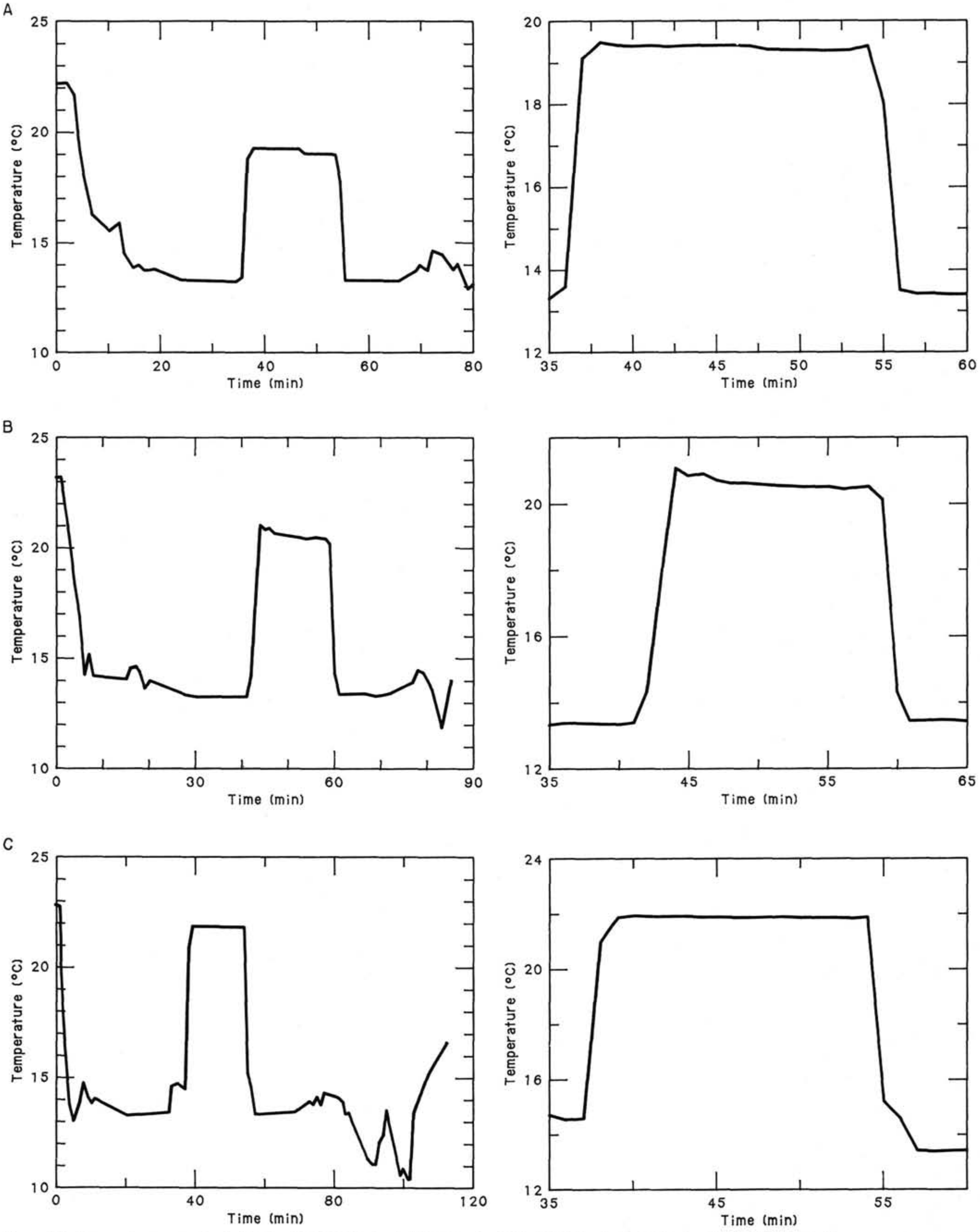

Figure 31. Temperature records. A. Station HF 3 (127.4 mbsf). B. Station HF 4 (165.8 mbsf). C. Station HF 5 (203.8 mbsf).

Table 9. Interval temperature, gradient, thermal conductivity, and heat flow for Site 654.

Interval between measurements	Sub-bottom interval m	Interval temperature difference °C	Thermal gradient °C/km	Thermal conductivity $Wm^{-1} K^{-1}$	n*	Heat flow [mW $m^{-2} s^{-1}$]	Heat flow HFU
[0 #1]	0-40.3	2.05 ± 0.04	50.9 ± 0.8	1.1	22	56	1.34
[0 #3]	0-127.4	5.9 ± 0.04	46.3 ± 1.2	1.22	53	56.5	1.35
[0 #4]	0-165.8	7.2 ± 0.04	43.4 ± 1.6	1.22	78	52.75	1.26
[0 #5]	0-203.8	8.6 ± 0.05	42.2 ± 1.6	1.24	95	49.7	1.19
[1 #2]	40.3-88.7	0.15 ± 0.15	—	1.22	16	—	—
[1 #3]	40.3-127.4	3.85 ± 0.04	44.2 ± 0.6	1.28	31	56.6	1.35
[1 #4]	40.3-165.8	5.15 ± 0.04	41.0 ± 1.2	1.25	56	51.4	1.23
[1 #5]	40.3-203.8	6.55 ± 0.04	40.1 ± 1.6	1.28	73	51.2	1.22
[4 #5]	165.8-203.8	1.4 ± 0.04	36.8 ± 0.8	1.35	17	49.7	1.19
[3 #4]	127.4-165.8	1.3 ± 0.04	33.9 ± 0.8	1.20	25	40.7	0.97
[3 #5]	127.4-203.8	2.7 ± 0.04	35.4 ± 1.2	1.27	42	44.9	1.07
	203.8-252	—	—	1.30	23	—	

*n; Number of thermal conductivity measurements.

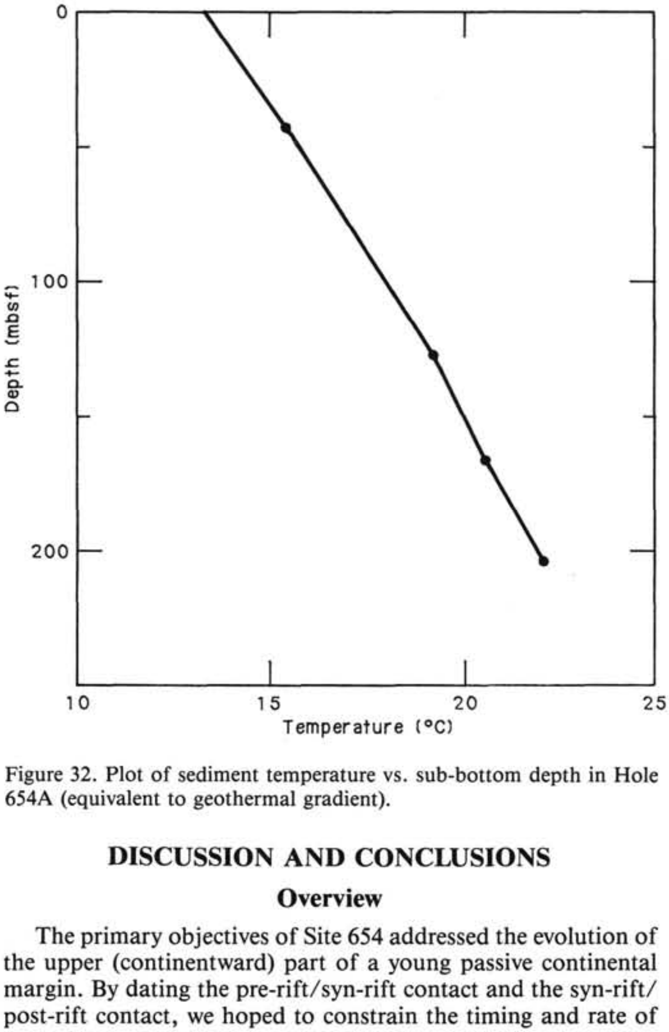

Figure 32. Plot of sediment temperature vs. sub-bottom depth in Hole 654A (equivalent to geothermal gradient).

DISCUSSION AND CONCLUSIONS

Overview

The primary objectives of Site 654 addressed the evolution of the upper (continentward) part of a young passive continental margin. By dating the pre-rift/syn-rift contact and the syn-rift/post-rift contact, we hoped to constrain the timing and rate of extension and subsidence of the margin, and to compare these results to those from the lower continental margin (Site 652). Results from Site 654 date the post-rift sequence as uppermost Messinian, Pliocene, and Quaternary, whereas the recovered portion of the syn-rift sequence includes lower and middle Messinian and upper Tortonian sediments. The lower portion of the recovered section shows a classic example of a transgressive sequence, which we attribute to subsidence of the Sardinian margin during block faulting and extension. In this context, the Messinian desiccation event appears as a short-term regression superimposed on the subsidence-driven transgression. Penetration was halted for technical reasons in coarse conglomerates before reaching the pre-rift sequence. However, we believe that the pre-rift sedimentary basement is represented in the numerous pebbles of conglomerate recovered at the base of the hole.

Pliocene-Pleistocene Sediments

The Pliocene-Pleistocene section (lithostratigraphic Unit I) was deposited under open marine conditions, with a tendency toward intermittently reducing conditions. Volcanic ash is more common in the upper Pliocene and the Pleistocene than in the lower Pliocene, following a trend observed throughout the leg. Terrigenous clastic content is rather low, probably due to damming of clastics derived from Sardinia behind Monte Baronie. Several sapropels and/or sapropelic layers are attributed to short-lived intervals of bottom-water stagnation. Careful correlation of sapropels and sapropelic layers of Site 654 with those of Site 652 may constrain the water depth range and lateral extent of these inferred bodies of stagnant water.

An interval of basalt was encountered close to the Pliocene/Pleistocene boundary. The depth of the basalt coincides with a diffracting horizon on seismic reflection records which had been interpreted as coarse-grained channel fill. Although only 30 cm were recovered, observation of the rate of penetration while drilling suggests that the basalt interval was approximately 2 m thick. Recovery of such a small, isolated basalt fragment within the pelagic sequence was unanticipated, although alkaline basalts of similar age have been dredged along slopes of the Sardinian margin (Keller, 1981) and outcrop in eastern Sardinia (Marinelli, 1975). Preliminary chemical data suggest that Site 654 basalts have alkaline or transitional affinity; thus they may represent basaltic injections related to progressive rifting of the Sardinian margin. The lower basalt/sediment contact was not recovered. The sediment recovered immediately above the basalt appears unaltered. Because of this apparent lack of alteration and because the fine-grained texture of the basalt suggests rapid cooling, the basalt interval is interpreted as a flow rather than a sill. It is possible, however, that the basalt is a cobble carried to Site 654 down a submarine channel, rather than an *in-situ* flow basalt.

As at Sites 652 and 653, the lowermost Pliocene sediments at Site 654 contain red, yellow, and brown-colored layers. The brilliant coloration is attributed to the presence of iron oxides derived from subaerial weathering.

Messinian Sediments

The Evaporitic Messinian Sediments

The uppermost Messinian consists of alternations of gypsum-dominated intervals (primarily laminated balatino-type gypsum) and gypsum-poor intervals (primarily clastic sediments with minor nannofossil ooze). Sedimentary structures within the intra-gypsum horizons indicate significant bottom current activity. Recovery was fragmentary in the alternating hard/soft layers. Observations of rate of penetration while drilling suggest that four or five major gypsum layers as thick as 7.5 m were penetrated. In the cores, five major gypsum cycles as thick as 5.2 m (or eleven minor gypsum horizons) can be identified. An interesting comparison can be made with the upper evaporites of Sicily where seven gypsum-rich/gypsum-poor cycles are described (Decima and Wezel, 1973; Heiman and Mascle, 1974; Garrison et al., 1978).

The gypsum-rich/gypsum-poor cycles are thought to represent an alternation between intervals of hypersaline conditions during which chemical sedimentation dominated, and less saline conditions during which the clastic sediments and rare chalks were deposited. The sedimentary cycles may have been driven by fluctuations in climate.

The evaporitic Messinian sediments correlate very well with a series of very fine, closely spaced, high-amplitude seismic reflectors. These reflectors dip slightly westward, and are subparallel with a barely discernible increase in reflector spacing toward the west. Toward the east, the reflectors onlap the underlying units. This geometry suggests that if tilting of the block occurred while these sediments were being deposited it must have been minor. This inference is supported by the infrequent presence of microfaults and slumps. We thus tentatively place the syn-rift/post-rift contact at or near the base of the evaporitic Messinian.

The Silica-Bearing Messinian

The evaporitic facies immediately overlies a dark brown, organic-carbon-rich, pyrite-bearing, finely laminated, sedimentary sequence containing siliceous biogenic remains (radiolarians, sponge spicules, and diatoms). This unit is thought to have been deposited in an organically productive sea, possibly in a setting analogous to the modern Gulf of California (McKenzie et al., 1980). Siliceous sediments immediately underlying marginal Messinian evaporites are known elsewhere in the circum-Mediterranean; this unit may be considered as a basinal equivalent of, for example, the diatomites of the Tripoli formation in Sicily (Decima and Wezel, 1973). The reason for the silica enrichment at this time remains unclear, both at Site 654 and in land sections. It has been proposed that paleoceanographic conditions in the early part of the Messinian drawdown were such that upwelling was vigorous and continual delivery of fresh nutrients encouraged diatom blooms (McKenzie et al., 1980). Alternatively, bottom water geochemistry may have been such as to encourage carbonate dissolution and silica preservation.

Microfaults are abundant and vividly displayed by the fine laminations of lithostratigraphic Unit III. On seismic reflection profiles, the silica-bearing Messinian sediments fall within the wedge interpreted as the syn-rift sequence. Together, these observations imply that at the onset of the Messinian salinity crisis, rifting-related subsidence was proceeding rapidly on the upper Sardinian margin.

The Open Marine Messinian

A light gray nannofossil ooze, with open marine benthic and planktonic fauna, underlies the silica-bearing Messinian sediments. This open marine portion of the Messinian sequence is lithologically indistinguishable from the underlying upper Tortonian sediments.

The Syn-Rift Transgressive Sequence

The lowermost 140 m of Hole 654A contain a textbook example of a transgressive sequence. Unit VI is interpreted as an alluvial fan deposit; the shallow-water macrofauna and benthic foraminifers of Unit V suggest a coastal environment; and the nannofossil oozes of Unit IV suggest a gradually deepening, fertile, fully marine sea. We attribute this transgressive sequence to rapid subsidence of the continental crust during the rifting stage of formation of the Tyrrhenian margin.

The lowermost Messinian and uppermost Tortonian sediments of Cores 654A-40R through 654A-44R record a fertile, fully-marine environment with sufficiently oxygenated bottom waters to support a vigorous community of burrowing infauna. Benthic foraminifer assemblages suggest a water depth of several hundred meters. The position of the Messinian/Tortonian boundary is recorded at slightly different levels by different fossil groups: the nannofossil boundary NN11a/NN11b occurs between 654A-43R-5, 92 cm, and 654A-43R, CC, whereas the planktonic foraminifer boundary occurs at 654A-42R-2, 70–72 cm. Slightly downsection, Cores 654A-44R and 654A-45R still contain a marine community, but benthic assemblages indicate that the water is shallower. In Core 654A-45R, sand fraction increases, suggesting the shoreline may be nearer. Then, in Core 654A-46R, a nearshore assemblage including large oyster shells was recovered.

The subaerial, continental deposits of lithostratigraphic Unit VI are characterized by a distinctive red colored matrix attributed to iron oxide formation during subaerial weathering. The pebbles in the Unit VI conglomerate are inferred to be derived from an erosional unconformity which is observed on seismic reflection profiles updip (i.e., east) of the site. In dozens of pebbles, only four lithologies were seen: recrystallized limestone, marble, dolostone, and minor quartzite. The lithologies recovered suggest that the pre-rift unit of the tilted block is a deformed and metamorphosed carbonate platform with underlying quartzitic basement, both probably of Paleozoic age.

Tectonic Implications

In summary, a brief comparison between the drilling results and the seismic stratigraphy suggests the following sequence of events.

1. At some time earlier than latest Tortonian, listric normal faults cut through the limestone cover and metamorphosed basement of a continental area. The time of onset of rifting is not yet firmly dated. However, seismic reflection profiles suggest that the syn-rift sequence below the maximum penetration of Site 654 is of similar character to lithostratigraphic Unit VI. Although there are no dates in lithostratigraphic Unit VI, such coarse alluvial fan deposits typically accumulate very rapidly, in excess of 100 m/1000 yr. At such rates, the 140 m of sediment between the base of lithostratigraphic Unit IV and V and the pre-rift/syn-rift contact, would be instantaneous in geologic time. Thus we estimate that the onset of rifting would be in Tortonian time, most likely late Tortonian.
2. As the listric faults slipped, the fault-bounded blocks tilted and subsided, and half-grabens were created offshore from each fault outcrop. Erosion was active, particularly on the crest of each fault-bounded tilted block, where an erosional unconformity is evident updip from Site 654. Rapid subaerial erosion, at a short distance from the site, provided the coarse clastics of lithostratigraphic Unit VI.
3. In the late Tortonian, sea level transgressed over the rapidly subsiding continental margin. Several hundred meters of

subsidence occurred during the time required to deposit only a few tens of meters of sediment.

4. In the early Messinian, restricted circulation and/or high productivity contributed to anoxic bottom water. Since Site 654 had not yet subsided to its present depth, its paleocirculation could have been quite sensitive to changes in water depth. A relatively minor drop in Messinian water depth might have been sufficient to turn the Site 654 half-graben into a silled basin bounded by the crest of the tilted fault block. Abundant microfaults suggest that subsidence and/or tilting were rapid at this time.

5. In the late Messinian, gypsum-bearing sediments were deposited onlapping onto the earlier syn-rift sediments (Fig. 7). At this time rifting-related subsidence and tilting seemed to have slowed or stopped.

6. During the Pliocene and Quaternary, marine sediments were deposited conformably over the upper Messinian sequences. The Quaternary, Pliocene, and uppermost Messinian are classified as post-rift sediments. However, minor extension probably continued throughout this time interval. The slight tilt of the evaporitic Messinian acoustic reflectors may have been acquired during the Pliocene-Quaternary. The olivine basalt recovered at 78–79 mbsf may indicate local volcanism in earliest Pleistocene.

REFERENCES

Broecker, W. S., and Van Donk, J., 1970. Insolation changes, ice volume, and the ^{18}O record in deep-sea cores. *Rev. Geophys. Space Phys.*, 8:169–198.

Catalano, R., Ruggieri, G., and Sprovieri, R. (Eds.), 1978. Messinian evaporites in the Mediterranean. *Mem. Soc. Geol. Ital.*, 16.

Cifelli, R., 1974. Planktonic Foraminifera from the Mediterranean and adjacent Atlantic waters (cruise of the Atlantic II, 1969). *J. Foraminiferal. Res.*, 4:171–183.

Cita, M. B., 1975. Studi sul Pliocene e gli strati di passaggio del Miocene al Pliocene, VIII. Planktonic foraminiferal biozonation of the Mediterranean deep sea record: a revision. *Riv. Ital. Paleontol. Stratigr.*, 81,527–544.

Colantoni, P., Fabbri, A., Gallignani, P., Sartori, R., and Rehault, J.-P., 1981. Carta Lithologica e Stratigraphica del Mari Italiani. *Consiglio Naz. Ricerche Publ.* 4.

Decima, A., and Wezel, F. C., 1973. Late Miocene evaporites of the central Sicilian Basin. *In* Ryan, W.B.F., and Hsü, K. J., et al., *Init. Repts. DSDP*, 13: Washington (U.S. Govt. Printing Office), 1234–1240.

Della Vedova, B., Pellis, G., Foucher, J. P., Rehault, J.-P., 1984. Geothermal structure of the Tyrrhenian Sea. *Mar. Geol.*, 55:271–289.

D'Onofrio, S., Giannelli, L., Iaccarino, S., Morlotti, E., Romeo, M., Salvatorini, G., Sampo', M. and Sprovieri, R., 1975. Planktonic foraminifera from some Italian sections and the problem of the lower boundary of the Messinian. *Bol. Soc. Paleontol. Ital.*, 14:177–196.

Duschenes, J., Sinha, M. C., and Louden, K. E., 1986. A seismic refraction experiment in the Tyrrhenian Sea. *Geophys. J. R. Astron. Soc.*, 85:139–160.

Fabbri, A., and Curzi, P., 1979. The Messinian of the Tyrrhenian Sea. Seismic evidences and dynamic implications. *G. Geol.*, 2,43:215–248.

Fabbri, A., Gallignani, P., and Zitellini, N., 1981. Geologic evolution of the Peri-Tyrrhenian sedimentary basin. *In* Wezel, F. C. (Ed.) *Sedimentary basins of Mediterranean margins*: Bologna (Tecnoprint) 101–126.

Garrison, R. E., Schreiber, B. C., Bernoulli, D., Fabricius, F., Kidd, R. B., and Melieres, F., 1978. Sedimentary petrology and structures of Messinian evaporitic sediments in the Mediterranean Sea, Leg 42A, Deep Sea Drilling Project. *In* Hsü, K. J., and Montadert, L., et al., *Init. Repts. DSDP*, 42, Pt. 1: Washington (U.S. Govt. Printing Office) 571–612.

Heimann, K. O., and Mascle, G., 1974. Les séquences de la series évaporitique méssiniénne. *C. R. Acad. Sci. Paris Ser.* 2,279:1967–1970.

Hutchison, I., Von Herzen, R., Louden, K., Sclater, J., and Jemsek, J., 1985. Heat flow in the Balearic and Tyrrhenian basins, Western Mediterranean. *J. Geophys. Res.*, 90(B1):685–701.

Keller, J., 1981. Alkali basalts from the Tyrrhenian sea basin: magmatic and geodynamic significance. *Bull. Volcanol.*, 44:327–337.

Malinverno, A., Cafiero, M., Ryan, W.B.F., and Cita, M. B., 1981. Distribution of Messinian sediments and erosional surfaces beneath the Tyrrhenian Sea: geodynamic implications. *Oceanol. Acta*, 4: 489–496.

Marinelli, G., 1975. Magma evolution to Italy. *In* Squyres, C. (Ed.), *Geology of Italy, Tripoli, Libya*: Earth Sci. Soc. Libyan Arab Republic, 165–219.

Mazzei, R., Raffi, I., Rio, D., Hamilton, N., and Cita, M. B., 1979. Calibration of late Neogene calcareous plankton datum planes with the paleomagnetic record of Site 397 and correlation with Moroccan and Mediterranean sections. *In* Von Rad, U., Ryan, W.B.F., et al., *Init. Repts. DSDP*, 47, Pt. 1: Washington (U.S. Govt. Printing Office), 375–389.

McKenzie, D., 1978. Some remarks on the development of sedimentary basins. *Earth Planet. Sci. Lett.*, 40:25–32.

McKenzie, J. A., Jenkyns, H. C., and Bennett, G. C., 1979. Stable isotope study of the cyclic diatomite-claystones from the Tripoli formation, Sicily: A prelude to the Messinian salinity crisis. *Paleogeogr., Paleoclimatol., Paleoecol.*, 29(1/2):125–142.

Moussat, E., 1983. Evolution de la Mer Tyrrhénienne centrale et orientale et de ses marges septentrionales en relation avec la néotectonoque dans l'Arc Calabrais [Thesis]. Univ. Pierre et Marie Curie, Paris.

Moussat, E., Rehault, J.-P., Fabbri, A., and Mascle, G., 1985. Evolution géologique de la mer Tyrrhénienne. *C. R. Acad. Sci. Paris, Ser.* 2, 301:491–496.

Murray, J. W., 1973. *Distribution and Ecology of Living Benthic Foraminiferids.* Portsmouth, NH (Heinemann Educational Books).

Parker, F. L., 1955. Distribution of planktonic foraminifera in some Mediterranean sediments. *Papers in Marine Biology and Oceanography*: London (Pergamon Press), 204–241.

________, 1958. Eastern Mediterranean foraminifera. *Rep. Swed. Deep-Sea Exped.*, 8:219–283.

Recq, M., Rehault, J.-P., Steinmetz, L., and Fabbri, A., 1984. Amincicement de la croute et accrétion au centre du bassin Tyrrhénien d'aprés la sismique réfraction. *Mar. Geol.*, 55:411–428.

Rehault, J.-P., Tisseau, C., and Fouchet, J. P., 1984. Structure, subsidence et flux thermique de la Mer Tyrrhénienne Centrale: éssais de modelisation. CIESM, (29th meeting) 11–19 October 1984, Lucerne.

Rio, D., Sprovieri, R., Di Stefano, I., and Raffi, I., 1984a. *Globorotalia truncatulinoides* (d'Orbigny) in the Mediterranean upper Pliocene geologic record. *Micropaleontology*, 30:121–137.

Rio, D., Sprovieri, R., and Raffi, I., 1984b. Calcareous plankton biostratigraphy and biochronology of the Pliocene-lower Pleistocene succession of the Capo Rossello area (Sicily). *Mar. Micropaleontol.*, 9:135–180.

Ruggieri, G., and Sprovieri, R., 1983. Recenti progressi nella stratigraffia del Pleistocene inferiore. *Bol. Soc. Paleontol. Ital.,* 22:3, 315–321.

Ruggieri, G., Rio, D., and Sprovieri, R., 1984. Remarks on the chronostratigraphic classification of Lower Pleistocene. *Bol. Soc. Geol. Ital.*, 103:252-259.

Steinmetz, L., Ferrucci, F., Hirn, A., Morelli, C., and Nicolich, R., 1983. A 550 km long moho traverse in the Tyrrhenian Sea from O.B.S. recorded Pn waves. *Geophys. Res. Lett.*, 10(6):428–431.

Thunell, R. C., 1978. Distribution of Recent planktonic foraminifera in surface sediments of the Mediterranean Sea. *Mar. Micropaleontol.*, 3:147–173.

Todd, R., 1958. Foraminifera from Western Mediterranean Deep-Sea cores. *Rep. Swed. Deep-Sea Exped.*, 3:169–215.

SITE 654 HOLE A CORE 1 R CORED INTERVAL 2208.0-2212.6 mbsl; 0.0-4.6 mbsf

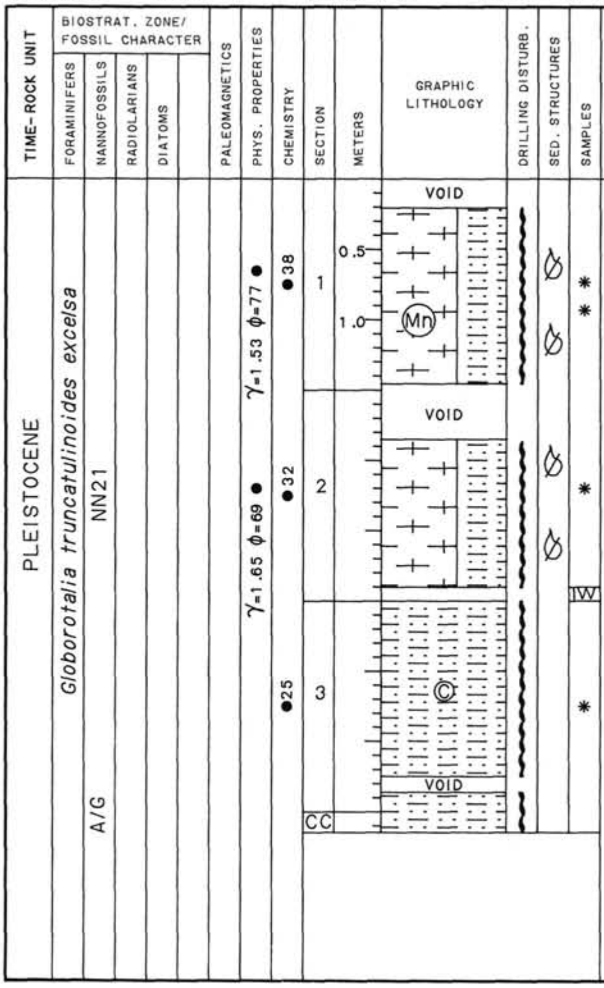

LITHOLOGIC DESCRIPTION

MARLY FORAMINIFER-NANNOFOSSIL OOZE and CALCAREOUS MUD

Marly foraminifer-nannofossil ooze and calcareous mud, very disturbed by drilling, with thin intervals rich in black manganese micronodules and scattered, mostly broken, pteropod shells. No obvious textures or coarse layers. Colors are light olive-brown (2.5Y 5/4) in Section 1, 0–130 cm, becoming light olive-gray (5Y 6/2) downcore throughout Section 2. Section 3 and CC are grayish brown (2.5Y 5/2). One oxidized layer, olive-yellow (2.5Y 6/6), exists in Section 1, 135 cm, and a few dark patches and specks in Section 3.

SMEAR SLIDE SUMMARY (%):

	1, 75 D	1, 95 M	2, 75 D	3, 75 D
TEXTURE:				
Sand	20	15	15	15
Silt	20	20	20	20
Clay	60	65	65	65
COMPOSITION:				
Quartz	7	8	10	5
Mica	3	1	3	2
Clay	21	47	32	36
Volcanic glass	5	4	8	5
Dolomite	4	8	5	5
Accessory minerals	3	3	2	2
Pyrite	2	2	1	2
Limonite/oxides	—	1	3	—
Organic matter	—	2	—	3
Foraminifers	12	4	8	5
Nannofossils	30	10	20	30
Diatoms	Tr	2	Tr	—
Radiolarians	1	1	Tr	Tr
Sponge spicules	1	Tr	—	—
Silicoflagellates	1	—	—	—
Fish remains	—	—	Tr	—
Plant debris	Tr	—	—	Tr
Micrite	5	7	8	5
Gypsum?	—	—	—	Tr

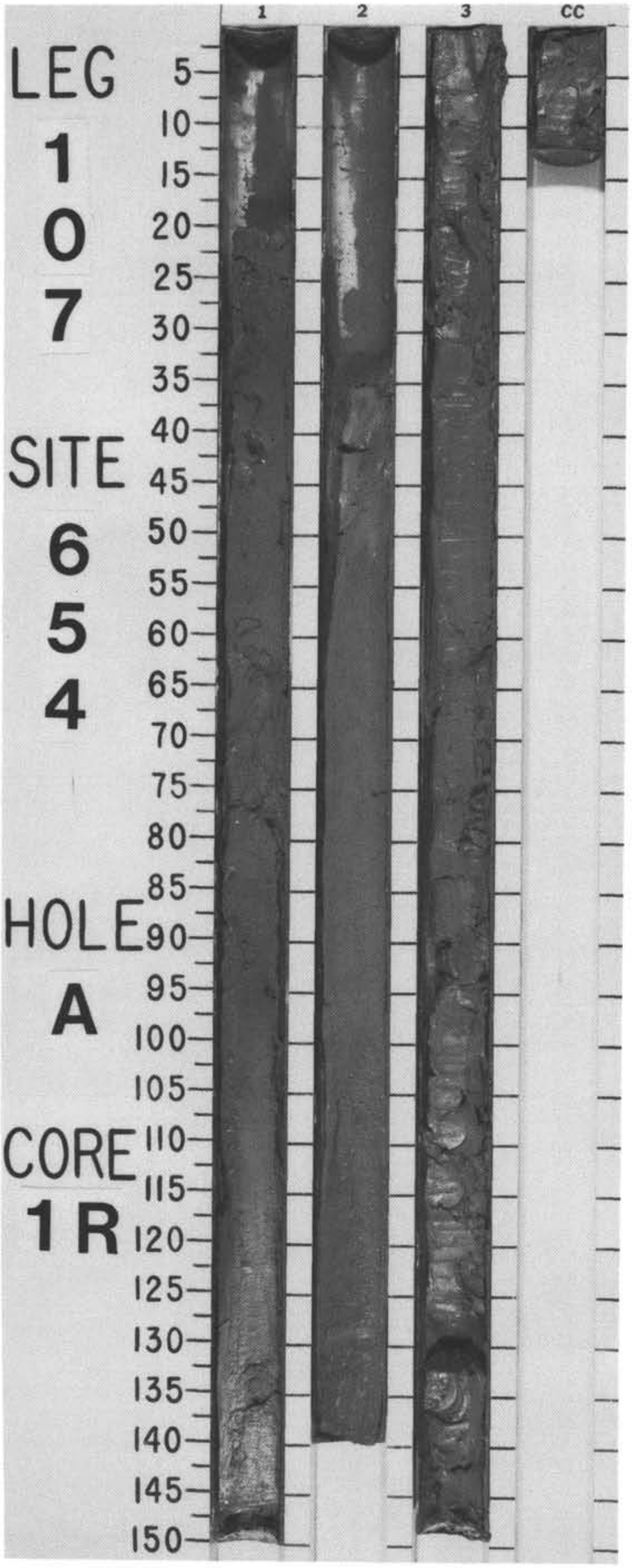
1
2
3
CC
LEG
107
SITE
654
HOLE
A
CORE
1R
5
10
15
20
25
30
35
40
45
50
55
60
65
70
75
80
85
90
95
100
105
110
115
120
125
130
135
140
145
150

SITE 654 HOLE A CORE 2 R CORED INTERVAL 2212.6-2220.0 mbsl; 4.6-12.0 mbsf

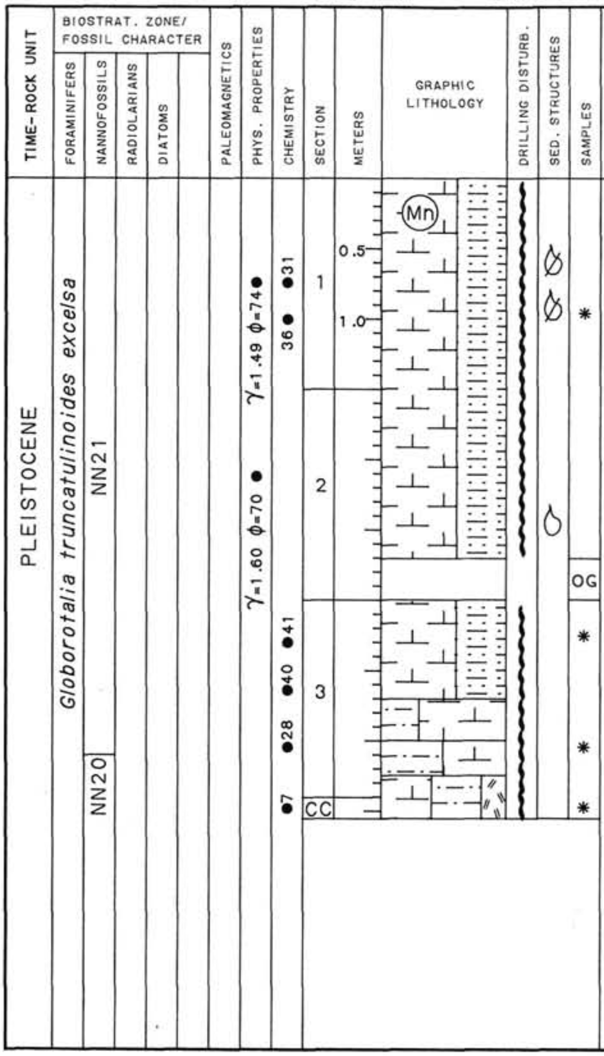

LITHOLOGIC DESCRIPTION

MARLY NANNOFOSSIL OOZE and VOLCANIC ASH-RICH SAND

Marly nannofossil ooze and minor volcanic ash-rich sand, very disturbed by drilling; top portion of core is grayish brown (2.5Y 5/2) becoming olive-gray (5Y 5/2) in most of Sections 1, 2, and 3; minor interbedded colors are light olive-brown (2.5Y 5/6) (oxidation layer in Section 1, 30 cm), light gray (N 6/), and pale olive (5Y 6/3) (discrete intervals in Section 3); bottom 15 cm in Section 3 and CC show various gray and brownish-gray tones; sand in CC is dark olive-gray (5Y 3/2).

Details: Section 1 has a thin interval rich in black manganese micronodules. Some pteropods are scattered throughout core; their shells are usually broken, with the exception of a cluster of entire skeletons in Section 2, 97–100 cm. Two coarser grained zones are observed: the first one contains scattered chunks in Section 3, 70–120 cm; the second is a dark, sandy layer in CC. The coarse layers are terrigenous; some volcaniclastics appear in the CC sand and in the dominant ooze.

SMEAR SLIDE SUMMARY (%):

	1, 100 D	3, 30 M	3, 104 M	CC, 9 M
TEXTURE:				
Sand	5	5	25	55
Silt	15	10	20	30
Clay	80	85	55	15
COMPOSITION:				
Quartz	10	5	10	15
Feldspar	—	—	—	10
Rock fragments	—	—	—	8
Mica	1	1	1	6
Clay	36	38	39	15
Volcanic glass	10	2	2	18
Calcite	—	—	—	10
Dolomite	8	5	6	1
Accessory minerals	—	1	1	5
Foraminifers	3	3	5	3
Nannofossils	25	45	20	6
Diatoms	Tr	Tr	Tr	—
Radiolarians	Tr	—	—	Tr
Sponge spicules	1	—	—	—
Micrite	—	—	15	2
Gypsum?	1	—	1	—

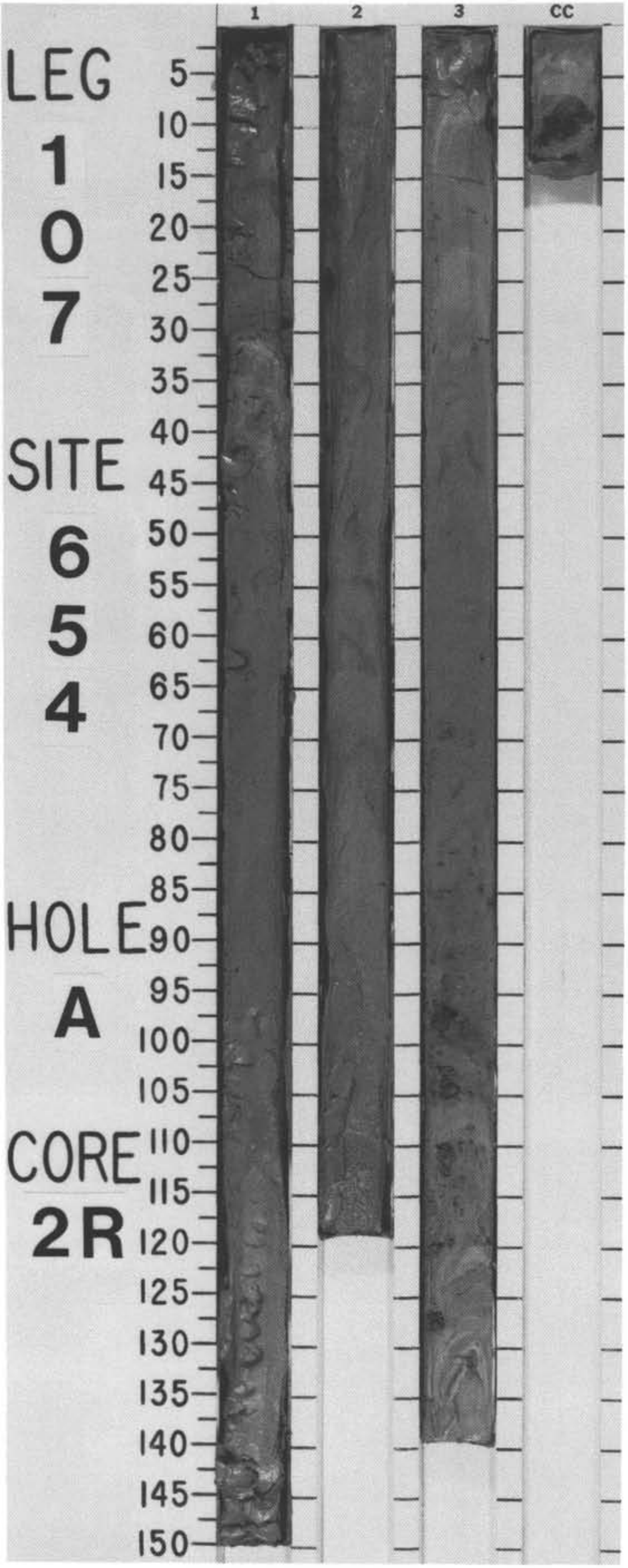
LEG
107
SITE
654
HOLE
A
CORE
2R
1
2
3
CC
5
10
15
20
25
30
35
40
45
50
55
60
65
70
75
80
85
90
95
100
105
110
115
120
125
130
135
140
145
150

SITE 654 HOLE A CORE 3 R CORED INTERVAL 2220.0-2229.4 mbsl; 12.0-21.4 mbsf

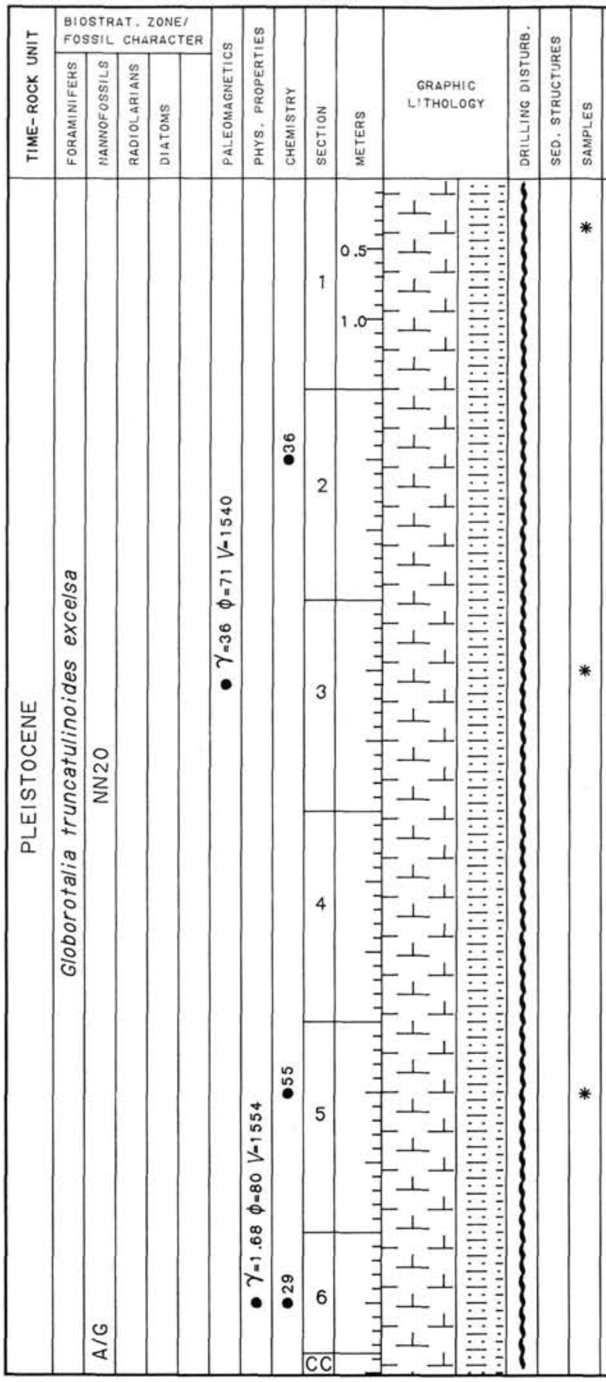

LITHOLOGIC DESCRIPTION

MARLY NANNOFOSSIL OOZE and VOLCANIC ASH

Marly nannofossil ooze and minor volcanic ash, very disturbed; rare volcanic ash in Section 1, 20–23 cm. Core was apparently originally color banded; colors are light olive-gray (5Y 6/2), pale olive (5Y 6/3), light gray (5Y 7/2), olive (5Y 5/6), white (5Y 8/2, 8/1), and olive-gray (5Y 5/2).

Details: Section 3, 90–140 cm, is less disturbed and contains scattered foraminifers; Section 4, 0–150 cm, contains mottled, gray, sulfide-rich areas; in Section 5 there is a progressive upward change from yellowish green (10GY 6/2) to light gray (5Y 7/2); in Section 6, 38 cm, a miliolid is present.

SMEAR SLIDE SUMMARY (%):

	1, 22 M	3, 3 D	6, 10 D
TEXTURE:			
Sand	40	5	5
Silt	50	15	30
Clay	10	80	65
COMPOSITION:			
Quartz	10	4	5
Feldspar	Tr	1	—
Mica	Tr	1	Tr
Clay	12	39	25
Volcanic glass	50	3	1
Dolomite	—	Tr	2
Opaques	5	1	5
Pyroxene	8	—	—
Zeolite/analcite	Tr	—	—
Nepheline/limonite?	Tr	—	—
Foraminifers	—	10	10
Nannofossils	—	40	44
Sponge spicules	—	—	1
Silicoflagellates	—	1	—
Intraclasts	5	—	—
Bioclasts	—	Tr	5
Gypsum	—	—	2
Pteropods	—	—	Tr

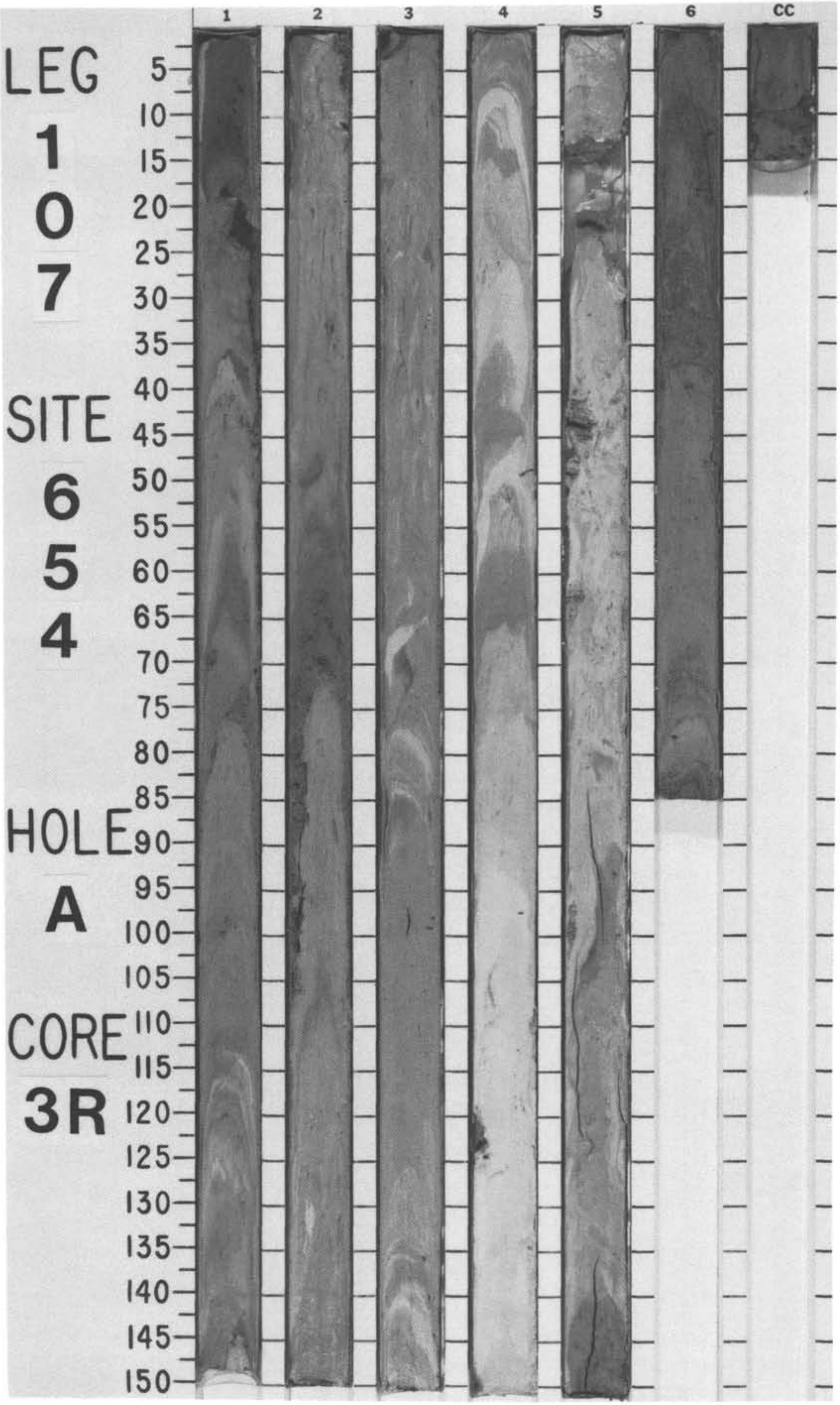
LEG 107
SITE 654
HOLE A
CORE 3R
1
2
3
4
5
6
CC
5
10
15
20
25
30
35
40
45
50
55
60
65
70
75
80
85
90
95
100
105
110
115
120
125
130
135
140
145
150

SITE 654 HOLE A CORE 4 R CORED INTERVAL 2229.4-2238.8 mbsl; 21.4-30.8 mbsf

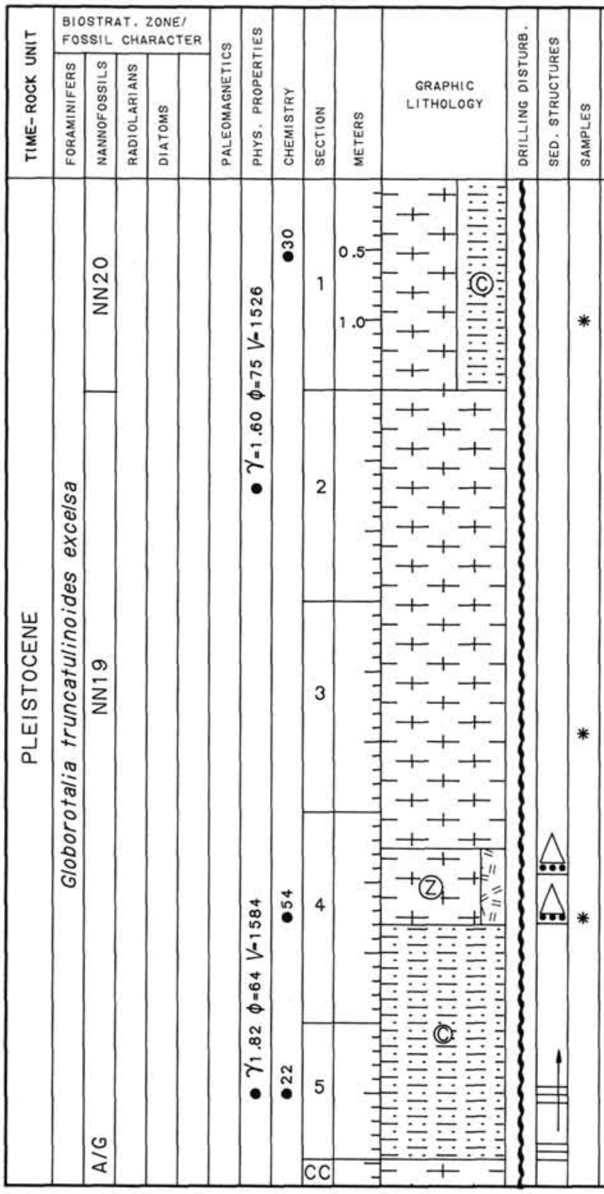

LITHOLOGIC DESCRIPTION

FORAMINIFER-NANNOFOSSIL OOZE and CALCAREOUS MUD

Foraminifer-nannofossil ooze and calcareous mud, very disturbed, with minor volcaniclastic-bearing ooze, light olive-gray (5Y 6/2), pale olive (5Y 6/3), pale yellow (5Y 7/3, 7/4), gray (5Y 5/1, 6/1), white (5Y 8/2), light gray (5Y 7/1, 7/2), and olive-gray (5Y 5/2).

Details: Sections 1, 2, and 3 contain gray (5Y 5/1), mottled areas of FeS_2 (iron sulfide?); in Section 4 there are two graded units made by marly nannofossil ooze with 20% volcanic glass that shows some alteration to zeolites.

SMEAR SLIDE SUMMARY (%):

	1, 100 D	3, 100 D	4, 76 M
TEXTURE:			
Sand	5	5	30
Silt	15	10	40
Clay	85	85	30
COMPOSITION:			
Quartz	1	Tr	5
Feldspar	—	—	Tr
Mica	—	Tr	3
Clay	26	21	20
Volcanic glass	Tr	—	20
Dolomite	Tr	Tr	—
Accessory minerals	1	1	—
Opaques	—	—	5
Foraminifers	10	5	5
Nannofossils	60	70	30
Sponge spicules	—	—	2
Fish remains	—	1	—
Intraclasts	1	—	5
Zeolite	—	—	2
Pyroxenes	—	—	3

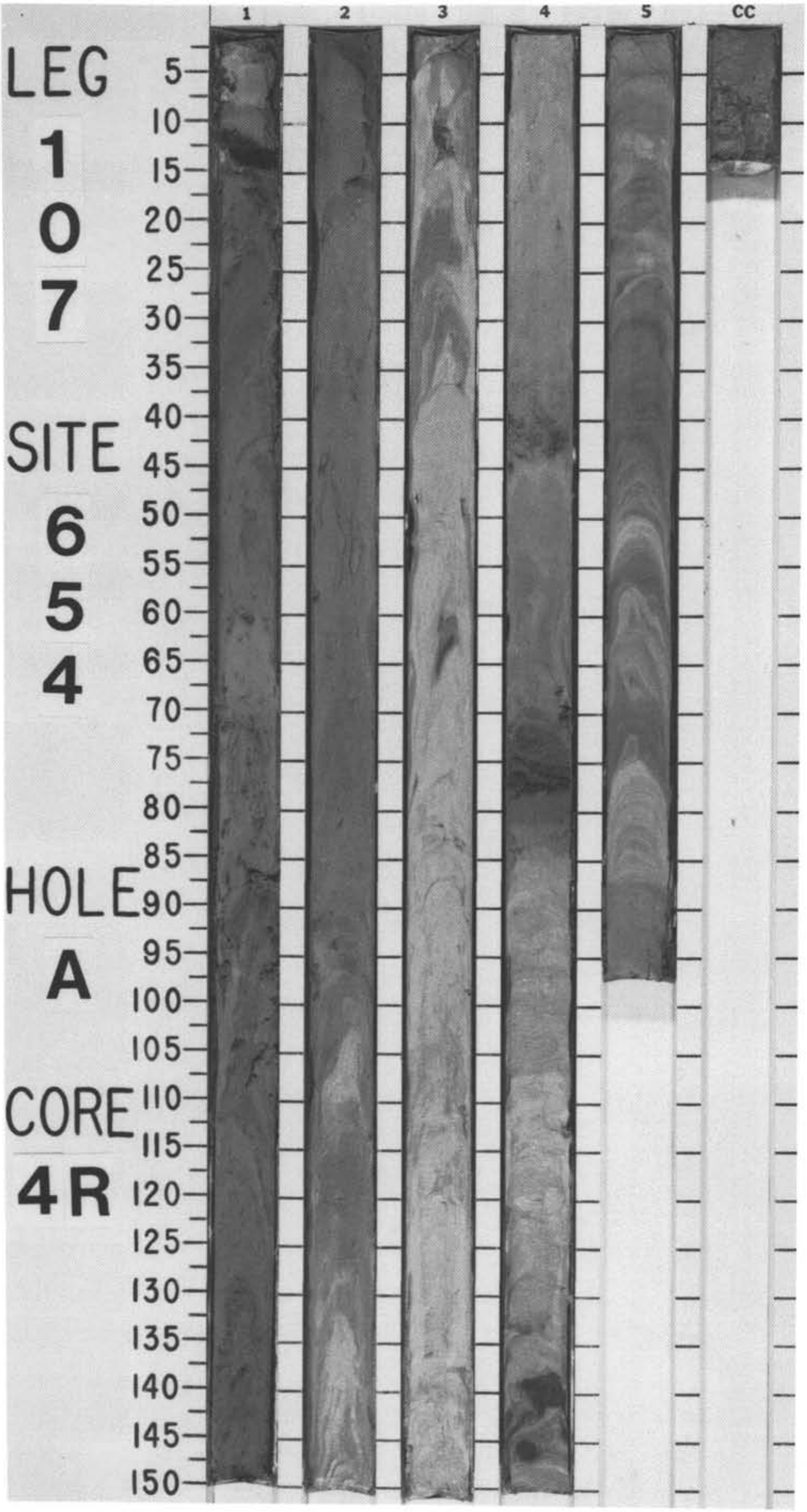
LEG
1
0
7
SITE
6
5
4
HOLE
A
CORE
4R
1
2
3
4
5
CC
5
10
15
20
25
30
35
40
45
50
55
60
65
70
75
80
85
90
95
100
105
110
115
120
125
130
135
140
145
150

SITE 654 HOLE A CORE 5 R CORED INTERVAL 2238.8-2248.3 mbsl; 30.8-40.3 mbsf

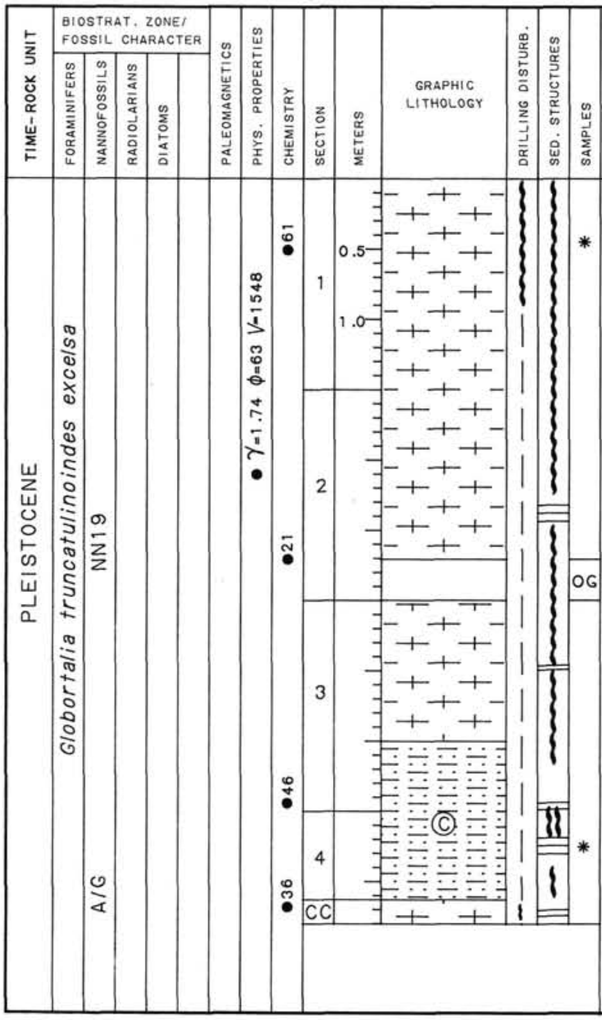

LITHOLOGIC DESCRIPTION

FORAMINIFER-NANNOFOSSIL OOZE and CALCAREOUS MUD

Foraminifer-nannofossil ooze and calcareous mud, with subordinate organic-rich nannofossil ooze, white (5Y 8/1), pale olive (5Y 6/3), gray (5Y 5/1), olive (5Y 5/3), dark olive-gray (5Y 3/2), pale yellow (5Y 7/3), light olive-gray (5Y 6/2), very pale brown (10YR 7/4), yellow (2.5Y 7/6), light brownish gray (2.5Y 6/2), light gray (2.5Y 7/2, N 6/), and dark grayish brown (2.5Y 4/2).

Details: above Section 1, 90 cm, the degree of disturbance increases and there are many FeS_2 (iron sulfide?) mottled areas; in Section 2, 80–84 cm, and Section 3, 128–130 cm, there is an orange, limonitic stain; Section 4 contains two organic-rich layers, gray mud (40–50 cm) and whitish mud (33-40 cm) which pass upward into a gray, organic-rich layer (28–32 cm), whitish mud (23–28 cm) and gray, organic- rich, nannofossil ooze layer (0–23 cm). CC, 0–6 cm, contains similar organic-rich nannofossil ooze. A smear slide of Section 4, 30.5 cm, contains muscovite in the organic-rich layer.

SMEAR SLIDE SUMMARY (%):

	1, 52 D	4, 30 M
TEXTURE:		
Sand	—	15
Silt	5	10
Clay	95	75
COMPOSITION:		
Quartz	Tr	2
Mica	Tr	6
Clay	35	13
Volcanic glass	—	Tr
Dolomite	Tr	—
Organic matter	—	15
Foraminifers	12	15
Nannofossils	35	45
Sponge spicules	3	3
Flagellates	Tr	—
Intraclasts	5	—
Micrite	10	—
Pellets	—	1

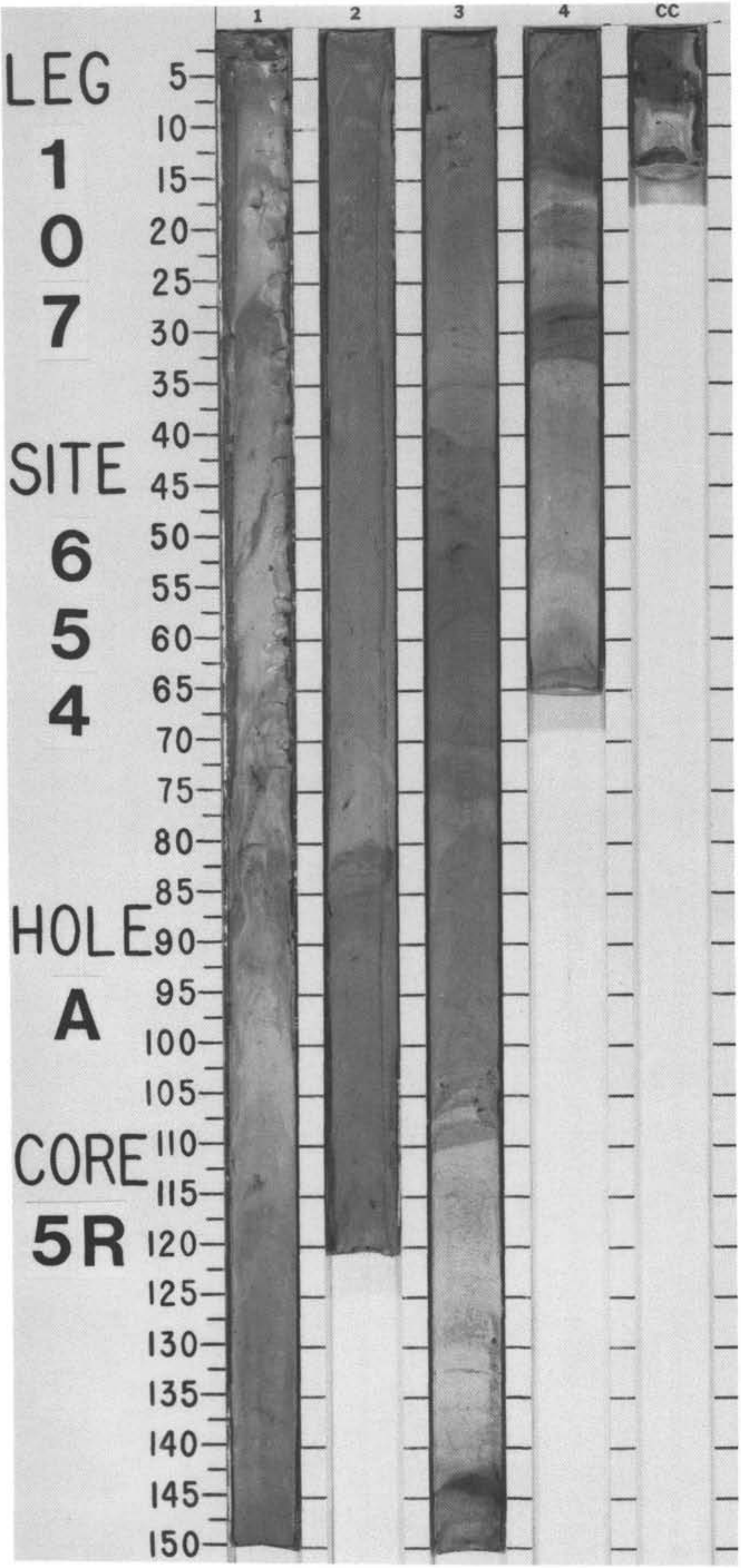
LEG
1
0
7
SITE
6
5
4
HOLE
A
CORE
5R
1
2
3
4
CC
5
10
15
20
25
30
35
40
45
50
55
60
65
70
75
80
85
90
95
100
105
110
115
120
125
130
135
140
145
150

SITE 654 HOLE A CORE 6 R CORED INTERVAL 2248.3-2257.7 mbsl; 40.3-49.7 mbsf

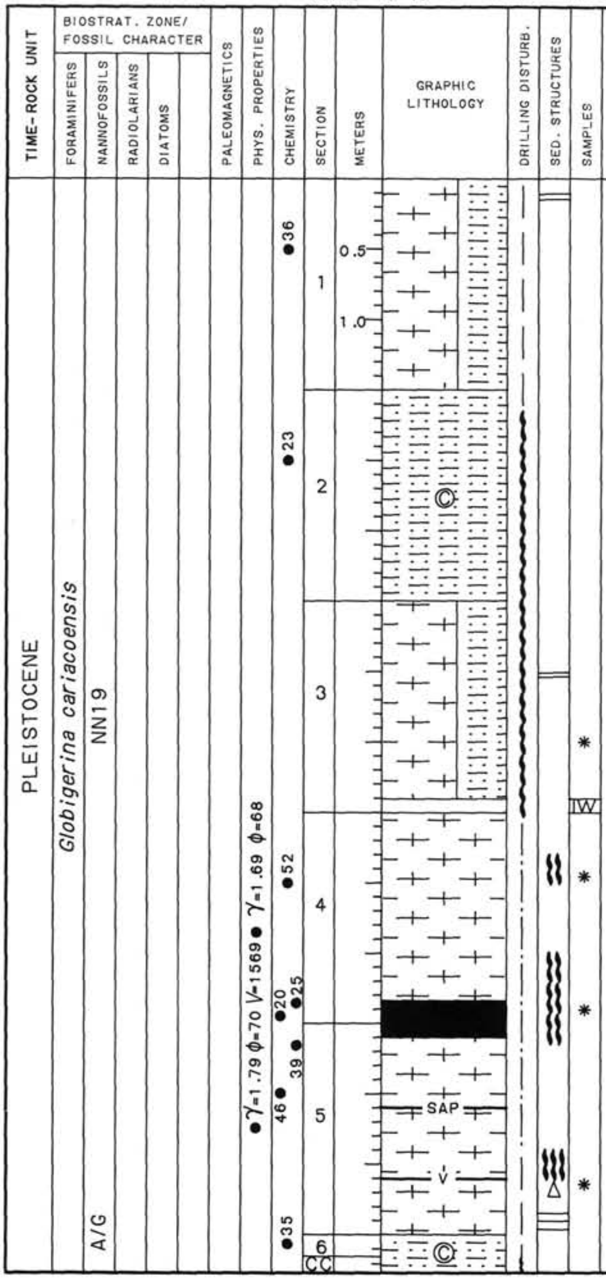

LITHOLOGIC DESCRIPTION

MARLY FORAMINIFER-NANNOFOSSIL OOZE and SAPROPEL

Marly foraminifer-nannofossil ooze and minor sapropel, light gray (2.5Y 7/0, 5Y 7/1-7/2), gray (5Y 5/1, 6/1), dark gray (5Y 4/1), very dark gray (5Y 3/1), pale yellow (5Y 7/3), yellow (5Y 7/6, 8/6), light olive-gray (5Y 6/2), olive-gray (5Y 4/2), and pale olive (5Y 6/3).

Details: foraminifers are scattered throughout Section 1, and coring disturbance gives rise to streaky texture; Sections 2 and 3 are very disturbed, giving rise to vertical streaky lamination; Section 4 is composed of strongly disturbed mud with a probable pyritized worm burrow at 60 cm (50 × 10 × 5 mm, 1/2 round) and a sapropel layer, very dark gray (5Y 3/1), at 135–150 cm; in Section 5, the sapropel layer continues to 7 cm, and there is another sapropelic layer at 60 cm; a 2-cm-thick silty-ash layer is present at 108–110 cm, and the rest of this Section is very disturbed mud; Section 6 is homogeneous gray mud; CC is weakly calcareous, homogeneous mud.

SMEAR SLIDE SUMMARY (%):

	3, 100 D	4, 50 M	4, 145 M	5, 107 M
TEXTURE:				
Sand	—	10	—	30
Silt	5	10	10	60
Clay	95	80	90	10
COMPOSITION:				
Quartz	5	—	3	35
Mica	—	—	5	5
Clay	40	40	35	10
Volcanic glass	1	—	—	—
Dolomite	4	5	Tr	—
Accessory minerals	1	5	—	—
Gypsum	2	Tr	—	—
Zeolite needles	5	—	Tr	5
Opaques	12	—	12	15
Foraminifers	5	10	2	10
Nannofossils	35	30	33	20
Sponge spicules	—	1	—	—
Flagellates	2	3	—	—
Plant debris	—	—	Tr	—
Limonite	10	—	10	—
Bioclasts	—	1	—	—
Intraclasts	—	5	—	—

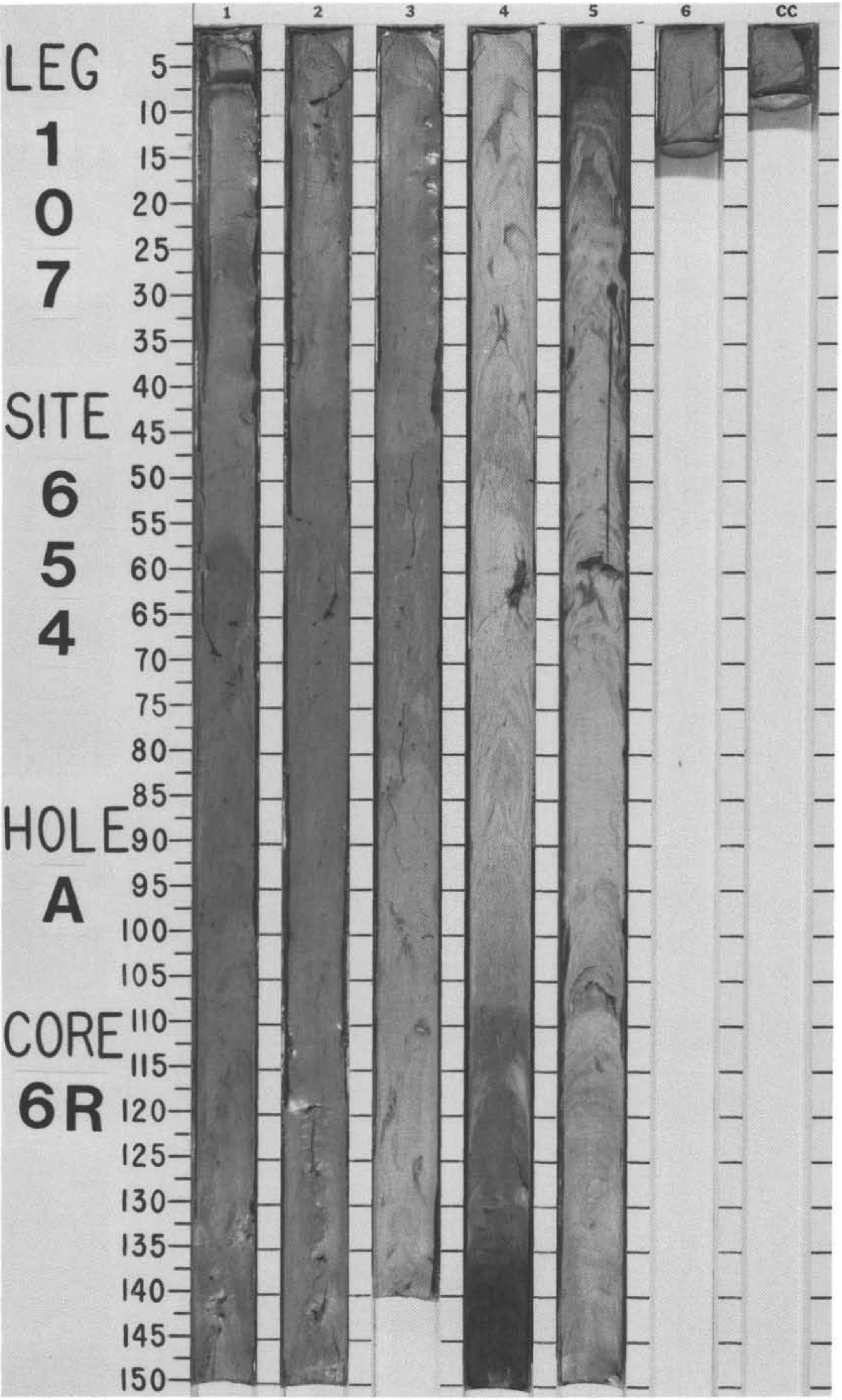
LEG
107
SITE
654
HOLE
A
CORE
6R
1
2
3
4
5
6
CC
5
10
15
20
25
30
35
40
45
50
55
60
65
70
75
80
85
90
95
100
105
110
115
120
125
130
135
140
145
150

SITE 654 HOLE A CORE 7 R CORED INTERVAL 2257.7-2267.1 mbsl; 49.7-59.1 mbsf

TIME-ROCK UNIT	BIOSTRAT. ZONE/ FOSSIL CHARACTER				PALEOMAGNETICS	PHYS. PROPERTIES	CHEMISTRY	SECTION	METERS	GRAPHIC LITHOLOGY	DRILLING DISTURB.	SED. STRUCTURES	SAMPLES
	FORAMINIFERS	NANNOFOSSILS	RADIOLARIANS	DIATOMS									
PLEISTOCENE	*Globigerina cariacoensis*	C/G NN19					26 ●	CC					*

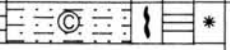

LITHOLOGIC DESCRIPTION

CALCAREOUS MUD

Calcareous mud; 25 cm of olive-gray (5Y 4/2, 5/2), homogeneous mud were recovered.

SMEAR SLIDE SUMMARY (%):

	CC, 11 D
TEXTURE:	
Sand	15
Silt	30
Clay	55
COMPOSITION:	
Quartz	15
Clay	35
Volcanic glass	5
Dolomite	5
Gypsum	3
Foraminifers	10
Nannofossils	27

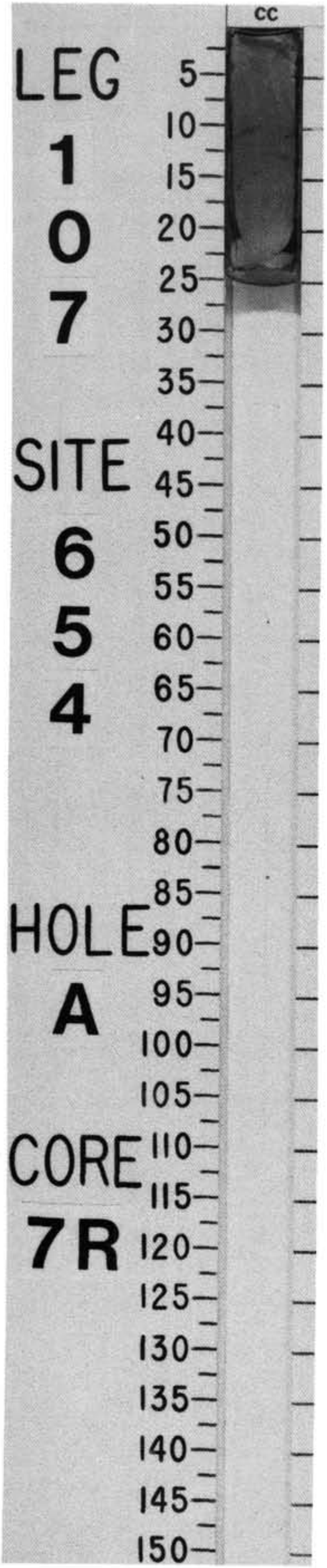
CC
LEG
107
SITE
654
HOLE
A
CORE
7R
5
10
15
20
25
30
35
40
45
50
55
60
65
70
75
80
85
90
95
100
105
110
115
120
125
130
135
140
145
150

SITE 654 HOLE A CORE 8 R CORED INTERVAL 2267.1-2277.3 mbsl; 59.1-69.3 mbsf

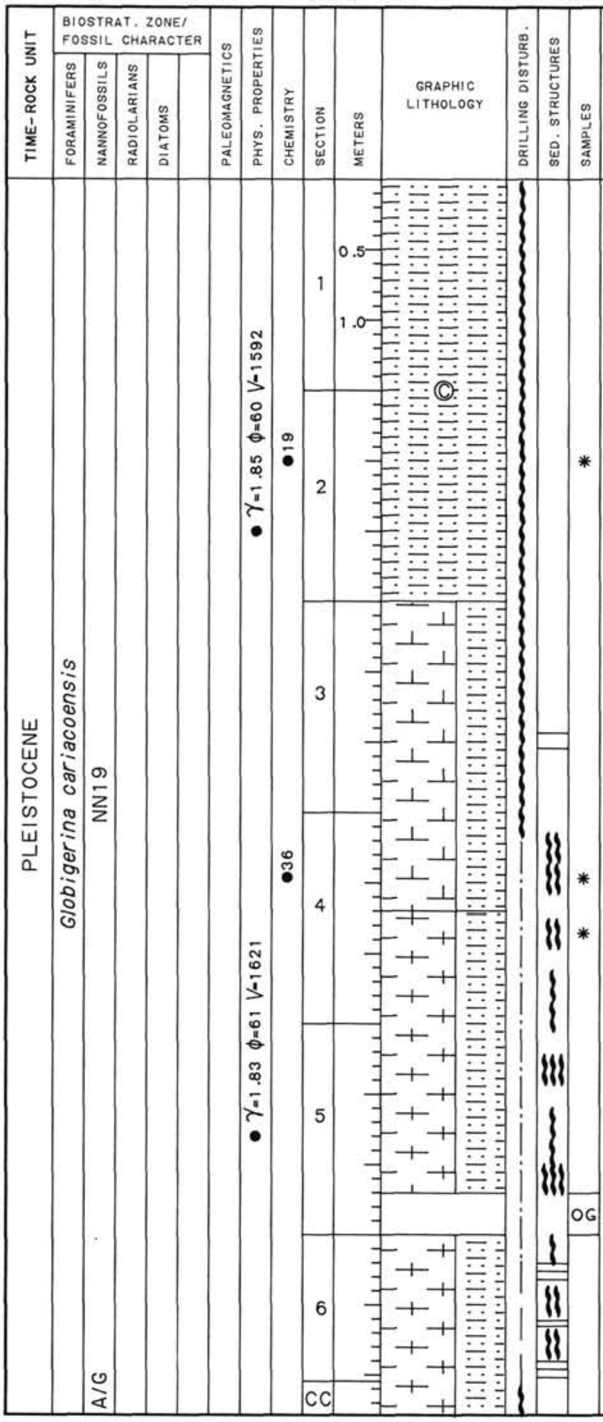

LITHOLOGIC DESCRIPTION

MARLY FORAMINIFER-NANNOFOSSIL OOZE, MARLY NANNOFOSSIL OOZE, and CALCAREOUS MUD

Marly foraminifer-nannofossil ooze, marly nannofossil ooze, and calcareous mud, very disturbed to moderately disturbed, light gray (2.5Y 7/0, 5Y 7/1–7/2), gray (5Y 6/1), dark gray (5Y 4/1), light olive-brown (2.5Y 5/6), light olive-gray (5Y 6/2), and olive-gray (5Y 5/2).

Details: Section 1 is very soupy; Section 2 contains FeS_2 hydrotroilite blebs throughout; Section 3 is very disturbed; Section 4 is burrowed, clay-rich, nannofossil ooze with many blackish patches at 0–30 cm and a darker, organic-rich layer at 40–60 cm; Section 5, FeS_2 hydrotroilite blebs; Section 6 and CC are very homogeneous.

SMEAR SLIDE SUMMARY (%):

	2, 50 D	4, 40 M	4, 83 M
TEXTURE:			
Sand	—	—	—
Silt	15	15	5
Clay	85	85	95
COMPOSITION:			
Quartz	3	1	Tr
Mica	1	Tr	—
Clay	11	4	30
Volcanic glass	Tr	—	—
Dolomite	1	4	Tr
Accessory minerals	1	—	—
Zeolite	2	—	—
Organics	—	23	—
Foraminifers	10	2	10
Nannofossils	70	65	60
Sponge spicules	1	—	—
Fish remains	—	1	—

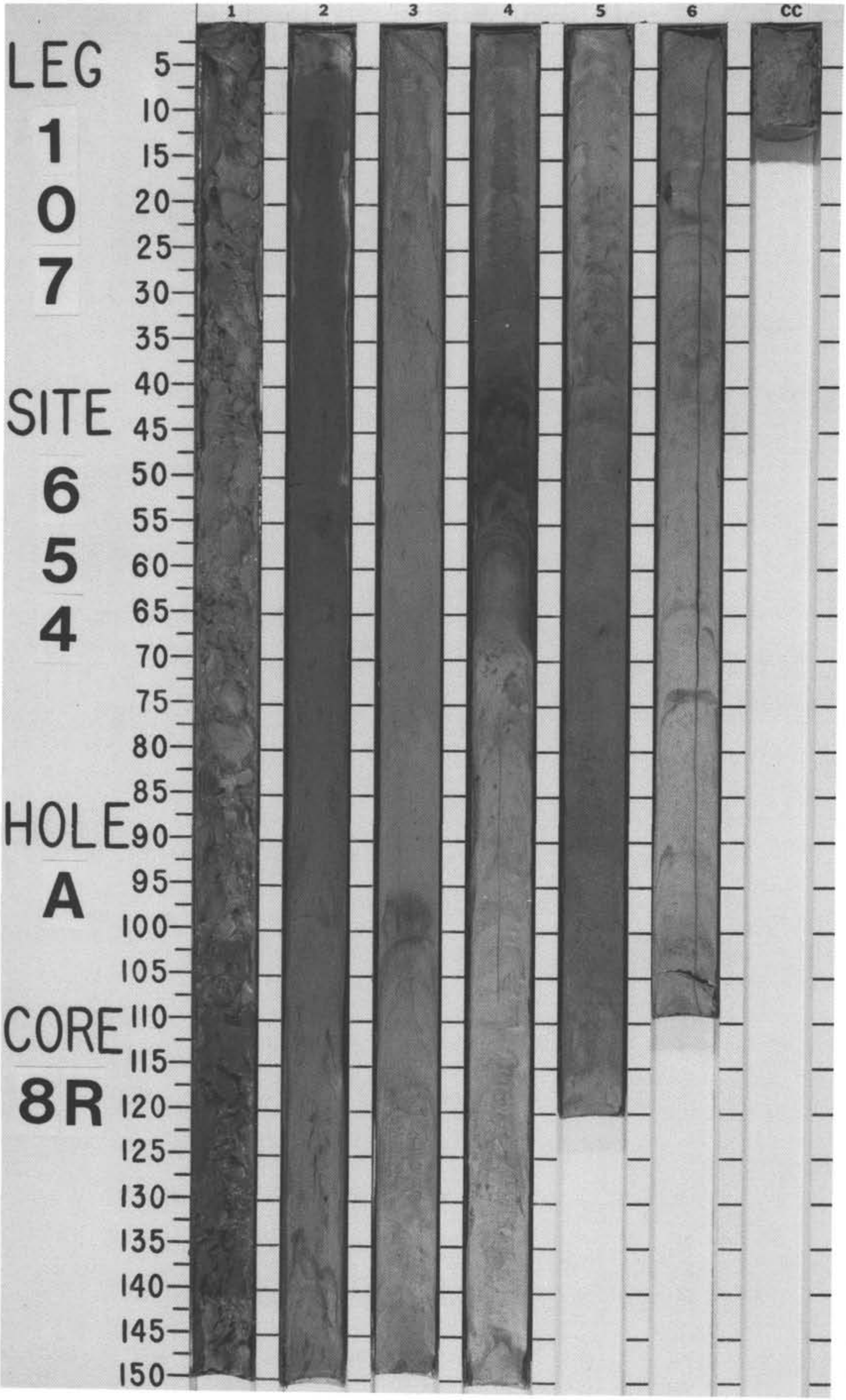
LEG
107
SITE
654
HOLE
A
CORE
8R
1
2
3
4
5
6
CC
5
10
15
20
25
30
35
40
45
50
55
60
65
70
75
80
85
90
95
100
105
110
115
120
125
130
135
140
145
150

SITE 654 HOLE A CORE 9 R CORED INTERVAL 2277.3-2287.0 mbsl; 69.3-79.0 mbsf

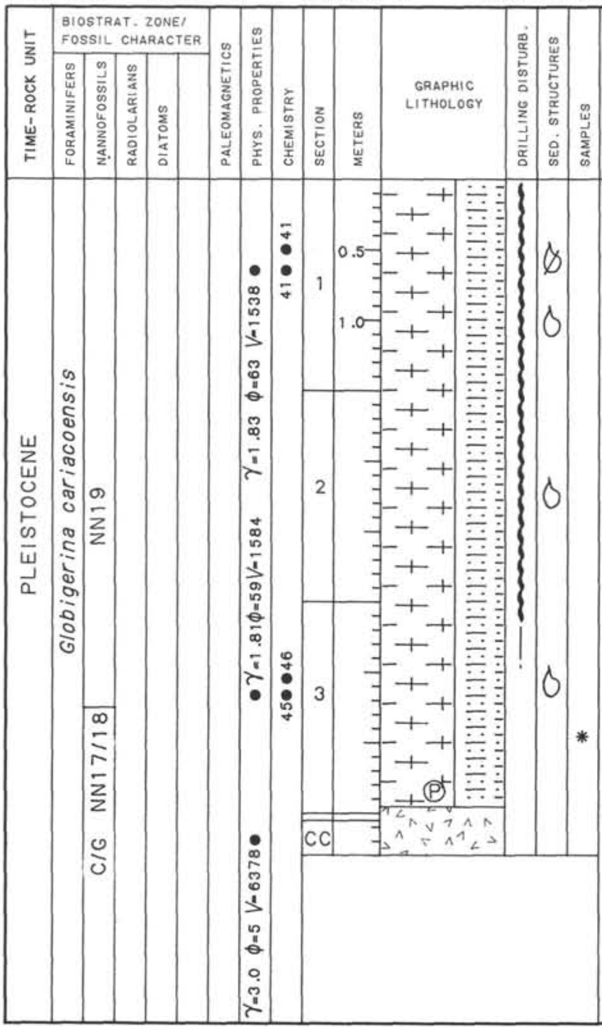

LITHOLOGIC DESCRIPTION

MARLY FORAMINIFER-NANNOFOSSIL OOZE and BASALT PEBBLES

Marly foraminifer-nannofossil ooze and basalt pebbles; sediment is gray (5Y 5/1, 5GY 5/1) and contains scattered foraminifer tests, rare mollusc fragments, and a few dark gray specks and streaks (possibly pyrite bearing); one greenish gray (5G 5/1) pyrite-rich zone occurs in Section 3, 135–145 cm, just above the occurrence of basalt. The true contact between ooze and basalt was not recovered. Dark gray olivinic basalt pebbles occur, one in Section 3, one in Section 4, and two in CC.

SMEAR SLIDE SUMMARY (%):

	3, 100 D
TEXTURE:	
Sand	25
Silt	10
Clay	65
COMPOSITION:	
Quartz	12
Mica	Tr
Clay	29
Volcanic glass	3
Dolomite	15
Accessory minerals	1
Pyrite	2
Foraminifers	15
Nannofossils	15
Diatoms	Tr
Radiolarians	2
Sponge spicules	1
Silicoflagellates	Tr
Micrite	5

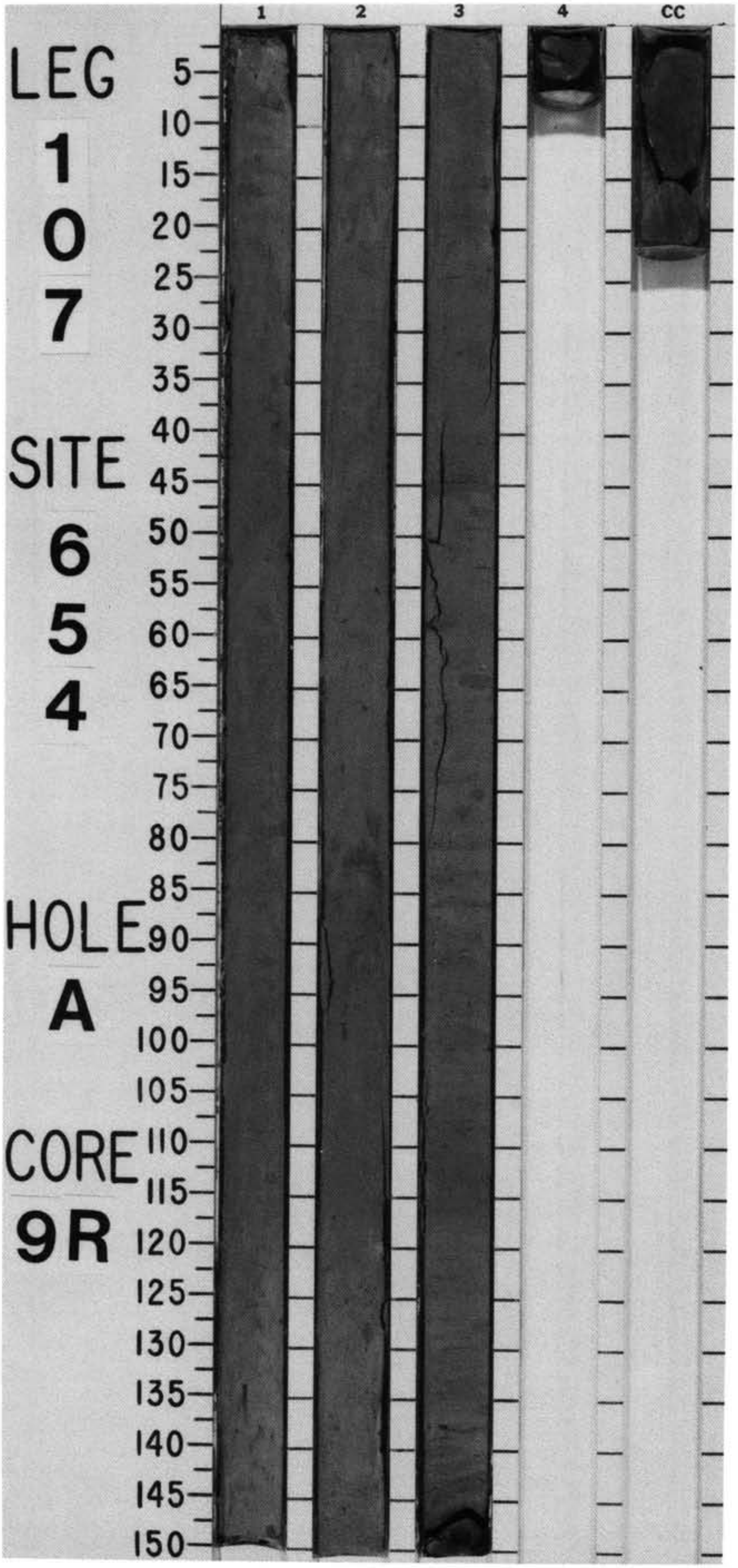
LEG
1
0
7
SITE
6
5
4
HOLE
A
CORE
9R
1
2
3
4
CC
5
10
15
20
25
30
35
40
45
50
55
60
65
70
75
80
85
90
95
100
105
110
115
120
125
130
135
140
145
150

SITE 654 HOLE A CORE 10 R CORED INTERVAL 2287.0-2296.7 mbsl; 79.0-88.7 mbsf

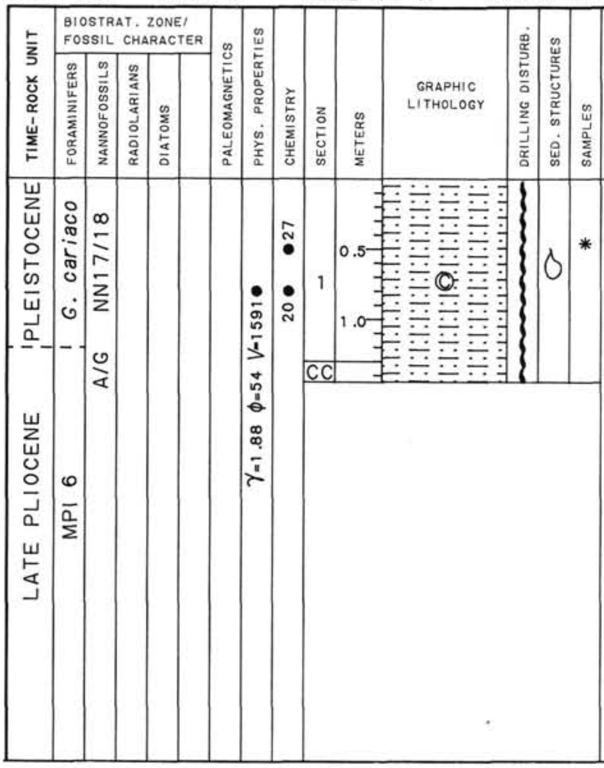

LITHOLOGIC DESCRIPTION

CALCAREOUS MUD

Calcareous mud, severely deformed, olive-gray (10Y 6/1, 5Y 5/2), with very dark gray specks and abundant, scattered foraminifer tests.

SMEAR SLIDE SUMMARY (%):

	1, 50 D
TEXTURE:	
Sand	15
Silt	15
Clay	70
COMPOSITION:	
Quartz	10
Mica	1
Clay	15
Volcanic glass	Tr
Dolomite	4
Accessory minerals	1
Pyrite	1
Zeolites	Tr
Foraminifers	12
Nannofossils	45
Diatoms	1
Radiolarians	1
Sponge spicules	Tr
Silicoflagellates	Tr
Micrite	8

SITE 654 HOLE A CORE 11 R CORED INTERVAL 2296.7-2306.4 mbsl; 88.7-98.4 mbsf

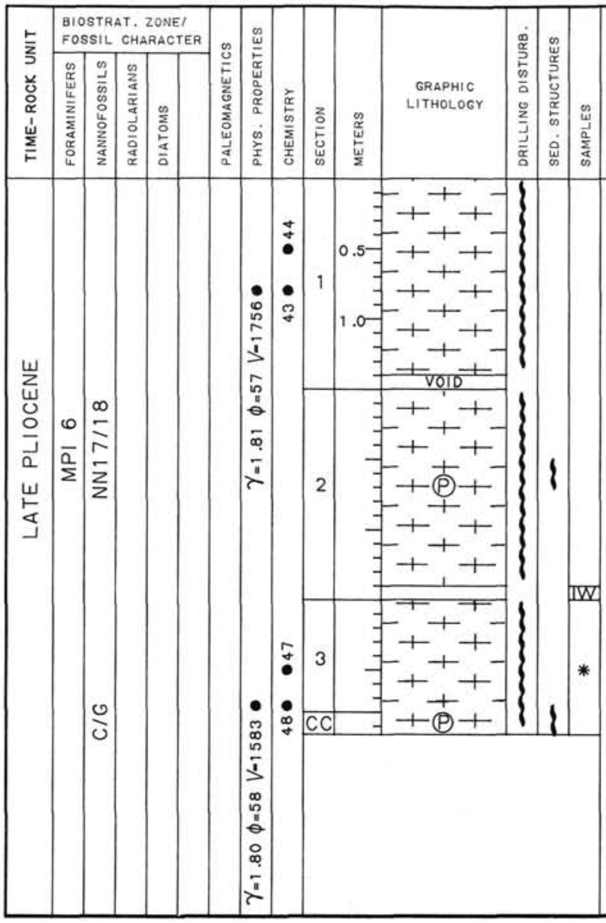

LITHOLOGIC DESCRIPTION

FORAMINIFER-NANNOFOSSIL OOZE

Foraminifer-nannofossil ooze, very severely disturbed, gray (5Y 6/1) in Sections 1 and 2, light olive-gray (5Y 6/2) in Section 3 and CC, with one olive (5Y 5/3) interval in Section 3, 60–90 cm. Pyrite-rich patches occur as displaced former burrow molds. In Section 3, 67–72 and 103–104.5 cm, framboidal pyrite encloses foraminifer tests, sometimes pyritized.

SMEAR SLIDE SUMMARY (%):

	3, 50 D
TEXTURE:	
Sand	15
Silt	15
Clay	70
COMPOSITION:	
Quartz	6
Mica	Tr
Clay	12
Volcanic glass	2
Dolomite	15
Accessory minerals	1
Pyrite	1
Limonite	1
Glauconite	Tr
Foraminifers	8
Nannofossils	35
Diatoms	1
Radiolarians	1
Sponge spicules	Tr
Silicoflagellates	Tr
Micrite	8

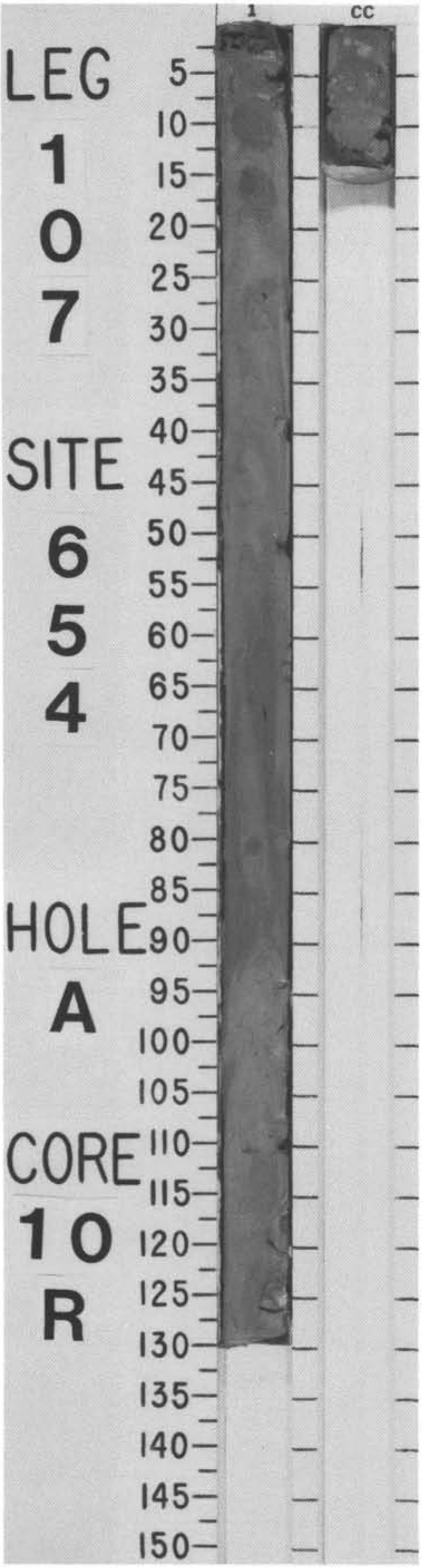
1
CC
LEG
107
SITE
654
HOLE
A
CORE
10
R
5
10
15
20
25
30
35
40
45
50
55
60
65
70
75
80
85
90
95
100
105
110
115
120
125
130
135
140
145
150

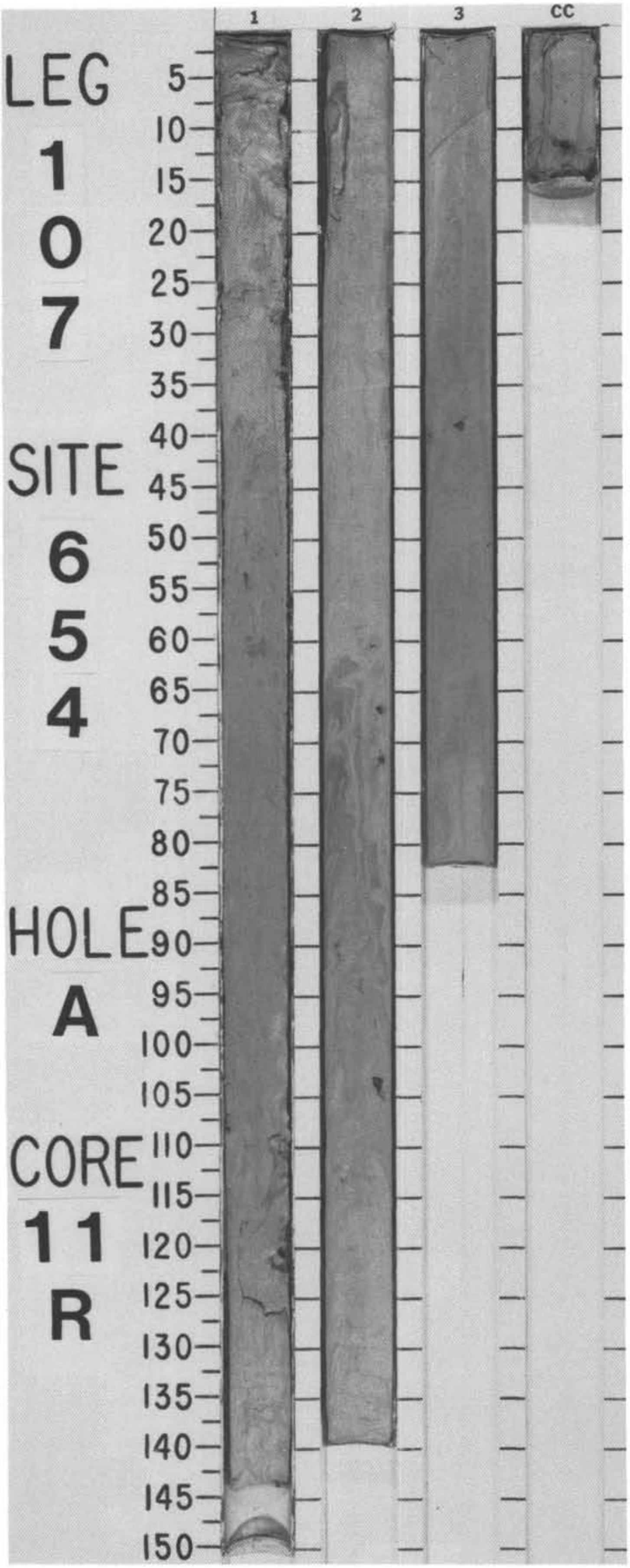
1
2
3
CC
LEG
107
SITE
654
HOLE
A
CORE
11
R
5
10
15
20
25
30
35
40
45
50
55
60
65
70
75
80
85
90
95
100
105
110
115
120
125
130
135
140
145
150

SITE 654 HOLE A CORE 12 R CORED INTERVAL 2306.4-2316.0 mbsl; 98.4-108.0 mbsf

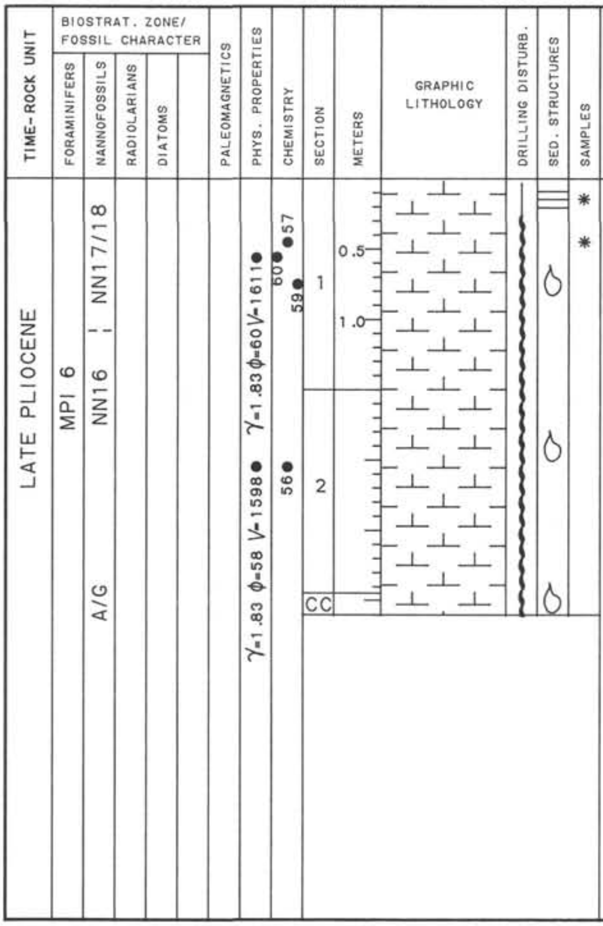

LITHOLOGIC DESCRIPTION

NANNOFOSSIL OOZE

Nannofossil ooze; colors grade downcore from olive-gray (5Y 5/2 to 5Y 6/2) in Section 1, through gray (5Y 6/1) in Section 2, to light olive-gray (5Y 6/2) in CC; exceptions are a thin interval that includes gray (5Y 5/1) laminae in Section 1, 18–21 cm, and a pale olive (5Y 6/3) flow-in interval in Section 2, 50–100 cm, overlying disturbed, FeS_2-rich layers. Abundant, scattered foraminifer tests occur throughout the whole core.

SMEAR SLIDE SUMMARY (%):

	1, 20 M	1, 50 D
TEXTURE:		
Sand	10	15
Silt	10	15
Clay	80	70
COMPOSITION:		
Quartz	10	10
Mica	1	Tr
Clay	46	9
Volcanic glass	3	—
Dolomite	5	6
Accessory minerals	1	1
Pyrite	1	1
Limonite	—	1
Foraminifers	5	10
Nannofossils	25	55
Diatoms	—	1
Radiolarians	2	2
Sponge spicules	1	Tr
Silicoflagellates	Tr	—
Micrite	—	6

13R-NO RECOVERY

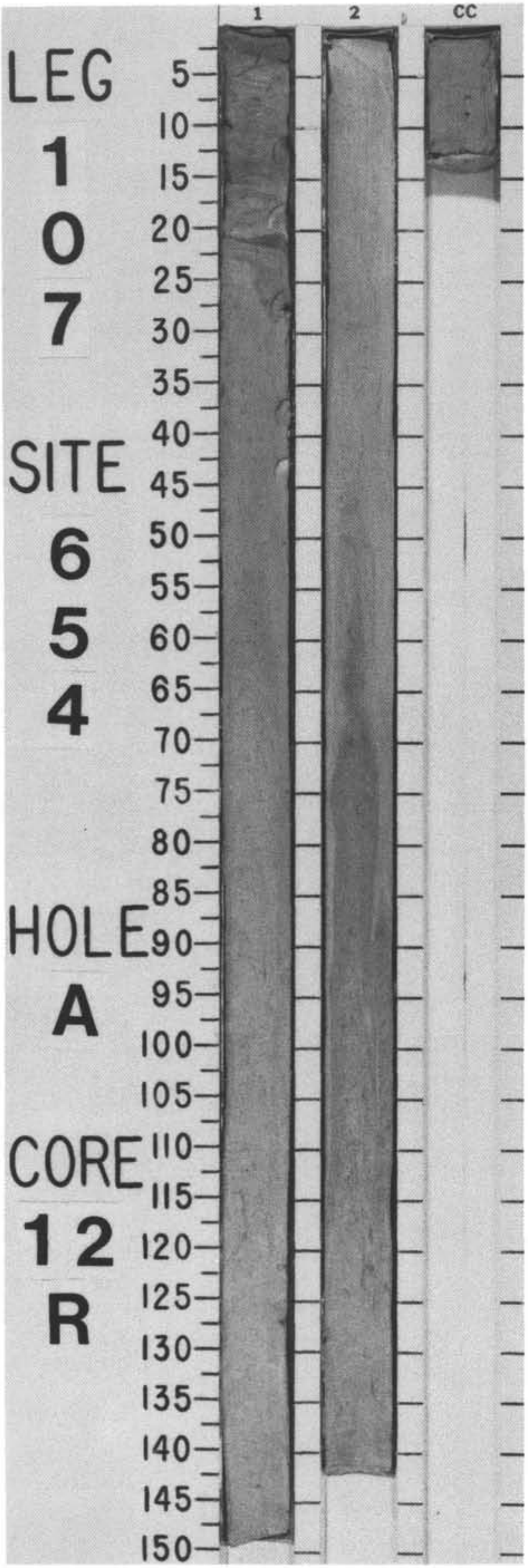
LEG
1
0
7
SITE
6
5
4
HOLE
A
CORE
1 2
R
1
2
CC
5
10
15
20
25
30
35
40
45
50
55
60
65
70
75
80
85
90
95
100
105
110
115
120
125
130
135
140
145
150

SITE 654 HOLE A CORE 14 R CORED INTERVAL 2325.7-2335.3 mbsl; 117.7-127.3 mbsf

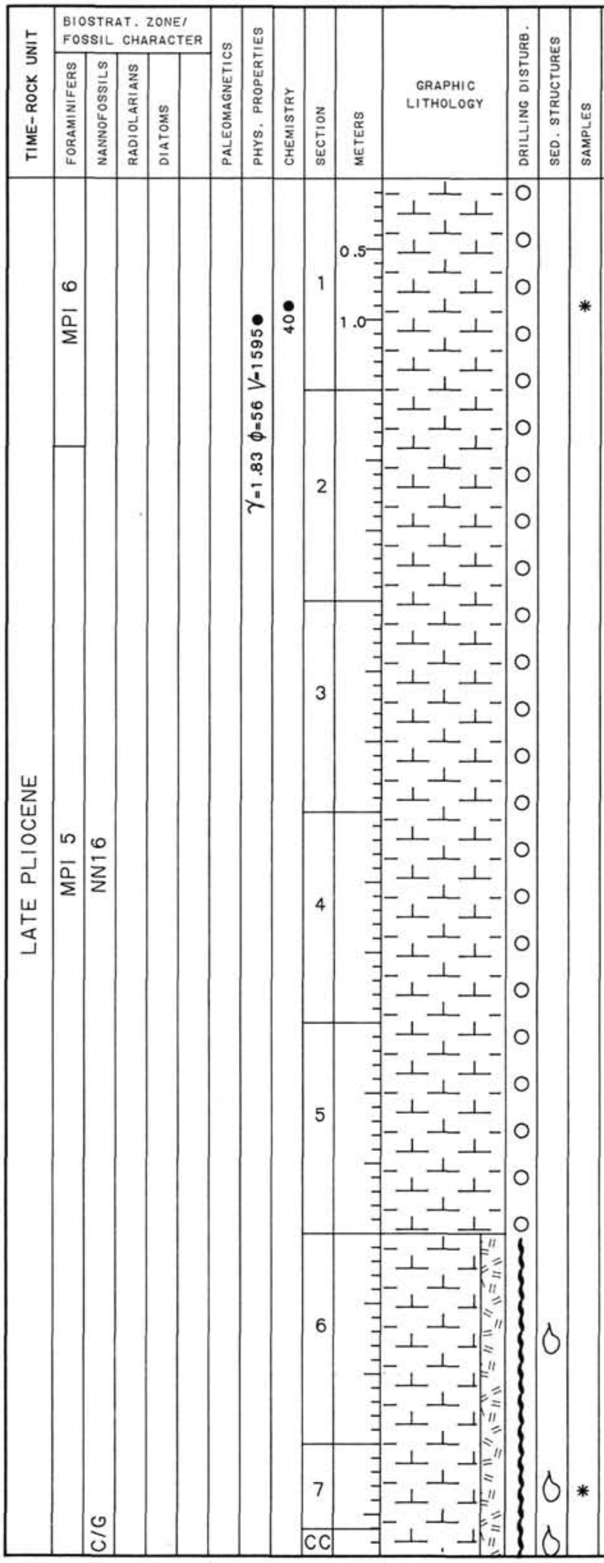

LITHOLOGIC DESCRIPTION

NANNOFOSSIL OOZE and VOLCANIC ASH-BEARING NANNOFOSSIL OOZE

Nannofossil ooze and volcanic ash-bearing nannofossil ooze; soupy, totally brecciated sequence in Sections 1 through 5; very severely disturbed in Sections 6 and 7 and CC. In Sections 1–5, gray (5Y 6/1) foraminifer tests are frequent. In other sections foraminifer tests are common, gray (5Y 5/1, 6/1) and light olive-gray (5Y 6/2), with more darker and lighter tones and a few very dark gray specks and bands. An increase in silt-sized volcanic ash seems to occur in these lowermost sections.

SMEAR SLIDE SUMMARY (%):

	1, 94 D	7, 35 D
TEXTURE:		
Sand	5	15
Silt	10	30
Clay	85	55
COMPOSITION:		
Quartz	2	8
Feldspar	6	6
Rock fragments	Tr	Tr
Mica	2	2
Clay	17	20
Volcanic glass	7	15
Dolomite	1	—
Accessory minerals	Tr	1
Foraminifers	3	2
Nannofossils	59	42
Diatoms	1	2
Radiolarians	Tr	Tr
Micrite	2	2
Gypsum	Tr	—

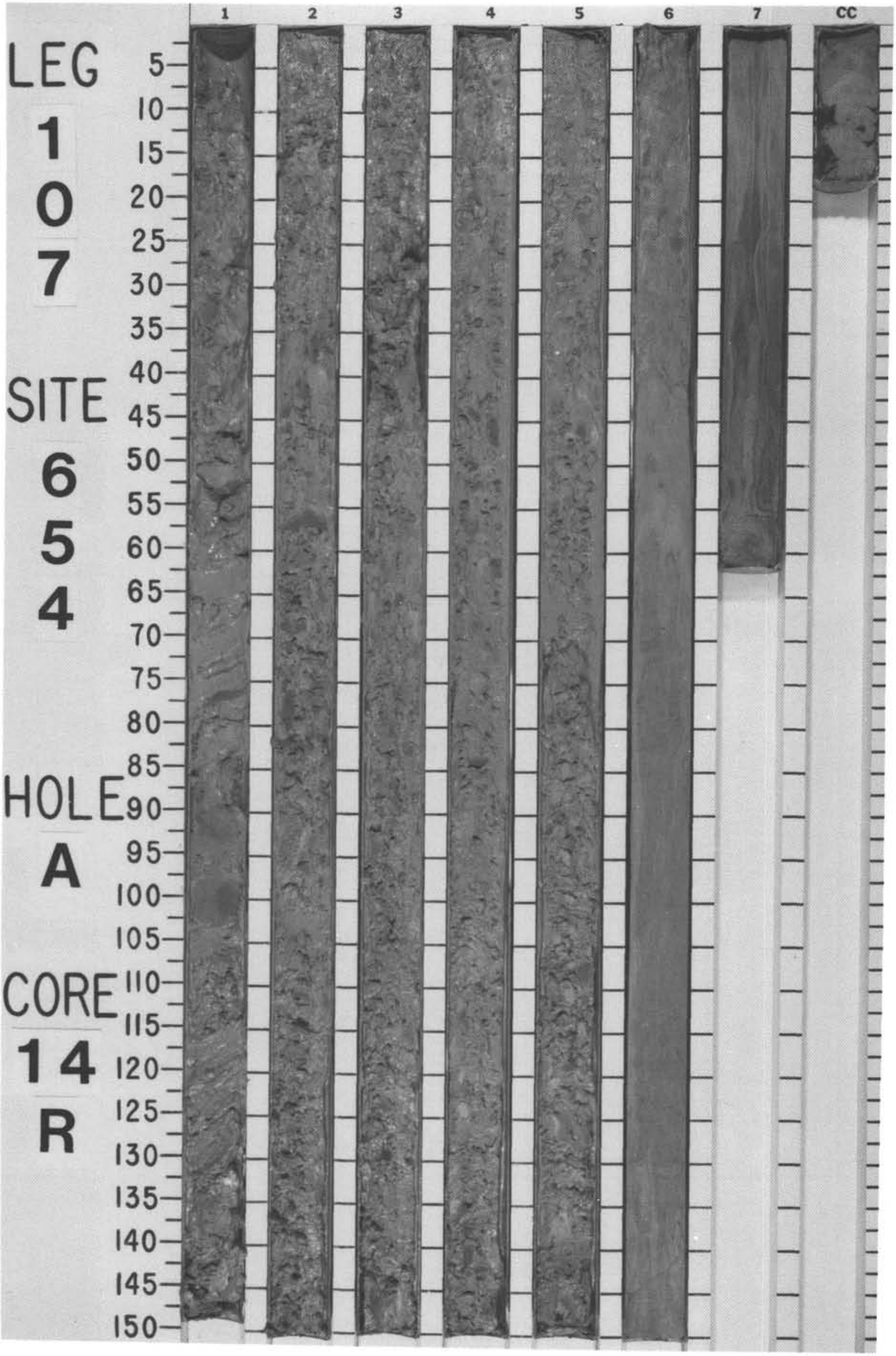
LEG
107
SITE
654
HOLE
A
CORE
14
R
1
2
3
4
5
6
7
CC
5
10
15
20
25
30
35
40
45
50
55
60
65
70
75
80
85
90
95
100
105
110
115
120
125
130
135
140
145
150

SITE 654 HOLE A CORE 15 R CORED INTERVAL 2335.3-2344.8 mbsl; 127.3-136.8 mbsf

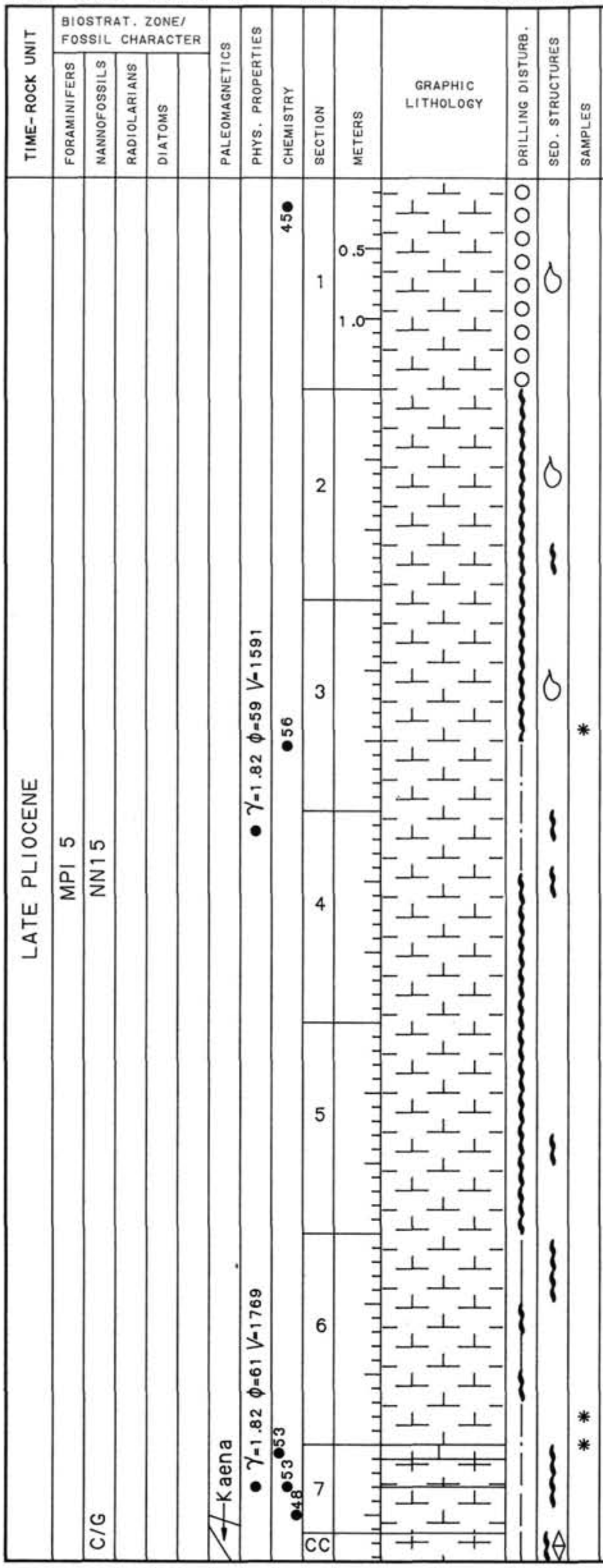

LITHOLOGIC DESCRIPTION

FORAMINIFER-NANNOFOSSIL OOZE and NANNOFOSSIL OOZE

Foraminifer-nannofossil ooze and nannofossil ooze; foraminifer-nannofossil ooze is found from Section 7 downcore. The sediments are extremely disturbed and mainly arranged in complex swirls. Scattered foraminifer tests occur throughout. The less disturbed intervals display burrowing; one large, pyritized burrow tube occurs in Section 6, 141–143 cm. General colors are gray (5Y 6/1) in Sections 1, 2, and the upper part of Section 3, and variously intermixed in Sections 1 and 2 with gray (5Y 5/1) and light olive-gray (5Y 6/2). Alternations, often irregular, of light olive-gray (5Y 6/2) and gray (5Y 5/1, 6/1) occur in lower Sections 3 and 4; greenish gray (5GY 6/1) with minor gray (5Y 5/1, 5GY 5/1) predominates in Sections 5 and 6; gray (5Y 5/1, 6/1) with rare, light olive-gray (5Y 6/2) alternates regularly in Section 7 and CC, possibly indicating alternating foraminifer-rich and foraminifer-poor ooze intervals.

SMEAR SLIDE SUMMARY (%):

	3, 100 D	6, 132 M	7, 5 D
TEXTURE:			
Sand	5	5	20
Silt	10	10	15
Clay	85	85	65
COMPOSITION:			
Quartz	4	4	8
Mica	2	3	Tr
Clay	13	10	9
Volcanic glass	2	3	1
Dolomite	12	10	15
Accessory minerals	1	1	1
Pyrite	1	2	1
Limonite	—	1	—
Foraminifers	3	3	12
Nannofossils	50	50	45
Diatoms	—	Tr	1
Radiolarians	1	2	2
Sponge spicules	Tr	1	Tr
Silicoflagellates	—	—	Tr
Micrite	10	10	5
Gypsum	1	—	—

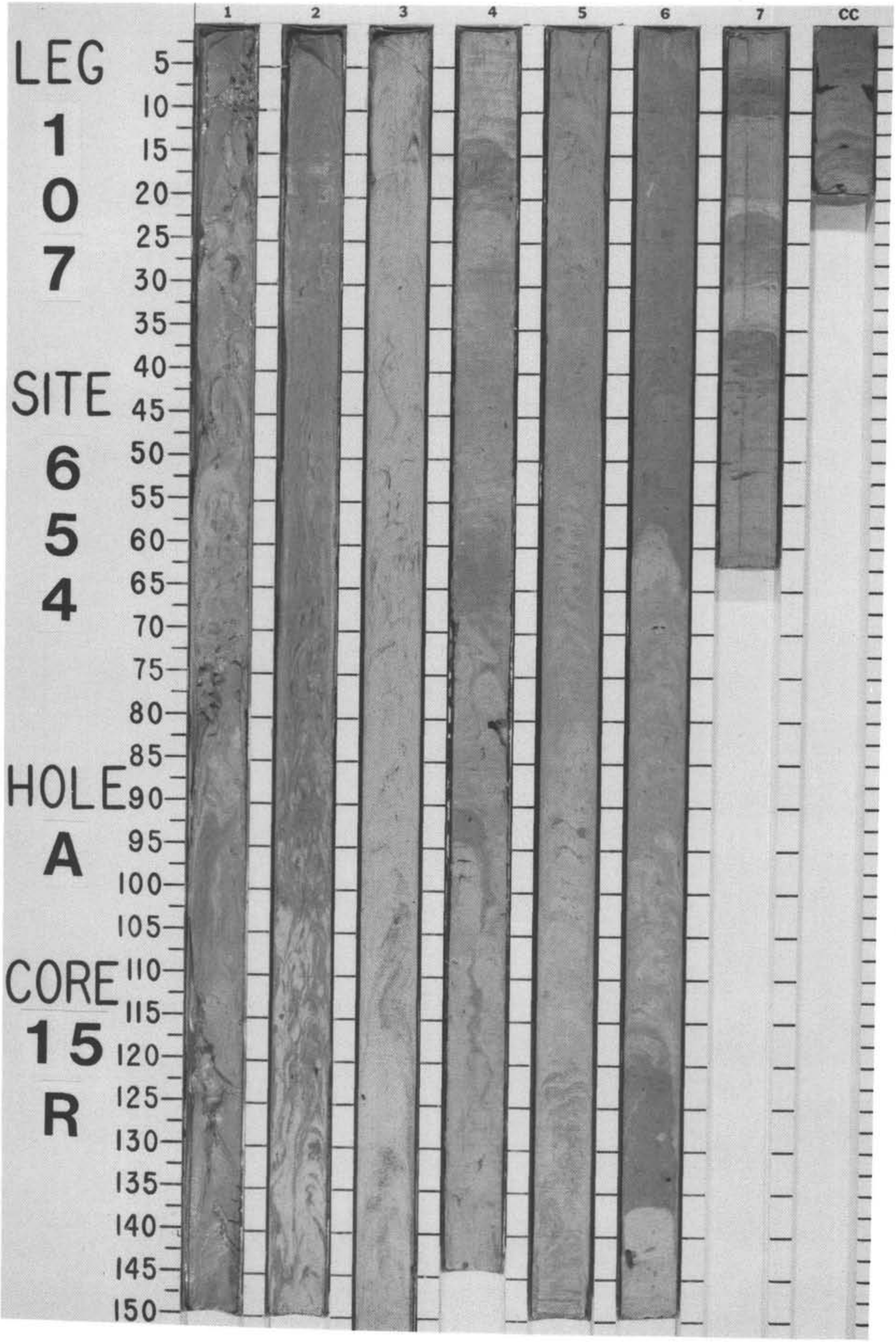
LEG 107
SITE 654
HOLE A
CORE 15 R
1
2
3
4
5
6
7
CC
5
10
15
20
25
30
35
40
45
50
55
60
65
70
75
80
85
90
95
100
105
110
115
120
125
130
135
140
145
150

SITE 654 HOLE A CORE 16 R CORED INTERVAL 2344.8-2354.5 mbsl; 136.8-146.5 mbsf

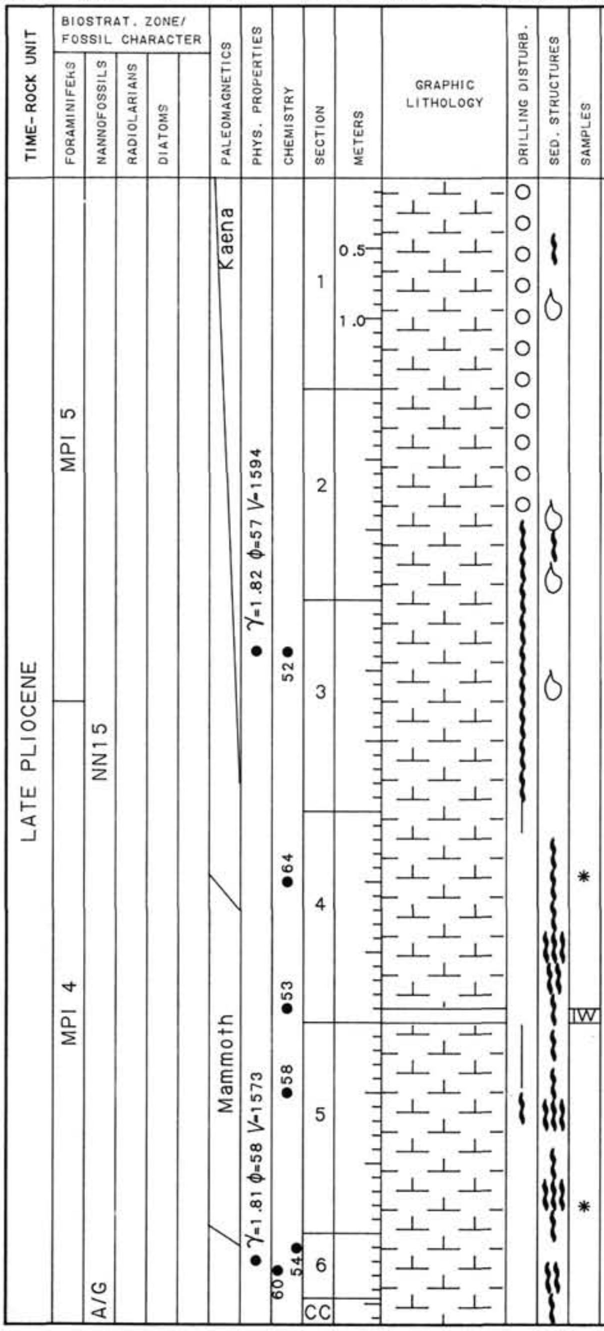

LITHOLOGIC DESCRIPTION

NANNOFOSSIL OOZE and FORAMINIFER-RICH NANNOFOSSIL OOZE

Nannofossil ooze and foraminifer-rich nannofossil ooze; Sections 1 through 3 are severely disturbed and show background colors of light gray (5Y 7/1) and gray (5Y 6/1), with some dark gray (5Y 4/1) or gray (5Y 5/1) specks and one stretched halo burrow in Section 2, 97–117 cm. Scattered foraminifers are common. The remaining sections are less disturbed and show regular alternating of the two previous colors, with minor light olive-gray (5Y 6/2), light greenish gray (5GY 7/1), and greenish gray (5GY 6/1). Burrowing is common to abundant, sometimes enhanced by FeS_2-rich fillings and/or by foraminifer concentrations. Scattered foraminifers are abundant; one lamina of foraminifer-rich ooze occurs in Section 6, 100–101 cm. One very dark spot, weakly indurated and with FeS_2 (iron sulfide?) occurs in Section 5, 97 cm.

SMEAR SLIDE SUMMARY (%):

	4, 50 D	5, 132 D
TEXTURE:		
Sand	15	4
Silt	15	12
Clay	70	84
COMPOSITION:		
Quartz	10	3
Mica	1	Tr
Clay	12	15
Volcanic glass	1	3
Calcite/dolomite	3	15
Accessory minerals	1	1
Pyrite	1	1
Foraminifers	7	2
Nannofossils	50	55
Diatoms	Tr	—
Radiolarians	2	Tr
Sponge spicules	1	—
Silicoflagellates	Tr	—
Micrite	10	5
Gypsum	1	—

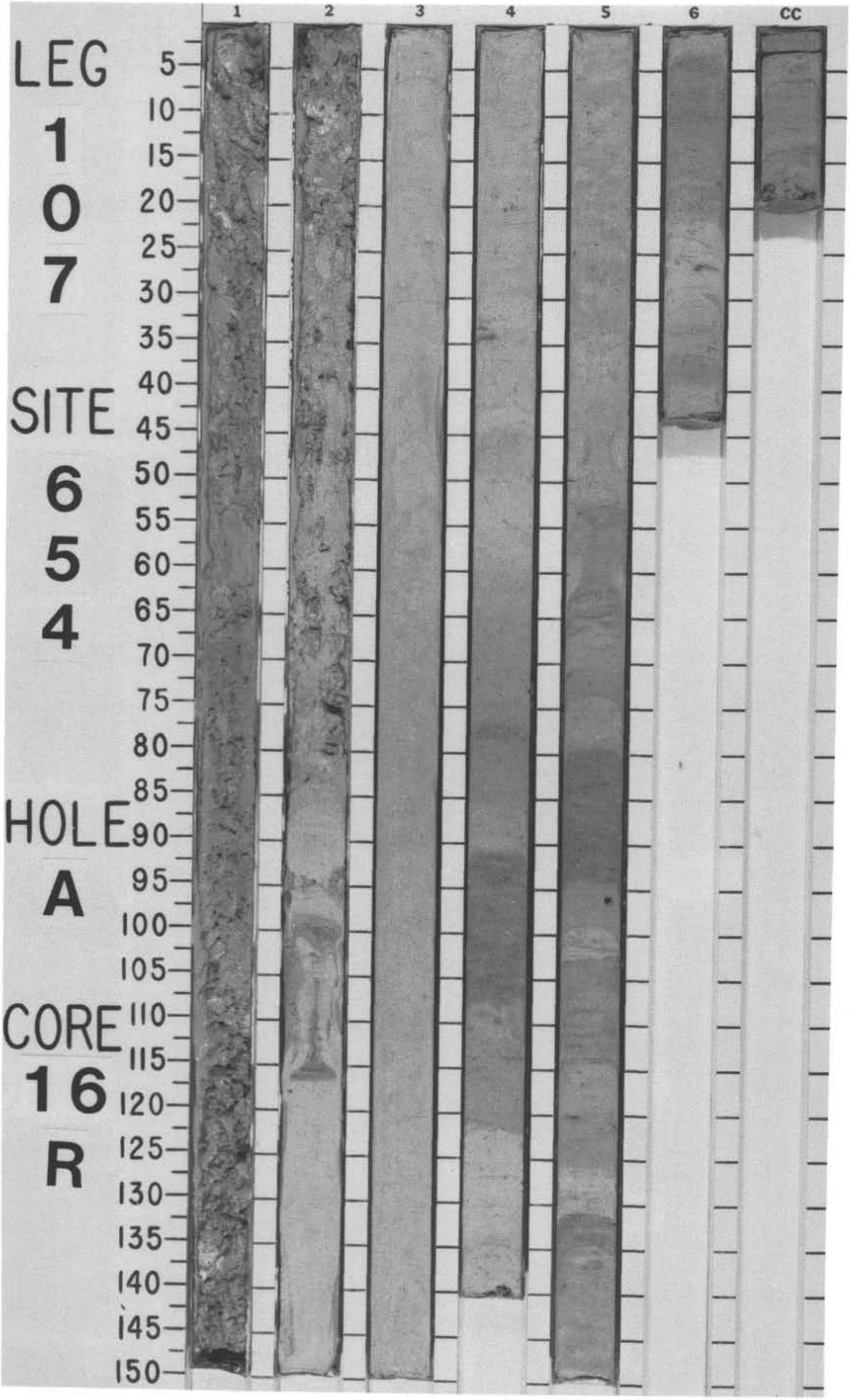
LEG
107
SITE
654
HOLE
A
CORE
16
R
1
2
3
4
5
6
CC
5
10
15
20
25
30
35
40
45
50
55
60
65
70
75
80
85
90
95
100
105
110
115
120
125
130
135
140
145
150

SITE 654 HOLE A CORE 17 R CORED INTERVAL 2354.5-2364.1 mbsl; 146.5-156.1 mbsf

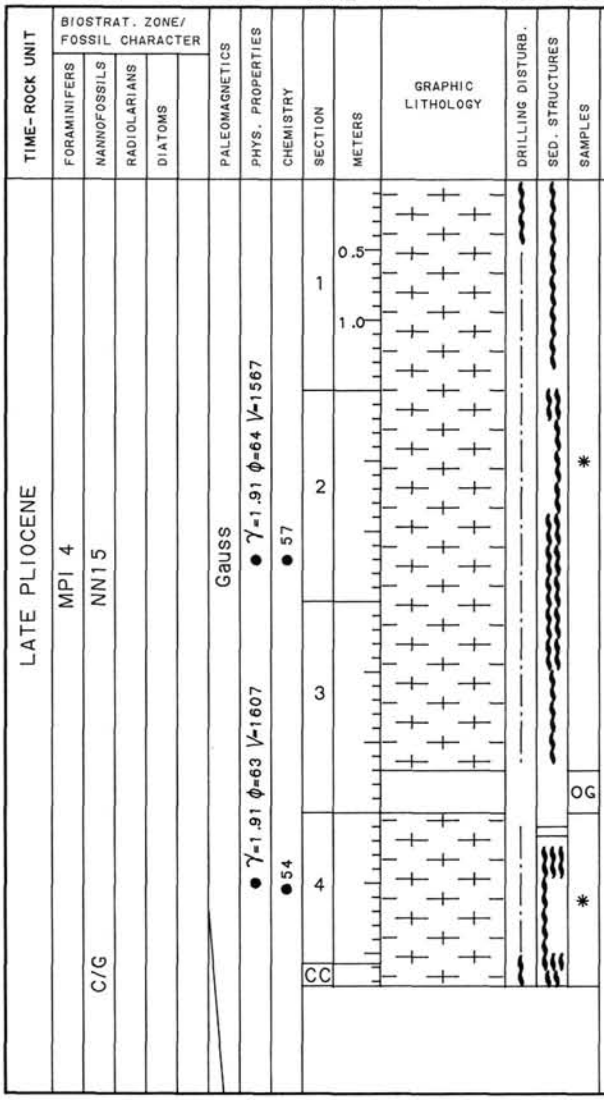

LITHOLOGIC DESCRIPTION

FORAMINIFER-NANNOFOSSIL OOZE

Foraminifer-nannofossil ooze, moderately to very disturbed and burrowed, white (5Y 8/2), light gray (5Y 7/1, 7/2), gray (5Y 6/1), pale yellow (5Y 8/3), yellow (5Y 7/8), olive-yellow (5Y 6/6), light olive-gray (5Y 6/2), and dark olive-gray (5Y 3/2).

Details: Section 1 is uniform light gray (5Y 7/2) with streaky FeS_2 (hydrotroilite) mottled areas; Section 2 is similar but with an olive-yellow (5Y 6/6), limonitic stain at 100–110 cm; Section 3, 15–20 cm, has similar limonitic areas; Section 4 contains foraminifer-rich zones at 25–30 and 50–60 cm; a blackish layer is present at 63 cm; CC contains more typical sulfide mottles.

SMEAR SLIDE SUMMARY (%):

	2, 50 D	4, 63 M
TEXTURE:		
Sand	—	10
Silt	15	10
Clay	85	80
COMPOSITION:		
Quartz	2	1
Clay	18	—
Dolomite	—	7
Pyrite	—	12
Gypsum	—	2
Zeolites	—	2
Foraminifers	25	8
Nannofossils	45	59
Flagellates	—	2
Cellulose	Tr	—
Micrite	10	—
Foraminifer debris	—	7

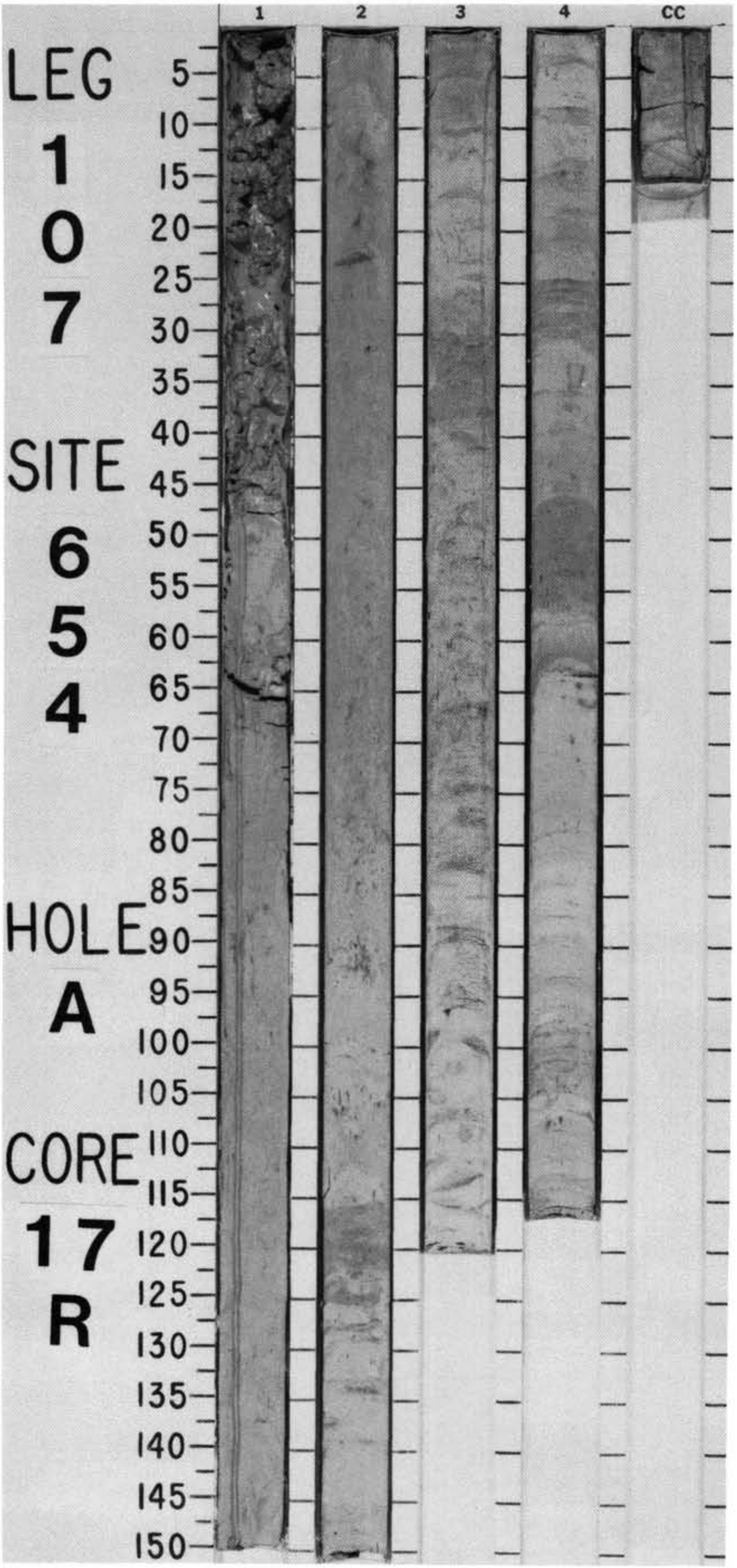
LEG
1
0
7
SITE
6
5
4
HOLE
A
CORE
17
R
1
2
3
4
CC
5
10
15
20
25
30
35
40
45
50
55
60
65
70
75
80
85
90
95
100
105
110
115
120
125
130
135
140
145
150

SITE 654 HOLE A CORE 18 R CORED INTERVAL 2364.1-2373.8 mbsl; 156.1-165.8 mbsf

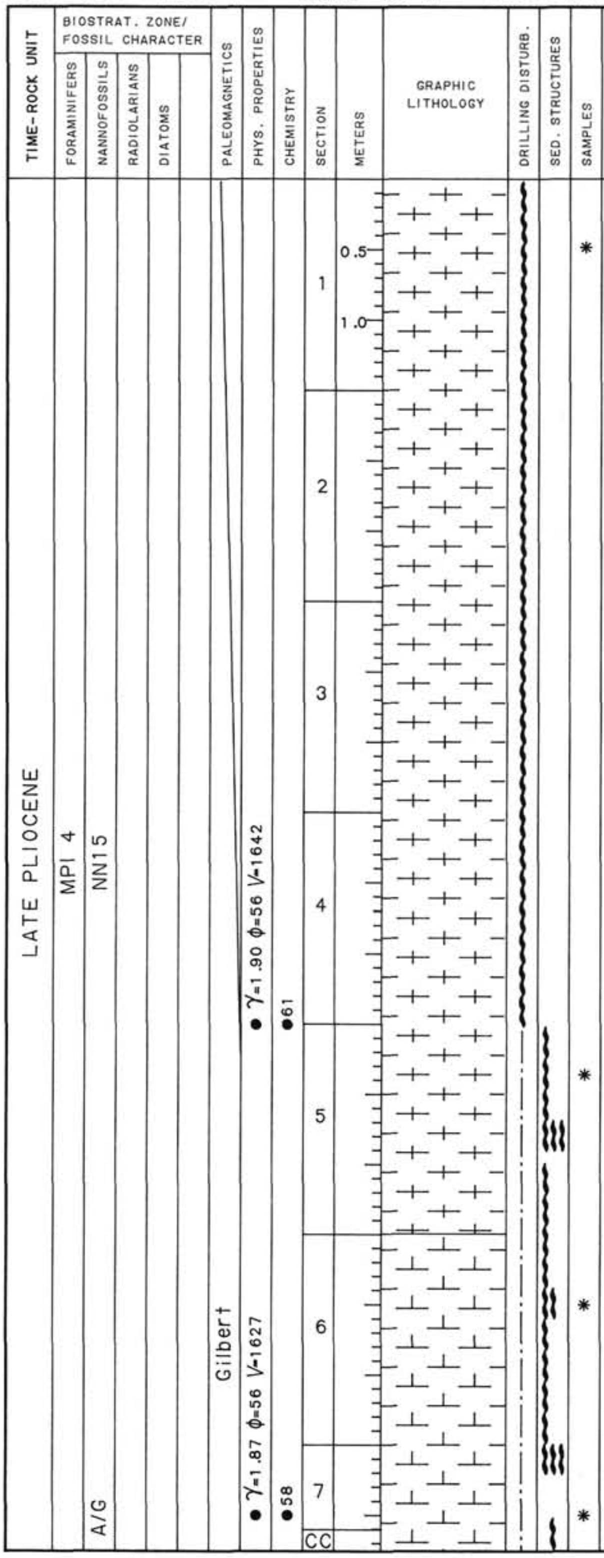

LITHOLOGIC DESCRIPTION

FORAMINIFER-NANNOFOSSIL OOZE and NANNOFOSSIL OOZE

Foraminifer-nannofossil ooze and nannofossil ooze; Sections 1 through 4 are soupy and homogenized by drilling; below this the core is relatively undisturbed. Colors are white (5Y 8/1), light gray (5Y 7/1, 7/2), pale yellow (5Y 7/3), and minor yellow (10YR 7/6).

Details: Sections 1 through 4 appear to be homogeneous nannofossil ooze; Section 5 is homogeneous ooze with FeS_2 mottled areas and scattered foraminifers; Section 6 shows primary color banding emphasized by subtle variations in gray color; Section 7 is similar, but a slight orange (10YR 7/6) stain is present at 20–23 cm. CC contains color-banded ooze, white (5Y 8/1, 8/2), light gray (5Y 7/2), and pale yellow (5Y 7/3); bands are 3–4 cm thick.

SMEAR SLIDE SUMMARY (%):

	1, 50 D	5, 30 D	6, 50 D	7, 50 D
TEXTURE:				
Sand	—	—	—	—
Silt	5	5	8	1
Clay	95	95	92	99
COMPOSITION:				
Quartz	—	Tr	—	Tr
Mica	—	Tr	—	—
Clay	15	15	—	15
Volcanic glass	—	—	2	—
Dolomite	Tr	Tr	5	—
Accessory minerals	—	—	4	—
Micrite	10	10	—	10
Gypsum	—	—	Tr	—
Foraminifers	20	10	5	5
Nannofossils	65	65	78	70
Carbonate spherules	—	Tr	—	—
Bioclasts	—	—	5	—
Aragonite needles	—	—	—	Tr

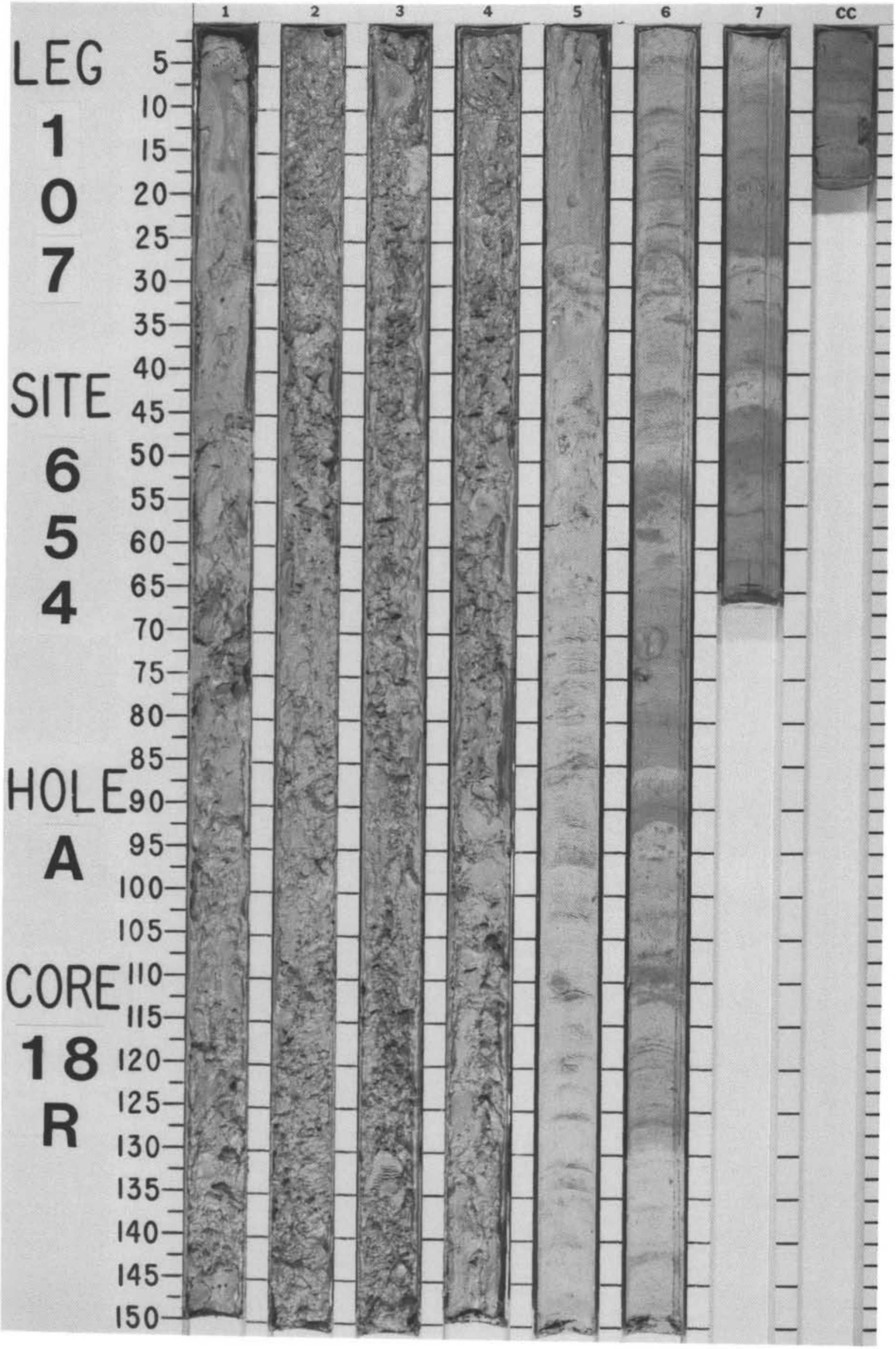
LEG
1
0
7
SITE
6
5
4
HOLE
A
CORE
18
R
1
2
3
4
5
6
7
CC
5
10
15
20
25
30
35
40
45
50
55
60
65
70
75
80
85
90
95
100
105
110
115
120
125
130
135
140
145
150

SITE 654 HOLE A CORE 19 R CORED INTERVAL 2373.8-2383.0 mbsl; 165.8-175.0 mbsf

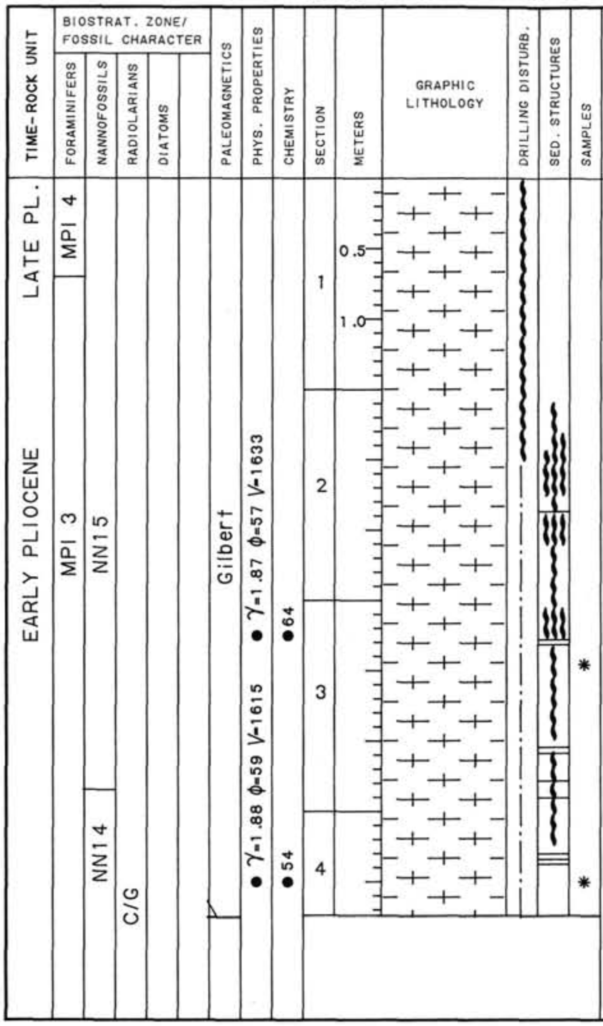

LITHOLOGIC DESCRIPTION

FORAMINIFER-NANNOFOSSIL OOZE

Nearly homogeneous foraminifer-nannofossil ooze, white (2.5Y 8/0), light gray (2.5Y 7/1–7/2, 5Y 7/2), and gray (5Y 6/1).

Details: Sections 1 and 2 are soupy due to drilling disturbance; Section 2 contains scattered foraminifers and streaks of gray sulfide mottles; in Section 3, 48 cm, black patches may indicate a sulfide-rich burrow; in Section 3, 50–60 and 90–120 cm, there are foraminifer-rich areas. Section 4 is markedly color banded: gray (5Y 6/1), light gray (5Y 7/2), gray (5Y 6/1), light gray (5Y 7/1), gray (5Y 6/1), and light gray (5Y 7/1), in downward order of appearance. There was no CC recovery.

SMEAR SLIDE SUMMARY (%):

	3, 50 D	4, 50 D
TEXTURE:		
Sand	—	—
Silt	5	5
Clay	95	95
COMPOSITION:		
Quartz	Tr	Tr
Mica	Tr	—
Clay	15	15
Aragonite	—	Tr
Foraminifers	11	11
Nannofossils	60	60
Bioclasts	2	2
Intraclasts	2	2
Micrite	10	10

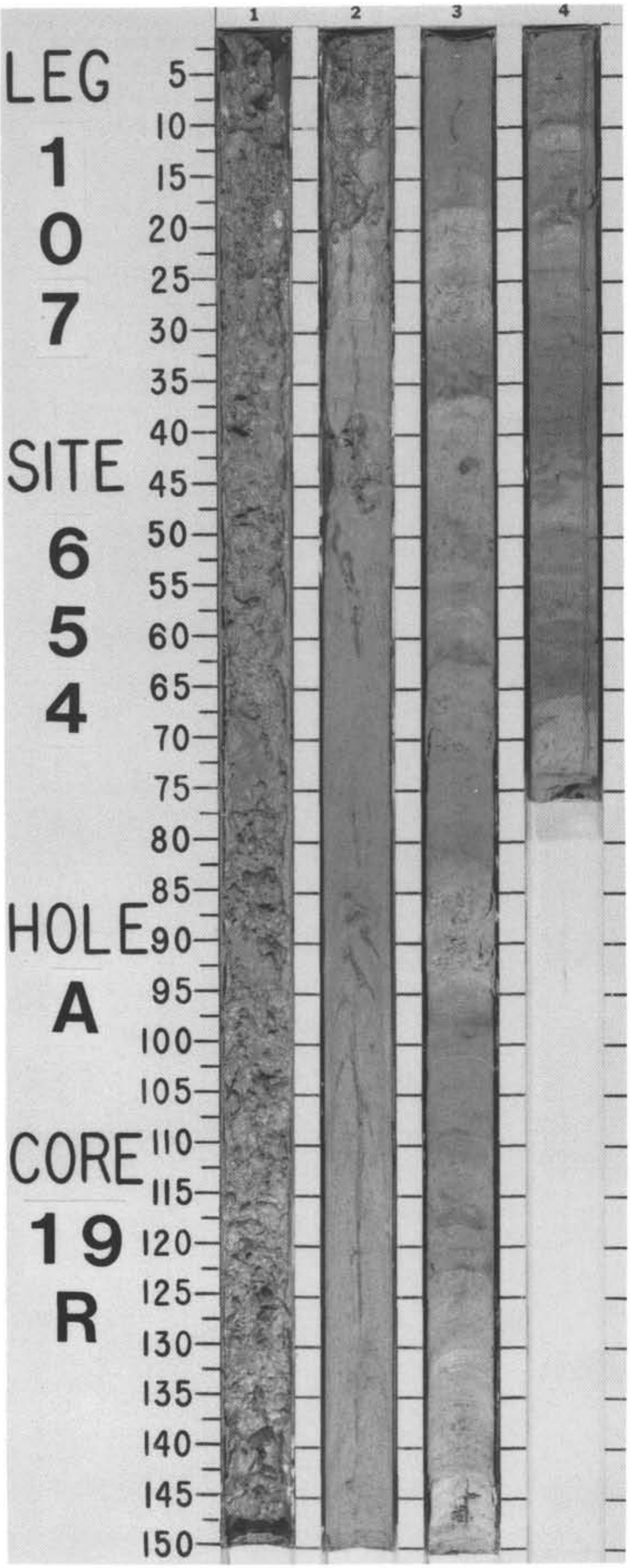
1
2
3
4
LEG
1
0
7
SITE
6
5
4
HOLE
A
CORE
19
R
5
10
15
20
25
30
35
40
45
50
55
60
65
70
75
80
85
90
95
100
105
110
115
120
125
130
135
140
145
150

SITE 654 HOLE A CORE 20 R CORED INTERVAL 2383.0-2392.6 mbsl; 175.0-184.6 mbsf

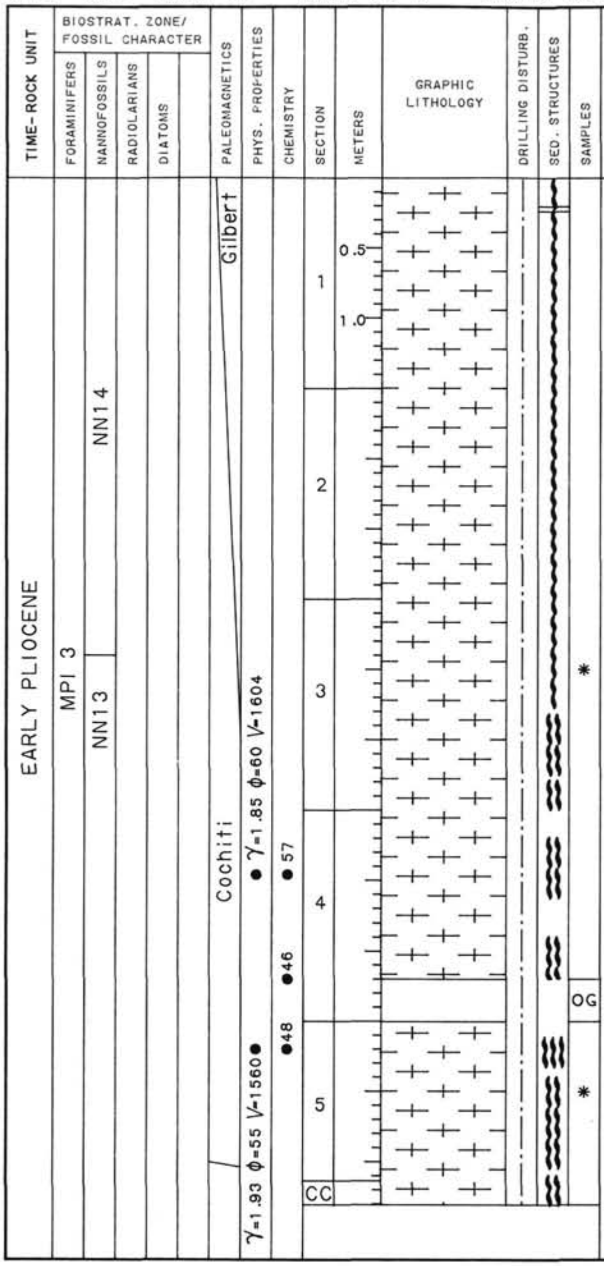

LITHOLOGIC DESCRIPTION

FORAMINIFER-NANNOFOSSIL OOZE

Foraminifer-nannofossil ooze, nearly homogeneous throughout the core, white (2.5Y 8/1, 8/2), light gray (2.5Y 7/1, 5Y 7/1–7/2, N 7/), gray (5Y 6/1), light olive-gray (5Y 6/2), and pale yellow (2.5Y 8/4).

Details: Section 1 has scattered mottled sulfide areas and vague yellow (2.5Y 7/2) patches; foraminifers are abundant; Section 2 has abundant foraminifers and, at 16 cm, a vague yellow stain; Section 3 is highly burrowed with a vague pale yellow (2.5Y 8/4) stain at 24–26 and 148–150 cm; FeS_2 mottled areas common; Section 4 has foraminifer-rich zones at 10–23, 45–62, and 70–90 cm; burrowing is locally intense; Section 5 shows only a vague color banding; CC is homogeneous and burrowed.

SMEAR SLIDE SUMMARY (%):

	3, 50 D	5, 50 D
TEXTURE:		
Sand	—	—
Silt	5	10
Clay	95	90
COMPOSITION:		
Quartz	Tr	—
Clay	15	—
Dolomite	Tr	5
Accessory minerals	—	2
Zeolite	—	1
Foraminifers	8	10
Nannofossils	55	82
Plant debris	Tr	—
Bioclasts	7	—
Micrite	15	—

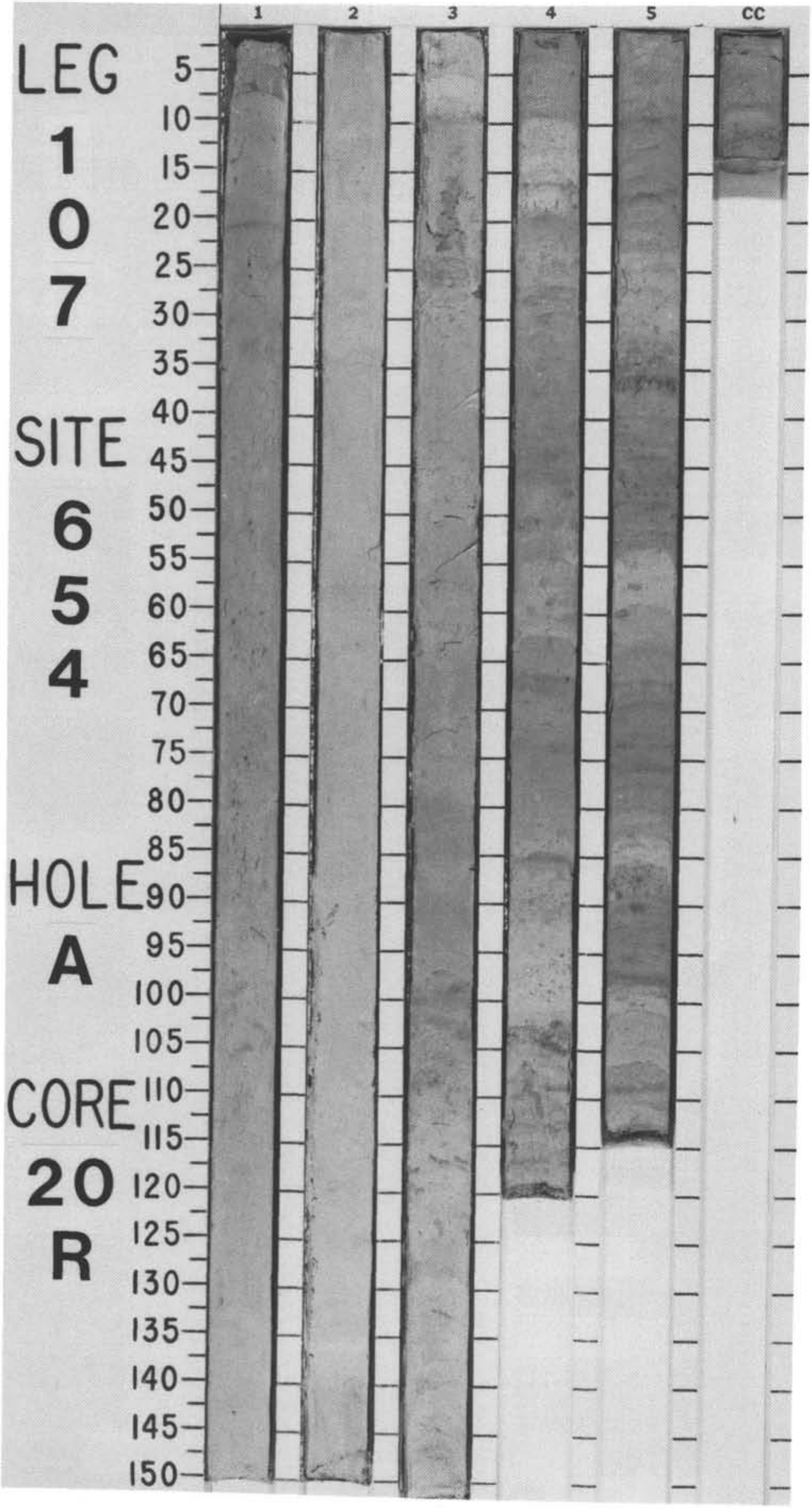
LEG
107
SITE
654
HOLE
A
CORE
20
R
1
2
3
4
5
CC
5
10
15
20
25
30
35
40
45
50
55
60
65
70
75
80
85
90
95
100
105
110
115
120
125
130
135
140
145
150

SITE 654 HOLE A CORE 21 R CORED INTERVAL 2392.6-2402.2 mbsl; 184.6-194.2 mbsf

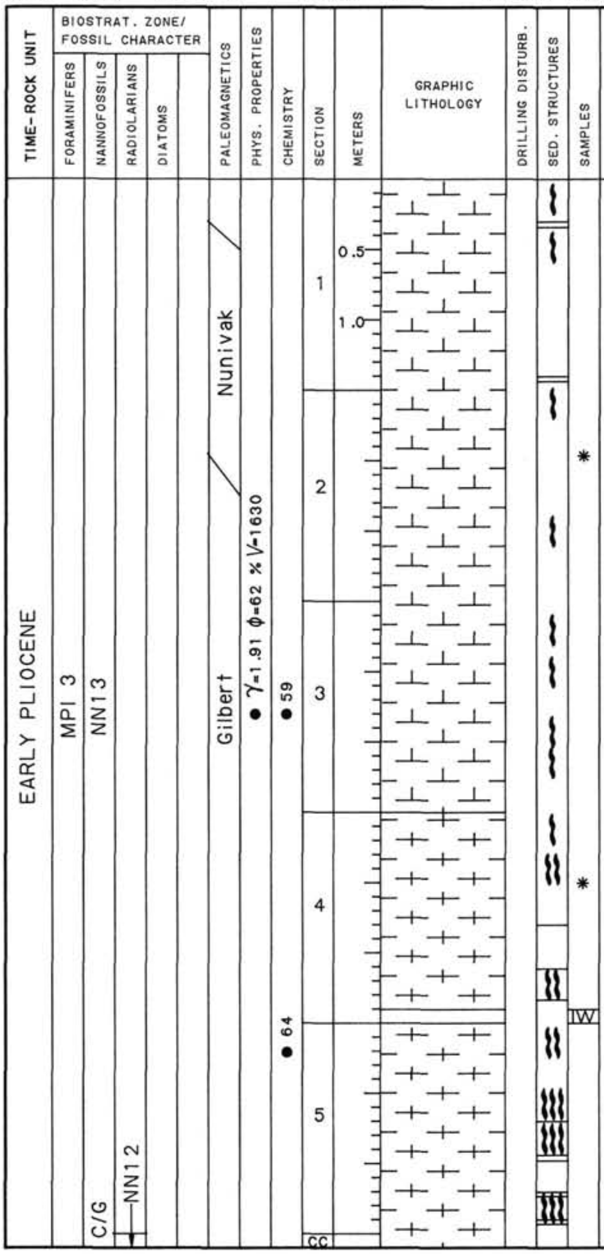

LITHOLOGIC DESCRIPTION

NANNOFOSSIL OOZE and FORAMINIFER-NANNOFOSSIL OOZE

Nannofossil ooze and foraminifer-nannofossil ooze, light gray (2.5Y 7/1, 7/2) and light brownish gray (2.5Y 6/2).

Details: Section 1 is homogeneous with numerous black specks and blebs of hydrotroilite(?); Section 2 has vague gray lamination at 50–52 cm and a yellowish zone at 102 cm; Section 3 has a large light gray burrow at 21 cm and a mottled yellowish zone at 63 cm; Section 4 is very homogeneous, with FeS_2 mottled areas; Section 5 has foraminifer-rich zones at 10–22, 59–69, 89–101, 116–124, and 136–148 cm and has FeS_2 blebs and local patches of oxidation at 13–14 and 116–117 cm; CC is homogeneous ooze.

SMEAR SLIDE SUMMARY (%):

	2, 50 D	4, 50 D
TEXTURE:		
Sand	—	—
Silt	5	5
Clay	95	95
COMPOSITION:		
Quartz	Tr	1
Clay	10	10
Dolomite	Tr	Tr
Accessory minerals	—	1
Intraclasts	10	1
Micrite	20	10
Aragonite	Tr	—
Foraminifers	5	10
Nannofossils	55	65
Fish remains	—	1
Plant debris	Tr	—
Bioclasts	—	1

22R-NO RECOVERY

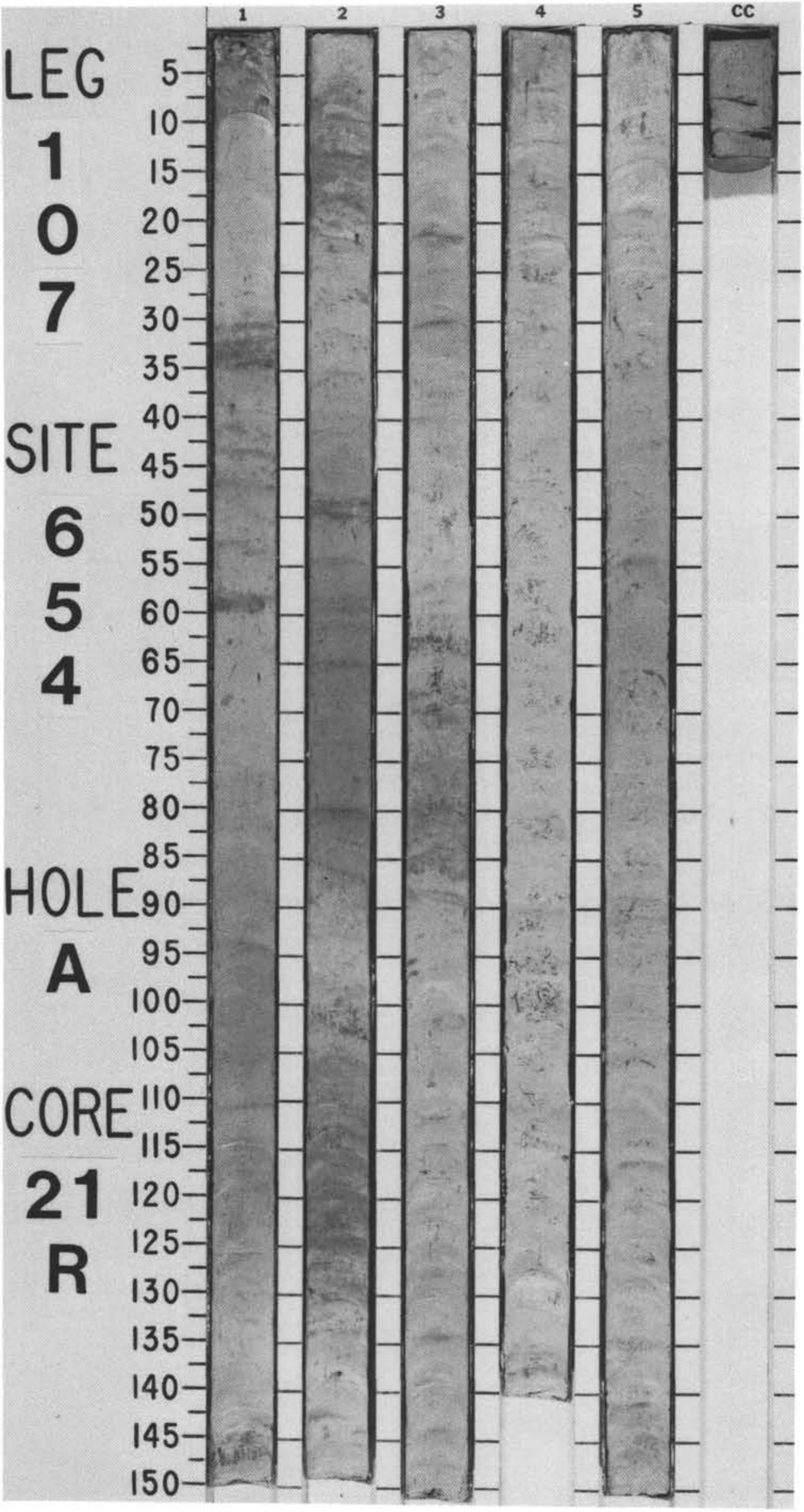
LEG
107
SITE
654
HOLE
A
CORE
21
R
1
2
3
4
5
CC
5
10
15
20
25
30
35
40
45
50
55
60
65
70
75
80
85
90
95
100
105
110
115
120
125
130
135
140
145
150

SITE 654 HOLE A CORE 23 R CORED INTERVAL 2411.8-2421.4 mbsl; 203.8-213.4 mbsf

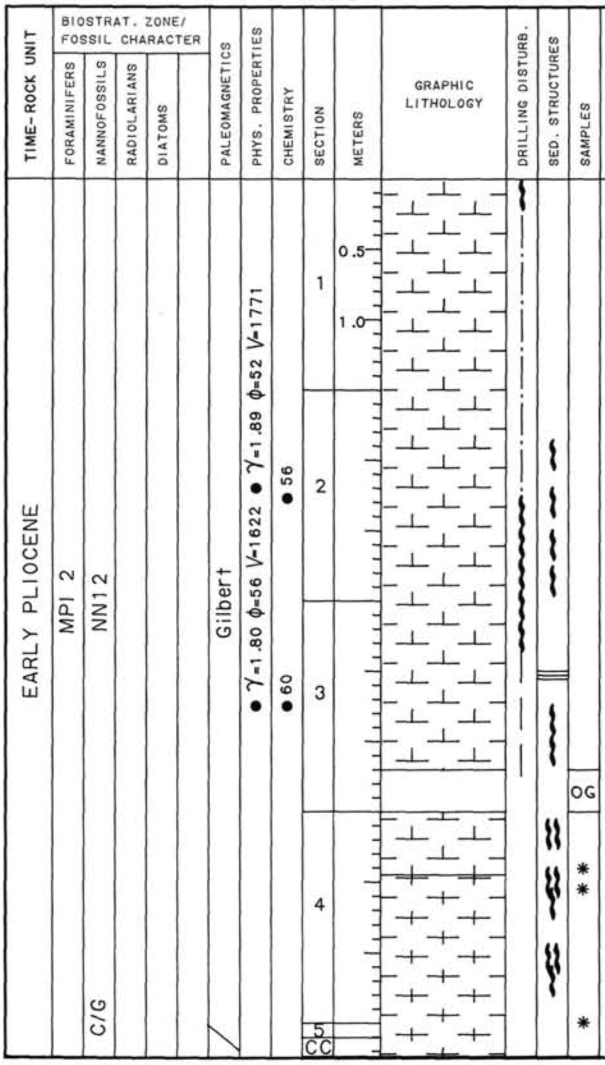

LITHOLOGIC DESCRIPTION

NANNOFOSSIL OOZE and FORAMINIFER-NANNOFOSSIL OOZE

Nannofossil ooze and foraminifer-nannofossil ooze; the upper portion is very disturbed, with drilling biscuits made alternately of homogeneous ooze and sediment containing some preserved structures; gray (5Y 6/1), grading in Sections 4 through CC to alternation with light olive-gray (5Y 6/2, 7/1).

Details: burrows are common, including typical halo burrows in Section 2; a few are pyritized; most are dark gray (5Y 4/1, 5/1) and pale olive (5Y 6/3). Other streaks and irregular bands in Sections 1 and 2 are olive-gray (5Y 5/2) and light olive-brown (2.5Y 5/4); faint traces of original parallel banding or color lamination in olive-gray (5Y 5/1, 5/2, 6/1) occur in Section 3, 50–55 cm.

SMEAR SLIDE SUMMARY (%):

	4, 45 D	4, 50 D	5, 2 M
TEXTURE:			
Sand	10	10	12
Silt	10	5	8
Clay	80	85	80
COMPOSITION:			
Quartz	6	2	8
Mica	Tr	Tr	1
Clay	23	7	10
Volcanic glass	Tr	—	—
Dolomite	3	2	1
Accessory minerals	2	1	—
Pyrite	1	—	1
Zeolite	—	Tr	—
Aragonite needles	—	Tr	—
Foraminifers	6	10	8
Nannofossils	50	70	60
Radiolarians	1	2	3
Sponge spicules	Tr	1	—
Silicoflagellates	Tr	—	—
Micrite	8	5	4

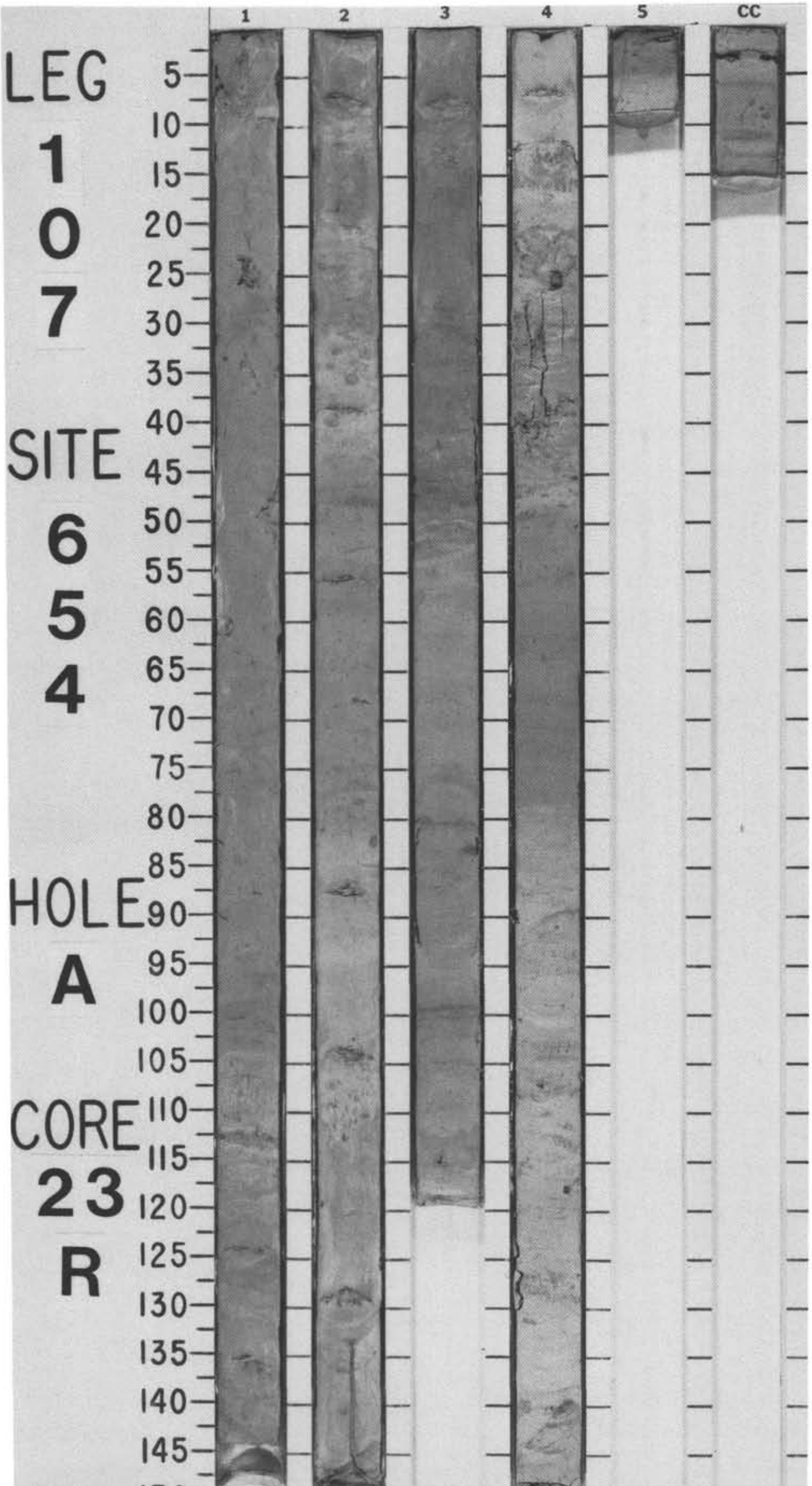
LEG
107
SITE
654
HOLE
A
CORE
23
R
1
2
3
4
5
CC
5
10
15
20
25
30
35
40
45
50
55
60
65
70
75
80
85
90
95
100
105
110
115
120
125
130
135
140
145
150

SITE 654 HOLE A CORE 24 R CORED INTERVAL 2421.4-2431.1 mbsl; 213.4-223.1 mbsf

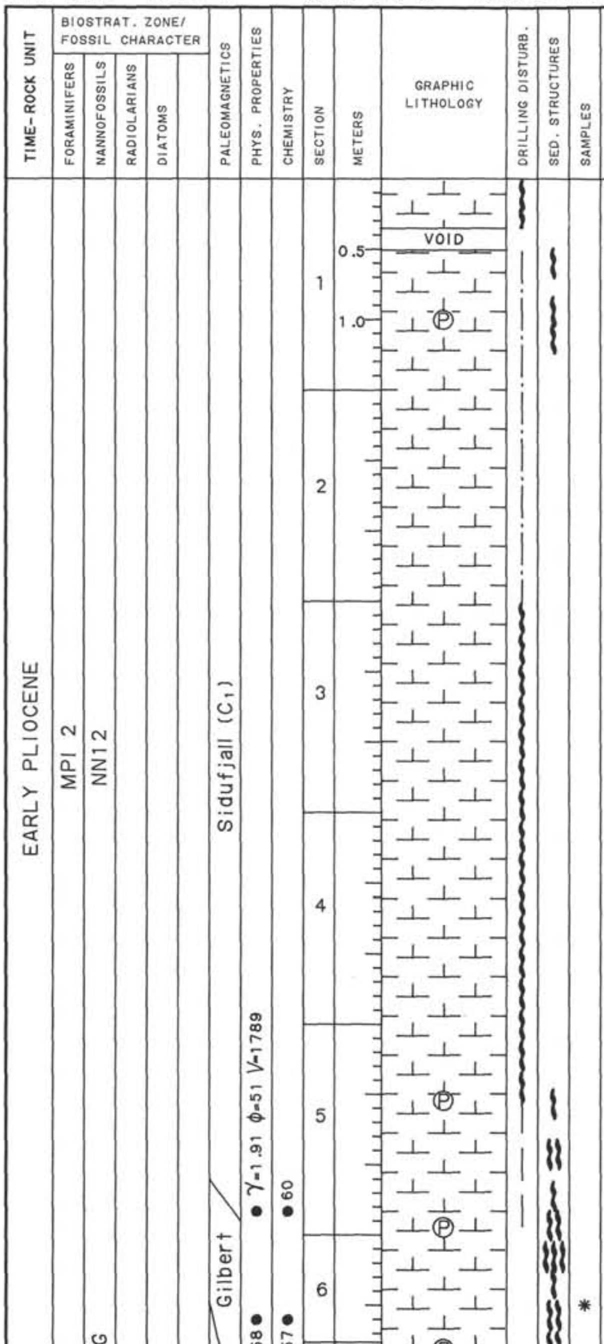

LITHOLOGIC DESCRIPTION

NANNOFOSSIL OOZE

Nannofossil ooze, very disturbed; in Sections 1 through 5 ooze is light gray (10Y 6/1, 5Y 6/1–7/1). Burrows, sometimes large and pyritized, occur and are usually darker than the surrounding sediment. From Section 6 downward are several 2–5-cm-thick alternations of oozes of different colors, including light gray (5Y 7/1), gray (5Y 5/1, 6/1), and greenish gray (5GY 6/1). Bioturbation is strong to moderate in these intervals, usually with darker FeS_2-induced stains (one pyritized burrow tube in CC, 10 cm).

SMEAR SLIDE SUMMARY (%):

	6, 50 D
TEXTURE:	
Sand	5
Silt	20
Clay	75
COMPOSITION:	
Quartz	3
Mica	Tr
Clay	27
Volcanic glass	3
Accessory minerals	1
Foraminifers	5
Nannofossils	50
Diatoms	5
Radiolarians	2
Sponge spicules	1
Silicoflagellates	Tr
Micrite	3

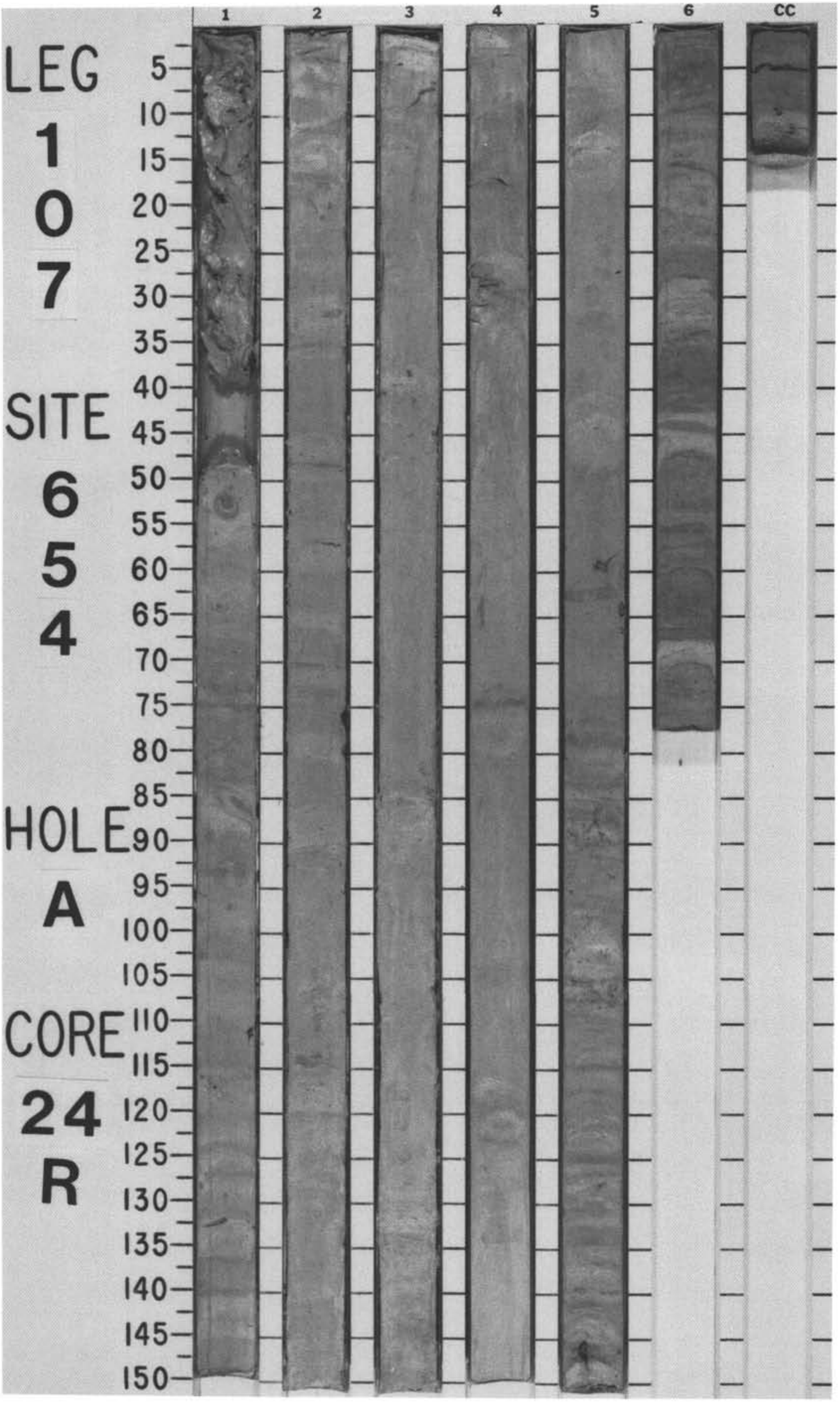
LEG
1
0
7
SITE
6
5
4
HOLE
A
CORE
24
R
1
2
3
4
5
6
CC
5
10
15
20
25
30
35
40
45
50
55
60
65
70
75
80
85
90
95
100
105
110
115
120
125
130
135
140
145
150

SITE 654 HOLE A CORE 25 R CORED INTERVAL 2431.1-2440.7 mbsl; 223.1-232.7 mbsf

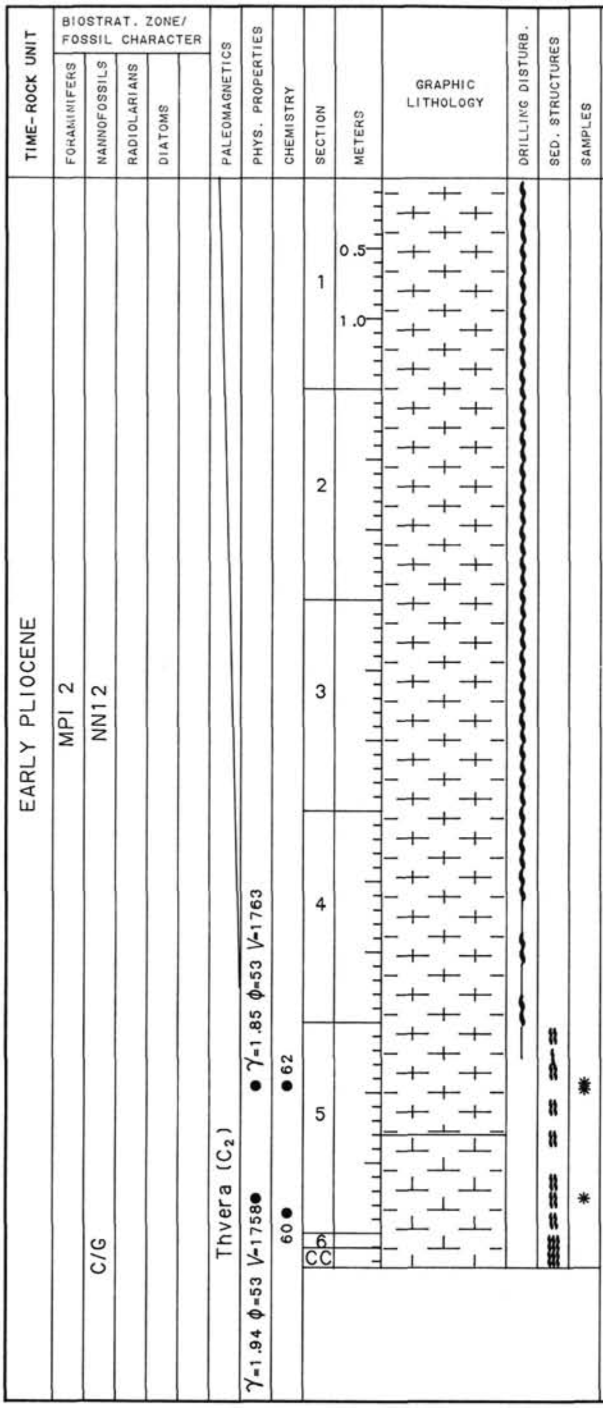

LITHOLOGIC DESCRIPTION

FORAMINIFER-NANNOFOSSIL OOZE and NANNOFOSSIL OOZE

Foraminifer-nannofossil ooze and nannofossil ooze; Sections 1 through 4 are very disturbed; light gray (5Y 7/1), gray (5Y 6/1), light olive (10Y 6/1), and minor olive-gray (5Y 5/2); dark gray specks and foraminifers are common. Starting from Section 5, which is less disturbed, sediment color gradually changes from gray (5Y 5/1, 6/1), olive-gray (5Y 5/2), olive (5Y 4/3), light olive-gray (5Y 6/2), to olive-gray (5Y 5/2), becoming olive-gray (5Y 4/2) in the CC. In Section 5, olive-brown (2.5Y 4/4), 1- cm-thick layers cyclically occur every 5–15 cm down section from 20 to 133 cm (relatively foraminifer-poor layers). Burrowing is intense, in colors darker or lighter than the host sediment, and sometimes appears as concentric color layers.

SMEAR SLIDE SUMMARY (%):

	5, 50 M	5, 51 D	5, 131 D
TEXTURE:			
Sand	15	35	2
Silt	10	15	7
Clay	75	50	91
COMPOSITION:			
Quartz	6	Tr	Tr
Feldspar	—	1	Tr
Mica	Tr	—	—
Clay	20	18	20
Volcanic glass	—	1	—
Calcite	—	1	—
Dolomite	5	—	1
Accessory minerals	1	—	—
Pyrite/hydrotroilite	3	—	—
Opaques (oxides)	—	1	—
Foraminifers	12	25	4
Nannofossils	46	50	65
Diatoms	—	1	4
Radiolarians	2	2	3
Sponge spicules	Tr	—	—
Silicoflagellates	—	Tr	—
Micrite	5	Tr	2
Ostracods	—	—	1
Gypsum	—	Tr	—

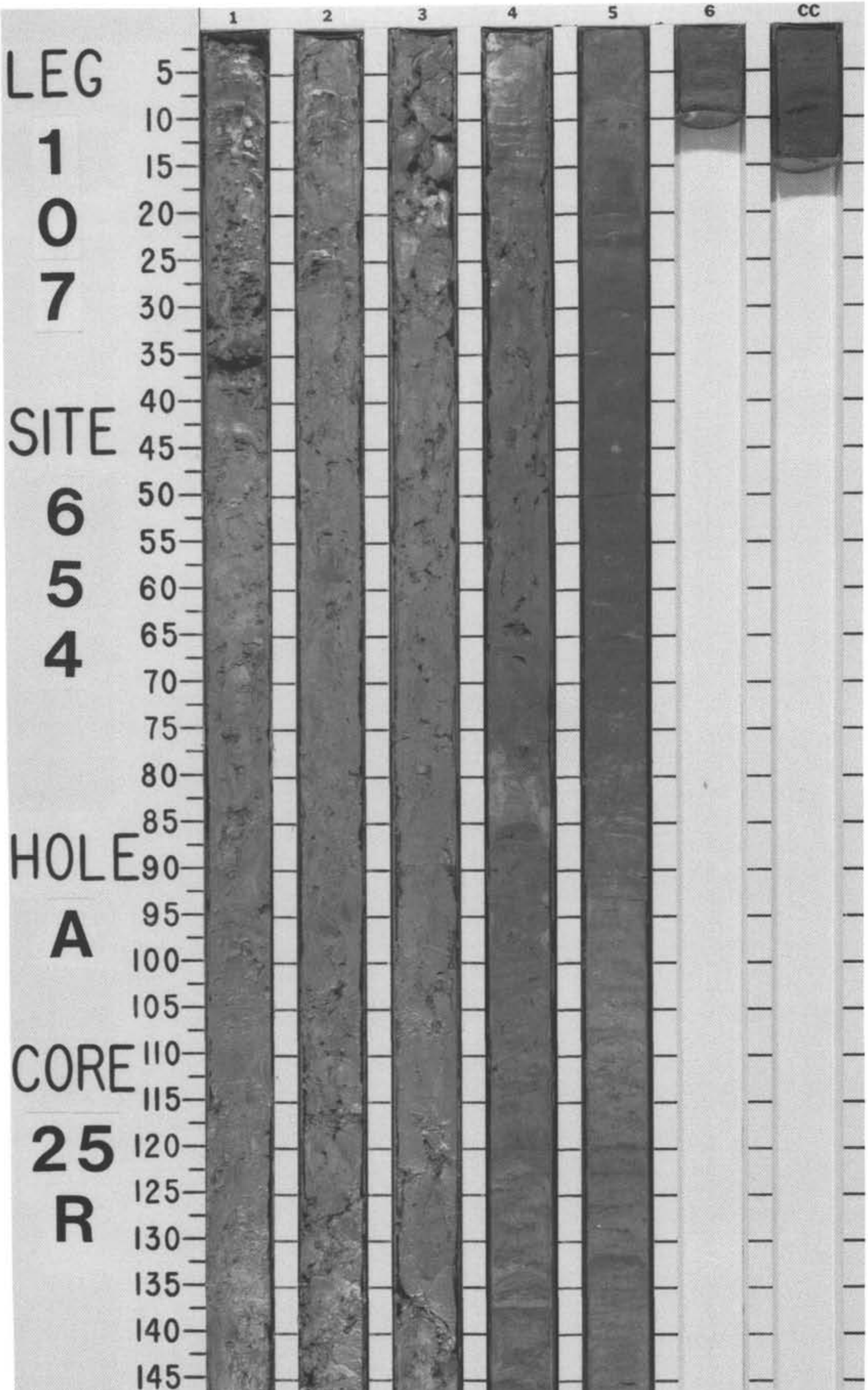
LEG
107
SITE
654
HOLE
A
CORE
25
R
1
2
3
4
5
6
CC
5
10
15
20
25
30
35
40
45
50
55
60
65
70
75
80
85
90
95
100
105
110
115
120
125
130
135
140
145
150

SITE 654 HOLE A CORE 26 R CORED INTERVAL 2440.7-2450.4 mbsl; 232.7-242.4 mbsf

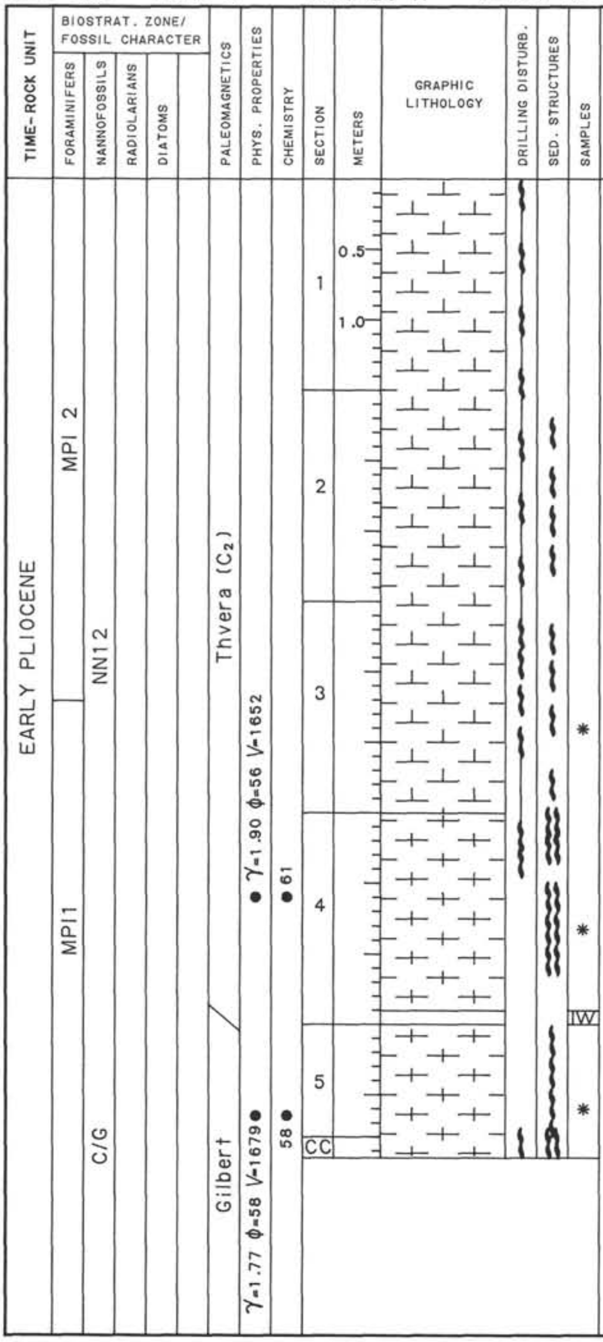

LITHOLOGIC DESCRIPTION

NANNOFOSSIL OOZE and FORAMINIFER-NANNOFOSSIL OOZE

Nannofossil ooze and foraminifer-nannofossil ooze, Sections 1 through 3 are alternations of less disturbed biscuits and of totally homogenized intervals, Section 1, 0-70 cm, has gray (5Y 6/1) as a background color, turning to olive (5Y 4/6), olive-brown (2.5Y 4/4), and finally grayish olive (10Y 5/2) below 127 cm. The latter color is also found in Sections 2 and 3. In these intervals, dark gray to light gray specks seem to indicate intense burrowing. Sections 4 through CC contain alternations of olive-gray (5Y 5/2), olive (5Y 4/3, 4/4, 5/3), and olive-brown (2.5Y 4/4) oozes, all intensively bioturbated with burrows containing abundant foraminifer tests. Some olive-brown, 2–5-cm-thick, burrowed bands occur in Section 4, 50–110 cm, and in Section 5, 55–79 cm.

SMEAR SLIDE SUMMARY (%):

	3, 95 D	4, 91 M	5, 67 D
TEXTURE:			
Sand	10	7	20
Silt	10	15	10
Clay	80	78	70
COMPOSITION:			
Quartz	5	3	4
Mica	—	—	Tr
Clay	9	6	11
Volcanic glass	—	2	—
Dolomite	10	5	4
Accessory minerals	1	1	1
Pyrite/hydrotroilite	1	1	4
Foraminifers	4	15	10
Nannofossils	60	60	60
Radiolarians	—	—	1
Sponge spicules	—	—	Tr
Micrite (dolomicrite?)	10	7	5

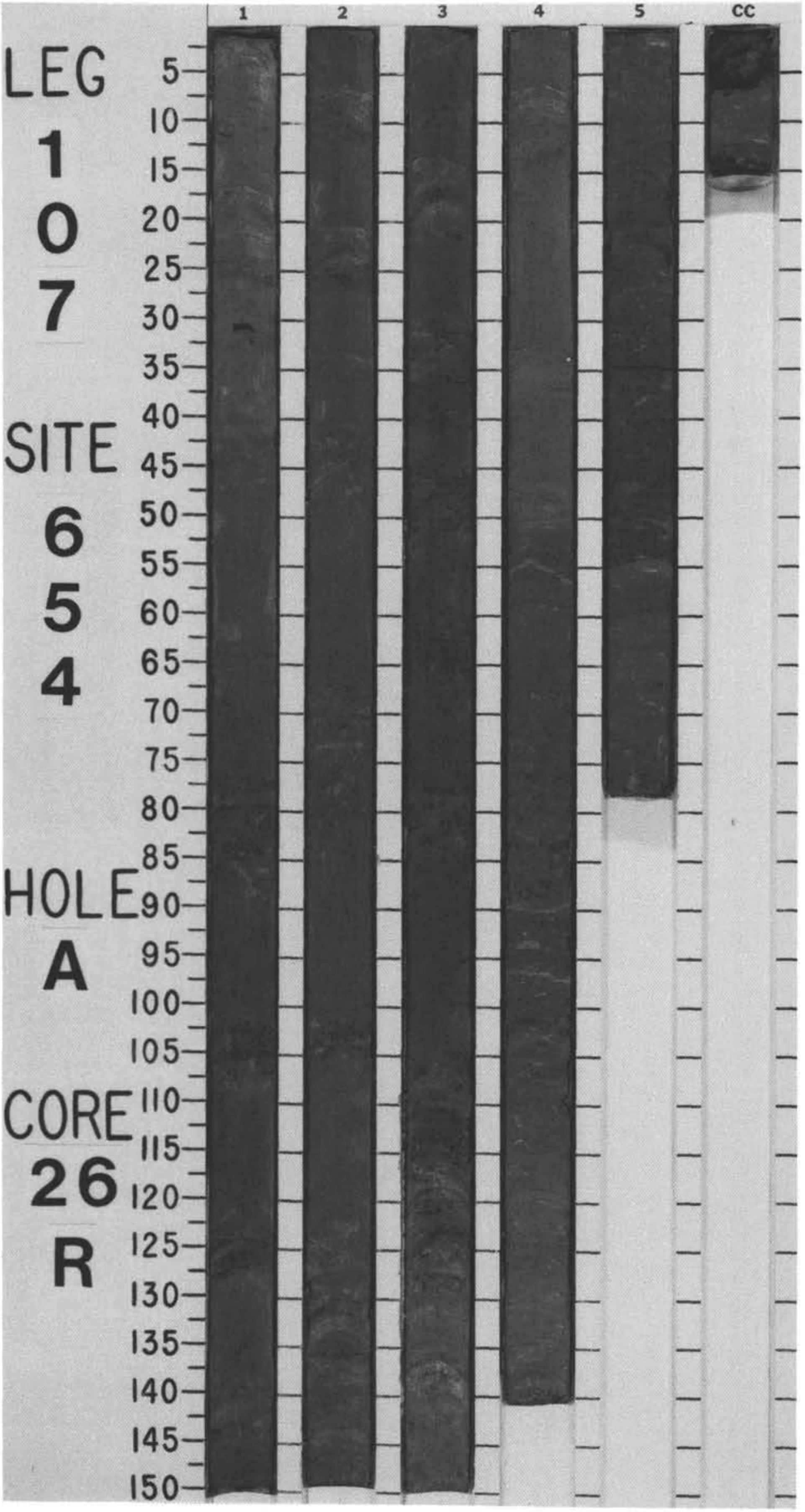

LEG
107
SITE
654
HOLE
A
CORE
26
R
1
2
3
4
5
CC
5
10
15
20
25
30
35
40
45
50
55
60
65
70
75
80
85
90
95
100
105
110
115
120
125
130
135
140
145
150

SITE 654 HOLE A CORE 27 R CORED INTERVAL 2450.4-2460.0 mbsl; 242.4-252.0 mbsf

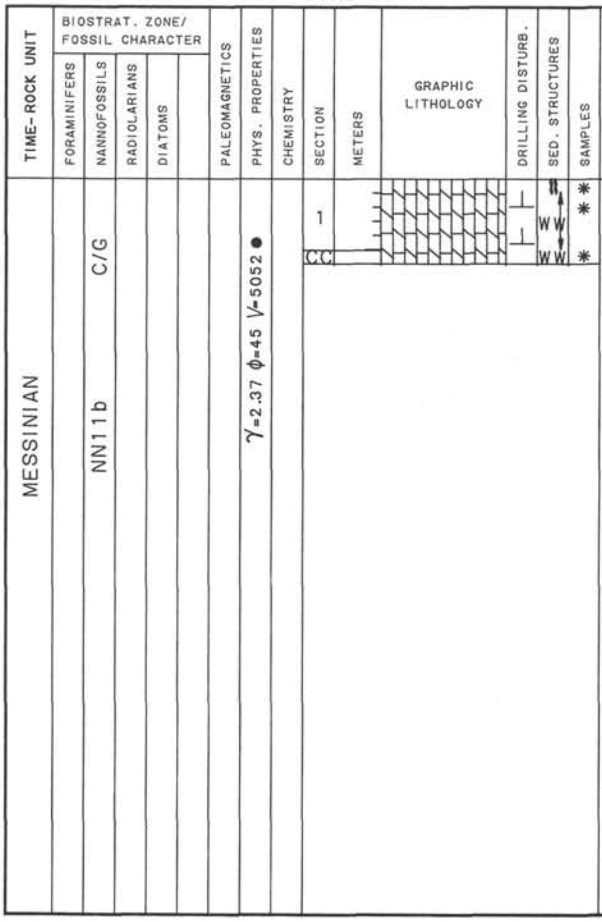

LITHOLOGIC DESCRIPTION

GYPSUM and FORAMINIFER-NANNOFOSSIL OOZE

Gypsum with minor olive-gray (5Y 4/2) foraminifer-nannofossil ooze found only in Section 1, 0–3 cm. True contact not recovered; gypsum occupies remainder of core. Gypsum is greenish gray (5GY 5/1), except for CC, 0–3 cm, where a gray (5Y 5/1), calcareous interval occurs. The gypsum is usually finely crystalline and displays wavy lamination describing various sedimentary cycles. The most common occurrences include fining-upward gypsum layer sandwiches between two thin laminae of greenish gray sediment; two laminae of gypsum separated by a dissolution surface, sometimes draped or filled by orange sediment; and coarsening-upward gypsum laminae (reverse-graded bedding) capped by greenish gray sediment. Authigenic minerals, probably zeolites, are common in some smear slides.

SMEAR SLIDE SUMMARY (%):

	1, 2 M	1, 20 M	CC, 5 M
TEXTURE:			
Sand	20	35	40
Silt	10	15	20
Clay	70	50	40
COMPOSITION:			
Quartz	5	—	—
Clay	12	20	17
Dolomite	3	30	30
Accessory minerals	1	1	—
Gypsum	1	8	20
Pyrite	1	1	—
Foraminifers	12	5	—
Nannofossils	60	—	3
Micrite	5	5	—
Dolomicrite	—	—	10
Zeolites	—	30	20

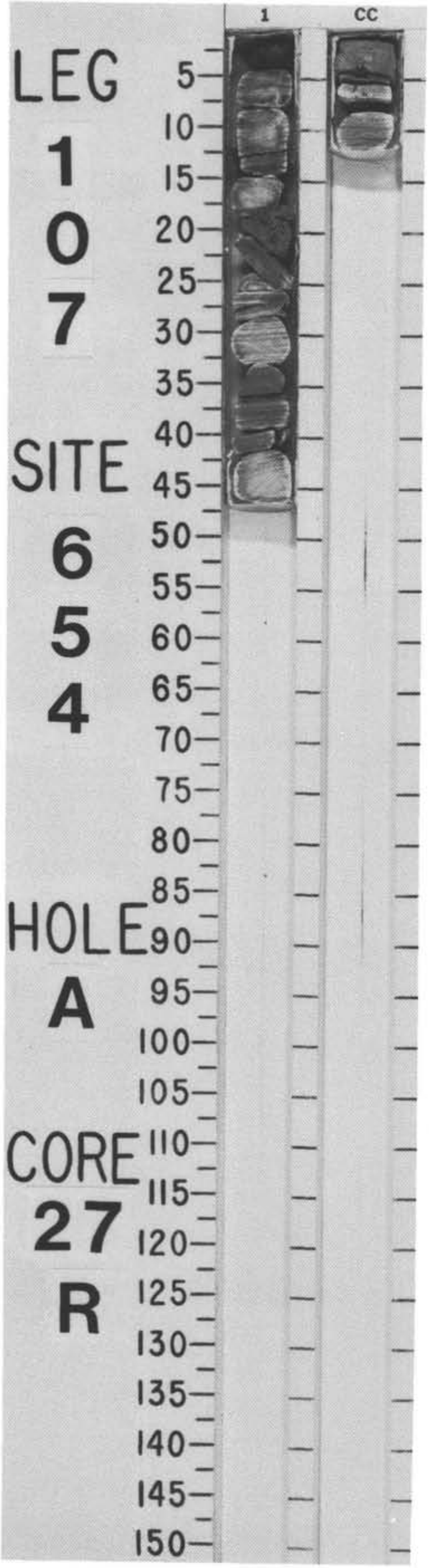
LEG
107
SITE
654
HOLE
A
CORE
27
R
1
CC
5
10
15
20
25
30
35
40
45
50
55
60
65
70
75
80
85
90
95
100
105
110
115
120
125
130
135
140
145
150

SITE 654 HOLE A CORE 28 R CORED INTERVAL 2460.0-2469.7 mbsl; 252.0-261.7 mbsf

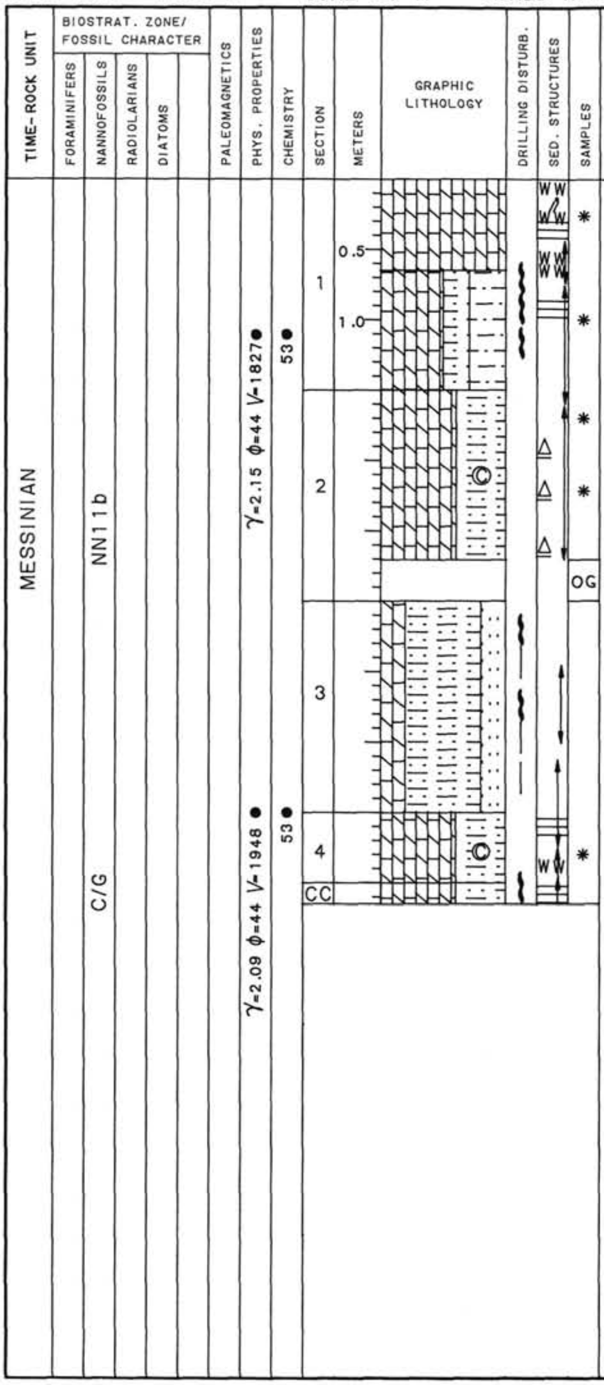

LITHOLOGIC DESCRIPTION

GYPSIFEROUS and DOLOMITIC SEDIMENT

Gypsiferous and dolomitic sediment, including complex and variable alternations of laminated gypsum, gypsiferous and calcareous sand, gypsiferous mud, dolomitic mud, and silty clay.

Section 1, 0–68 cm, is laminated gypsum (10G 8/2) and finely laminated gypsum, separated by 1–3-mm-thick grayish green (5G 5/2) laminae; 5–6 and 31–43 cm have gypsiferous, calcareous sands; there are cyclic alternations of darker layers (containing organic matter) and lighter layers with elongate gypsum clasts; at 14–26 cm the laminated gypsum is cracked and brecciated, offset, and filled with gypsum sand; at 60–70 cm the laminae are deformed due to gypsum crystal growth; at 50–150 cm are very finely laminated, gypsum-calcite mud and greenish gray (5GY 6/1) sand with very thin scour partings.

Section 2, 0–40 cm, is weakly consolidated gypsiform-dolomitic mud with pale yellowish green (10GY 7/2–7/1), graded, gypsiferous silt and mud; at 26–41 cm are large (up to 6-cm diameter) selenitic gypsum concretions; at 40–70 cm are repeated graded units, which at the base are silty and light green (10G 7/1) and at the top are pale yellowish green (10GY 7/2), which is parallel-laminated with tiny *Chondrites* burrows; ripples also occur (3-cm spacing, 1.1-cm height); 70–120 cm contains about 80 depositional units with silt and mud, often graded.

Section 3 is largely disturbed and typically shows units (at 91–94 cm) with scoured bases and greenish silt or clay, which coarsens upward into finely laminated, silty clay, gray (5Y 5/1), then into dark gray (5Y 4/1), homogeneous clay.

Section 4, 0–21 cm, contains 1–12-mm-thick, greenish gray (5BG 5/1) laminae, laterally continuous but with some wavy or flaser bedding; at 21–40 cm are hundreds of very fine, grayish green (10GY 5/2) laminae, tiny mud intraclasts, and many grains (rounded, 1/2-mm diameter) of detrital gypsum; at 40 cm is a 4.5-cm large, secondary selenitic gypsum concretion with disrupted lamination; at 40–50 cm is a series of discontinuous wavy laminae and 1-mm thin, selenitic gypsum layers with some laminae containing detrital gypsum; secondary gypsum crystals disrupt lamination. Colors are greenish gray (5BG 5/1) and grayish green (10GY 5/2, 5G 5/2).

CC contains white (5Y 8/1) anhydrite nodules and lenses within finely laminated, gypsiferous and/or anhydrite sand beds with generally sharp bases.

SMEAR SLIDE SUMMARY (%):

	1, 28 D	1, 106 M	2, 17 D	2, 78 M	4, 32 D
TEXTURE:					
Sand	—	50	—	50	25
Silt	50	25	50	25	50
Clay	50	25	50	25	25
COMPOSITION:					
Quartz	2	5	2	5	5
Feldspar	—	15	2	3	—
Clay	15	16	6	28	14
Dolomite	—	4	90	4	10
Accessory minerals	Tr	—	—	—	1
Gypsum	3	40	—	35	5
Micrite	80	—	—	—	60
Dolomicrite	2	—	—	—	—
Inorganic calcite	—	20	—	15	—
Limonite	—	—	—	10	2
Pyrite	—	—	—	—	3

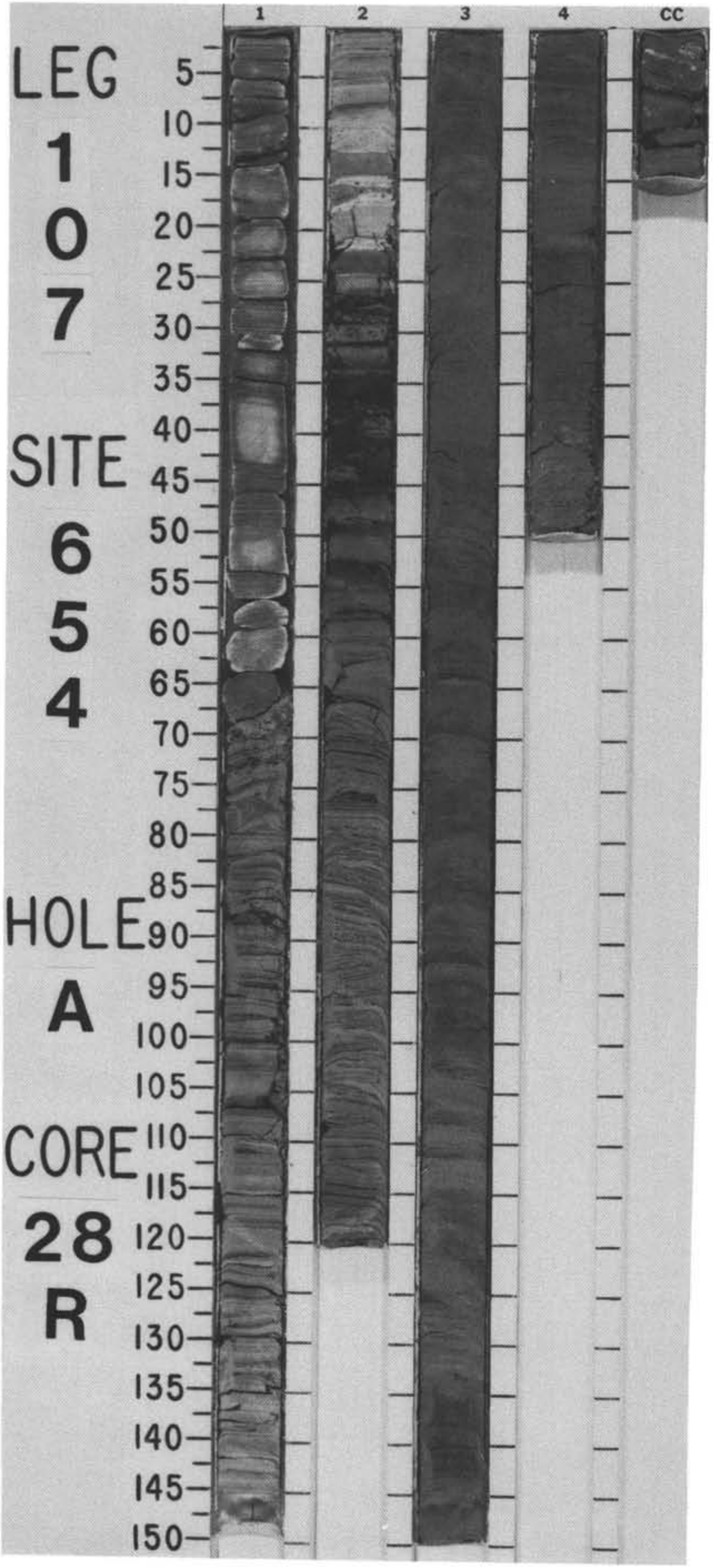
LEG 107
SITE 654
HOLE A
CORE 28 R
1
2
3
4
CC
5
10
15
20
25
30
35
40
45
50
55
60
65
70
75
80
85
90
95
100
105
110
115
120
125
130
135
140
145
150

SITE 654 HOLE A CORE 29 R CORED INTERVAL 2469.7-2479.3 mbsl; 261.7-271.3 mbsf

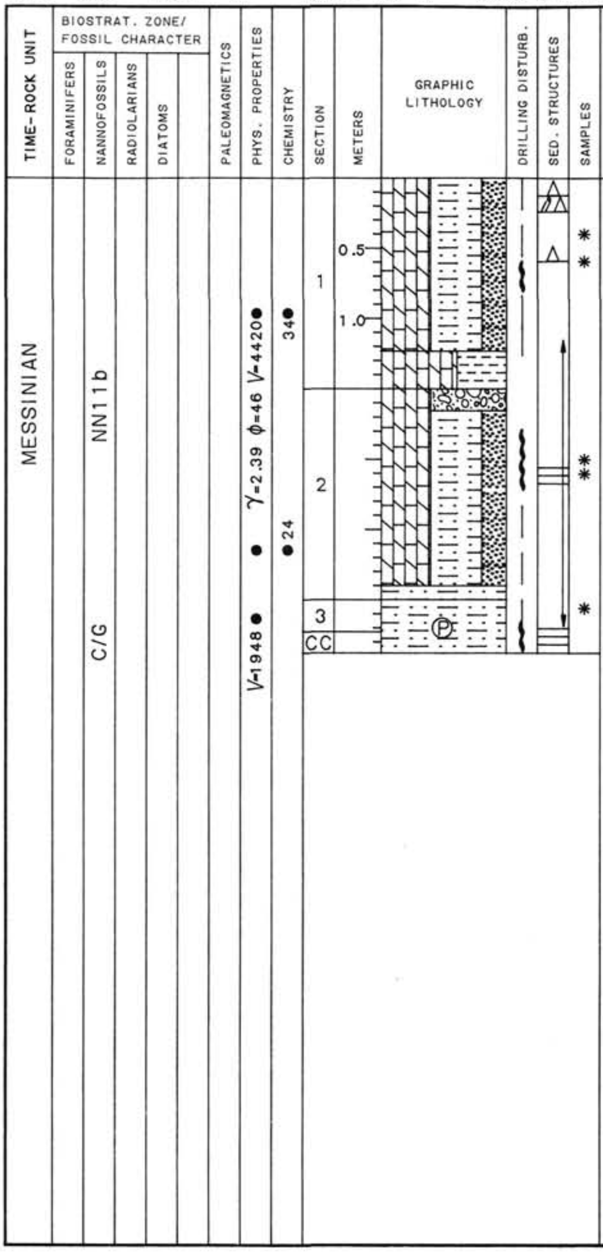

LITHOLOGIC DESCRIPTION

BALATINO GYPSUM, GYPSUM-RICH SAND, SILTY SAND, and CALCAREOUS MUDSTONE

Balatino gypsum, gypsum-rich sand, silty sand, and calcareous mudstone.

Section 1 is mostly gypsiferous mud and silty clay with subordinate Balatino gypsum; a subvertical fracture is infilled with gypsiferous sand and silty sand; 10–12 cm is a breccia partly disturbed by drilling; 50–60 cm is a graded breccia composed of gypsiferous pebbles as large as 0.6 cm in diameter; 70–73 cm is Balatino gypsum; 70–80 cm is disturbed, but contains anhydrite nodules; 85–100 cm is weakly calcareous, homogeneous mud; 110–120 cm is Balatino gypsum; 125–150 cm is about 50 clay-gypsum couplets each <4-mm thick.

Section 2, 5–14 cm, is breccia disturbed by drilling; 15–21 cm is 14 Balatino gypsum/clay couplets; 21–80 cm is very disturbed, but comprises some fragments of Balatino, passing into alternations of sandy, gypsiferous, silty clay layers; at 97–128 cm elongate selenite gypsum as long as 7 cm, with centripetal growth patterns; 132–133 cm is crystal-like gypsum; colors are light olive-brown (2.5Y 5/6), light olive-gray (5Y 6/2), dusky yellow-green (5GY 5/2), and brownish yellow (10YR 6/8); 138–150 cm is well-laminated, gray (5Y 5/1), calcareous mud.

Section 3 is gray (5Y 5/1) calcareous mud with a pyrite layer.

CC has alternations of darker and lighter gray (5Y 5/1), poorly calcareous mudstone with a pyrite layer.

SMEAR SLIDE SUMMARY (%):

	1, 49 D	1, 57 M	2, 54 D	2, 70 D	3, 10 D
TEXTURE:					
Sand	25	50	5	—	—
Silt	40	40	35	5	10
Clay	35	10	60	95	90
COMPOSITION:					
Quartz	18	15	4	5	1
Feldspar	—	—	2	—	—
Mica	5	—	—	—	—
Clay	30	10	30	—	25
Dolomite	4	—	5	5	10
Accessory minerals (pyrite)	—	—	15	—	3
Zeolite	Tr	5	5	—	1
Gypsum	8	30	23	20	30
Anhydrite	2	—	5	—	5
Foraminifers	Tr	Tr	1	—	—
Nannofossils	20	20	10	10	25
Bioclasts	13	10	—	—	—
Opaques	—	3	—	—	—
Limonite	—	7	—	60	—
Aragonite	—	Tr	—	—	—
Analcite	—	Tr	—	—	—

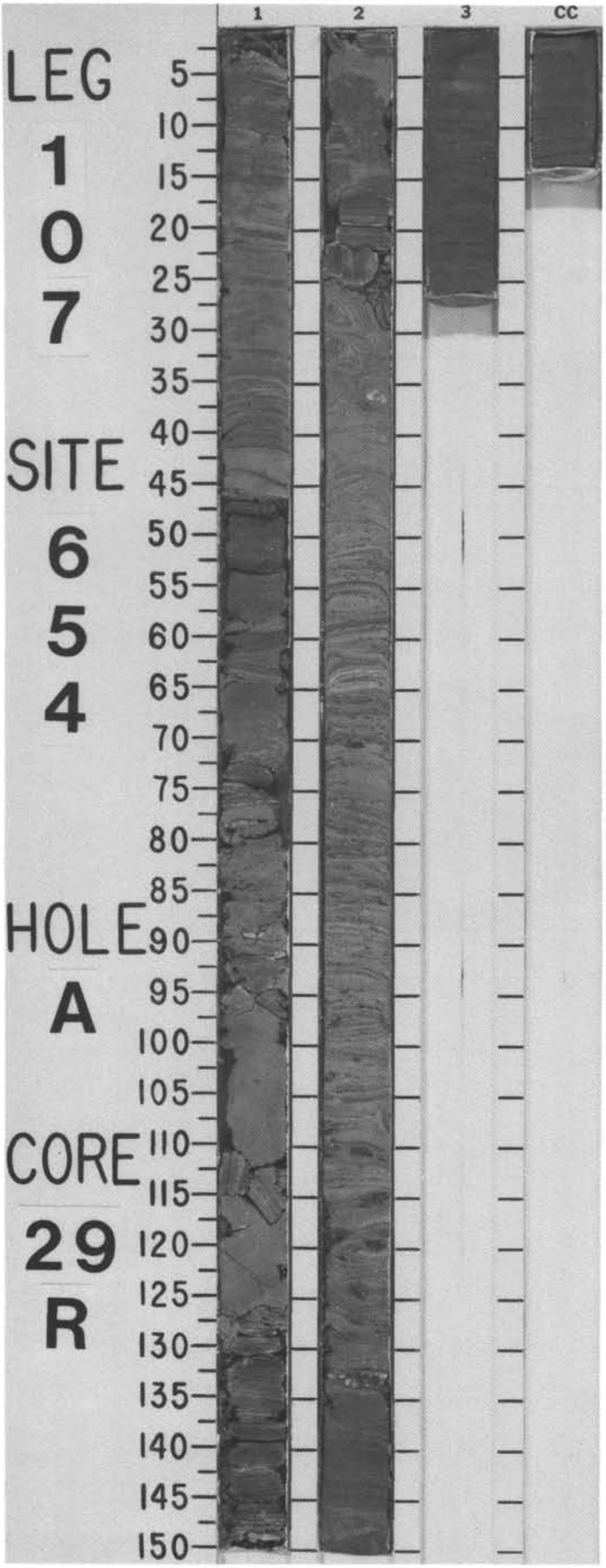
1
2
3
CC
LEG
107
SITE
654
HOLE
A
CORE
29
R
5
10
15
20
25
30
35
40
45
50
55
60
65
70
75
80
85
90
95
100
105
110
115
120
125
130
135
140
145
150

SITE 654 HOLE A CORE 30 R CORED INTERVAL 2479.3-2484.3 mbsl; 271.3-276.3 mbsf

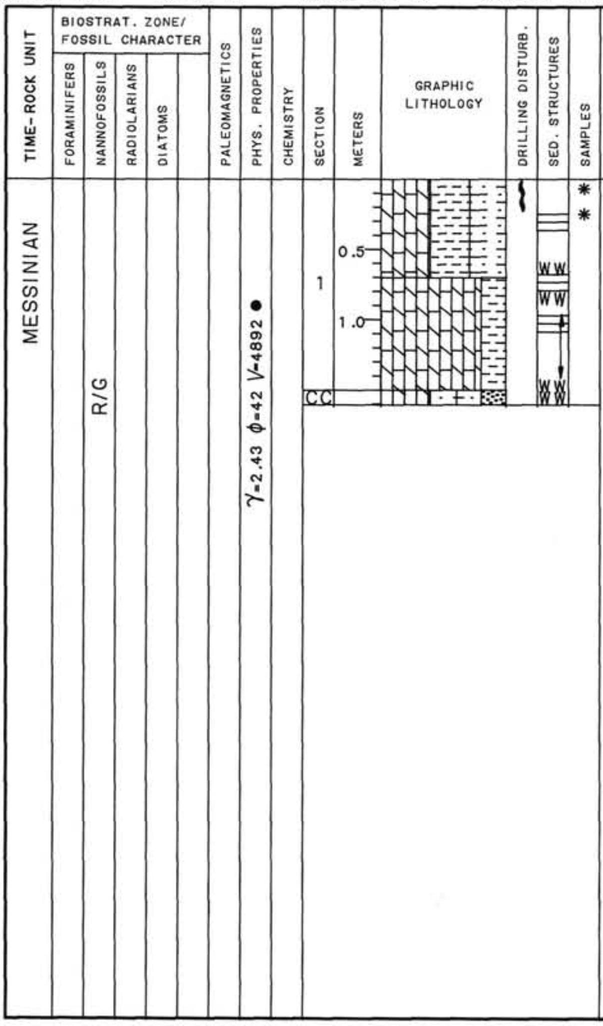

LITHOLOGIC DESCRIPTION

BALATINO GYPSUM, MUDSTONE, CLAYSTONE, and SANDSTONE

Balatino gypsum, mudstone, claystone, and minor sandstone.

Section 1, 0–68 cm, has 90 units, each <1-cm-thick, of reverse-graded, very finely laminated, gypsiferous mud, light yellowish brown (2.5Y 6/4), light olive-brown (2.5Y 5/4), and light gray (2.5Y 7/2), with very small *Chondrites* burrows, grading to calcareous-gypsiferous silt with small ripples. The 70–150 cm interval is composed of Balatino gypsum with both parallel and wavy lamination (the latter mostly convex upward). The finely-laminated, white (5GY 6/1), alabastrine gypsum is interlaminated with green (5G 5/2) laminae, some wavy and discontinuous; the convex-upward, wavy lamination is especially well developed at 140–150 cm. There is a prominent normal fault at 100–122 cm; the apparent dip of the bedding here is 34° and the dip of the fault is 85°, with a throw of 1.5 cm; the fault plane is filled and cemented by sparry gypsum.

CC contains a pale yellowish green (10GY 7/2), silty mud at 0–1.5 cm. From this unit to 9 cm is a prominent reverse-graded unit composed of greenish gypsiferous mud, passing up through medium- and coarse-grained sand with numerous rip-up clasts of gypsum. The unit is well cemented.

SMEAR SLIDE SUMMARY (%):

	1, 5 D	1, 29 M
TEXTURE:		
Sand	—	30
Silt	10	50
Clay	90	20
COMPOSITION:		
Quartz	10	20
Clay	15	—
Volcanic glass	2	2
Dolomite	15	10
Accessory minerals	5	25
Anhydrite	30	10
Gypsum		26
Zeolite	3	—
Foraminifers	—	5
Nannofossils	20	2

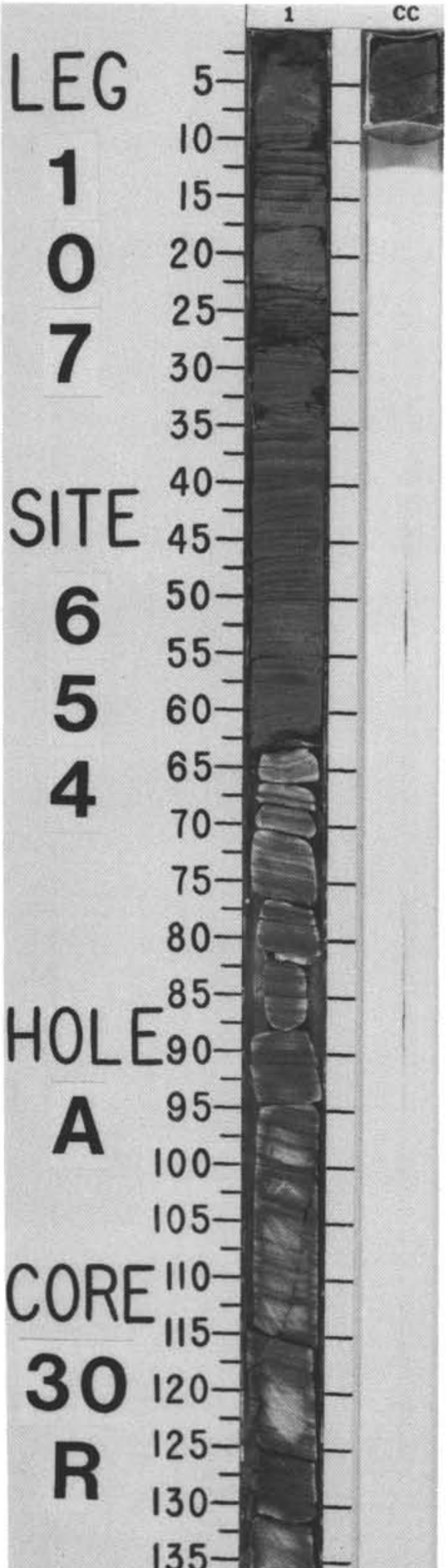
LEG
107
SITE
654
HOLE
A
CORE
30
R
1
CC
5
10
15
20
25
30
35
40
45
50
55
60
65
70
75
80
85
90
95
100
105
110
115
120
125
130
135
140
145
150

SITE 654 HOLE A CORE 31 R CORED INTERVAL 2484.3-2488.9 mbsl; 276.3-280.9 mbsf

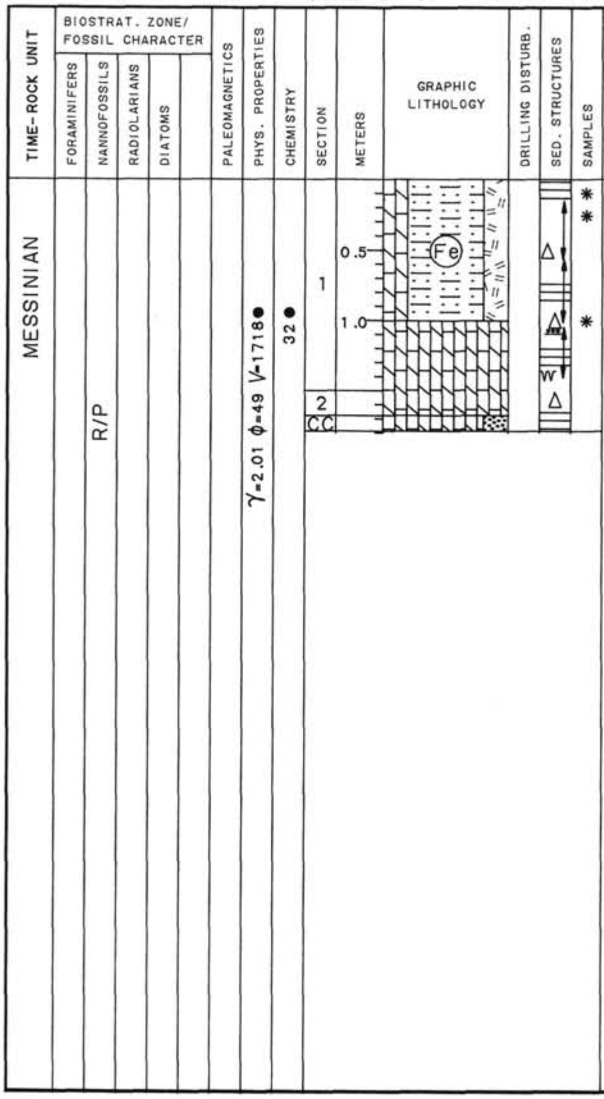

LITHOLOGIC DESCRIPTION

VOLCANIC ASH-RICH MUDSTONE, DOLOMITIC MUDSTONE, BRECCIA, and BALATINO GYPSUM

Volcanic ash-rich mudstone, dolomitic mudstone, minor breccia, and balatino gypsum.

Section 1, 0–8 cm, is very coarse gypsum crystals; 8–21 cm has 2–5-cm-thick, grayish olive (10GY 5/2) and olive-yellow (2.5Y 6/5), gypsiferous mud units with a sharp base; these are underlain by flat lying, whitish flaser beds (gypsum?) and homogeneous mud; 30–60 cm is alternations of graded units, <5-cm thick, composed of thin sandy, silty layers at the base, passing into poorly calcareous, silty mud at the top, rich in limonite; 62–95 cm is gray (2.5Y 5/0) mud (fizzes in HCl), with alternations of lighter gray; 95–105 cm is a microbreccia layer, grayish green (10GY 5/2) and yellowish green (10GY 6/5), containing scattered rounded sand grains of possibly eolian origin. The breccia is matrix supported, with a slight color change in the middle; 105–110 cm is greenish gray (5GY 6/1), crystalline gypsum showing twinning; 110–140 cm is Balatino gypsum (mm thick, and a few cm thick); 138–145 cm is finely crystalline gypsum at the base with a wavy, possibly algal, lamination at the top; 145–150 cm is a dolomitic layer.

Section 2 contains numerous Balatino gypsum units as in Section 1.

CC is more Balatino cycles, the last one beginning with a thin, graded microbreccia containing clay pebbles and reworked iron oxide.

SMEAR SLIDE SUMMARY (%):

	1, 11 D	1, 27 D	1, 102 D
TEXTURE:			
Sand	—	10	5
Silt	10	50	30
Clay	90	40	65
COMPOSITION:			
Quartz	—	—	5
Clay	30	25	25
Volcanic glass	2	35	30
Calcite/dolomite	28	2	—
Accessory minerals	10	—	—
Zeolite	Tr	—	5
Gypsum	30	5	5
Foraminifers	Tr	Tr	—
Nannofossils	Tr	10	10
Bioclasts/intraclasts	—	28	20

SITE 654 HOLE A CORE 32 R CORED INTERVAL 2488.9-2495.6 mbsl; 280.9-287.6 mbsf

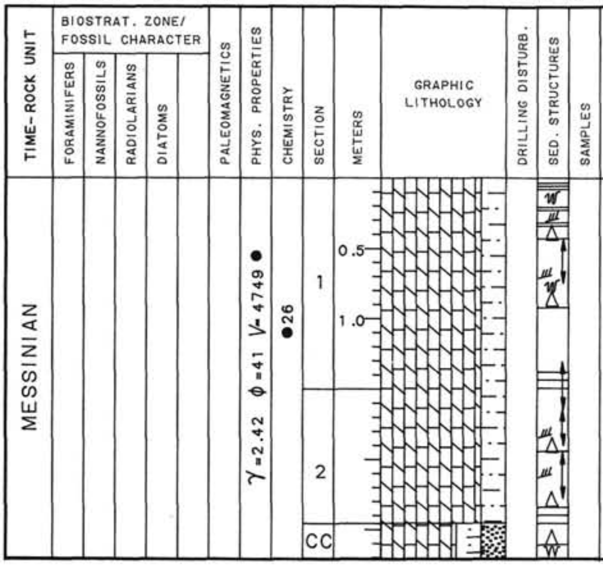

LITHOLOGIC DESCRIPTION

BALATINO GYPSUM, SILTSTONE, and SANDSTONE

Balatino gypsum and minor siltstone and sandstone, hard and well lithified.

Section 1 is well-laminated Balatino gypsum with some ripple cross-bedding and graded-bedding; a well-developed ripple is present at 87 cm; colors are grayish green (10GY 5/2), moderate greenish yellow (10Y 7/4), dark gray (5Y 4/1), white (10YR 8/1), and light yellowish brown (10YR 6/4). There is some recrystallization of the gypsum at 140–150 cm.

Section 2 is well-layered Balatino gypsum; dominant color is (10GY 5/12), but there are 1-mm-thick alternations of greenish, grayish, yellowish, and white. Some layers of sandy gypsum which coarsen downward occur; and some cross lamination is visible.

CC contains more Balatino gypsum, probably stromatolitic; at 15–16 cm is a sandy siltstone and mudstone layer.

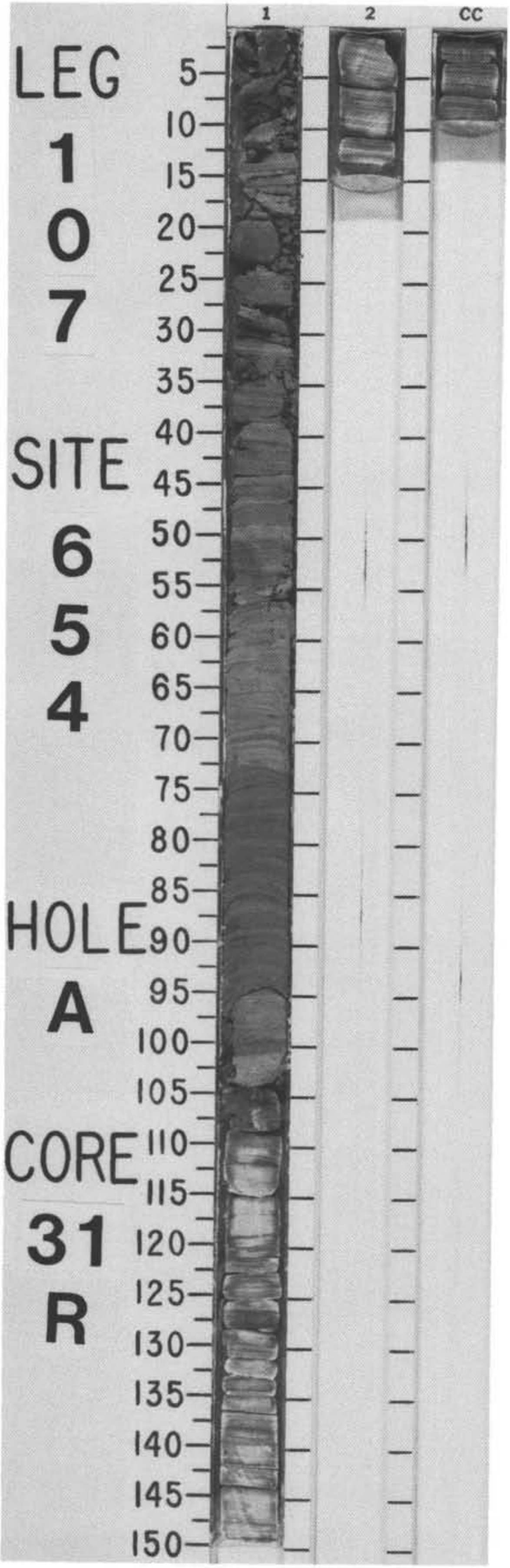
LEG 1 0 7
SITE 6 5 4
HOLE A
CORE 31 R
1
2
CC
5
10
15
20
25
30
35
40
45
50
55
60
65
70
75
80
85
90
95
100
105
110
115
120
125
130
135
140
145
150

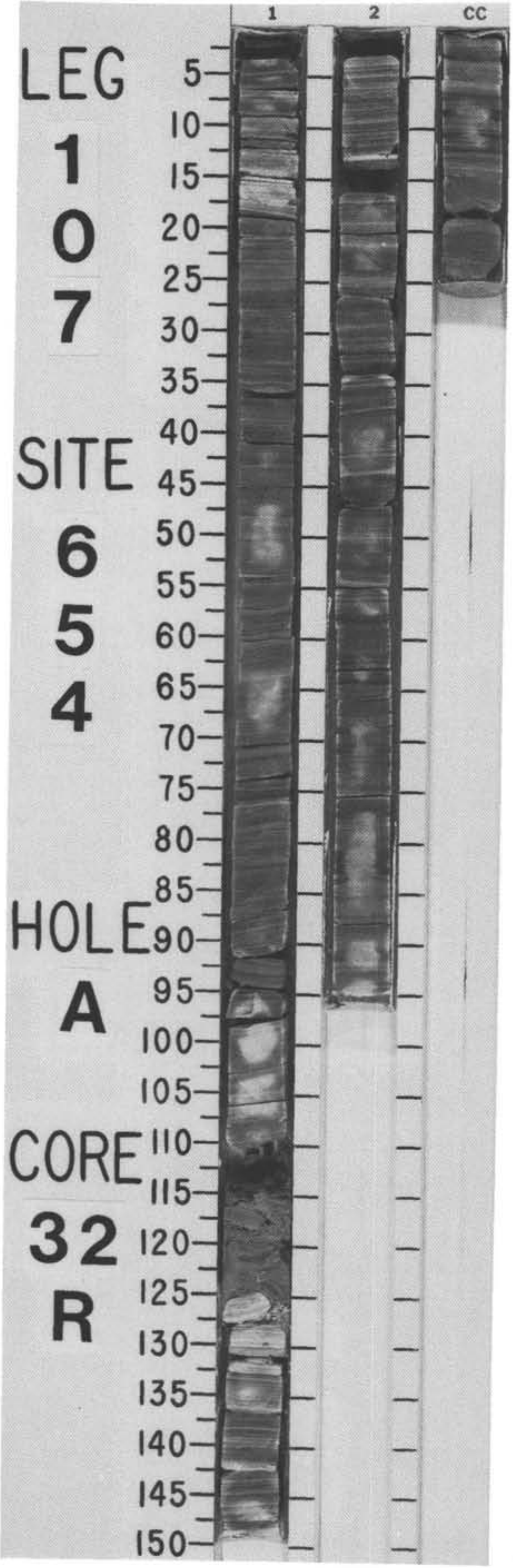
LEG 1 0 7
SITE 6 5 4
HOLE A
CORE 32 R
1
2
CC
5
10
15
20
25
30
35
40
45
50
55
60
65
70
75
80
85
90
95
100
105
110
115
120
125
130
135
140
145
150

SITE 654 HOLE A CORE 33 R CORED INTERVAL 2495.6-2498.6 mbsl; 287.6-290.6 mbsf

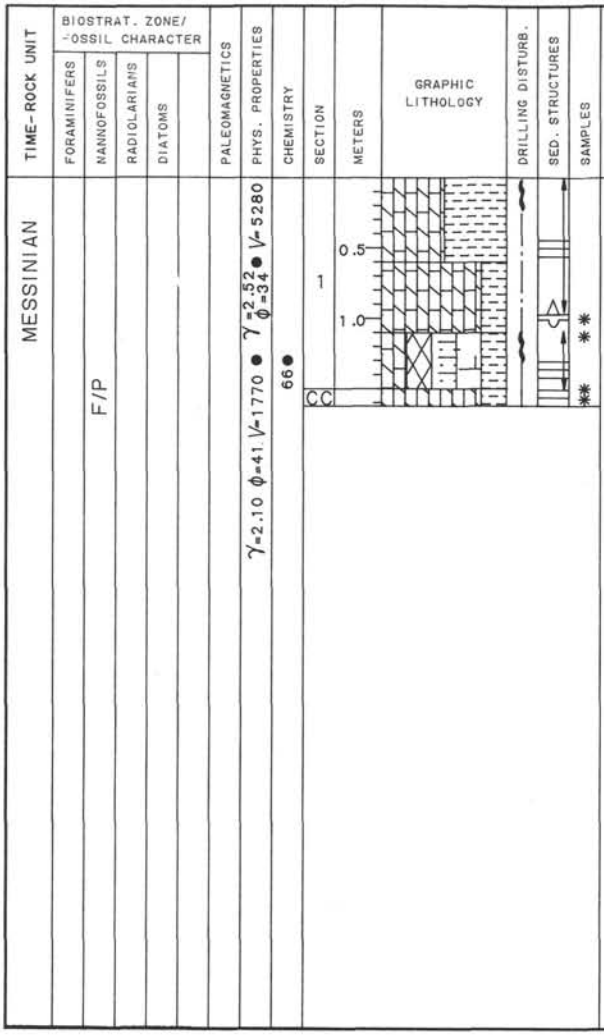

LITHOLOGIC DESCRIPTION

GYPSIFEROUS MUDSTONE, SANDY SILTSTONE, ANHYDRITE, and NANNOFOSSIL CHALK

Gypsiferous mudstone, sandy siltstone, anhydrite, and minor nannofossil chalk.

Section 1: drilling breccia at 10–11 cm; 11–40 cm is composed of varicolored mud, with alternations of thin, well-layered, dark gray, calcareous mudstone and very thin, gray (5Y 5/1), gypsum laminae; at 40–60 cm the units are thicker, up to 2–3 cm each; 60–75 cm is crystalline gypsum; 75–102 cm is composed of Balatino gypsum sequences, light yellowish brown (10YR 6/4) and greenish gray (5GY 5/1), mm-thick alternations, some of which are undulose and could be stromatolitic; 102–114 cm is white, nannofossil-bearing marls that are very disturbed by drilling and well-lithified, gray (5Y 6/1) layers of gypsum showing small-scale grading and wavy lamination; at 114 cm is a sandy gypsiferous layer; 114–150 cm is well-laminated, varicolored, calcareous mud (10GY 5/12) and light gray (5Y 7/1).

CC is well-laminated, very dark gray (5Y 3/1), gypsiferous mud.

SMEAR SLIDE SUMMARY (%):

	1, 106 M	1, 113 M	1, 146 D	CC, 14 D
TEXTURE:				
Sand	—	15	—	10
Silt	25	55	100	40
Clay	75	30	—	50
COMPOSITION:				
Quartz	10	15	—	5
Clay	20	15	—	35
Volcanic glass	10	—	—	—
Dolomite	—	Tr	—	9
Accessory minerals	—	—	—	15
Micrite	15	—	—	—
Gypsum	—	35	—	30
Anhydrite	—	5	100	5
Foraminifers	3	5	—	—
Nannofossils	27	5	—	—
Bioclasts/intraclasts	15	20	—	—
Aragonite needles	Tr	—	—	—
Zeolites	—	—	—	1

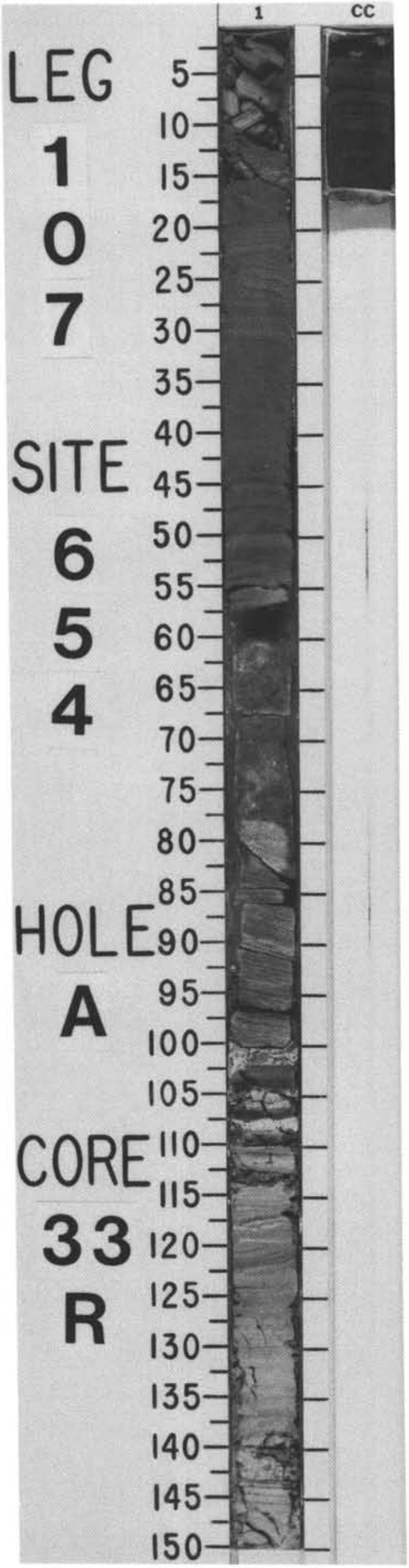
LEG
1
0
7
SITE
6
5
4
HOLE
A
CORE
33
R
1
CC
5
10
15
20
25
30
35
40
45
50
55
60
65
70
75
80
85
90
95
100
105
110
115
120
125
130
135
140
145
150

SITE 654 HOLE A CORE 34 R CORED INTERVAL 2498.6-2508.3 mbsl; 290.6-300.3 mbsf

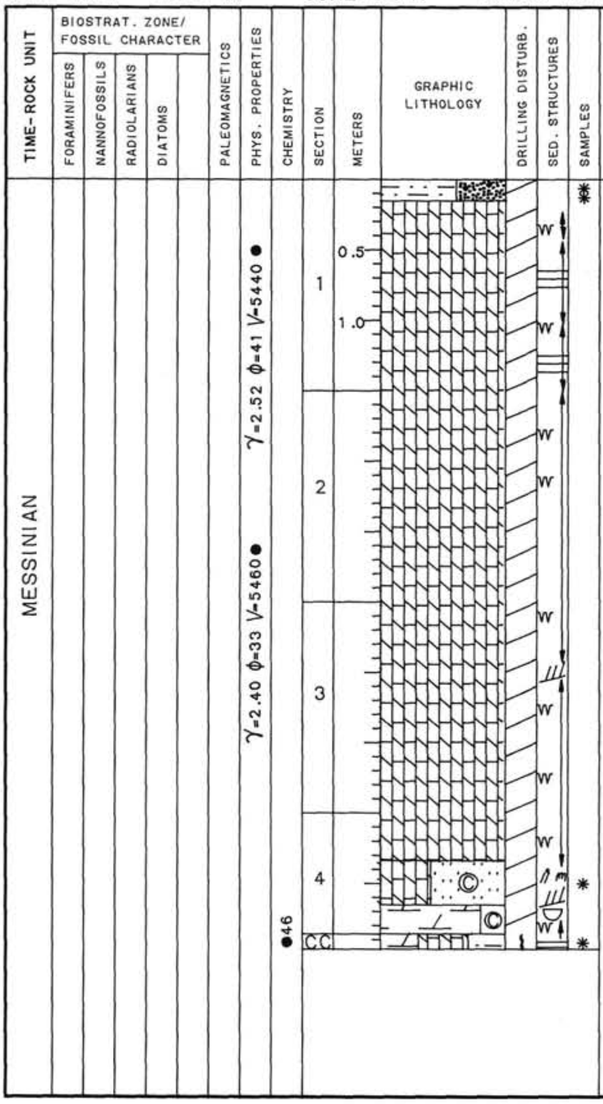

LITHOLOGIC DESCRIPTION

GYPSUM with traces of DOLOMITIC MARLSTONE, GYPSUM- and CARBONATE-RICH SANDSTONE, and SANDY MUDSTONE

Gypsum with traces of dolomitic marlstone, gypsum- and carbonate-rich sandstone, and sandy mudstone; except for the top of Section 1, where gypsum shows large secondary crystals, the gypsum occurs in laminae 0.5–1.0-cm thick, mostly with wavy lamination; arranged in cycles showing coarsening-upward grains; each cycle begins with fine-grained greenish gray sediments overlain by grayish fine-grained gypsum and by clear, coarser grained gypsum.

Section 1, 98–100 cm, and Section 2, 100–103 cm, contain redeposited elongated coarse grains of gypsum (rip-up brecciation); laminae in these evaporitic intervals are white (5Y 8/1), light gray (5Y 7/1), olive-gray (5Y 5/2), and dusky yellow-green (5GY 5/2).

Section 4, 38–66 cm, contains two intervals of gypsum-rich carbonate sandstone and siltstone with gypsum, white biogenic material, and in situ *in situ* pyrite crystals; from 66 cm to end of Section are numerous white laminae, <mm-thick, having a carbonate composition.

CC contains a drilling admixture, light gray (5Y 7/1), gray (5Y 5/1), and dark gray (5Y 4/1), of gypsum-rich carbonate mudstone to sandy mudstone, finely parallel-laminated with secondary gypsum crystals and pyrite framboids growing along the laminae.

SMEAR SLIDE SUMMARY (%):

	1, 10	1, 12	4, 50	CC, 10
	M	M	M	D
TEXTURE:				
Sand	—	70	60	15
Silt	50	15	20	25
Clay	50	15	20	60
COMPOSITION:				
Quartz	4	2	2	2
Feldspar	—	—	—	5
Mica	—	6	—	—
Clay	9	—	16	30
Dolomite	—	2	3	15
Accessory minerals	—	—	1	—
Pyrite	—	—	3	8
Nannofossils	2	—	—	—
Micrite (dolomicrite)	80	30	20	30
Gypsum	5	35	30	10
Zeolites	—	25	25	—

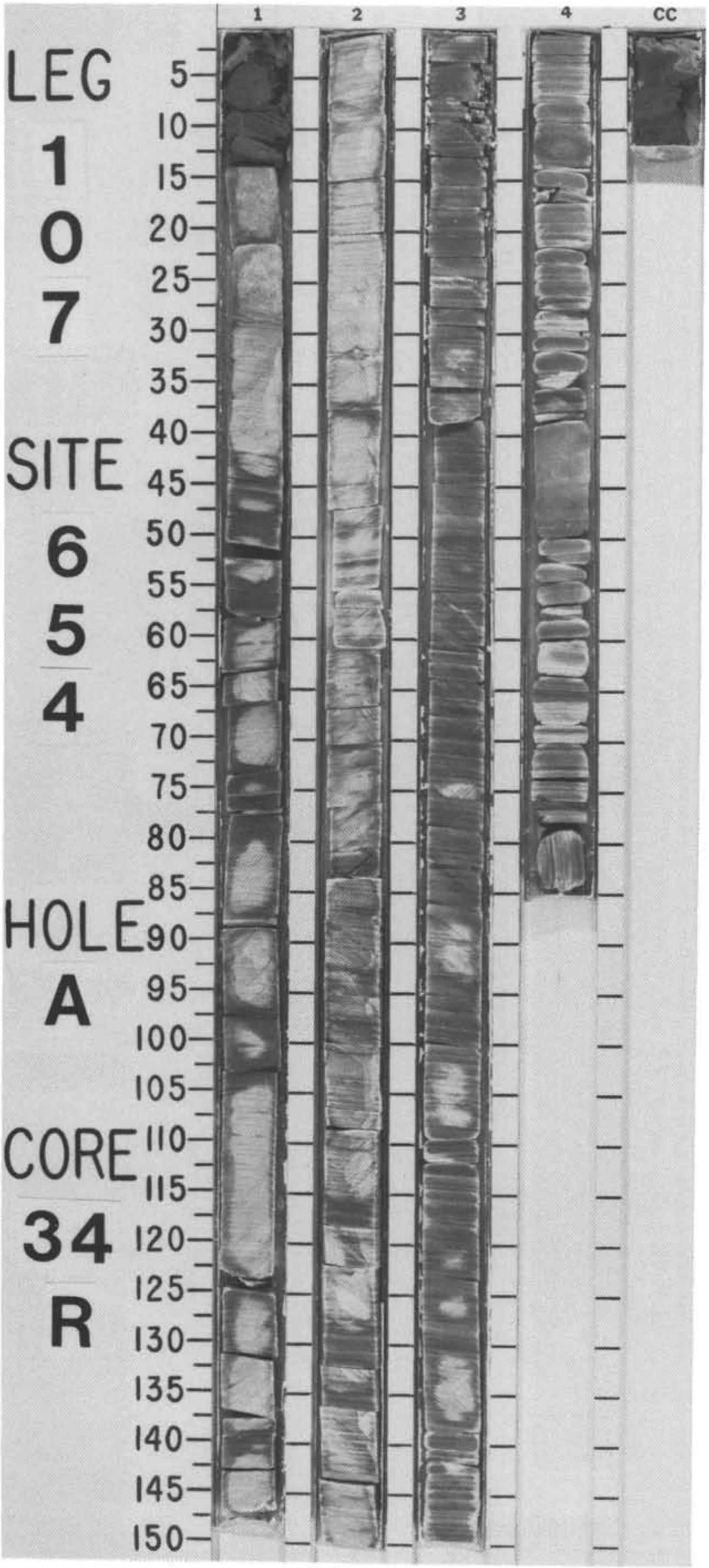
LEG
107
SITE
654
HOLE
A
CORE
34
R
1
2
3
4
CC
5
10
15
20
25
30
35
40
45
50
55
60
65
70
75
80
85
90
95
100
105
110
115
120
125
130
135
140
145
150

SITE 654 HOLE A CORE 35 R CORED INTERVAL 2508.3-2518.0 mbsl; 300.3-310.0 mbsf

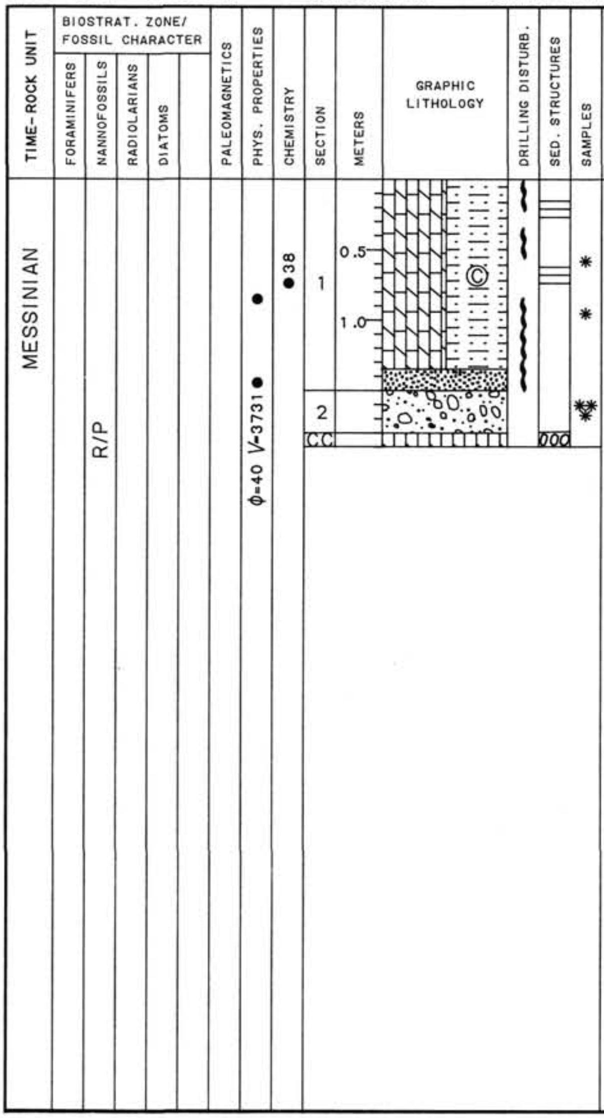

LITHOLOGIC DESCRIPTION

GYPSUM, CALCAREOUS MUDSTONE, SANDSTONE, and BRECCIA

Gypsum, calcareous mudstone, sandstone, and breccia.

Section 1 is largely disturbed and homogenized by drilling; where less disturbed, it shows layers of gypsiferous and calcareous mudstone containing pockets of secondary gypsum crystals (sometimes discoidal, as at 35 cm) and of abundant pyrite, the latter mainly associated with laminae surfaces or secondary gypsum crystals; color is gray (5Y 5/1), becoming light gray (5Y 7/1) in the homogenized intervals. The lowermost 15 cm contains a poorly sorted gypsiferous-calcareous sandstone with elongate gypsum clasts, showing internal parallel lamination in a fine-grained, gray (5Y 5/1) matrix.

In Section 2 this lithology becomes a gray (5Y 5/1, 6/1) poorly sorted, gypsiferous-calcareous breccia with large (up to 2-cm diameter) clasts, which include laminated gypsum and authigenic zeolite-rich lithologies and first-generation breccia clasts. The matrix is finely crystalline carbonate.

CC contains gray (5Y 5/1, 6/1), finely laminated gypsum, showing mud cracks or dissolution cracks, as well as gypsiferous sandstone with elongate, curved, and imbricated gypsum crystals.

SMEAR SLIDE SUMMARY (%):

	1, 61 M	1, 100 D	2, 21 M	2, 21 M	2, 23 M
TEXTURE:					
Sand	25	3	90	80	35
Silt	40	20	5	15	10
Clay	35	77	5	5	55
COMPOSITION:					
Quartz	5	2	—	—	—
Feldspar	3	—	—	—	—
Rock fragments	Tr	—	—	—	—
Mica	1	—	—	—	—
Clay	24	7	6	—	—
Volcanic glass	2	—	—	—	—
Calcite	1	—	—	—	—
Dolomite	Tr	—	—	—	—
Accessory minerals	Tr	—	—	—	—
Pyrite	—	6	Tr	—	—
Nannofossils	Tr	—	—	—	—
Micrite	50	85	7	15	40
Gypsum	15	—	7	25	30
Zeolites	—	—	80	60	30

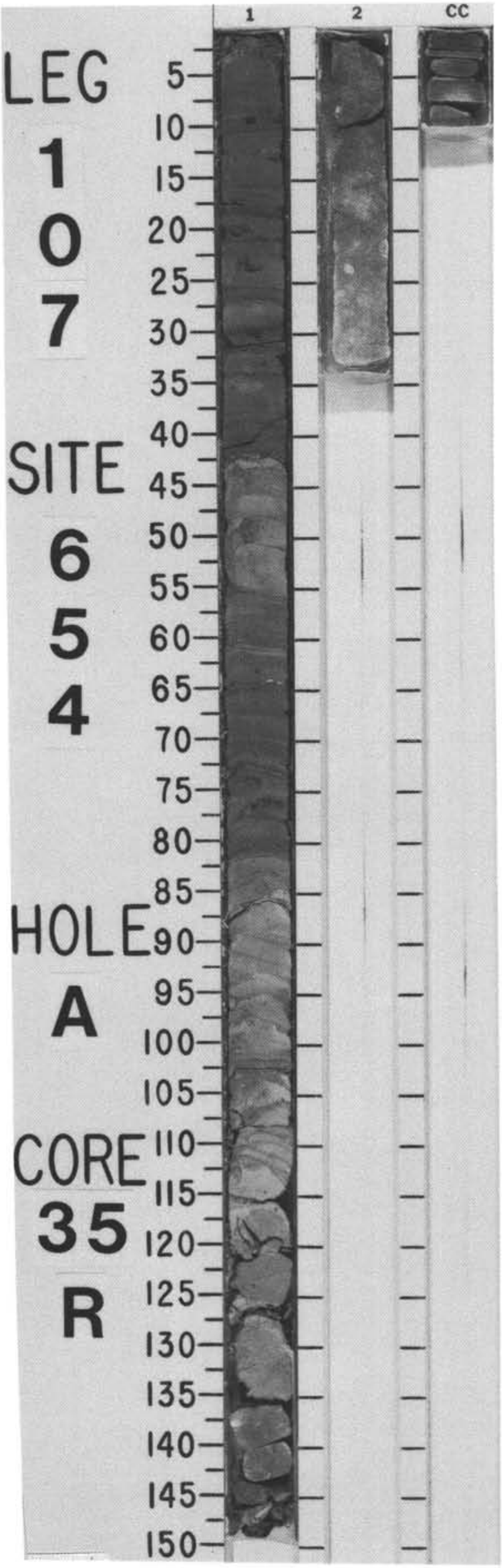
LEG
1
0
7
SITE
6
5
4
HOLE
A
CORE
35
R
1
2
CC
5
10
15
20
25
30
35
40
45
50
55
60
65
70
75
80
85
90
95
100
105
110
115
120
125
130
135
140
145
150

SITE 654 HOLE A CORE 36 R CORED INTERVAL 2518.0-2527.6 mbsl; 310.0-319.6 mbsf

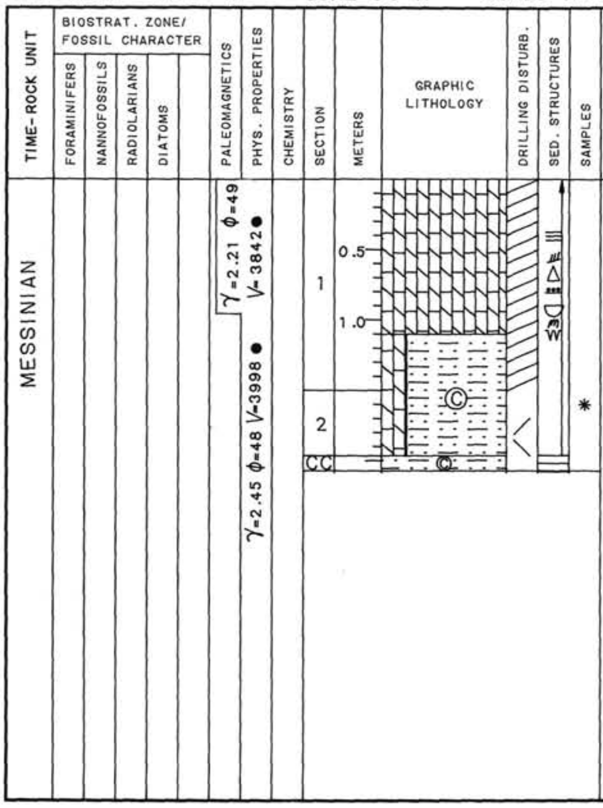

LITHOLOGIC DESCRIPTION

GYPSUM and GYPSIFEROUS-CALCAREOUS MUDSTONE

Gypsum and gypsiferous-calcareous mudstone.

Section 1, 0–110 cm, contains finely laminated (<0.5 mm) gypsum in colors alternating from light olive-gray (5Y 6/2) to gray (5Y 5/1, 6/1); several structures alternate at a cm-scale length, including parallel laminations, small asymmetrical ripples, and scours. From Section 1, 110 cm, to the bottom of the core, laminated, gypsum-bearing, gray (5Y 6/1), carbonate mudstone occurs. The mudstone contains all the previous structures, plus reworked elongate and rounded particles laid down by currents (fecal pellets?). Calcareous mudstone becomes homogeneous in CC, 7–10 cm.

SMEAR SLIDE SUMMARY (%):

	2, 15 D
TEXTURE:	
Sand	10
Silt	—
Clay	90
COMPOSITION:	
Quartz	1
Feldspar	3
Clay	1
Micrite	90
Gypsum	5

SITE 654 HOLE A CORE 37 R CORED INTERVAL 2527.6-2537.3 mbsl; 319.6-329.3 mbsf

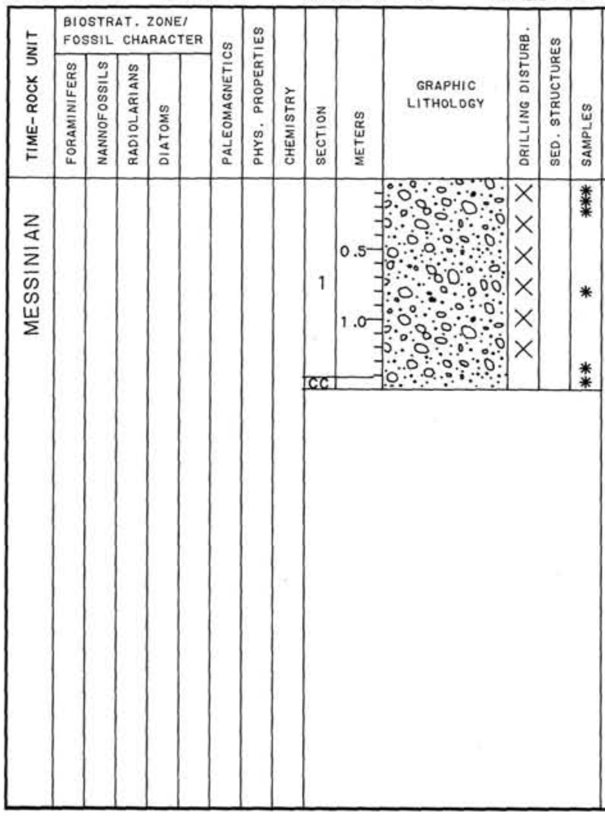

LITHOLOGIC DESCRIPTION

DRILLING BRECCIA

Drilling breccia of various lithologies, including a Pliocene nannofossil ooze (s.s. minor, Section 1, 7 cm). Most lithologies have been encountered in previous Messinian cores, but in addition, in the CC there were two pieces, one of which showed flaser bedding.

SMEAR SLIDE SUMMARY (%):

	1, 4 M	1, 7 M	1, 18 M	1, 84 M	1, 134 M	CC, 6 D
TEXTURE:						
Sand	15	2	80	95	3	35
Silt	15	3	10	—	30	25
Clay	70	95	10	5	67	40
COMPOSITION:						
Quartz	3	3	—	1	3	2
Clay	—	24	10	—	—	6
Dolomite	10	2	—	—	—	8
Accessory minerals	2	1	—	—	—	—
Pyrite	1	—	—	—	7	12
Limonite	2	—	—	95	—	—
Organic matter	—	—	—	—	—	2
Nannofossils	—	50	—	—	—	—
Plant debris	—	—	—	—	—	2
Micrite	67	20	20	—	79	25
Gypsum	15	—	70	4	10	8
Zeolites	—	—	—	—	—	35

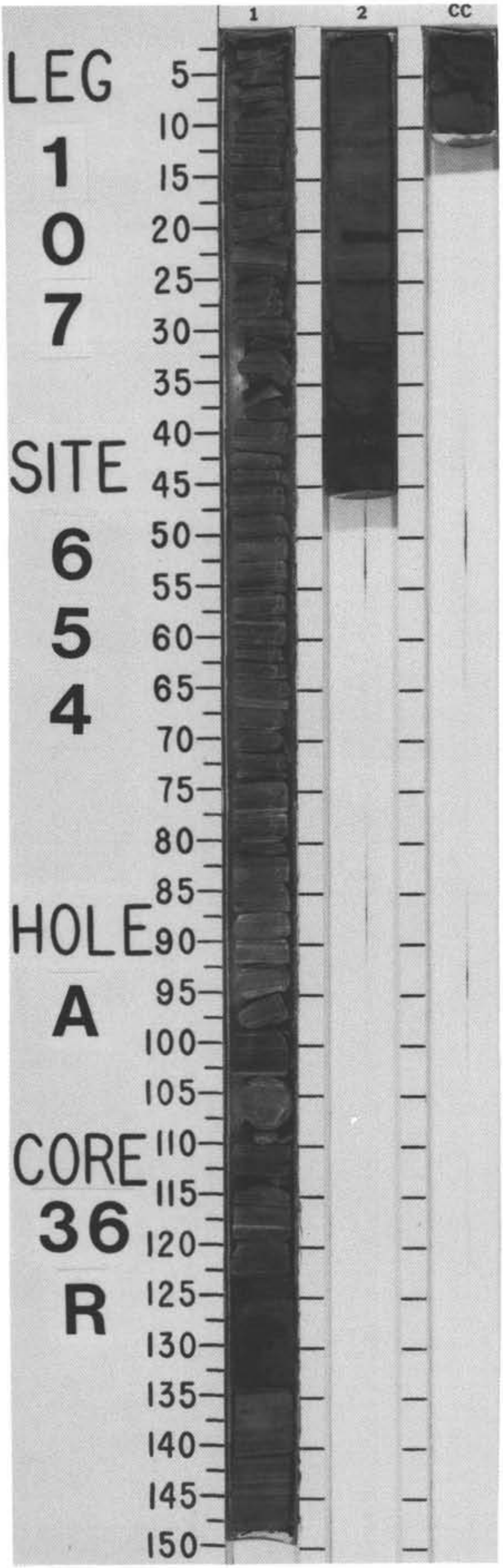
LEG
107
SITE
654
HOLE
A
CORE
36
R
1
2
CC
5
10
15
20
25
30
35
40
45
50
55
60
65
70
75
80
85
90
95
100
105
110
115
120
125
130
135
140
145
150

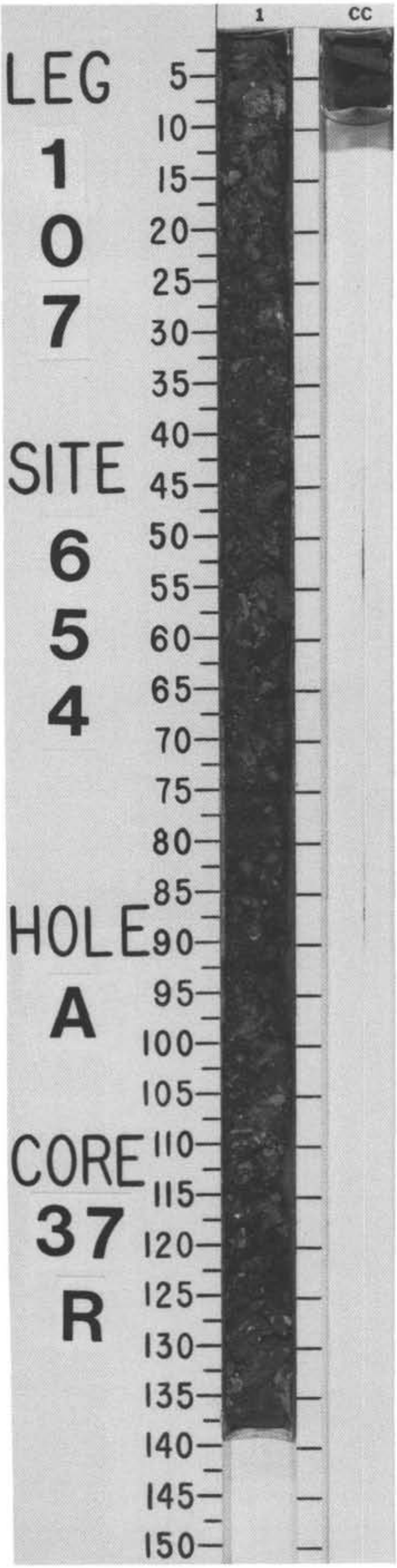
LEG
107
SITE
654
HOLE
A
CORE
37
R
1
CC
5
10
15
20
25
30
35
40
45
50
55
60
65
70
75
80
85
90
95
100
105
110
115
120
125
130
135
140
145
150

SITE 654 HOLE A CORE 38 R CORED INTERVAL 2537.3-2546.6 mbsl; 329.3-338.6 mbsf

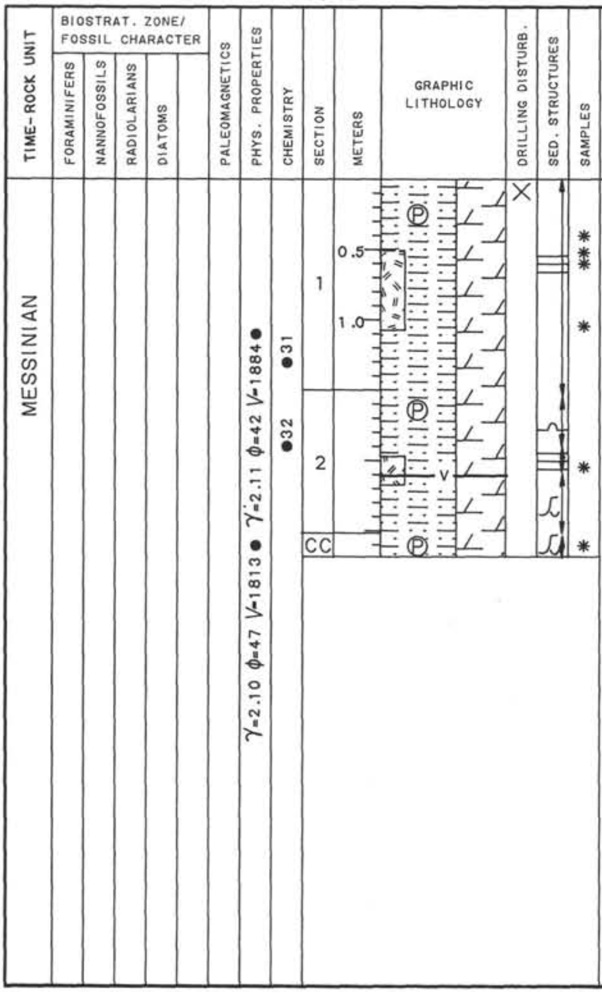

LITHOLOGIC DESCRIPTION

PYRITE-BEARING CLAYSTONE, alternating with DOLOMITIC MUDSTONE, and VOLCANIC TUFF-RICH DOLOMITIC MUDSTONE

Pyrite-bearing claystone, alternating with dolomitic mudstone, minor volcanic tuff-rich dolomitic mudstone; very fine millimeter- to centimeter-thick parallel lamination occurs throughout, with color alternations in the main lithologies of very dark gray (5Y 3/1), dark gray (5Y 4/1), gray (5Y 5/1, 6/1), and light gray (5Y 7/1), down to Section 2, 40 cm. Beneath this depth flaser lamination prevails in colors of black (5Y 2.5/1), very dark gray (5Y 3/1), and dark gray (5Y 4/1). Volcanic tuff-rich dolomicrite appears in Section 1 as hard, black nodules at 56, 77, and 96 cm, as compact layers at 60 cm, and as coarse-grained intervals at 70 and 104–108 cm; the latter interval is light gray (5Y 7/1) and contains probable authigenic zeolites. Millimeter-thick white laminae, possibly volcanic tuff-rich, also occur in Section 2, 60–62 cm.

Apparent dip is about 12°. Core contains several low-angle direct faults which in some cases cross high-angle direct faults.

SMEAR SLIDE SUMMARY (%):

	1, 40 D	1, 43 D	1, 60 M	1, 107 D	2, 60 D	CC, 16 M
TEXTURE:						
Sand	1	3	25	15	2	10
Silt	35	—	20	50	10	10
Clay	64	97	55	35	88	80
COMPOSITION:						
Quartz	1	3	3	2	—	2
Feldspar	—	—	—	—	—	5
Clay	55	4	9	10	2	—
Volcanic glass	—	—	20	—	—	—
Dolomite	—	—	—	5	—	—
Accessory minerals	—	1	—	—	—	—
Pyrite	25	2	4	6	6	5
Fish remains	—	—	1	—	—	—
Micrite	15	90	60	62	90	85
Gypsum	4	—	3	—	2	3
Zeolites	—	—	—	15	—	—

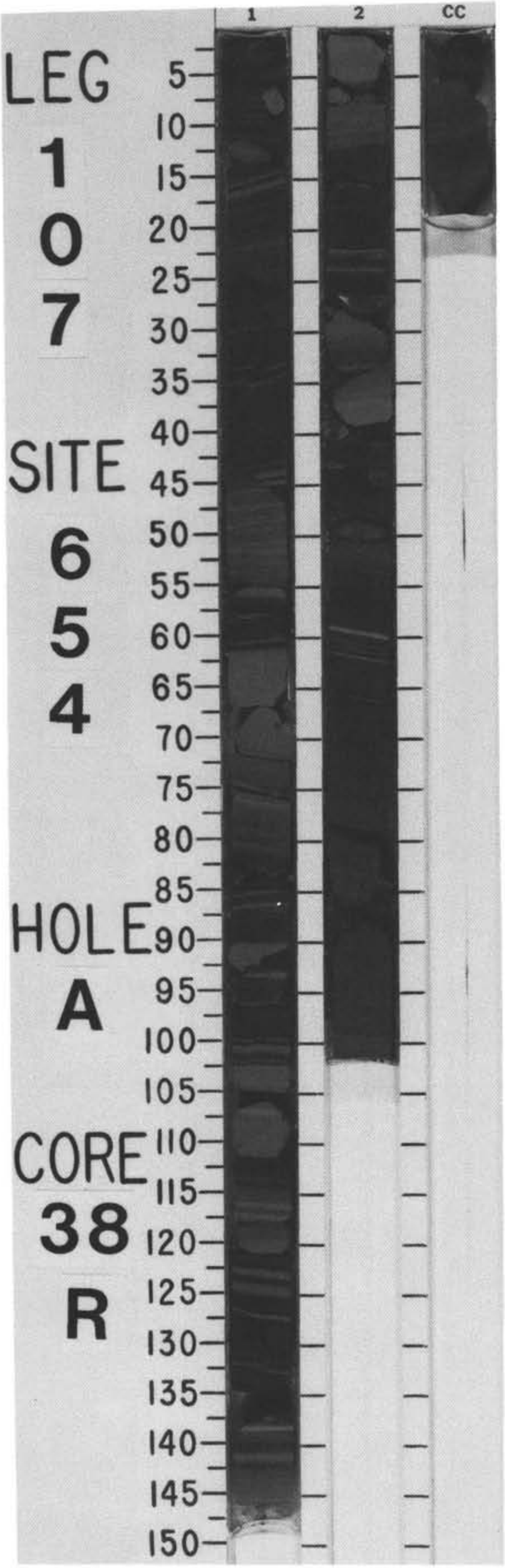
LEG
107
SITE
654
HOLE
A
CORE
38
R
1
2
CC
5
10
15
20
25
30
35
40
45
50
55
60
65
70
75
80
85
90
95
100
105
110
115
120
125
130
135
140
145
150

SITE 654 HOLE A CORE 39 R CORED INTERVAL 2546.6-2556.2 mbsl; 338.6-348.2 mbsf

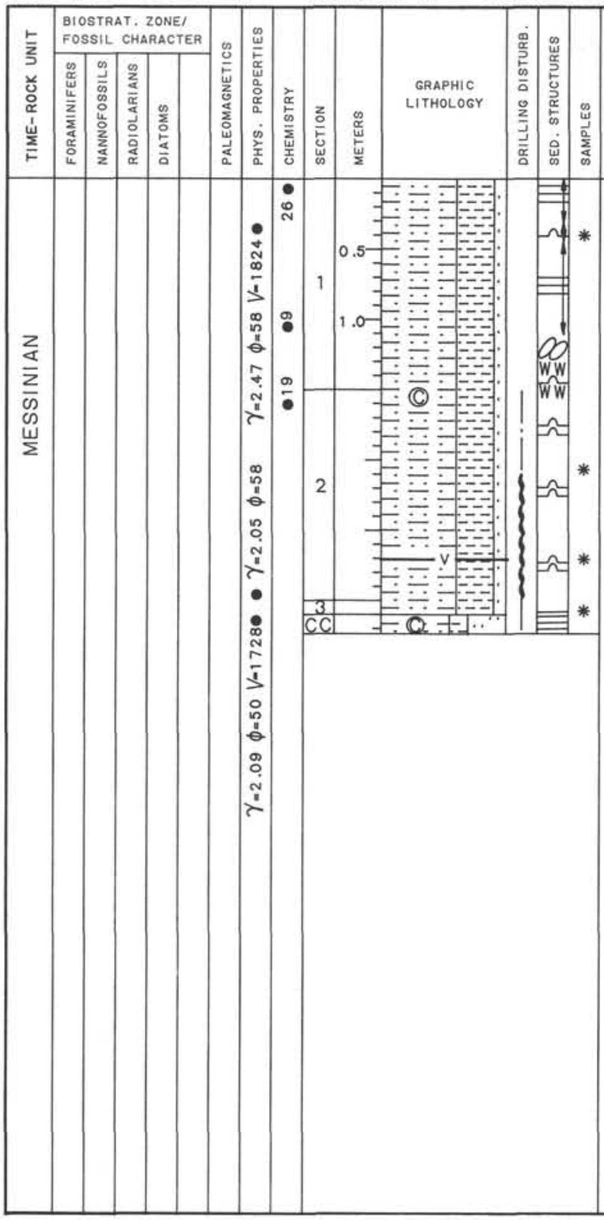

LITHOLOGIC DESCRIPTION

DOLOMITIC CLAYSTONE and SILTSTONE

Varve-type, laminated, dark dolomitic claystone and siltstone.

Section 1, 0–15, 36–75, and 81–93 cm, contain centimeter-thick, olive (5Y 5/3) laminae of claystone and siltstone, with each lamina appearing to be normally graded; where claystone is present at the top the contact is sharp, otherwise it is indistinct; 15–36 cm is same lithology, but contains rounded and stretched clasts floating in a clay matrix (debis flow textures); 71-81 cm is same lithology as 15-36 cm, but at the base is a debris flow composed of mudstone and a few siltstone intraclasts floating in a mud matrix; 93–150 cm is a debris flow with mud clasts in a mud matrix, with many yellow (2.5Y 7/10) wavy and parallel laminations; 129–130, 137, 138–139, and 141–142 cm have disrupted laminae.

Section 2 is a continuation of Section 1 lithologies, but more deformed; 25–36 cm is another debris flow of mud clasts in a mud matrix; 57-58 cm is a white-gray layer (2.5Y 7/0); 75–118 cm is orange lamination, but very disturbed; 77–78 cm is a white layer; 118–120 cm is a disturbed sandy layer; 120–150 cm is a disturbed, nearly homogeneous claystone, light gray (2.5Y 7/0), gray (10YR 5/1), dark gray (10YR 4/1), and olive (5Y 5/3), with remnants of two whitish layers.

Section 3 and CC are dolomitic clay and sandy, silty claystone, gray (5Y 5/1, 6/1), olive-gray (5Y 5/2), olive (5Y 5/3), and olive-brown (2.5Y 4/4).

SMEAR SLIDE SUMMARY (%):

	1, 42 D	2, 58 M	2, 120 M	3, 4 D
TEXTURE:				
Sand	—	3	70	20
Silt	20	90	20	40
Clay	80	7	10	40
COMPOSITION:				
Quartz	5	—	—	5
Feldspar	—	—	Tr	2
Mica	2	—	—	1
Clay	—	8	—	41
Volcanic glass	—	2	90	—
Dolomite	50	85	2	30
Cement	22	—	—	—
Accessory minerals	10	1	2	5
Zeolites	1	—	—	2
Gypsum	5	—	6	—
Hornblende	—	—	—	1
Diatoms	Tr	1	—	3
Sponge spicules	5	1	—	1
Fish remains	Tr	—	—	—
Intraclasts	—	1	—	—
Micrite	—	1	—	—
Organic matter	—	—	—	4
Bioclasts	—	—	—	4

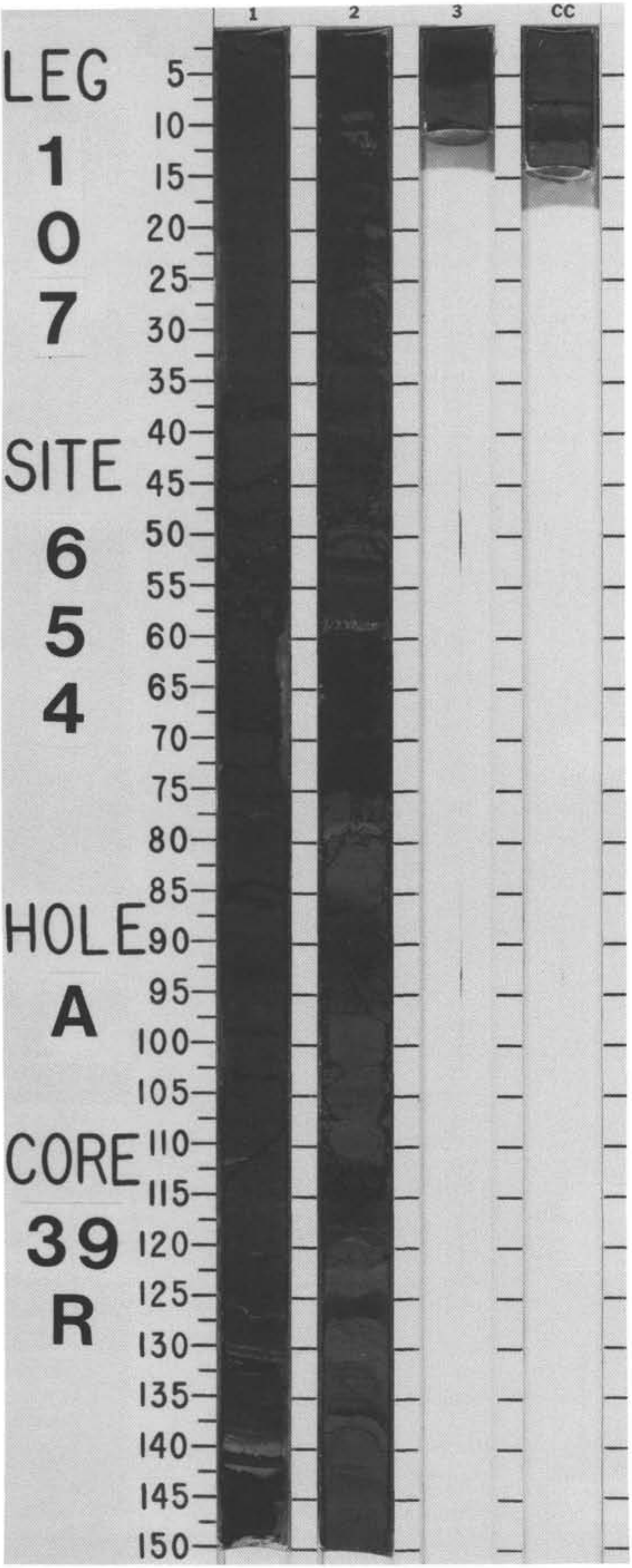
LEG
107
SITE
654
HOLE
A
CORE
39
R
1
2
3
CC
5
10
15
20
25
30
35
40
45
50
55
60
65
70
75
80
85
90
95
100
105
110
115
120
125
130
135
140
145
150

SITE 654 HOLE A CORE 40 R CORED INTERVAL 2556.2-2565.8 mbsl; 348.2-357.8 mbsf

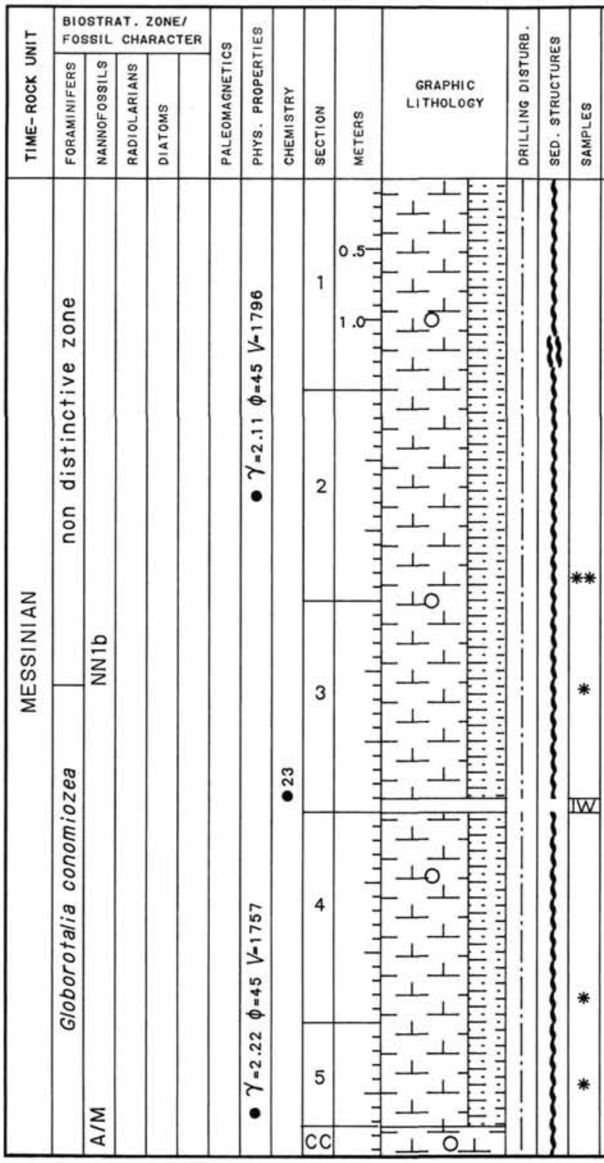

LITHOLOGIC DESCRIPTION

MARLY NANNOFOSSIL OOZE

Slightly petroliferous, marly nannofossil ooze, bioturbated throughout.

Section 1, 1–8 and 15–18 cm, contains two pieces of varve-type, laminated, dolomitic mudstone, as in Core 39R; 8–15 and 18–150 cm are foraminifer-bearing, light olive-brown (2.5Y 5/6) nannofossil ooze with a slight petroliferous smell; 18–50 cm contains numerous burrows exhibiting lighter gray halos; 50–150 cm contains scattered pyritized burrows 0.5–1 mm in diameter (worms).

Section 2 is same lithology as Section 1 below 50 cm, but is more disturbed; vague dark and light laminae are visible, and scarce pyritized worm burrows occur, again has a petroliferous smell.

Section 3 is gray (2.5Y 5/0) in color; oil appears to be mostly in black worm burrows; again pyritized burrows are present, 1-mm in diameter.

Section 4 is gray (5Y 5/0), with a black (5Y 2/0) local patch at 135 cm.

Section 5 contains disseminated foraminifers; very dark gray (2.5Y 3/0), oil-rich laminae occur, especially at 48–50 cm, with general colors light yellowish brown (2.5Y 6/4) and gray (2.5Y 5/0).

CC is gray (2.5Y 5/0) in color.

(O indicates oil in graphic lithology.)

SMEAR SLIDE SUMMARY (%):

	2, 132 M	2, 133 D	3, 61 D	4, 136 M	5, 48.5 M
TEXTURE:					
Sand	—	5	2	50	—
Silt	35	15	12	50	15
Clay	65	80	86	—	85
COMPOSITION:					
Quartz	Tr	3	2	—	2
Feldspar	—	Tr	—	—	1
Clay	40	14	12	—	—
Volcanic glass	—	1	—	—	25
Dolomite	Tr	3	—	—	3
Cement (spar)	—	25	20	—	—
Accessory minerals	—	2	—	—	—
Opaques	20	—	—	48	—
Organic matter	Tr	—	—	50	3
Zeolites	—	—	—	—	3
Foraminifers	10	5	2	—	1
Nannofossils	20	45	60	2	60
Bioclasts	10	2	—	—	—
Intraclasts	—	—	3	—	1

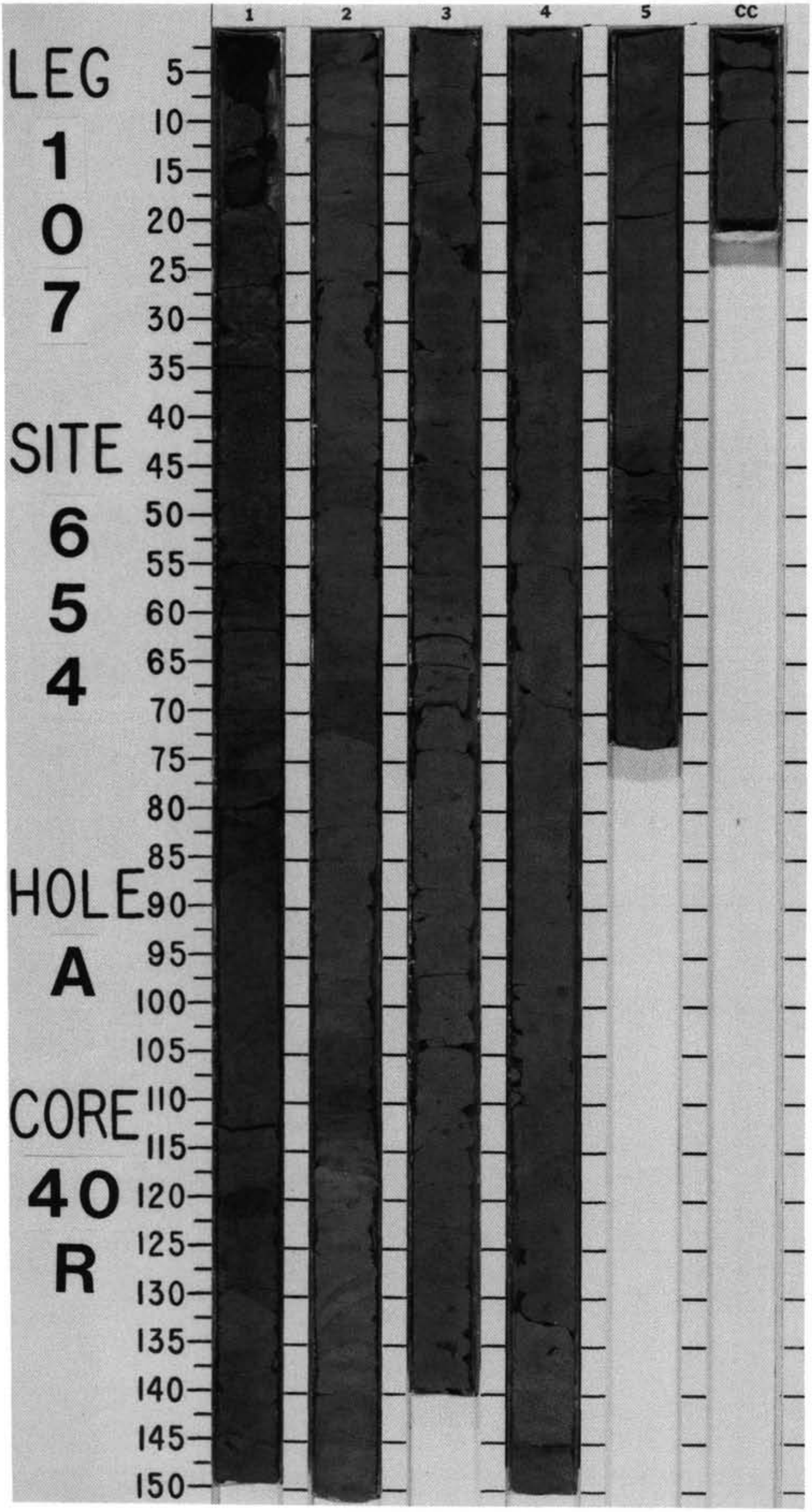
LEG
1
0
7
SITE
6
5
4
HOLE
A
CORE
40
R
1
2
3
4
5
CC
5
10
15
20
25
30
35
40
45
50
55
60
65
70
75
80
85
90
95
100
105
110
115
120
125
130
135
140
145
150

SITE 654 HOLE A CORE 41 R CORED INTERVAL 2565.8-2575.4 mbsl; 357.8-367.4 mbsf

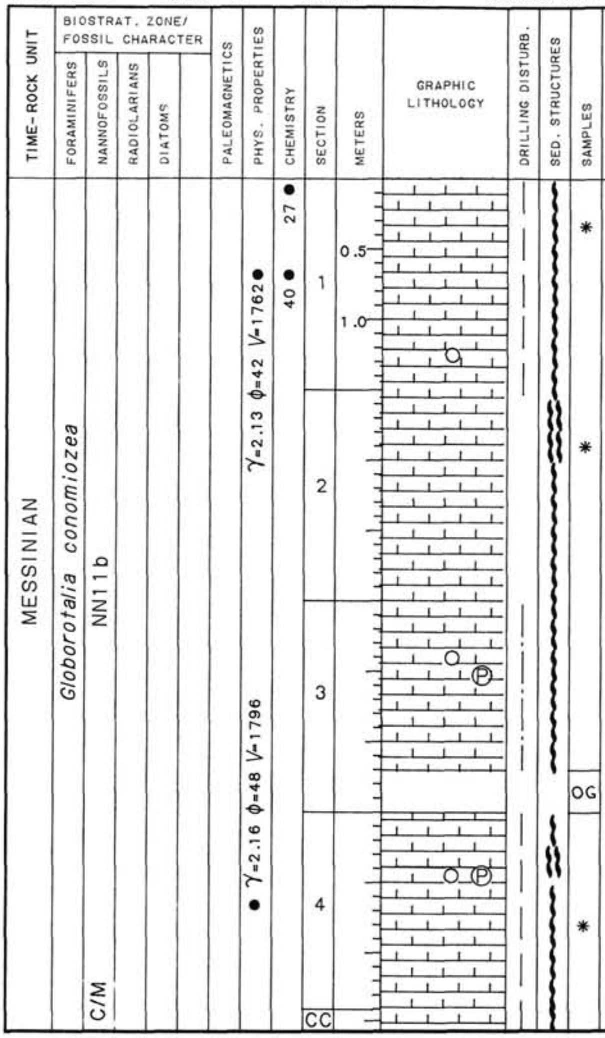

LITHOLOGIC DESCRIPTION

MARLY NANNOFOSSIL CHALK

Slightly petroliferous marly nannofossil chalk.

In Section 1, the ooze is gray (2.5Y 5/0); 0–10 cm is disturbed, but a vague plane lamination is visible; 10–16 and 27–41 cm are mud or debris flows; 41–150 cm is burrowed nannofossil ooze with few other primary sedimentary structures preserved.

Section 2 is burrowed with many blackish patches; a sharp color change from gray (2.5Y 5/0) to brownish gray (5Y 5/1) occurs at 35 cm; at 90–150 cm is a gradual color change to gray (2.5Y 5/0).

Section 3, contains pyrite concentrations at 55–60, 103, and 112–115 cm; color is gray (2.5Y 5/0).

Section 4, 0–60 cm, is gray (2.5Y 5/0); 60–143 cm is gray (5Y 5/1); rich in disseminated pyrite.

CC is gray (2.5Y 5/0) in color.

SMEAR SLIDE SUMMARY (%):

	1, 36 M	2, 41 M	4, 81 D
TEXTURE:			
Sand	1	5	2
Silt	16	10	15
Clay	83	85	83
COMPOSITION:			
Quartz	4	3	2
Feldspar	1	1	—
Mica	—	1	—
Clay	23	14	26
Dolomite	2	2	1
Cement	—	15	—
Pyrite	10	2	35
Foraminifers	2	4	1
Nannofossils	40	45	35
Fish remains	1	1	—
Bioclasts	1	1	—
Cement (spar)	15	—	—
Micrite	—	11	—

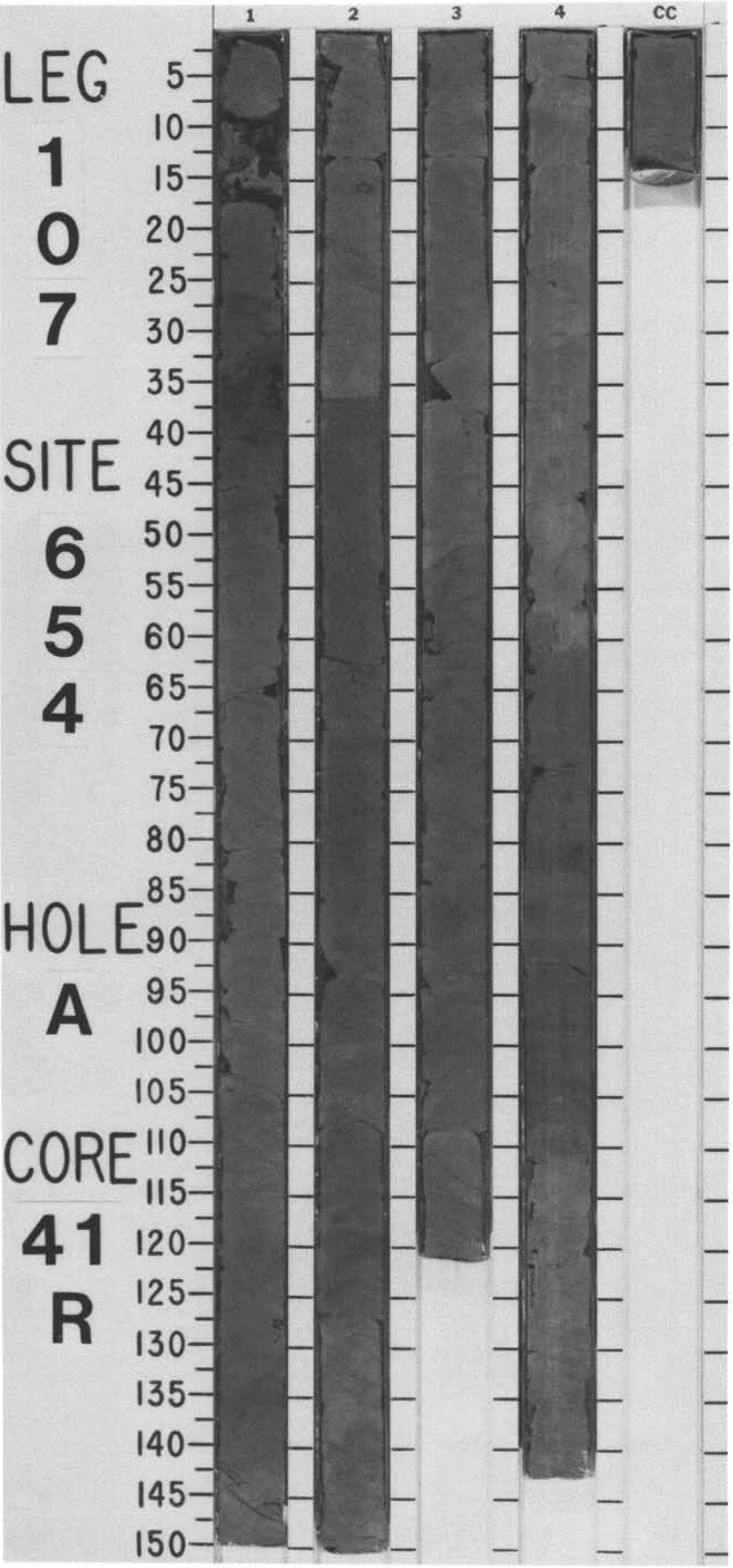
LEG
107
SITE
654
HOLE
A
CORE
41
R
1
2
3
4
CC
5
10
15
20
25
30
35
40
45
50
55
60
65
70
75
80
85
90
95
100
105
110
115
120
125
130
135
140
145
150

SITE 654 HOLE A CORE 42 R CORED INTERVAL 2575.4-2585.1 mbsl; 367.4-377.1 mbsf

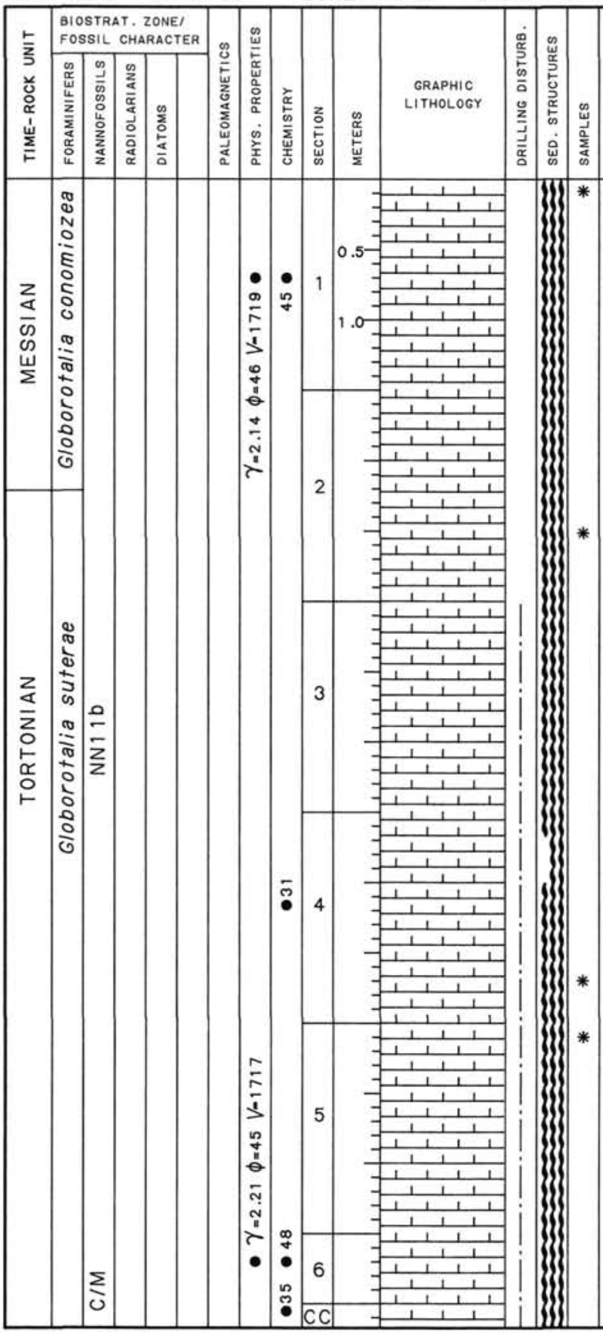

LITHOLOGIC DESCRIPTION

NANNOFOSSIL CHALK

Homogeneous nannofossil chalk, very bioturbated.

Section 1, 0–8.5 cm, is silty, light gray (5Y 7/1), and burrowed; the rest of the Section contains local pyrite enrichments (especially at 11–16, 72–73, and 82–84 cm), mostly disseminated or infilling foraminifer shells.

Section 2 contains pyrite at 70–71, 100–102, and 120–122 cm.

Section 3 is gray (5Y 6/1) and has pyrite at 10, 40, and 50 cm.

Section 4 is more disturbed and gray (5Y 6/1); 0–35 and 95-110 cm are particularly highly burrowed; at 115 cm pyrite is present; at 121–122 cm chalk is more silty, with pyritized foraminifers.

Section 5 contains pyrite at 50–60 cm and pyrite concretions at 145–150 cm.

Section 6 is gray (2.5Y 6/0); at 0–9 cm is a siltier horizon.

CC is gray (5Y 6/1) in color.

SMEAR SLIDE SUMMARY (%):

	1, 5 D	2, 100 D	4, 121 D	5, 5 D
TEXTURE:				
Sand	5	5	5	5
Silt	20	15	15	35
Clay	75	80	80	60
COMPOSITION:				
Quartz	5	2	2	—
Mica	Tr	1	—	—
Clay	23	32	28	40
Volcanic glass	—	—	1	—
Dolomite	15	5	—	—
Pyrite	15	3	2	10
Glauconite	Tr	—	—	—
Gypsum	2	—	—	3
Calcite	—	—	2	—
Foraminifers	10	3	3	5
Nannofossils	30	45	55	25
Diatoms	—	1	—	—
Sponge spicules	—	1	1	—
Cement (spar)	—	10	5	—
Bioclasts	—	—	1	7
Micrite	—	—	—	10

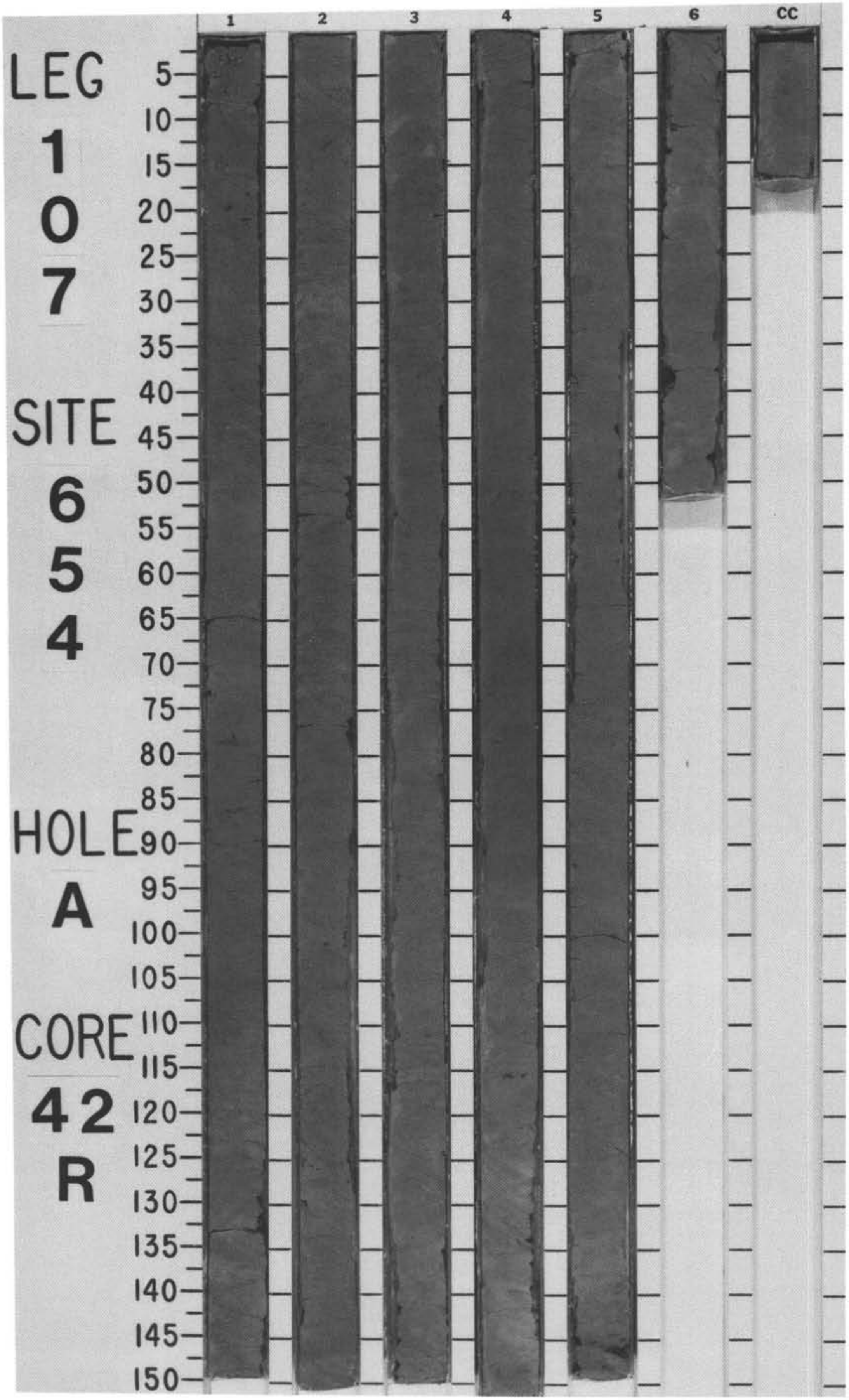
LEG
107
SITE
654
HOLE
A
CORE
42
R
1
2
3
4
5
6
CC
5
10
15
20
25
30
35
40
45
50
55
60
65
70
75
80
85
90
95
100
105
110
115
120
125
130
135
140
145
150

SITE 654 HOLE A CORE 43 R CORED INTERVAL 2585.1-2594.8 mbsl; 377.1-386.8 mbsf

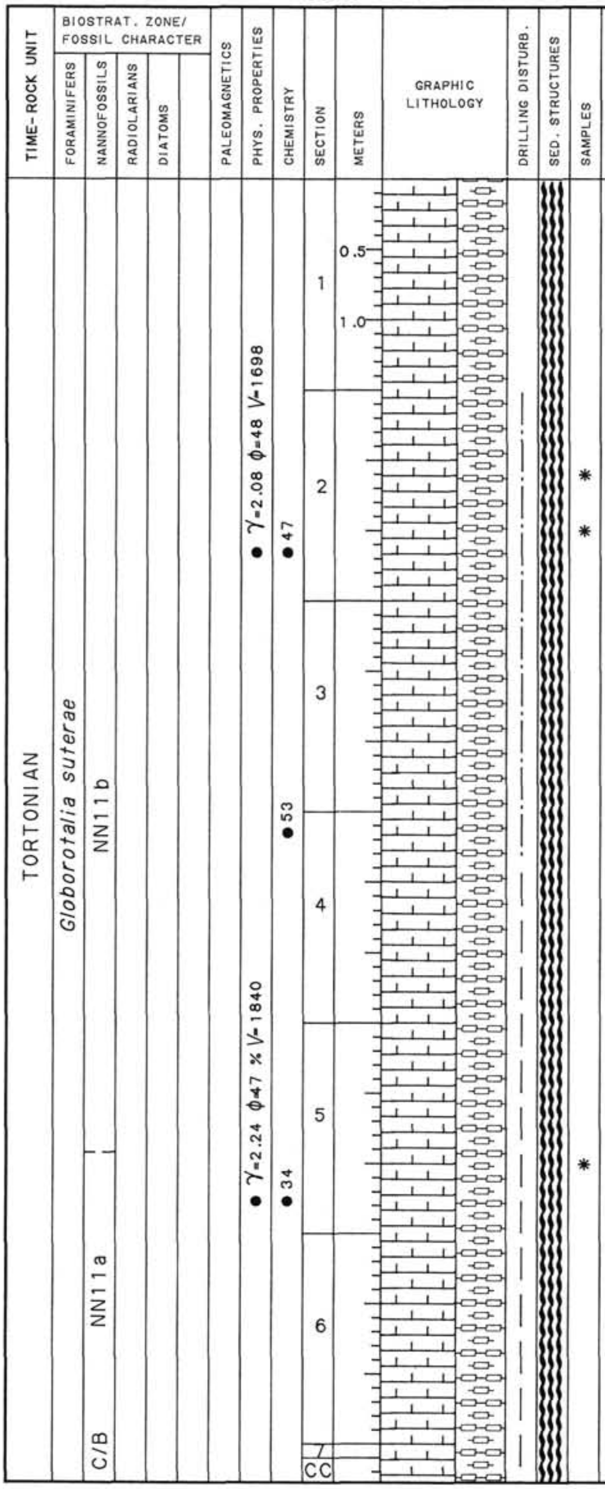

LITHOLOGIC DESCRIPTION

NANNOFOSSIL CHALK and SILTY CALCAREOUS CHALK

Nannofossil chalk and silty calcareous chalk, very burrowed and homogeneous.

Section 1 contains framboidal pyrite at 40, 80, and 125 cm; chalk is light gray (5Y 7/1).

Section 2 is more disrupted into drilling biscuits; pyrite occurs at 10, 26, 51, and 82–83 cm; 120–126 cm is more silty.

Section 3 is gray (5Y 6/1); pyrite is at 89 cm; well-formed pyrite cubes occur at 102 cm; more silty calcareous chalk occurs at 100–102 cm.

Section 4 is a little more silty than general lithology; contains numerous white foraminifer shells (*Orbulina* sp.); pyrite layers occur at 55 and 96 cm.

Sections 5, 6, and CC are gray (10YR 5/1) in color; pyrite and mica occur at Section 5, 0–11, 33, 80, and 93 cm.

SMEAR SLIDE SUMMARY (%):

	2, 70 M	2, 100 D	5, 10 D	5, 95 D
TEXTURE:				
Sand	12	—	5	5
Silt	20	20	20	10
Clay	68	80	75	85
COMPOSITION:				
Quartz	6	Tr	3	—
Feldspar	1	—	Tr	—
Rock fragments	1	—	—	—
Mica	—	—	5	2
Clay	—	29	30	18
Volcanic glass	—	2	—	3
Dolomite	2	10	10	8
Pyrite	9	3	—	4
Gypsum	—	3	2	—
Foraminifers	5	5	10	7
Nannofossils	20	45	40	40
Diatoms	—	1	—	—
Fish remains	—	—	—	1
Pellets	2	—	—	—
Bioclasts	2	Tr	—	2
Intraclasts	1	—	—	1
Micrite	25	—	—	5
Microspar	20	—	—	—

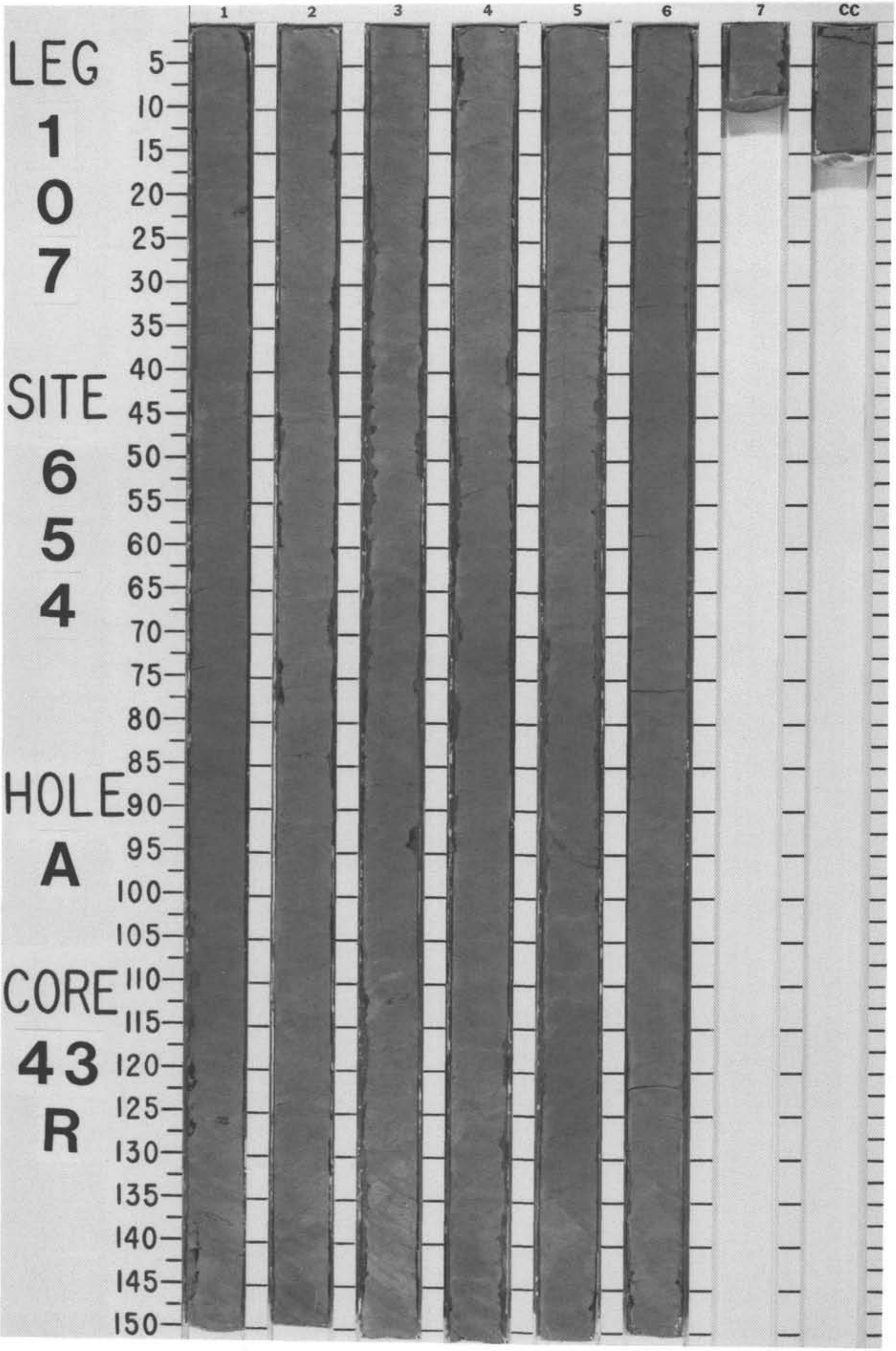
LEG
1
0
7
SITE
6
5
4
HOLE
A
CORE
43
R
1
2
3
4
5
6
7
CC
5
10
15
20
25
30
35
40
45
50
55
60
65
70
75
80
85
90
95
100
105
110
115
120
125
130
135
140
145
150

SITE 654 HOLE A CORE 44 R CORED INTERVAL 2594.8-2604.4 mbsl; 386.8-396.4 mbsf

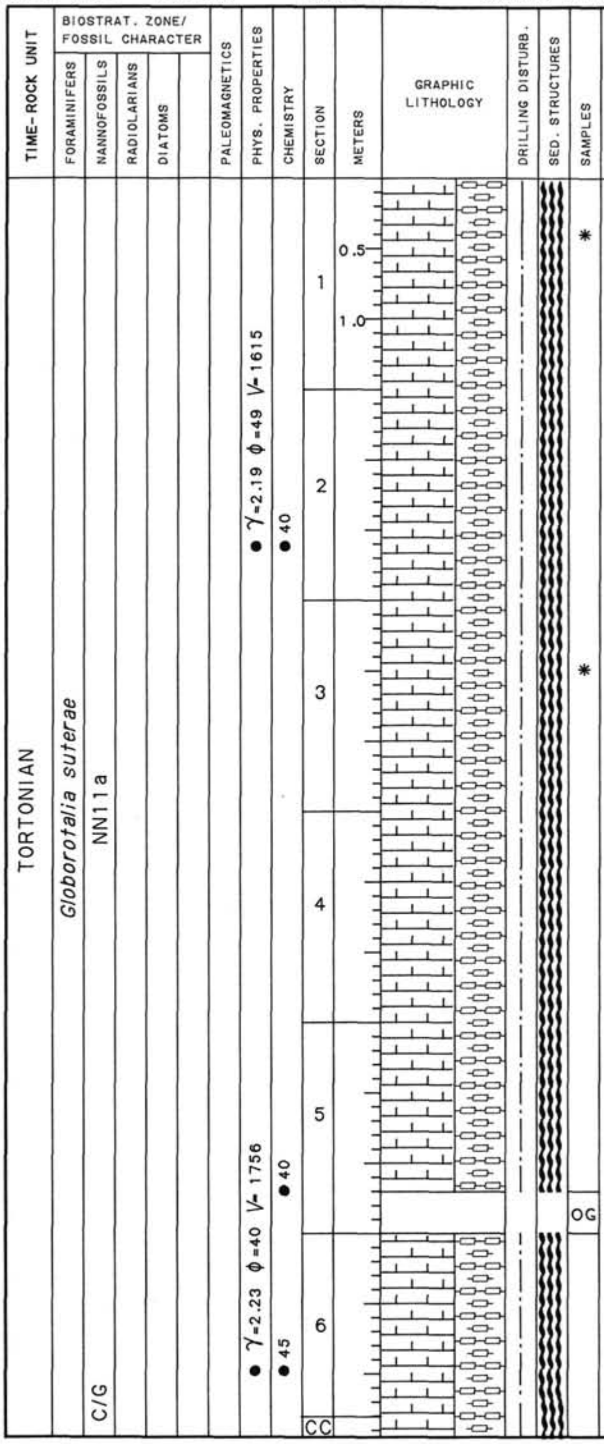

LITHOLOGIC DESCRIPTION

NANNOFOSSIL CHALK and CALCAREOUS CHALK

Nannofossil chalk and calcareous chalk, light gray (5Y 7/2, 5Y 7/1), nearly homogeneous, very bioturbated.

Section 1 contains burrows that are mostly *Chondrites* and scattered orbulinid foraminifers.

Section 2 contains abundant *Chondrites* burrows at 57–60 cm and silty layers at 120 and 140 cm.

Section 3 is silty at 45–62 cm and sand is present at 62 cm.

Section 4 contains a large burrow at 110 cm.

Sections 5, 6, and CC contain conspicuous *Orbulina* shells.

SMEAR SLIDE SUMMARY (%):

	1, 50 D	3, 44 M
TEXTURE:		
Sand	—	—
Silt	15	90
Clay	85	10
COMPOSITION:		
Quartz	—	Tr
Clay	25	—
Dolomite	2	30
Cement	—	15
Pyroxene	Tr	—
Gypsum	Tr	10
Opaques	—	15
Foraminifers	8	Tr
Nannofossils	60	8
Bioclasts/intraclasts	5	12
Glauconite	—	10

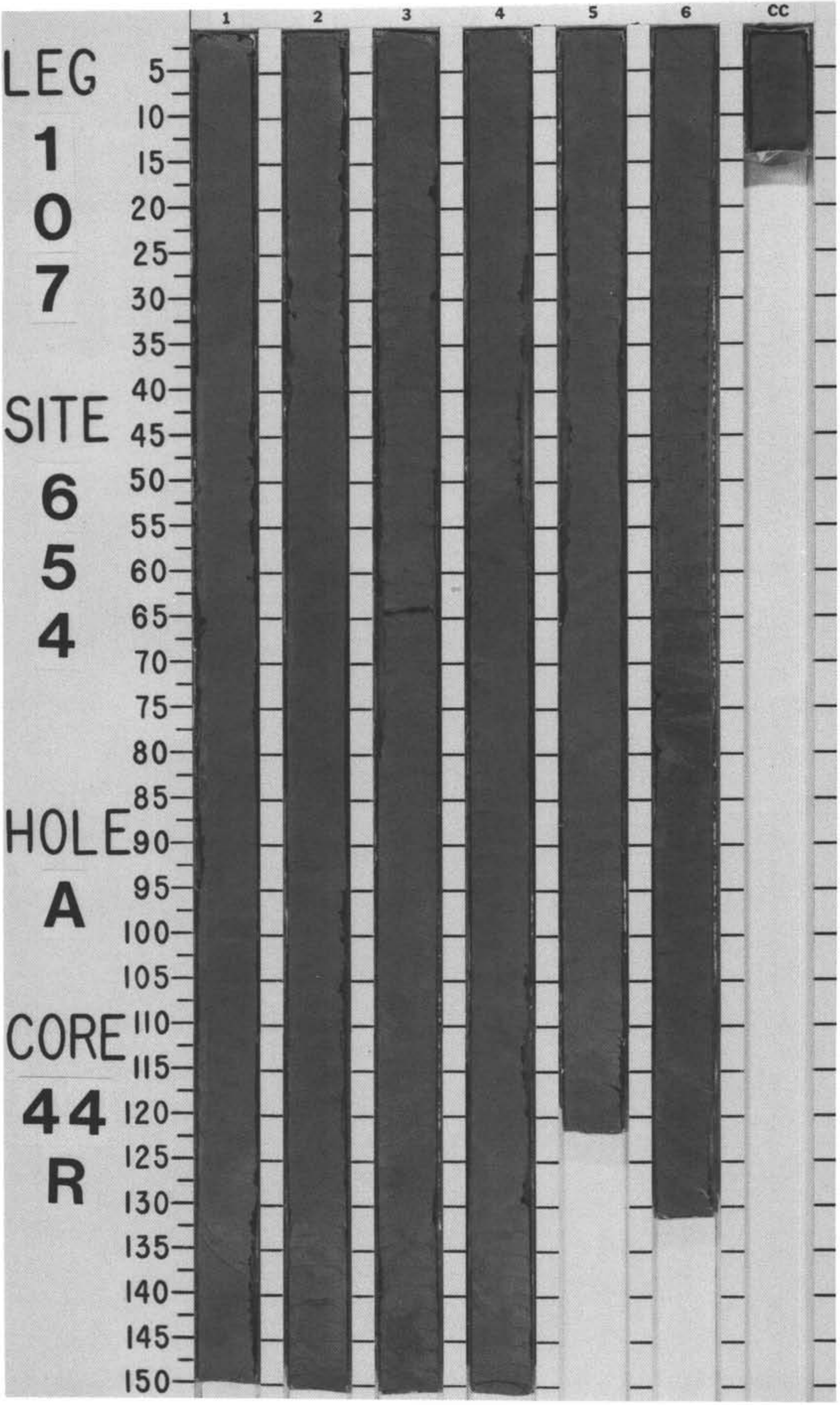
LEG
107
SITE
654
HOLE
A
CORE
44
R
1
2
3
4
5
6
CC
5
10
15
20
25
30
35
40
45
50
55
60
65
70
75
80
85
90
95
100
105
110
115
120
125
130
135
140
145
150

SITE 654 HOLE A CORE 45 R CORED INTERVAL 2604.4-2614.1 mbsl; 396.4-406.1 mbsf

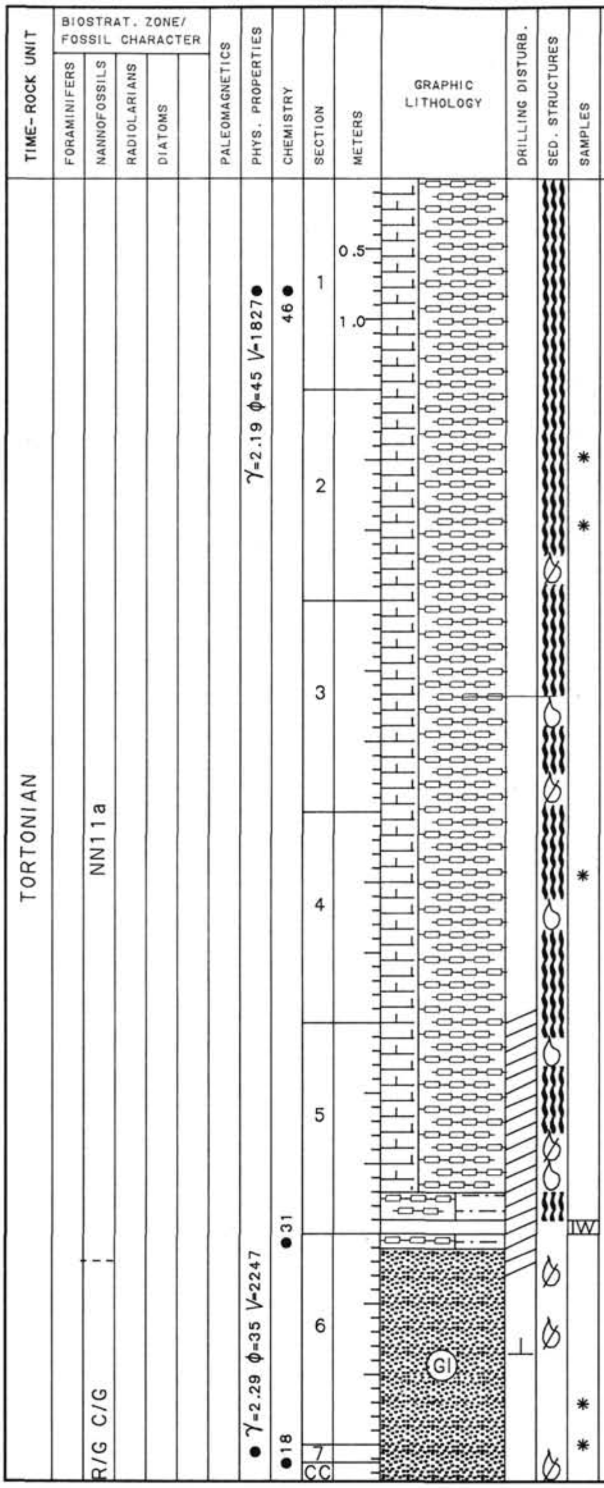

LITHOLOGIC DESCRIPTION

NANNOFOSSIL-RICH, CALCAREOUS CHALK and GLAUCONITE-RICH, POLYMICTIC SANDSTONE

Nannofossil-rich, calcareous chalk grading downcore to glauconite-rich, polymictic sandstone. Chalk occurs in Sections 1–5, becoming enriched in the sand fraction in Section 5, 125 cm; gray (5Y 5/1), with minor light olive-gray (5Y 6/2), grading to gray (2.5 YR) toward contact with the sandstone; chalk is strongly bioturbated and contains abundant foraminifers and a few large fragments of mollusks (*Ostrea* in Section 2, 131–138 cm); such bioclasts increase approaching the contact. Glauconite-rich (labeled Gl in the graphic lithology) polymictic sandstone appears in Section 6, 10 cm, beneath a 25-cm-thick interval of sandy calcareous mudstone; it is rich in matrix and contains scattered gravel- to pebble-sized clasts, mostly angular; these do not display imbrication or orientation, and some are made of firm, but not completely indurated, ooze. Some bioclasts are interspersed, their abundance increasing upward, including large foraminifers, molluscs, and possible echinid plates. Very crude gradation seems indicated by the increase in the matrix to large clasts ratio upward. The general color of the unit is dark gray (5Y 4/1), with the single components highly variable in color.

SMEAR SLIDE SUMMARY (%):

	2, 50 D	2, 96 M	4, 50 M	6, 125 D	7, 3 D
TEXTURE:					
Sand	25	25	15	40	40
Silt	25	20	30	20	25
Clay	50	55	55	40	35
COMPOSITION:					
Quartz	3	2	2	2	2
Feldspar	3	—	2	3	2
Mica	—	—	—	—	2
Clay	22	20	21	15	21
Dolomite	3	5	3	5	5
Accessory minerals	1	—	—	—	—
Pyrite	4	1	—	3	—
Zeolites	1	—	—	2	—
Foraminifers	5	3	2	2	3
Nannofossils	25	35	20	15	8
Radiolarians	1	—	Tr	Tr	2
Sponge spicules	Tr	—	Tr	—	—
Bioclasts	2	—	—	—	—
Micrite	30	30	40	35	30
Gypsum	—	4	10	15	10
Glauconite	—	—	—	15	15

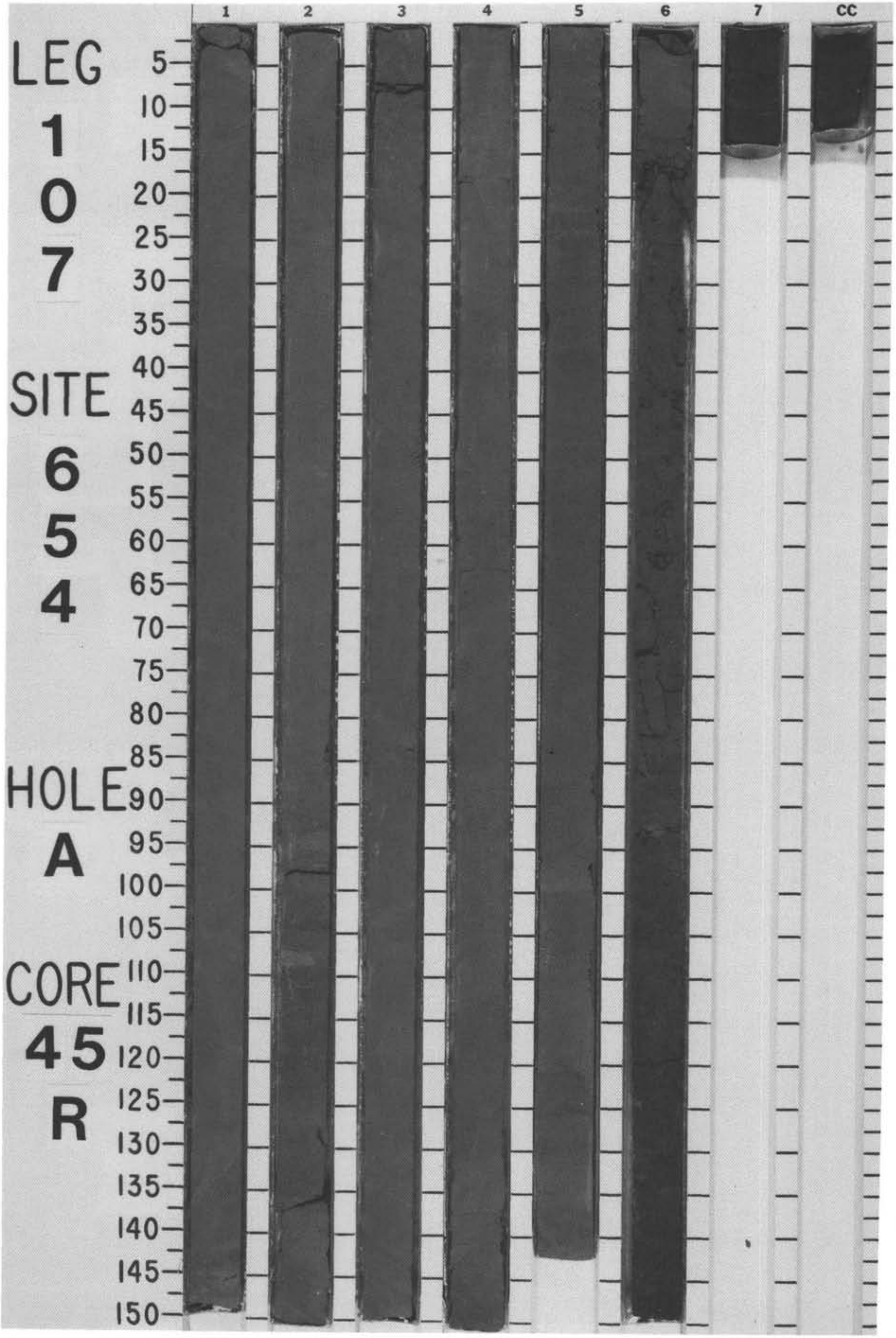
LEG
107
SITE
654
HOLE
A
CORE
45
R
1
2
3
4
5
6
7
CC
5
10
15
20
25
30
35
40
45
50
55
60
65
70
75
80
85
90
95
100
105
110
115
120
125
130
135
140
145
150

SITE 654 HOLE A CORE 46 R CORED INTERVAL 2614.1-2623.7 mbsl; 406.1-415.7 mbsf

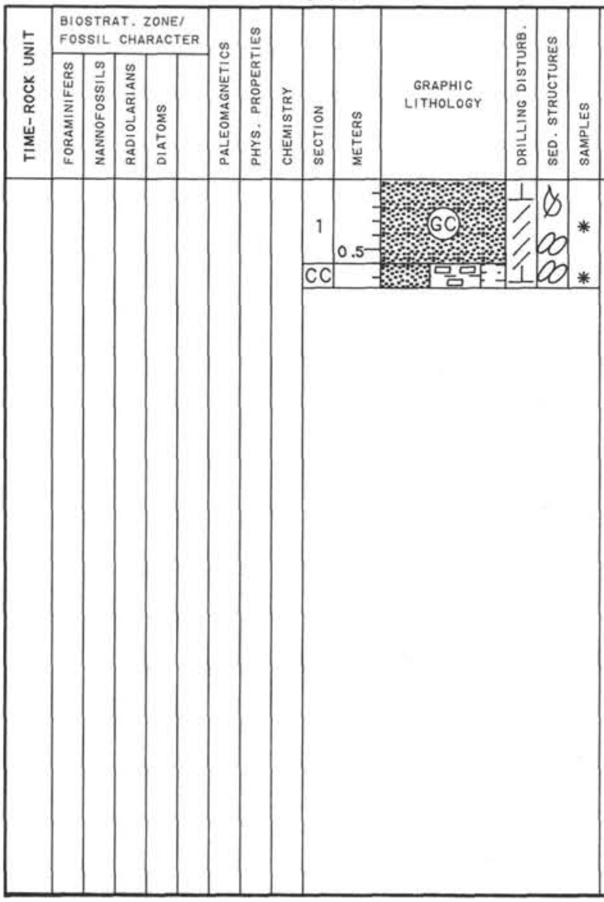

LITHOLOGIC DESCRIPTION

GLAUCONITE-RICH, POLYMICTIC SANDSTONE (with OSTREID fragments) and MARLY CALCAREOUS CHALK

Glauconite-rich polymictic sandstone, gray (5Y 6/1), occurs in Section 1 and the upper half of CC. It is rich in matrix, poorly sorted, and contains quartz, mica, gypsum, glauconite, pyrite, and carbonate. The most conspicuous fragments are bioclastics, among which are large and very thick walled Ostreids and large benthic foraminifers. Some of the latter are lenticular and display imbrication. At the base of the interval are the largest Ostreid specimens, some bored by *Cliona*-type sponges.

The bottom part of CC contains gray (5Y 5/1), marly calcareous chalk, with a few fragments of large mollusks.

SMEAR SLIDE SUMMARY (%):

	1, 36 D	CC, 12 M
TEXTURE:		
Sand	45	25
Silt	25	20
Clay	30	55
COMPOSITION:		
Quartz	3	6
Feldspar	—	2
Mica	1	—
Clay	—	30
Volcanic glass	2	—
Dolomite	—	5
Accessory minerals	—	1
Pyrite	3	2
Glauconite	16	—
Opaques (unspecified)	—	2
Bioclasts	Tr	—
Gypsum	30	4
Micrite	45	48

SITE 654 HOLE A CORE 47 R CORED INTERVAL 2623.7-2633.4 mbsl; 415.7-425.4 mbsf

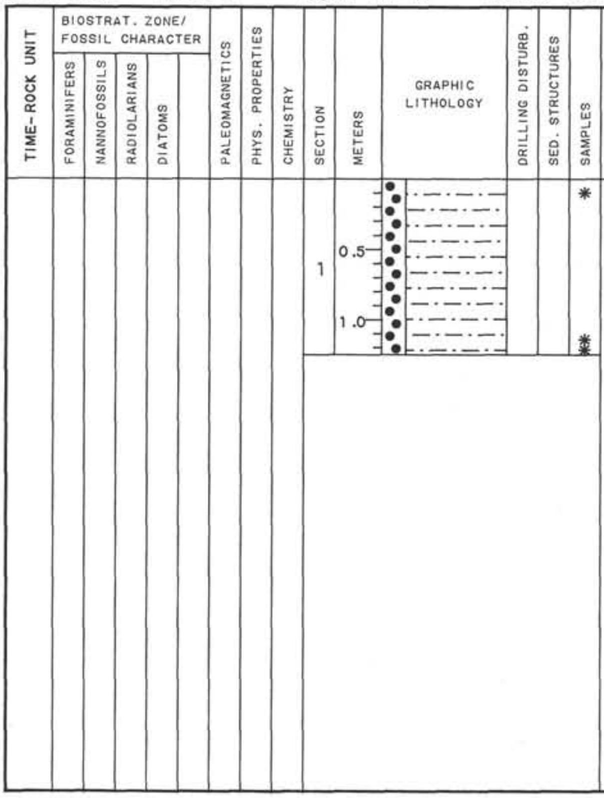

LITHOLOGIC DESCRIPTION

GRAVEL-BEARING, CALCAREOUS SANDY MUDSTONE

Gravel-bearing, calcareous sandy mudstone; a very plastic admixture of variously sized grains, gray (5Y 5/1) at the top becoming dominantly dark olive-yellow (7.5Y 4/6) with minor gray (5Y 5/1) downcore. Gravels contain pebbles as large as 10 mm in diameter, including one 3-cm dolomitic pebble at 119–122 cm; most components are angular to subrounded, and only few quartz grains are well rounded. The appearance is similar to materials washed by drilling, but preservation of color gradations and alternations suggests that a true stratigraphic interval has been recovered.

SMEAR SLIDE SUMMARY (%):

	1, 9 D	1, 113 M	1, 118 D
TEXTURE:			
Sand	30	30	15
Silt	35	35	30
Clay	35	35	55
COMPOSITION:			
Quartz	8	10	10
Feldspar	3	—	Tr
Rock fragments	—	5	—
Clay	39	38	50
Dolomite	5	7	5
Pyrite	8	—	—
Zeolites	2	—	—
Limonite	—	5	10
Micrite	25	15	25
Gypsum	10	20	—

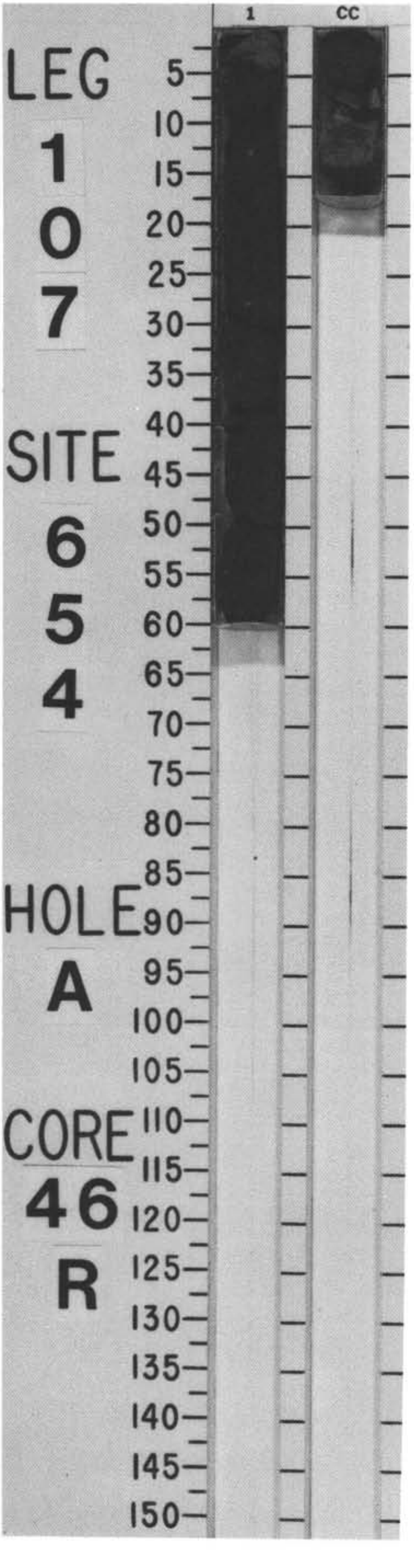
1
CC
LEG
107
SITE
654
HOLE
A
CORE
46
R
5
10
15
20
25
30
35
40
45
50
55
60
65
70
75
80
85
90
95
100
105
110
115
120
125
130
135
140
145
150

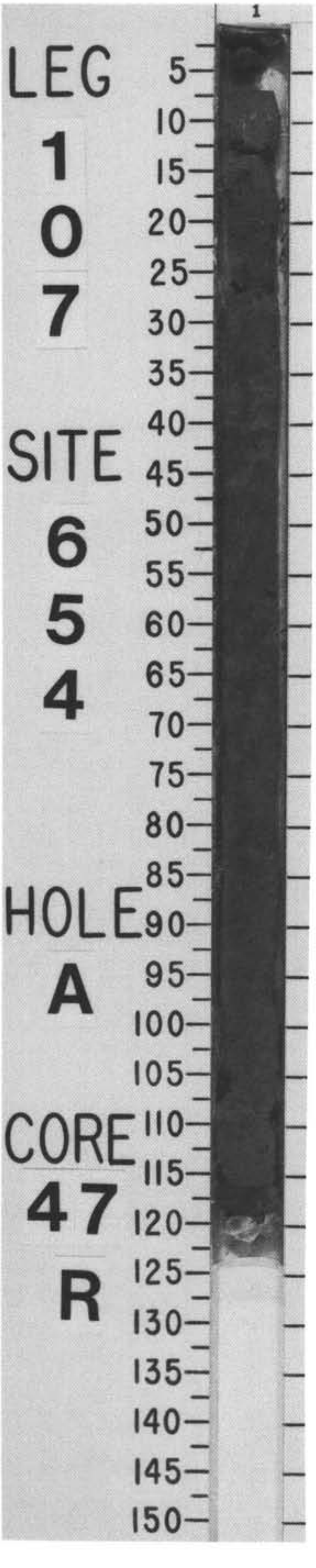
1
LEG
107
SITE
654
HOLE
A
CORE
47
R
5
10
15
20
25
30
35
40
45
50
55
60
65
70
75
80
85
90
95
100
105
110
115
120
125
130
135
140
145
150

SITE 654 HOLE A CORE 48 R CORED INTERVAL 2633.4-2643.1 mbsl; 425.4-435.1 mbsf

TIME-ROCK UNIT	BIOSTRAT. ZONE/ FOSSIL CHARACTER					PALEOMAGNETICS	PHYS. PROPERTIES	CHEMISTRY	SECTION	METERS	GRAPHIC LITHOLOGY	DRILLING DISTURB.	SED. STRUCTURES	SAMPLES	LITHOLOGIC DESCRIPTION
	FORAMINIFERS	NANNOFOSSILS	RADIOLARIANS	DIATOMS											
									CC						CONGLOMERATE Conglomerate, recovered only in the CC; angular to subrounded pebbles and very scarce, red calcareous mud that probably represents the matrix. Pebbles of the following lithologies have been described and measured (dimensions in millimeters): #1: several small pebbles in red matrix mud #2: 21 × 26 × 49 metalimestone with neomorphic quartz and quartz veins #3: 10 × 23 × 42 metacarbonate rock #4: 23 × 33 × 48 same as #3, with quartz veins #5: 30 × 40 × 47 same as #4 #6: 12 × 35 × 52 green quartzite, slightly metamorphosed #7: 20 × 40 × 44 same as #4 #8: 41 × 57 × 63 metacalcirudite

SITE 654 HOLE A CORE 49 R CORED INTERVAL 2643.1-2652.2 mbsl; 435.1-444.7 mbsf

TIME-ROCK UNIT	BIOSTRAT. ZONE/ FOSSIL CHARACTER					PALEOMAGNETICS	PHYS. PROPERTIES	CHEMISTRY	SECTION	METERS	GRAPHIC LITHOLOGY	DRILLING DISTURB.	SED. STRUCTURES	SAMPLES	LITHOLOGIC DESCRIPTION
	FORAMINIFERS	NANNOFOSSILS	RADIOLARIANS	DIATOMS											
							•2 V-5514 ●		1 CC						CONGLOMERATE Conglomerate; Section 1 yielded pebbles of the following lithologies (dimensions in millimeters): #1: 42 × 58 × 61 metalimestone (foliated marble) #2: 21 × 49 × 60 metalimestone #3: 30 × 51 × 58 same as #2 #4: 30 × 37 × 45 same as #1 #5: 48 × 55 × 56 quartzite with abundant veins #6: quartz pebble #7: quartz pebble #8: 32 × 37 × 52 same as #2 #9: 23 × 35 × 48 same as #2 #10: 34 × 45 × 56 same as #2 #11: 22 × 27 × 45 same as #2 #12: 33 × 50 × 53 same as #5 #13: 20 × 33 × 43 same as #1 #16: small pieces embedded in red mud In the CC the following two pebbles were recovered: #1: 27 × 51 × 52 gray-green quartzite #2: 23 × 42 × 53 same as #1

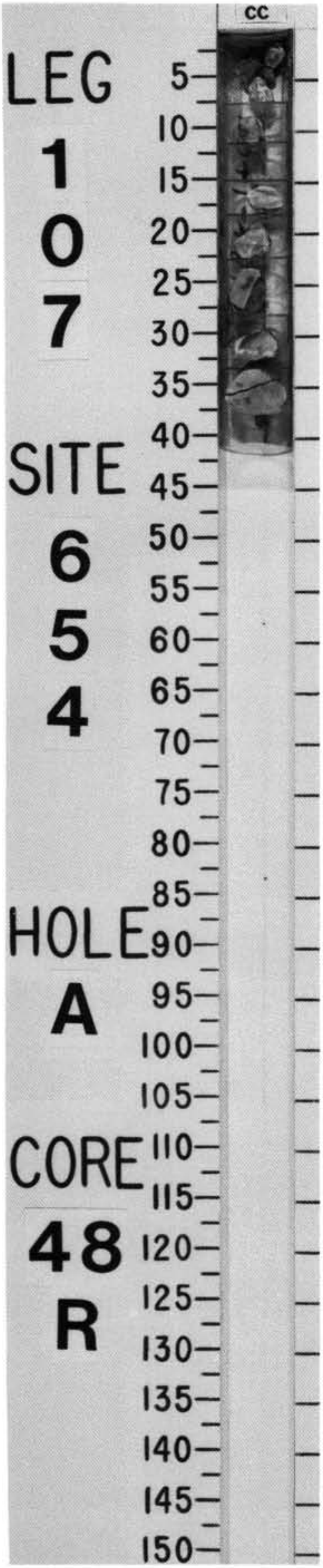
CC
LEG
1
0
7
SITE
6
5
4
HOLE
A
CORE
48
R
5
10
15
20
25
30
35
40
45
50
55
60
65
70
75
80
85
90
95
100
105
110
115
120
125
130
135
140
145
150

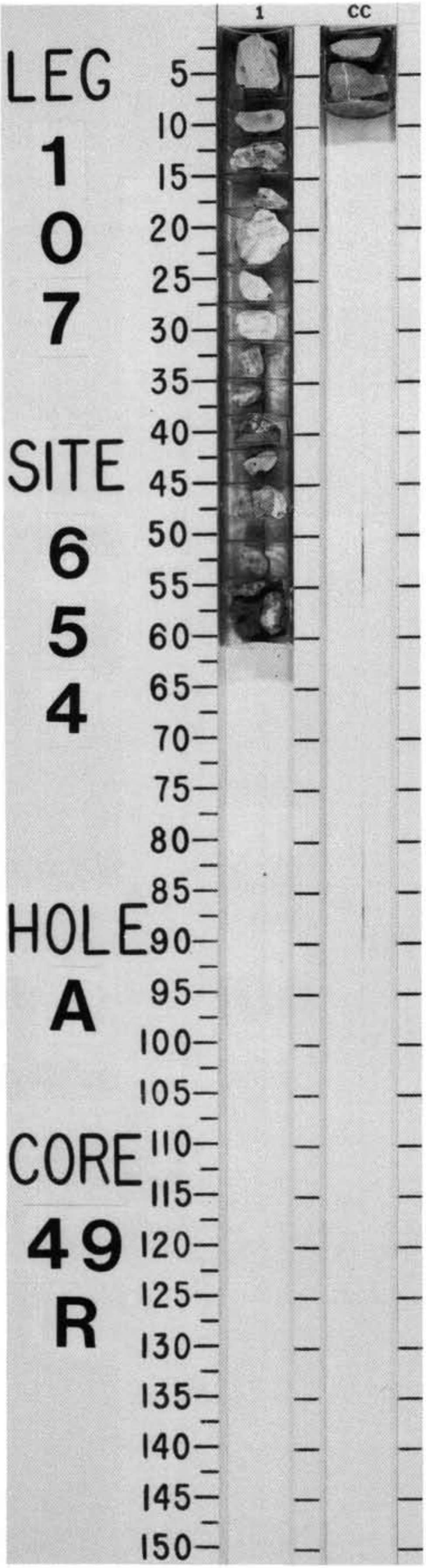
1
CC
LEG
1
0
7
SITE
6
5
4
HOLE
A
CORE
49
R
5
10
15
20
25
30
35
40
45
50
55
60
65
70
75
80
85
90
95
100
105
110
115
120
125
130
135
140
145
150

SITE 654 HOLE A CORE 50 R CORED INTERVAL 2652.2-2662.4 mbsl; 444.7-454.4 mbsf

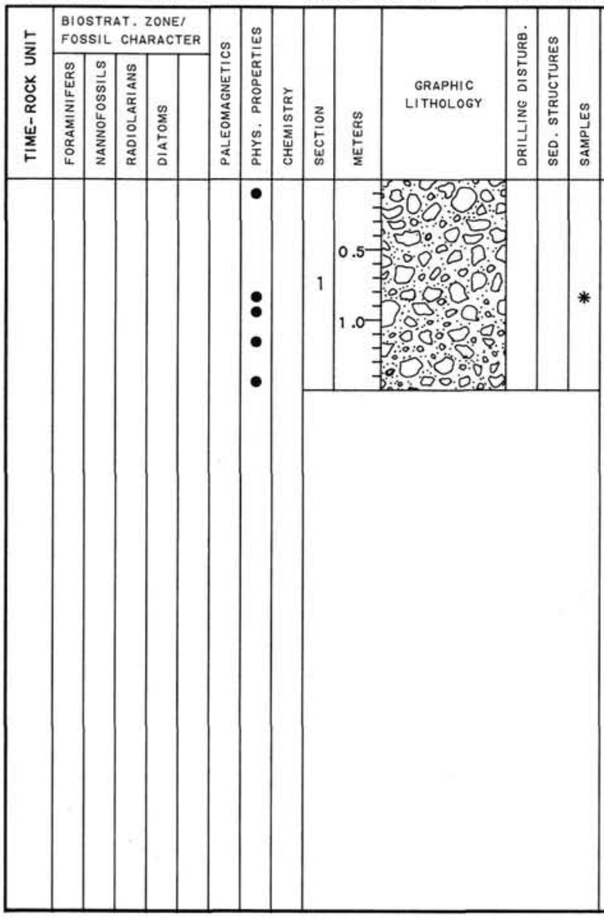

LITHOLOGIC DESCRIPTION

CONGLOMERATE

Conglomerate; Section 1 yielded pebbles of the following lithologies (dimensions in millimeters):
#1: 43 × 61 × 80 metalimestone/dolostone with quartz veins
#2: 52 × 59 × 82 laminated/foliated metalimestone
#3: 57 × 57 × 65 quartz pebble
#4: 58 × 59 × 61 same as #2
#5: 48 × 52 × 60 same as #1
#6: 38–60-cm small pebbles embedded in red mud matrix
#7: 50 × 58 × 63 same as #1
#8: 37 × 53 × 60 same as #1
#9: 44 × 51 × 55 same as #3
#10: 47 × 59 × 59 same as #1
#11: 36 × 55 × 57 same as #1
#12: 36 × 37 × 53 metacalcirudite
#13: 90–143 cm red mud with scattered small pebbles (smear slide)
#14A and #14B: 32 × 57 × 62 and 14 × 44 × 46 quartzite, metamorphic

SMEAR SLIDE SUMMARY (%):

	1, 90 D
TEXTURE:	
Sand	25
Silt	35
Clay	40
COMPOSITION:	
Quartz	18
Clay	33
Dolomite	4
Limonite	8
Gypsum	12
Micrite	25

SITE 654 HOLE A CORE 51 R CORED INTERVAL 2662.4-2672.1 mbsl; 454.4-464.1 mbsf

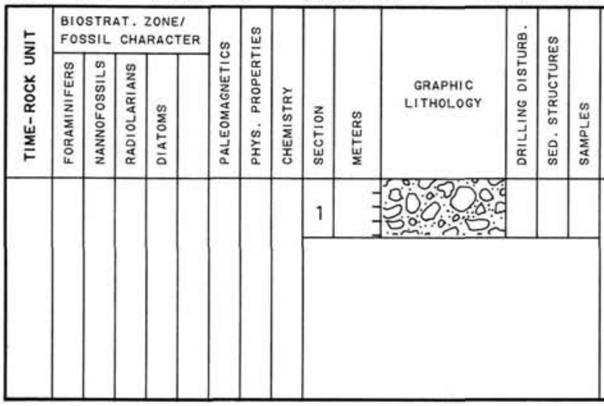

LITHOLOGIC DESCRIPTION

CONGLOMERATE

Conglomerate; recovery consisted of five pebbles of the following lithologies (without red matrix) (dimensions in millimeters):
#1: 30 × 57 × 61 quartzite, folded
#2: 40 × 61 × 68 metacarbonate rock
#3: 36 × 51 × 56 same as #1
#4: 43 × 57 × 63 same as #2
#5: 57 × 60 × 64 (two pieces) same as #2

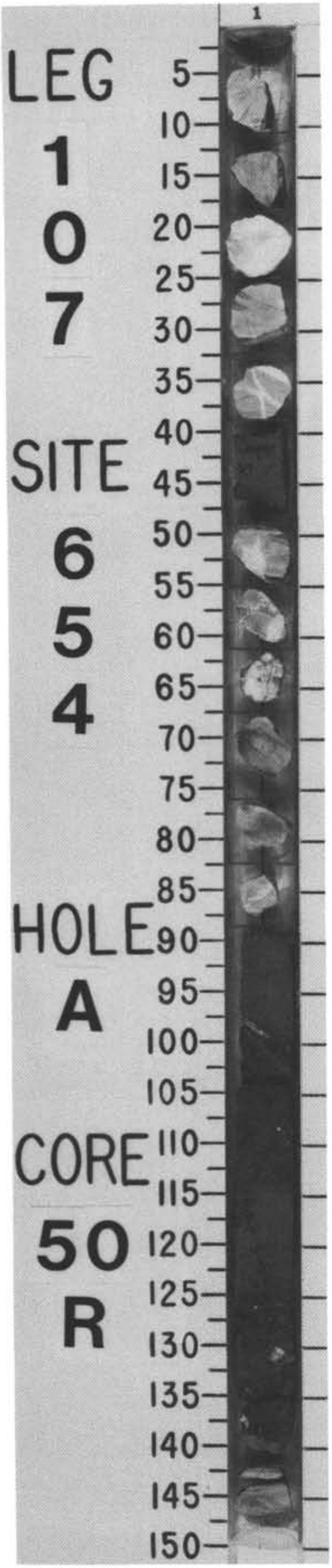
LEG
107
SITE
654
HOLE
A
CORE
50
R
1
5
10
15
20
25
30
35
40
45
50
55
60
65
70
75
80
85
90
95
100
105
110
115
120
125
130
135
140
145
150

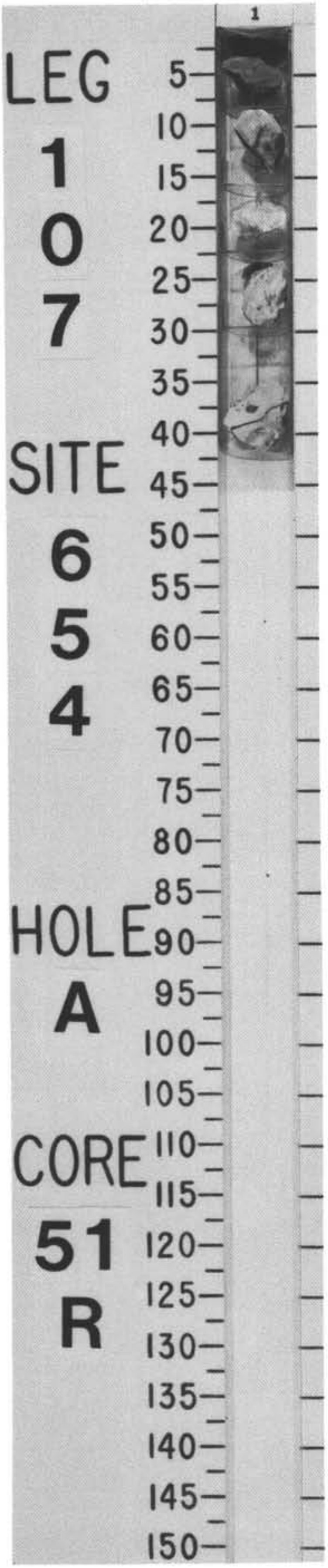
LEG
107
SITE
654
HOLE
A
CORE
51
R
1
5
10
15
20
25
30
35
40
45
50
55
60
65
70
75
80
85
90
95
100
105
110
115
120
125
130
135
140
145
150

SITE 654 HOLE A CORE 52 R CORED INTERVAL 2672.1-2681.8 mbsl; 464.1-473.8 mbsf

TIME-ROCK UNIT	BIOSTRAT. ZONE/ FOSSIL CHARACTER					PALEOMAGNETICS	PHYS. PROPERTIES	CHEMISTRY	SECTION	METERS	GRAPHIC LITHOLOGY	DRILLING DISTURB.	SED. STRUCTURES	SAMPLES
	FORAMINIFERS	NANNOFOSSILS	RADIOLARIANS	DIATOMS										
									1		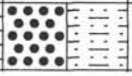			*

LITHOLOGIC DESCRIPTION

GRAVEL-RICH CLAYSTONE

Gravel-rich claystone, structureless; general color is yellowish red (5YR 4/6); contains angular clasts as large as 30 × 20 mm (at 40-cm depth), with average size 2 × 8 mm or less. The clasts are scattered throughout, but mainly concentrated at 24–27 and 39–44 cm; they show random orientation; also abundant whitish gray granule- to sand-sized clasts throughout.

SMEAR SLIDE SUMMARY (%):

	1, 16 D
TEXTURE:	
Sand	10
Silt	40
Clay	50
COMPOSITION:	
Quartz	15
Rock fragments	15
Clay	45
Volcanic glass	5
Dolomite	Tr
Limonite/hematite	10
Gypsum	10
Zeolite	5
Sponge spicules	Tr
Plant debris	Tr
Intraclasts	5


LEG
107
SITE
654
HOLE
A
CORE
52
R
1
5
10
15
20
25
30
35
40
45
50
55
60
65
70
75
80
85
90
95
100
105
110
115
120
125
130
135
140
145
150